Addressing the Multi-scale Lapsus of Landscape

Promotor: Prof. dr. ir. J. Bouma
Hoogleraar in de bodeminventarisatie en landevaluatie
Laboratorium voor Bodemkunde en Geologie
Wageningen Universiteit

Co-promotor: Dr. ir. A. Veldkamp
Universitair Hoofddocent
Laboratorium voor Bodemkunde en Geologie
Wageningen Universiteit

Samenstelling promotiecommissie (members of the promotion - examination committee):

Prof. dr. ir. L.O. Fresco	FAO, Rome, Italie
Prof. dr. A.C. Imeson	Universiteit van Amsterdam, Nederland
Prof. dr. López Bermúdez	Universiteit van Murcia, Spanje
Prof. dr. A.K. Bregt	Wageningen Universiteit, Nederland

Addressing the Multi-scale Lapsus of Landscape

Multi-scale landscape process modelling to support sustainable land use:

A case study for the Lower Guadalhorce valley South Spain

Jeroen Machiel Schoorl

PROEFSCHRIFT

ter verkrijging van de graad van doctor
op gezag van de rector magnificus
van Wageningen Universiteit
Prof. dr. ir. L. Speelman
in het openbaar te verdedigen
op maandag 11 maart 2002
des morgens te half elf in de Aula

CIP-DATA Koninklijke Bibliotheek, Den Haag

Schoorl, J.M.
Addressing the Multi-scale Lapsus of Landscape. Multi-scale landscape process modelling to support sustainable land use: a case study for the Lower Guadalhorce valley South Spain.

Thesis Wageningen University, The Netherlands. - With ref. - With summaries in Dutch, English and Spanish.

ISBN 90-5808-595-3

Propositions

1. As opposed to Van der Meer, the formation, functioning and subsequent closure of the sea-straits of Álora is an important tectonic indicator for the causes of the Messinian Salinity Crisis (*This thesis and Van der Meer, F., 1995. Triassic-Miocene palaeogeography and basin evolution of the Subbetic Zone between Ronda and Málaga, Spain. Geologie en Mijnbouw 74, 43-63*).
2. Under natural circumstances parent material affects modelled soil redistribution rates (*This thesis*).
3. The off-site effects from an exogenous driven change in land use (EC subsidies) might trigger endogenous land use changes in adjacent areas (*This thesis*).
4. To estimate soil redistribution, the ^{137}Cs technique is much cheaper than measuring and experimenting in the field during tens of years.
5. A "safe" calculated risk of a once in a thousand year flooding event can happen tomorrow.
6. To write a Dutch thesis in English for a Spanish research area you needed Belgium francs, have to have Mediterranean experience in Crete (Greece), learn French, speak Spanish, understand Valenciano and think Andalucian.
7. Since stress is causing RSI, AIO's or PhD's should live at walking distance from their office to avoid traffic jams and public transport, especially the Dutch railways.
8. Better one soil scientist in the field than ten behind a computer screen.
9. The steepest descent can break your ankle.

J.M. Schoorl, Addressing the Multi-scale Lapsus of Landscape, thesis defence on the 11th of March 2002 in the Lecture Hall of Wageningen University (Aula), Wageningen, The Netherlands

Aan mijn grootouders:
Gerardus Schoorl
Tini Schoorl-Straub
Joop Jansen
Willy Jansen-de Jongh

a Carolina

La ciencia es una estrategia
Es una forma de atar la verdad
Que es algo más que materia
Pues el misterio se oculta detrás

Cover illustrations by C. Boix Fayos and J.M. Schoorl. Cover illustration front: Digital Elevation Model of the Sabinal catchment just north of Álora indicating the differences in runoff generation between two land use related scenarios (see Chapter 7). Cover illustration back: Digital Elevation Model of the Lower Guadalhorce catchment area from El Chorro to the coast near Málaga. Every 10 meters coloured contour lines are given from 0 to 220 m.

Table of Contents

One slip, and down the hole we fall
It seems to take no time at all
A momentary lapse of reason
That binds a life for life

Preface

Acknowledgements, Dankwoord, Agradecimientos

A momentary lapse of reason was my only conclusion during the fieldwork of 1998 when I was crawling back to my car with a broken ankle doubting if I would ever finish this thesis. Nevertheless major part of the LAPSUS model source code were written during the weeks that I spend at home with my lap-top computer on the sofa and my leg in plaster, providing me with the base for this thesis. Anyway, over the years numerous acknowledgements have been written in many dissertations all over the world, including the thesis of my great-grandfather Prof. Dr. Nicolaas Schoorl exactly one hundred years ago (Schoorl, 1901). The message that can be found in most of them is that such a miracle as finishing your thesis is not the work of only one person. Therefore I can only hope that I mention all of you in the following paragraphs and that those who feel left out can forgive me for such a momentary "lapsus" of reason and memory.

In the first place I would like to thank Prof. dr. ir. Johan Bouma for creating the opportunities for the initial research project and this final thesis. Johan, you have given me the freedom and confidence to investigate along the various temporal and spatial levels combining the foundations of our laboratory namely: soil science and geology. You were also one of the initiators of the field practical "Sustainable Land Use" in Álora, more than ten years ago. Without interfering too much you were always interested in the progress of the work and you were always there for valuable suggestions, the occasional push and the finishing touch.

Without Dr. A. Veldkamp I could not have written this thesis. Tom, thank you for giving me the trust and confidence to become your first full AIO. I have enjoyed your informal way of working and I have learned that you are against pre-cooked thesis outlines. Consequently, I have appreciated very much the freedom I have enjoyed and to organise my own balance between modelling and fieldwork. I hope you agree with me that we did not achieve all the goals that we set at the beginning. Not because we could not do it, but because there were too much data, ideas and results for only four years and one single thesis. In the field your expertise and distinction of the general picture and at the same time an eye for the smallest details, are impressive, especially concerning geology, soils, fossils and mineralogy. Without getting lost in a "chicken-egg" discussion, I hope you at least let me believe that we were a good team and that I more or less prepared and located the sites where you could discover our gem quality *Schorl Tourmalines* and the *Stephanorhinus Veldkampschoorlus*. Finally I also want to thank Marga and your daughters for lending me "daddy Tom" in the field and for the occasional stays and night-overs at your house.

I would like to thank Prof. dr. ir. Louise Fresco for kidnapping me from Amsterdam University and introducing me in the scientific world of Wageningen University. Even when I was working on yours and Tom's CLUE-project you always encouraged me to try to find a way to obtain my PhD. You also played an important role in the development of the field practical "Sustainable Land Use" and the proposals that led to this research project and my thesis. So as you can see I have followed many of your advises except one, I still live in Amsterdam.
Concerning the Laboratory of Soil Science and Geology I would like to thank Willem Wielemaker for working with me in the Álora region and sharing his field (in all aspects) with me. One of the highlights for me and hopefully for you too, was the tenth anniversary of the Álora practical in June 2000. Willem, you know the soils there like nobody else and maybe in the future we can finish that paper about the gneiss hills. I also shared some good moments with Rob van den Berg van Saparoea at Duivendaal, in the field, negotiating with Conchi and Diego, as well as on the many terraces (both geomorphological as anthropogenic) that we visited during the past 5 years of warm and sunny practicals in the south of Spain. Rob, thank you for all those Álora logistics and Álora materials you have provided me over the years. This holds also partly true for Piet Peters although often you were leaving Álora by the time I arrived. I would like to thank Peter Buurman for valuable suggestions in the field and sharing his interest in the region. In addition to Joke, Henny and Thea for the valuable logistics, I would like to thank all other colleagues of BenG Duivendaal for sharing with me all sorts of things from dust-room to coffee-break, from electronic balance to lunch discussion, from excursion to Vlaamse reus (Aldo, Anne, Arie, Barend, Dennis, Douwe, Eef, Ellis, Eric, Ester, Esther, Gerrit, Harry, Hugo, Jan, Jeroen, Jetse, Joke, Gert, Hans, Kasper, Klaas, Koen, Leo, Lieven, Marcel, Michel, Mirjam, Neeltje, Nico, Norma, Paul, Peter, Peter, Piet, Pim, Renato, Rienk, Rob, Roel, Tini, Toine, Virginie, Willem). Only a few months I coincided with Jan Jaap van Dijke before he left for Delft, but I would have been helplessly lost without our initial discussions and his programming techniques.
During these years I enjoyed the company of several roommates: Roel Plant, Leo Tebbens and Marthijn Sonneveld. Thanks guys for providing me the necessary more and sometimes less scientific distractions, discussions, suggestions and evaluation of life in general. Thanks Leo, for your listening ear and advises, and also for all these times that I could spend the night in your guest room on those occasions when it was too late or too early to travel to Amsterdam. Thanks Marthijn and Leo for improving some of the manuscripts that led to this thesis. I also have enjoyed the company of six AV-students (supervising their Msc theses) who contributed to the progress of my research: Marthijn Sonneveld, Kjel Postema, Susanne Laven, Jan-Peter Lesschen, Arnaud Temme and Nynke Schulp.
All staff members of the field practical Sustainable Land Use are thanked for sharing Álora with me, especially John Stuiver for his discussions on flatless DEMs and aggregation levels and for giving me the necessary back up for all maters concerning GIS. John, thanks for everything and hopefully after this thesis I will find some time to write and finish one of those papers that we once started.
I would like to thank the people of the (Physical) Geography departments of Amsterdam and Valencia University that have inspired me to start a career in research. Especially Prof. Dr. Jaap van der Meer, Prof. Dr. Anton Imeson, Dr. Adolfo Calvo Cases and Dr. Erik Cammeraat. Thanks to Gijs Mesman Schultz I started to discover Spain and its inhabitants after which Ellen van Mulligen, Nienke Bouma and Ingeborg Tiemessen shared both the Mediterranean

field as well as the city of Valencia with me. Also the EEZA research group of Dr. J. Puigdefabregas, CSIC Almeria is greatly acknowledged where Dr. Matthias Boer introduced me to the inspiring Guadalentin region. The same holds true for Dr. Anja de Wit who taught me to never give up when she was investigating runoff in a semi-arid almost desert like environment. I will never forget the beautiful landscape, your field-Visa car and the "Mellow Yellow No Rain" song boosting through the speakers.

I would like to thank Prof. Dr. Alfred Stein and my fellow participants of the Methodology discussion group (1997-2000) of the C.T. de Wit Graduate School Production Ecology for many discussions and meetings. Starting initially as a member of the CLUE group I have enjoyed the company of Aldo Bergsma, Kasper Kok, Free de Koning, Peter Verburg, Nico de Ridder and others at the former department of Agronomy.

I would like to thank the following people of the Nuclear Geophysics Division at the KVI in Groningen for the analysis concerning the Cesium technique: Prof. Dr. R. J. de Meijer, Dr. E. R. van der Graaf and Ron ten Have. Concerning the investigation of our Pliocene Rhino teeth I would like to thank Dr. J. de Vos of the museum of natural history Naturalis in Leiden for his help and suggestions.

In addition to my co-authors mentioned at the beginning of each chapter, I would like to thank Prof. dr. M.J. Kirkby, Dr. Anne Mather, Dr. Martin Stokes, Dr. Darryl Maddy, Dr. Carlos Sanz de Galdeano, Dr. C. Huang and several anonymous reviewers for their useful comments on the manuscripts that have become chapters in this thesis.

En España quiero agradecer a Andalucía y en especial a la provincia de Málaga por su paisaje y por la inspiración para mis estudios. Gracias a los habitantes de Álora y sus alrededores por haberme dejado entrar en sus huertos, terrenos y caminos por el monte. Conchi Gordillo Fernández, Diego Aparicio Gómez-Lobo y Paco me han ayudado siempre durante todas mis visitas. Gracias a Conchi y Diego yo he siempre tenido las mejores casas para ver las procesiones de la magnífica Semana Santa en Álora. En las facultades de Ciencias en Granada y Málaga y específicamente en sus instalaciones de biblioteca he encontrado varias publicaciones interesantes. Los últimos años he tenido contacto con Dr. José Damián Ruiz y Prof. Dr. Emilio Ferré Bueno de la Universidad de Málaga, espero que podemos organizar algo en el futuro.

Aunque el fantástico paisaje ibérico no acabe nunca, mi vida en España no estaba solo dedicada a la ciencia. Quiero agradecer a toda la gente de la tierra valenciana que me ha ayudado de una forma u otra. Por ejemplo, los grupos de amigos políticos que aceptaron al "extraterrestre" que soy desde el primer momento, incluso con mi aspecto "guiri" con calcetines y sandalias en Vicoman (gracias Cristina, Mar, Carlos, Pilar, Mario, Pablito, Marisus y Carlos); y por Valencia y Madrid (gracias Isabel, Toni, Ester, Raúl, Angela, Miguel-Angel, Sara, Pilar, Emilio, Andrea y Carlota, Cristina, Rafa).

Todo lo que acabo de escribir es cierto también para mi familia española de la Avenida del Cid. Ellos no sólo me han proporcionado apoyo logístico en mis numerosos viajes al Sur de España en coche, cuando realizaba una parada técnica en Valencia, obligado descanso después de 1900 kms (en algunas ocasiones con estudiantes holandeses incluidos). Lo más importante, ¡Mare de Deu!, es que yo no se que habría hecho sin el apoyo psicológico, emocional y gastronómico proporcionado por la paella Fayos Camarena, las rutas turísticas Boix Tomás o las palabrotas y demás conocimiento de la cultura española aportado por els cuñats. Muchísimas gracias Mª Antonia, Rafa, Maite, Rafa, Mª Angeles y Pecas por toda la

ayuda, el cariño, lametones de brazo (Pecas), amor y todo lo que hacéis para la felicidad nuestra.
Wat betreft mijn "Nederlandse" vrienden en familie denk ik in de eerste plaats aan de mensen die dit helaas niet meer mee kunnen maken. Mijn grootouders aan wie ik dit werk opgedragen heb, zonder hen was dit alles niet mogelijk geweest (zowel biologisch, spiritueel als financieel). Zij kunnen alle vier, zeker wat het reizen betreft, tevreden zijn, Opa Ge Schoorl en Oma Willy wat betreft het vertoeven in en het bestuderen van de bergen, Oma Schoorl voor het langere schrijfwerk (zie dit dankwoord) en Opa Jansen wat betreft het zoeken van fossielen en het vinden van de kortste en mooiste routes. Vervolgens zijn mijn gedachten bij Tante Bert die altijd alle details wilde weten van mijn vorderingen in Latijn, Grieks en geografie en tot slot onlangs Anne-Mieke van Opstal die letterlijk en figuurlijk aan de wieg van mijn ontwikkelingen heeft gestaan.
De families van beide kanten zijn altijd betrokken geweest bij al mijn ontwikkelingen en vorderingen, helaas is het contact de laatste jaren wat minder geworden, mede ook door mijn vele verplichtingen in Spanje. In ieder geval wil ik Tante Ankie, Oom Tom, Oom Wim, Tante Inge, Oom Dick, Tante Rina, Tante Vallie, Oom Nico en alle neven en nichten plus aanwas, bedanken voor alles. In het bijzonder natuurlijk mijn lieve Peet-tante Vallie die altijd dicht bij mijn universitaire voortgang heeft gestaan, omdat we in dezelfde stad en zelfs een tijdje in dezelfde straat gewoond hebben. Het heeft ons (of mij) wel heel wat haren gekost op de Tweede Bloemdwarsstraat, maar dat was geheel vrijwillig. Bo, gaarne proclameer ik evolutioneel technisch dat den strijd reeds doch nog niet gecompleteerd is, ik werp U den handschoen om deze plausibele prestatie te evenaren of wellicht te excelleren. Tot slot wil ik mijn neef Paul (volgens mij nog steeds familie van Sting) en "the Joy of a Toy" bedanken voor een stukje muzikale ontwikkeling tijdens onze studententijd. Jammer dat het toen zo afgelopen is, maar ik heb de master tapes nog steeds en als we later rijk zijn moeten we de boel maar eens overmixen en opnieuw inzingen, MTV - TMF here we come.
Wat betreft mijn vrienden kring (Marc, Hugo, Vicky, Coen, Eva, Hans, Patrick, Ben, JB) is het altijd moeilijk om bepaalde personen niet te kort te doen. Maar een vriendschap van 29 jaar spant toch wel de kroon, bedankt Marc voor al die jaren van onvoorwaardelijke vriendschap, aandacht en ontelbare telefoongesprekken. Eigenlijk horen daar Gerrit en Magriet Volder ook een beetje bij door mij op jonge leeftijd al mee op reis te nemen naar nieuwe landschappen en culturen, en jullie onophoudelijke belangstelling voor mijn vorderingen tijdens mijn studies. Coen wil ik bedanken voor onze talloze discussies, etentjes en andere activiteiten tijdens onze Amsterdamse studenten jaren. Hugo, Vicky, Dik en Marijke wil ik bedanken voor een aantal mooie en bijzondere jaren op de "Nooit Volmaakt" en voor jullie gastvrijheid in de Leonardostraat, La Villeneuve en Cassà de la Selva.
Tot slot wil ik mijn eigen familie Hanki, Charles, Marije, Enya, Sena, Rochus en Saskia bedanken voor de nodige opvoeding, afleiding en steun door de jaren heen. Lieve Marije en Rochus, bedankt dat jullie het als broertje en zusje zolang met mij volgehouden hebben en jullie mogen mij blijven tutoyeren hoor! Lieve Hanki en Charles, ik denk dat er maar weinig mensen op de wereld zijn die zo'n fantastische, gelukkige en vrije jeugd gehad hebben als ik. Ondanks mijn soms pessimistische verwachtingen, mijn vaak ernstig serieuze gezichtsuitdrukkingen, mijn grappen, grollen en streken, mijn rare geluiden en mijn pluizige blonde piekhaar is alles dank zij jullie toch nog goed gekomen en kan ik in de voetsporen van mijn voorvaderen treden met de hoogste universitaire graad die mogelijk is.

Y finalmente en esta hoja blanca tengo sitio suficiente para llenar todo con miles de gracias a una sola persona. Aunque estoy dudando si tengo que escribir mejor en inglés o holandés? Pues no, castellano es la segunda linguae después el Chino. Ya que el Chino solo domino con el estomago, mejor escribo en Castellano así se enteren mas gente. Querida Carolina, paginas enteras dando las gracias a mucha gente, pero por mi esta claro que sin ti no hubiera llegado aquí. Simplemente por que sin ti no hubiera hecho tantos "estudios" en España y estuviera ahora mismo en Groenlandia viviendo con los Inuits in un iglú. Sea lo que sea, tu has estado en cada detalle de esta tesis y después de discutir un poco yo he podido tomar muchas decisiones (en la tesis, el trabajo y en la vida). A veces según mi opinión, a veces según la tuya. Pero no pasa nada, es como esta frase famosa de Fernando Sabater (ya sabes yo leo mucho) *"es mejor saber después de haber pensado y discutido que aceptar los saberes que nadie discute para no tener que pensar"*. Tu, doctora Boix, y tu impresionante potente tesis han sido mi ejemplo durante estos anos. Bonica, muchas gracias por todo lo que me has dado el ultimo decenio y un brindis para que se acaba la faena pronto para ti también. Pronto vamos a tomar esas vacaciones en la playa del paraíso Vicoman.

Gracies, Gracias, Bedankt, Merci, Thanks.

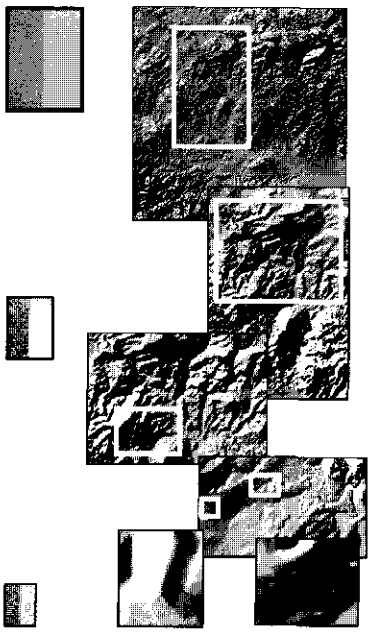

Chapter 1

General Introduction

"Addressing the Multi-scale Lapsus of Landscape" is the title of this thesis. Lapsus has the meaning of a slip of the tongue, a mistake or a missing link and refers to the underestimated importance of the landscape, in addition to serving as an acronym for the model developed and used in this thesis. The central role of the "landscape" is based on the consideration that the landscape is the main driving factor behind many processes at different temporal and spatial levels in geo-environmental sciences. At the same time landscape is the consequence of geological evolution and the result of geomorphological processes. Therefore landscape can be defined in terms of genesis (how formed, processes), geomorphology (its present form, shape), lithology/ soil (its composition), land cover (surface characteristics), land use (its use, human function) and even land management (human factor). Consequently both geological and soil science related issues are considered within this landscape context throughout this thesis.

1.1 Re-inventing the landscape

The role of the landscape in science was prominent in the early years of the nineteenth century when the first systematic geomorphological and geological descriptions and observations of the land surface were made. It was during this period that the first geological maps appeared. Meanwhile in Russia the first soil maps were produced by soil scientists who discovered the relation between soil and climate (Sibirtzev, 1897; Margulis, 1954). During these early years mainly geologists, chemists and agronomists were investigating the soil. Soil science as an individual discipline established itself in the Netherlands from the beginning of the twentieth century (see for review: Felix, 1995).

Soil science initially focussed on soil taxonomy and mapping issues for many years. All around the world major efforts were directed towards classifying soils and mapping of land surfaces at different scales. During the first half of the twentieth century the landscape still played an important role because of the widely applied physiographic mapping techniques, linking soil units to geomorphological features (de Bakker, 1995). Also during this period concepts like the "soil catena" and "chronosequence" were developed, placing the soils in their logical landscape context (Milne, 1936).

These soil survey efforts have resulted in the division of the earth surface in coloured polygons and classified entities with as culmination the FAO global soil map (FAO, 1988). In

the early years different classification systems have been developed all over the world. Later, the numbers of systems have been limited and some standards are now more widely accepted (e.g. USDA, 1999; FAO, 1988). However, still many countries have their "own" classification systems.

In the second half of the twentieth century "landscape" started to loose its visibility in soil science mainly because of the introduction of descriptive morphometric properties in the map legends such as texture, structure, pedogenesis etc. (de Bakker, 1995). The interest for using these chemical and physical soil properties in the soil surveys were a consequence of the more detailed mapping units that became standard in those days (< 1:50000) and the shift of interest from mapping units to taxonomy. Consequently the large scale landscape perspective and co-operation between soil science and geomorphology decreased (Jacob and Nordt, 1991).

Driven by the need for data in the taxonomy oriented scientific community the soil pedon obtained a central position. Soil properties were treated at this pedon scale only and therefore soil science (pedology) started to study the soil pedon inch by inch. The main focus was directed towards pedon dynamics mainly in a two-dimensional way (top-down). First mainly in vertical fluxes, much later also some horizontal and lateral inputs. As a consequence everything was focussed on profile dynamics and the landscape around the soil pedon was reduced to a variable set of boundary conditions.

However, we have to be aware of using soil maps with monotonous and generalised properties. In this sense we can consider the dualistic position of geostatistics. On the one hand useful and powerful in determining and even predicting of spatial variation, dependency and variability between and within soil classes, optimising sample strategies, predicting soil attributes and so on (Bouma et al., 1996; De Bruin and Stein, 1998; Saldaña et al., 1998). One the other hand giving an apparent accuracy for land-units that may need a complete new classification at the first place that properly reflects landscape processes (Lark and Beckett, 1998). At the same time it appears that sometimes geostatistics provides an elaborate statistical analysis for recognising soil properties or geomorphological features that can be recognised by simple observation or physiographic mapping (Park, 2001).

Another consequence of the lacking landscape component can be found at the policy makers level. Modern agriculture, especially in western Europe, is directed towards sustainable development within the landscape. However, many aspects of sustainability are investigated and evaluated at the profile level, ignoring and eliminating the effective processes operating at the higher landscape level. This implies that international, national and regional legislation is affected by generalisation, which may have undesirable and unrealistic effects. For example at the regional level the present day nitrate leaching legislation does not take into account site specific soil properties nor the position of a farmer in the landscape. Therefore neglecting the fact that the landscape is dynamic and that even the smallest gradient will have one farmer leaching his nitrate away to the other farmer. At the international level of the European Community, price controls and subsidies increasingly control land use and land use changes. However, for example in southern Spain land use conversions, changed tillage practises or land abandonment enhances significantly land degradation, which are not considered to enhance sustainable development of the Mediterranean landscape (Rubio and Bochet, 1998; De Graaf and Eppink, 1999).

Fortunately the landscape context surrounding the soil is starting to revive and to receive increasing attention again. Landscape was only a two dimensional carrier of soil information. Now, by means of information technology the realistic four-dimensional properties can be

addressed, thus re-inventing the landscape. In the context of land use and land management a re-invention if the soil in its landscape context is evidenced by the effect of years of management in cultivated areas. Recently studies in the Netherlands have revealed the importance of the management of the soil, showing that many years of agricultural management can alter significantly the most important soil physical and soil chemical properties and functioning of the system (e.g. Droogers and Bouma, 1997; Pulleman et al., 2000).
Nevertheless, in many fields of environmental sciences, including soil science and geology, the landscape context is often underestimated or even lacking at the different levels of investigation (both spatial as temporal) causing a "Multi-scale Lapsus of Landscape". Therefore this thesis will explicitly address the landscape following the issue raised by American scientists Jacob and Nordt (1991) at the end of the last century: "the soil-landscape paradigm is the natural path for pedology to follow".

1.2 Scale issues and modelling

Including the temporal component, landscape can be considered as having four dimensions (length, width, height and time). Therefore, as with all systems with more than two dimensions, scale issues or scale problems are a common point of discussion in environmental sciences. In addition to the multifunctional and sometimes confusing use of the word scale (e.g. hierarchical level, temporal and spatial resolution, temporal and spatial extension), these problems refer to the differences in observation, interpretation and calculation of processes at different organisational levels in the landscape. For example the relationships between the detailed level of individual processes such as infiltration, sediment and water redistribution, available soil water etc. as opposed to processes at global levels such as climate change and land use change.
Both in geomorphology and hydrology the issue of scale has been an important topic over the past years (e.g. Beven, 1995; Kalma and Sivapalan, 1995). Different causes of scale problems can be identified concerning the behaviour of processes at different scales (Schulze, 2000):

1. Emerging properties, new processes emerge at different levels.
2. Spatial heterogeneity of processes influenced by all sorts of spatial factors such as topography, soils and land use.
3. Non-linear behaviour of process rates in time.
4. Threshold dependency to trigger a process.
5. Varying dominant processes at different levels.
6. Response to disturbances.

Typical scale effects in geomorphology at the level of spatial resolution-extension are for example the decreasing erosion rates going from plot, hillslope, catchment to basin scale, where spatial heterogeneity of key processes, local resedimentation, sediment transport distances and the resolution of the measuring techniques play an important role. Another type of scale effect can be found in investigations concerning the impacts of rainfall and flooding events. Here an aspect of temporal resolution-extension is introduced: the magnitude-frequency distribution. For example at the scale of a slope, relations can be found between hillslope erosion, parent material and magnitude-frequency distribution of rainfall (De Ploey et al., 1991). At the catchment scale there are still uncertainties on the exact role of magnitude and frequency of floods, considering the impact of large catastrophic floods with a very low

frequency versus the cumulative effect of many minor flooding events. The large catastrophic floods seem important in the long term evolution of the catchment, whereas the smaller floods, depending on the timing, can have a larger cumulative impact (Coulthard et al., 2001).
In the geological sciences scale effects seem more accepted. For example, geological landscape evolution is driven by three major components: climate, sea level and tectonics. Long term dynamics of these components can be traced throughout the earth history, although one could state that their temporal and spatial resolution becomes coarser going further back in time. This increasing coarseness of geological observations and the resulting stratigraphical framework is in the first place a result of preservation. Secondly, even modern dating techniques show increasing coarseness in precision and validity.
As a consequence both temporal and spatial resolution of knowledge about climate, sea level and tectonics show much more detail for the Holocene than for the Pleistocene and even less for the Miocene. Although science advances rapidly in unravelling the earth history concerning global climate and sea level changes by for example ice core projects, spatially local conditions of specific regions are more difficult to trace back. In addition, the temporal resolution decreases rapidly, especially for global sea level and climate change when going beyond the validity of the Milankovitch glaciation cycles (Pliocene Miocene). Compared with the global to regional character of plate tectonics, climate and sea level changes, local uplift rates are spatially much more variable since in active areas uplift or subsidence rates often depend, in addition to the past and present position on the continents, on local fault systems.
Returning to the present day landscape forming processes, for many years, the tendency has been to model the processes with the most detail possible, small-scale short time, and to simply aggregate results to larger areas and longer time spans. However, as stated by Beven (1995) the hydrological or geomorphological modeller will have to accept that it is virtually impossible neither to model larger systems including the smallest details nor by simple aggregation. Therefore a model must be assembled with only those effective parameters at the grid scale of interest where the smaller sub-grid scales safely can be ignored (Kirkby et al., 1996).
Going back to the central landscape context, its evolution can be simulated by different processes, depending on the applied spatial and temporal resolution. In hydrology and geomorphology, different groups of scientists are working at different spatial and temporal levels. In hydrology there are 2 major groups focussing on: (i) slope and catchment behaviour dealing with event based predictions of runoff and hydrographs (e.g. Beven et al., 1984) and (ii) global and regional circulation models including climate change (e.g. Alcamo, 1994). The same division is found in geomorphology, since the hydrologic behaviour is one of the inputs for geomorphologic modelling: (i) slope and catchment event based erosion models (e.g. Morgan, 1994) and (ii) landscape evolution models including climate and tectonics (e.g. Howard, 1994).
To investigate the soil in the landscape context a spatial explicit model is needed at the multi-catchment level, where the temporal resolution will depend on the processes and observations involved. It is preferred not to use the empirical USLE or its derivatives (Wischmeier and Smith, 1958), since common experiments are limited to agricultural land, deep clayey soils and low gradient slopes. Furthermore there is no empirical basis for semi-arid to sub-humid Mediterranean conditions and in the previous sections on scale problems major constraints have been discussed of using plot data at any other level than the plot itself. The decision not to use sophisticated models like TOPMODEL or WEPP (Beven et al., 1984; Nearing et al.,

1989), in addition to the large amount of data needed, is the too detailed temporal spatial resolution that does not address the relevant processes and control factors at the resolution-extension needed for this thesis.
Actual field data is needed to calibrate and validate geomorphic landscape process models. Traditionally the type of field data that is collected shows a mixture of spatial and temporal resolutions. From point measurements of rainfall, profile data of infiltration, runoff and sediment yield of various plot sizes, catchment discharge and sediment load in flumes and so on. All these types of data have a variable spatial and event based temporal resolution. Consequently model calibration and validation becomes a difficult and uncertain procedure. One of the recently developed methods that shows a coarser temporal resolution is the ^{137}Cs technique. This technique enables monitoring soil redistribution over the last 30 to 40 years by measuring the soil related redistribution of the anthropogenic ^{137}Cs radionuclide, deposited in the environment in the sixties. However, the obtained rates are limited to point data and local soil profile conditions need various calibration techniques. Extension of the spatial resolution is achieved by increasing the number of sample sites in (transects or grids), which increases research costs. Still these costs are considerably lower as compared to the costs involved of long term monitoring with traditional techniques to achieve the same spatial and temporal resolution.

1.3 The fifth dimension and sustainability

As discussed in the previous sections the landscape in environmental sciences is considered to have three spatial dimensions. Together with the temporal dimension landscape becomes a four-dimensional entity within its bio-physical boundaries. However, at various spatial and temporal levels the human influence has become an important factor of consideration. At first this human factor was only considered to be important at short term temporal and limited spatial levels of local land use change and management practises. Recently many research efforts are directed towards the human role in past and future global environmental change (Turner et al, 1995). Gradually we become aware that anthropogenic influences may affect even geological development at regional to global scales (Van Loon, 2001). Therefore, the human influence is introduced here as the fifth dimension of landscape.
Over the past years the consequences of this human influences upon the environment has led to the need for sustainable development of this environment and the concept of sustainability. Numerous definitions of sustainability can be found for all the various disciplines involved in environmental sciences. However, the FAO (1992) uses one of the most elaborated definitions, defining sustainability as: "The management and conservation of the natural resource base, and the orientation of technological and institutional change in such a manner as to ensure attainment and continued satisfaction of human needs for present and future generations; such sustainable development conserves water, plant and animal genetic resources, is environmentally non-degrading, technically appropriate, economically viable and socially acceptable". This definition combines the ecological aspects of sustainability with the economic and social aspects, emphasising that sustainability comprises various dimensions. In other words, different perceptions on sustainable development exist and there is no single meaning or concept for sustainable agriculture and rural development.

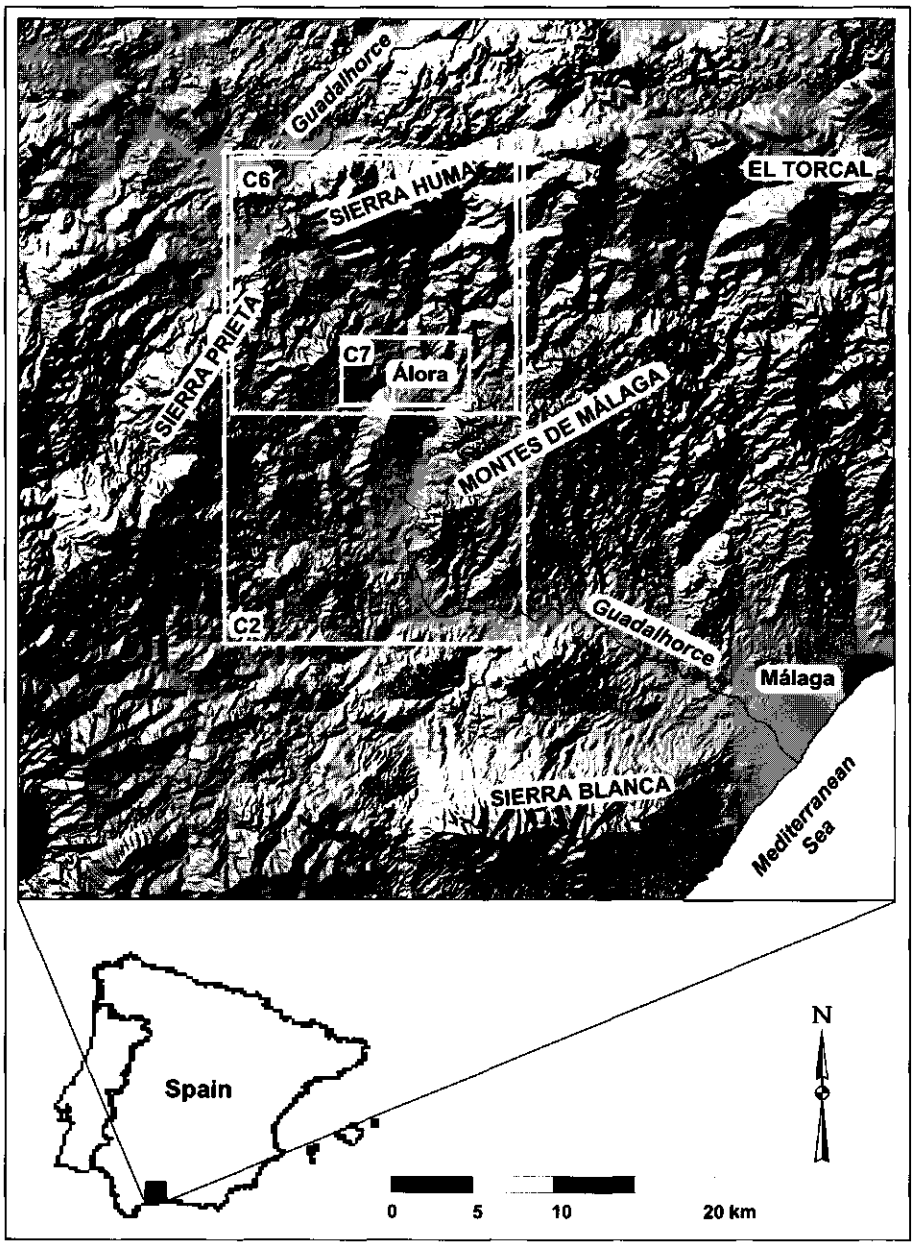

Fig. 1.1 Shaded relief image 50 by 50 km of the study area in the Málaga province, Andalucía, Spain. The white boxes indicate the extension of the areas studied in Chapter 2 (C2), Chapter 6 (C6) and Chapter 7 (C7). Chapters 4 and 5 are studied at a more detailed level, as a smaller part of C7.

It becomes clear that the concept of sustainability is not without discussion because of the various disciplines involved, from policy maker to earth scientist. All these disciplines have their own understanding, definition and implementation of the concept. However, for the earth scientists there are certain aspects of sustainable development that need some attention. By nature the earth is constantly changing, both gradual changes as apparently catastrophic ones. Sustainability in the form of environmental protection and nature conservation needs a framework of process rates and the interaction with the four-dimensional landscape. As stated by van Loon (2000) it is the task of earth scientists to rise awareness and to inform public and policy makers on the spatial and temporal impact of this geological evolution.

1.4 Study area

The study area is situated in the south of Spain surrounding the village of Álora in the river basin of the Guadalhorce, province of Málaga, Andalucía. This region is dominated by several mountain ranges up to 1500 m.a.s.l. high comprising the Montes de Málaga, Sierra Prieta, Sierra de Aguas, Sierra Blanca and Sierra Huma (Fig. 1.1). Geologically speaking, the area has been studied as early as 1859 by Ansted who gave a first geological and geomorphological description of the region surrounding the, in those days, small harbour city of Málaga.
This research area, comprising the middle to lower Guadalhorce river basin, was chosen for its dynamic landscape of mountains and hills, a variety of different lithologies within a small area, its interesting complex geological history and active landscape processes ranging from tectonics, land use changes to land degradation. Furthermore this area has been used for the past ten years by the Wageningen University field practical "Sustainable Land Use" integrating the disciplines of Agronomy, Irrigation, Soil and Water Conservation, Nature Conservation, GIS & Remote Sensing and Soil Science. Over the years this resulted in various publication about the research area of different disciplines (De Bruin and Stein, 1998; De Bruin et al., 1999; De Graaf and Eppink, 1999; De Bruin, 2000; De Bruin and Gorte, 2000; Schoorl and Veldkamp, 2000; Schoorl et al., 2000; Schoorl and Veldkamp, 2001; Veldkamp et al., 2001; Wielemaker et al., 2001; Schoorl and Veldkamp, 2002; Schoorl et al., 2002a; 2002b, 2002c). Consequently, the local infrastructure and resources of a growing database were available during this thesis project.
In this thesis, different spatial levels have been investigated around the village of Álora, situated in the northwestern part of the Málaga province, Andalucía (Fig. 1.1). Further details of the area concerning the level of observation, spatial and temporal resolution-extension, climate and other specific information, are given in each chapter in the introductionary and methodological sections. The geological background of the area will be discussed in detail in Chapter 2. Finally, details about the land use of the research area can be found in Chapter 7.

1.5 Objectives and research questions

The general objective of this thesis is to investigate the role of the landscape at different spatial and temporal levels (extension and resolution) in geomorphological processes, focussing on the sustainability of land use within a representative Mediterranean landscape. This general objective can be divided into the following 6 specific objectives for this thesis. Each of these objectives is achieved by trying to answer several research questions:

1. To explore the constraints of the geological context upon the landscape.
   - What is the geological background, composition and location of the different parent materials in the research area?
   - How does the present topography relate to geological processes in the past concerning changes in global sea level and global climate change?
   - What are the past and present uplift rates that have influenced landscape evolution?
2. To develop a simple multi-scale landscape process model valid on different temporal and spatial levels.
   - What is the effect of DEM resolution (i.e. the landscape representation) upon modelling erosion and deposition?
   - What are the effects of different flow routing algorithms at different resolutions and extensions?
3. To measure actual soil redistribution rates in the research area.
   - What is the validity of the Cs^{137} technique to measure net soil redistribution in the research area?
   - What is the influence of the typical Mediterranean environment concerning lithology, steep slopes and shallow stony soils upon both natural and anthropogenic radionuclides?
4. To compare measured soil redistribution rates with modelling landscape processes.
   - What are the commonly used calibration techniques and which one is the most suitable for the research area?
   - Can we calibrate the LAPSUS model with these measured ^{137}Cs soil redistribution rates?
   - What is the influence of land use and tillage upon these rates?
5. To investigate the influence of a dynamic landscape upon important soil qualities.
   - What is the influence of lithology upon the model input parameters of landscape process modelling?
   - How is the soil available water influenced by the dynamic landscape concept?
6. To research the effect of linking landscape process modelling and land use changes.
   - What parameters in modelling landscape processes are influenced by land use?
   - Which are the possible scenarios of land use change in the study area?

1.6 Outline of this thesis

Except the introduction (this Chapter 1) and the synthesis (Chapter 8), the Chapters 2 to 7 have been written at different spatial and temporal resolutions-extensions evolving around the central landscape theme (Fig. 1.2). All aspects around this theme have been investigated starting from the general geological background, to involving landscape processes, to model development, to calibration with field data, to landscape and soil properties, to integrating landscape processes and land use change.
As the base for the understanding of the landscape and its processes Chapter 2 is dealing with the landscape evolution of the research area at a geological timescale of 10^7 [a] with a difficult to determine temporal resolution of 10^4 to 10^5 [a]. The organisation of the landscape, concerning parent materials and topography, is investigated in relation to long term process rates of climate, sea level and tectonics. This study is directed towards the whole research area with a spatial extension in the order of 10^2 [km^2].

To investigate the most important landscape processes (water and soil redistribution) Chapter 3 is concerned with developing a multi-scale landscape process model valid at different spatial/ temporal resolutions called LAPSUS (see model source code in the Appendix). Model behaviour is tested within as many fixed boundary conditions as possible. This is achieved using a high level of abstraction with artificial DEMs and resolutions from 1 to 81 [m] and different extensions from 10^3 [m^2] to 10^5 [m^2].

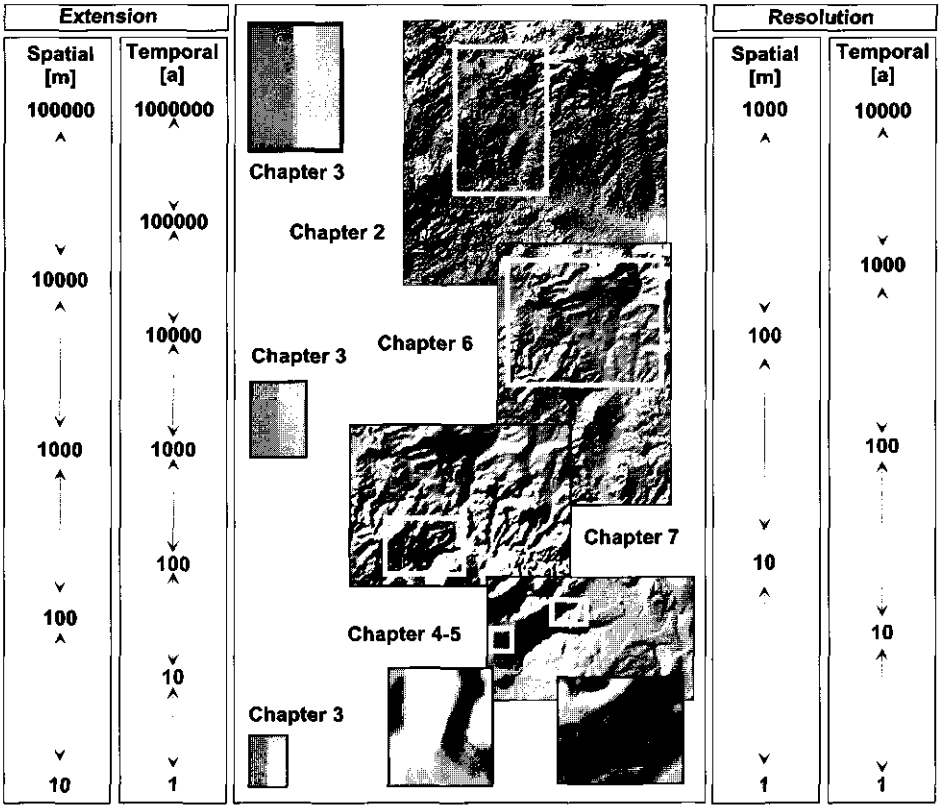

Fig. 1.2 Overview of the spatial and temporal resolution-extension applied in the different chapters.

To measure net rates of soil redistribution at the landscape level, and to overcome the limitations of extensive monitoring, the Caesium-137 (^{137}Cs) technique has been tested in the research area. Chapter 4 is investigating the applicability of the ^{137}Cs technique under typical Mediterranean conditions. The technique is applied at the slope transect to catchment scale within a spatial extension of 10^3 [m^2] to 10^5 [m^2]. In Chapter 5 the field-measured results are used to calibrate net soil redistribution on the temporal resolution of years and decades. Also in Chapter 5 the results of the ^{137}Cs monitored erosion and sedimentation patterns are compared with simulations of the LAPSUS model using 7.5 [m] resolution DEMs.

Knowing the possibilities but also the constraints of the Lapsus model, Chapter 6 moves up to the multi-catchment or basin scale with a spatial extension of 10^2 [km^2]. In this chapter the soil-landscape relations are evaluated using a DEM with 100 [m] resolution. Temporal resolution is again 1 to 10 [a] and the effects of soil redistribution upon water availability are simulated within this soil landscape context.
Finally Chapter 7 integrates landscape process modelling and changes in land use to evaluate onsite and offsite effects. Several scenarios of land use change are tested at a temporal resolution of 1 [a] and temporal extension of 10 [a]. The study area is the Sabinal catchment using a 25 [m] resolution DEM of around 1.7 10^1 [km^2].
Since each chapter is (to be) published in a peer reviewed scientific journal, the general layout of each chapter includes an introduction, materials and methods, results, discussion and conclusions section. Consequently only a brief synthesis is given in Chapter 8.

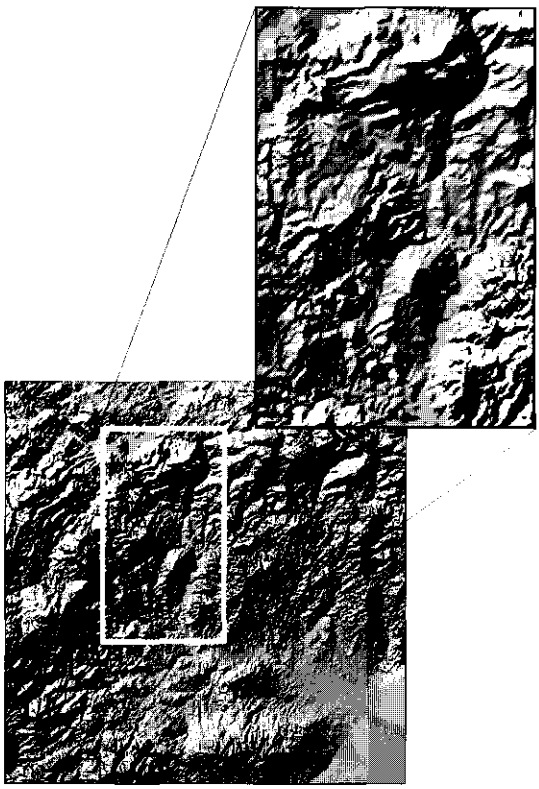

Chapter 2

Geology and Landscape Evolution

The first step in any soil-landscape oriented research is the investigation of the evolution of the landscape and the geological background in the study area. Landscape evolution is the result of a variety of geomorphological processes and their controls in time. In the south of Spain tectonics, climate and sea level fluctuations have mainly controlled Late Cenozoic landscape evolution. In this area, geomorphological reconstructions can be made using sedimentary evidence such as marine and fluvial deposits as well as erosional evidence such as terrain form and longitudinal profile analysis. Data is obtained and analysed from the Upper Miocene to present. These reconstructions add information and constraints to the uplift history and landscape development of the area. Main sedimentation phases are the Late Tortonian, Early Pliocene and Pleistocene. Important erosional hiatus are found for the Middle Miocene, Messinian and Late Pliocene to Early Pleistocene. This resulted in a relative large and elongated Tortonian marine valley filled with complex sedimentary structures. Next, a prolonged stage of erosion of these deposits and incision of the major valley system took place during the Messinian. In the Pliocene a short palaeo-Guadalhorce, in a narrow and much smaller valley existed, partly filled with marine sediments combined with prograding fan delta complexes. During the Pleistocene, a wider and larger incising river system resulted in rearrangements of the drainage network. Evaluating the uplift history of the area, we found that tectonic activity was higher during the Tortonian-Messinian and Upper Pleistocene, while tectonic activity was lower during the Pliocene. Relative uplift rates for the study area range for the Messinian between 160-276 [m Ma^{-1}], for the Pliocene between 10-15 [m Ma^{-1}] and for the Pleistocene 40-100 [m Ma^{-1}].

Based on: Schoorl, J.M. & Veldkamp, A., 2002. Late Cenozoic landscape development and its tectonic implications for the Guadalhorce valley near Álora (Southern Spain). Geomorphology.

2.1 Introduction

Landscape evolution is a continuing interplay of geomorphological processes and their controls in time. Most present-day landscapes are the net results of this evolution and many landscape properties, such as sediments and morphology, hold the keys to reconstruct their past. Using a framework that focuses on the main controlling factors of fluvial systems: climate, sea level and tectonics we can reconstruct landscape development. This approach combines the existing knowledge available from wider literature with local findings and data, especially when general curves of past sea level and climate changes are available (e.g. Harvey et al., 1999; Mather, 2000; Stokes and Mather, 2000).
In sedimentary basins, the lower reaches of fluvial systems are typically considered as the best records for upstream erosion in fluvial basins. While in tectonic actively uplifting areas the upper reaches are considered to be less suitable for the preservation of its history because of dominating erosional processes (Talling, 1998). This viewpoint is strongly contradicted by research of fluvial deposits in upper and middle reaches of uplifting fluvial systems (e.g. Maddy, 1997; Veldkamp and Van Dijke, 2000; Bridgland, 2000) and consequences of basin inversion and base level changes (e.g. Mather, 1993; Mather, 2000; Stokes and Mather, 2000). Fluvial terraces record both erosion and deposition events and although often sparsely distributed throughout the landscape, they do hold a more complete key of fluvial basin dynamics than stacked sediment bodies. Reconstruction and numerical modelling exercises demonstrate that stacked sediments in lower fluvial reaches have no direct link with the climate triggered erosion events upstream or the sea level triggered changes downstream (Veldkamp and Tebbens, 2001).
Most current landscapes in Europe were predominately shaped during the Pleistocene because of the major influence of Glacial eras (e.g. Ehlers, 1996). Only a few basins have remnants dating back to the Late Tertiary. The oldest known terraces in northwest Europe are from the Pliocene (Van den Berg, 1994; Bridgland, 2000). The landscapes in the South of Spain are exceptional because here much older landscape remnants can be found dating back to the Miocene (Sanz de Galdeano, 1990; Weijermars, 1991). These older landscapes make investigating landscape development in this area more complicated. Especially when for the Late Cenozoic only general knowledge of the climate and sea level dynamics are known. Also the tectonic history of the Betic Cordillera are considered complex and only partly known (Haq et al., 1987; Weijermars, 1991).
The aim of this chapter is to reconstruct several stages of the Late Cenozoic landscape development in the Guadalhorce valley near Álora. Published data and new field data will be combined to make a quantitative reconstruction of palaeo-landscapes. Subsequently the nature of regional tectonic activity will be assessed.

2.2 Location and geological setting

The investigated area is situated in the middle reach of the Guadalhorce river between El Chorro and Pizarra (Fig. 2.1) in the most northern part of the Málaga basin. This basin is one of many sedimentary basins in the Betic Cordillera of southern Spain (e.g. Sanz de Galdeano, 1990; Sanz de Galdeano and López Garrido, 1991; Weijermars, 1991; López Garrido and Sanz de Galdeano, 1999). Our study area is only part of this basin and is bounded by the Sierra de Huma and Sierra del Valle de Abdalajis in the north, the Sierra de Aguas in the central western sector and the Montes de Málaga in the southeast (see Fig. 2.1).

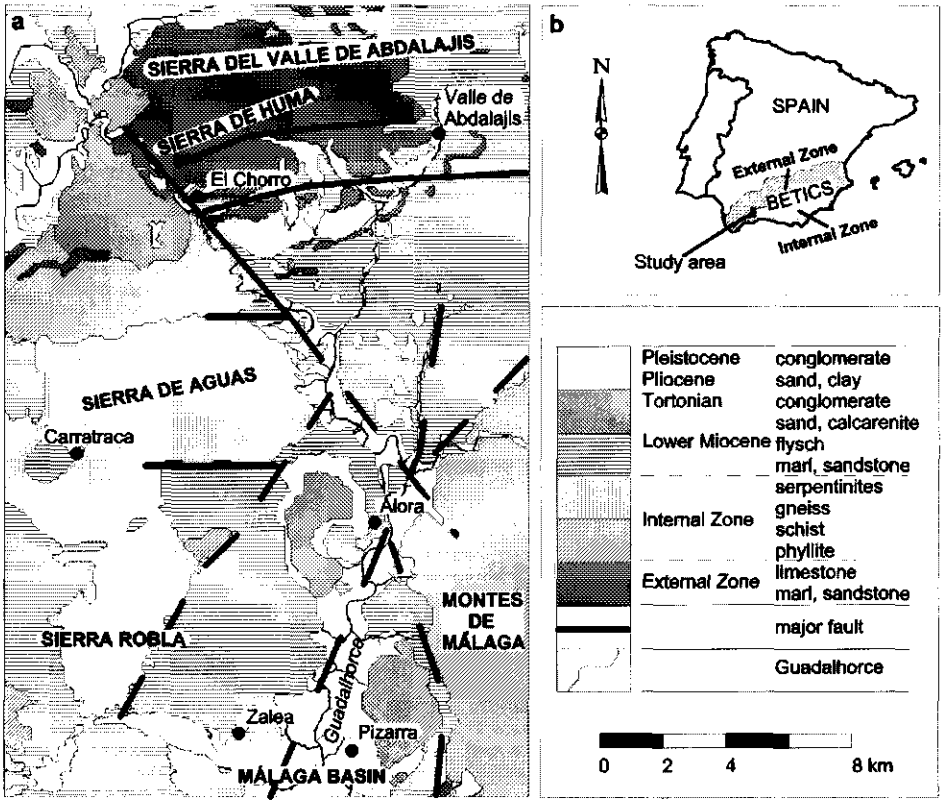

Fig. 2.1 Location of the study area with a) geological setting and b) position of the External and Internal zone of the Betic Cordillera in southern Spain.

Based on tectonics, lithology and palaeo-geography the Betic Cordilleras of southern Spain are divided into a northern External Zone (Prebetic and Subbetic) and a southern Internal Zone (e.g. Sanz de Galdeano, 1990; Weijermars, 1991; Biermann, 1995). In general, the External Zone includes non-metamorphic Mesozoic and Tertiary rocks. The Internal Zone is composed of three large, tectonically superposed complexes or nappes: the Nevado-Filabride, the Alpujarride and the Malaguide complex from bottom to top. The Nevado-Filabride and Alpujarride complexes include Palaeozoic to Triassic sediments, metamorphosed during the Alpine Orogeny. The Malaguide Complex comprises sediments from the rest of the Mesozoic and Tertiary, but only part of its Palaeozoic basement underwent metamorphism (e.g. Sanz de Galdeano, 1990; Sanz de Galdeano et al, 1993; Biermann, 1995).

Related with the (ongoing) interaction between the Iberian and African plates, structuring of the Internal Zone in nappes took place in the Late Oligocene to Early Miocene (Martín Algarra, 1987). In the lower Miocene the Internal zones began to be displaced towards the west causing deformation in the contacts with the External zones, associated with horizontal movements along N70-100 strike slip faults. From the Late Tortonian onwards movements in

the area are mainly vertical, controlled by NW-SE and NE-SW faults as a result of regional N-S compression (see faults in Fig. 2.1) and regional uplift of the Betic Cordillera (Sanz de Galdeano, 1990; Sanz de Galdeano and López Garrido, 1991).
The area comprises a variety of Neogene sediments, which were deposited mainly during the Early Miocene, Late Tortonian, Pliocene and Pleistocene (Fig. 2.1). Important erosional hiatus exist for the middle Miocene and the Messinian (e.g. Sanz de Galdeano, 1990; López Garrido and Sanz de Galdeano and literature cited within, 1999). As described in the previous section during the Early Miocene the area is still dominated by complex tectonic conditions such as extensional deformation and westward movement. Consequently, the Málaga basin and thus the study area acquired their present shape at the beginning of the Tortonian (Sanz de Galdeano and López Garrido, 1991). Therefore, our reconstructions start with the Late Tortonian sediments.

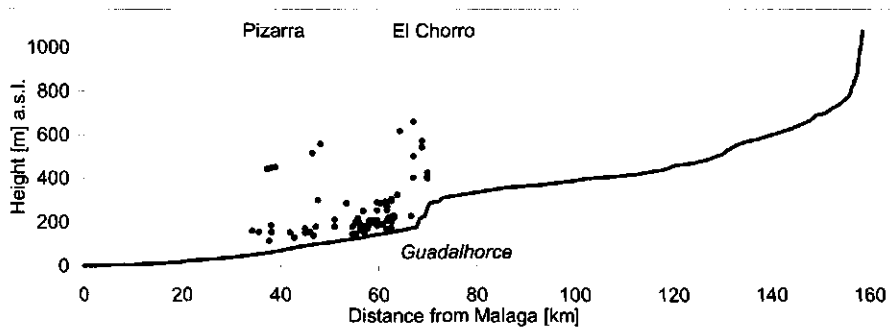

Fig. 2.2 Present day longitudinal profile of the Guadalhorce river from the coast near Málaga (left) towards the source area in the mountains east of Antequera (right). Dots represent observation points mentioned in the text.

2.3 Neogene deposits

All sites with Neogene deposits can be observed along the present day Guadalhorce longitudinal profile given from the present day coast near Málaga to the source area (Fig. 2.2). Present day topography clearly outlines the general geology as described in the previous section (Fig. 2.3). The different Sierras and Tortonian outcrops are clearly representing the higher areas (old or erosion resistant), while the lower areas are occupied by the Early Miocene flysch (less erosion resistant) and Pliocene and Pleistocene sediments (younger lithologies). Fig. 2.4 shows the Neogene deposits of the study area since Late Tortonian times. Some of these deposits can not be found on the more general outline of the geological maps of this area (IGME, 1978; ITGE, 1990). In the next sections the different units will be described in more detail from Late Tortonian to present.

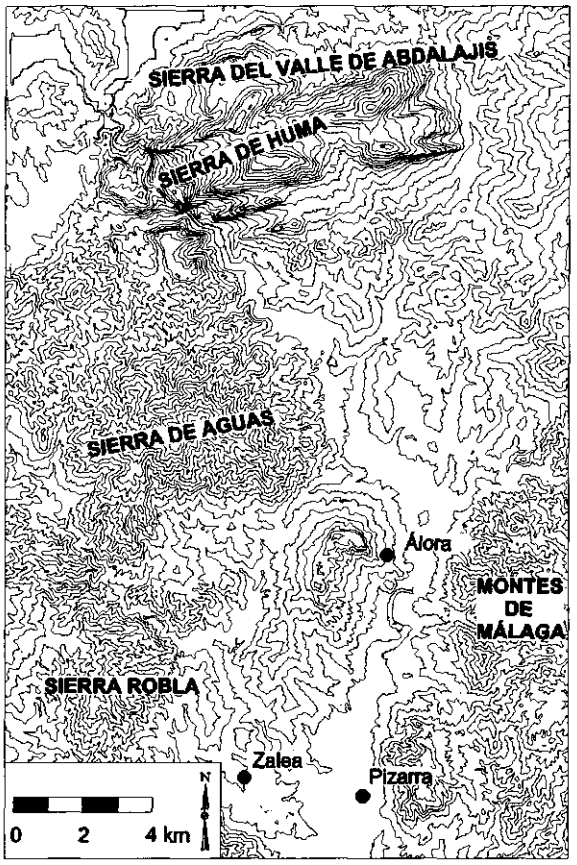

Fig. 2.3 Relief of the study area varying from 1100 [m] in the Sierra Huma, 900 [m] in the Sierra de Aguas towards 50 [m] south of Pizarra. Contour line interval is 50 [m].

2.3.1 Late Tortonian

In the study area several outcrops of sedimentary rocks can be found composed of micro to large boulder conglomerates, various sized sands, silts and calcarenites. At present they form tabular mountains of several hundreds of metres in altitude (Fig. 2.4). Sedimentary structures such as channels, bedding and (mega-)ripples are common as well as marine slumps and mudflows. In general the bottom layers contain the coarsest conglomerates while in the top layers undisturbed marine bio-clastic layers can be found. Throughout the whole outcrop from bottom to top macrofossils can be found. These macrofossils, especially pectinids, are surprisingly often well preserved in the coarser sequences (Jímenez et al., 1991). These materials are attributed to the Late Tortonian (López Garrido and Sanz de Galdeano, 1991) because of their stratigraphic similarity with outcrops near Antequera and Ronda, which were dated on their foraminifera content as Late Tortonian by Serrano (1979).

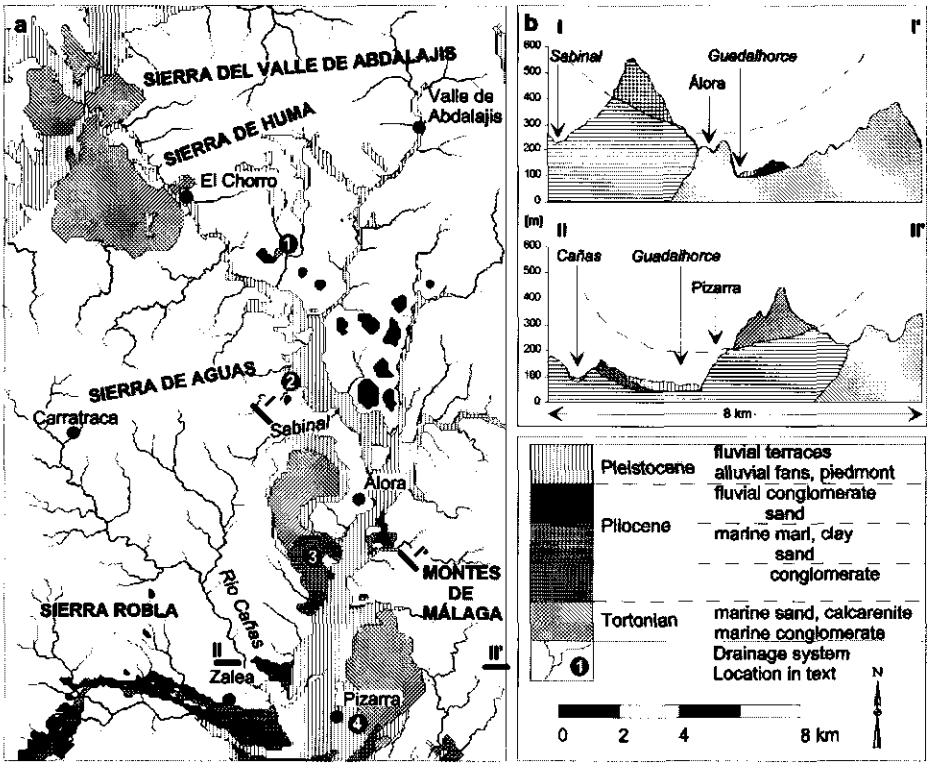

Fig. 2.4 Neogene deposits in the study area with a) geographical distribution and numbered important locations and b) schematic geological cross sections (basement units are described in Fig. 2.1).

Three main outcrops are situated in the study area, from north to south, near El Chorro, Álora and Pizarra (Fig. 2.4). According to detailed topographic maps the Tortonian rocks outcrop up to an elevation of 662 [m] at El Chorro with a base at 205 [m], at Álora they outcrop up to an elevation of 559 [m] with a base at 303 [m] and at Pizarra they outcrop at an elevation of 452 [m] with a base at 185 [m]. Although these elevations are slightly different, they compare well with altitudes previously recorded in the literature (e.g. Sanz de Galdeano and López Garrido, 1991). These highs and lows of the Tortonian, including two smaller remnants, can be observed along the present day Guadalhorce longitudinal profile (Fig. 2.5). The smaller remnants can be found between Álora and El Chorro (numbered locations 1 and 2 in Fig. 2.4) and consist of cemented Tortonian blocks, several tens of meters in size, composed of conglomerates and sandstones. Unfortunately the bases of these remnants are not exposed and there is a lot of interference with the surrounding materials.

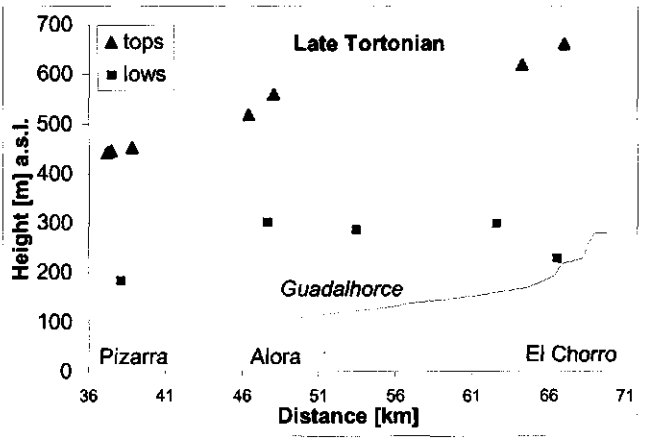

Fig. 2.5 Highest and lowest exposures of the present day Late Tortonian outcrops given as the absolute height above the present Guadalhorce river profile.

For the three major outcrops several observations of the basal bounding surface are possible. To the north of the El Chorro outcrop we find abrupt erosional contacts with Early Miocene marls and sandstones. Near the village of El Chorro erosional and abrupt contacts are clearly exposed with limestones from the External zone and phyllites from the Internal zone (Martín Algarra, 1987). Both outcrops near Álora and Pizarra are again situated directly on top of Early Miocene marls and sandstones. In a schematic cross section (Fig. 2.4) these Tortonian outcrops seem to be part of a large channel form of which the deepest part is difficult to determine.

2.3.2 Messinian

In general little is known about the Messinian in the middle and lower Guadalhorce valley. In literature and maps no deposits are attributed to this age and the Messinian is considered as an erosional hiatus in this area (e.g. IGME, 1978; ITGE, 1990; Sanz de Galdeano and López Garrido, 1991; López Garrido and Sanz de Galdeano, 1999).

2.3.3 Pliocene

In the Guadalhorce valley around Álora both marine and fluvial deposits represent the Pliocene. Downstream of Álora mainly marine clays, marls and fine sorted sands, upstream of Álora mainly fluvial sands and conglomerates can be found (Fig. 2.4). In general the fluvial deposits are found topographically higher than the marine deposits. This can be observed when the actual elevations of Pliocene fluvial and marine outcrops are plotted along the longitudinal profile of the present Guadalhorce river between El Chorro and Pizarra (Fig. 2.6). The well layered blue-grey marine marls and clays are rich in macrofossils and foraminifera, which date to the Early and Middle Pliocene (Sanz de Galdeano and López Garrido, 1991). In the studied area these marine sediments are 50 to > 100 [m] thick and are mostly deposited directly on the basement rocks. They can be found in large areas south of Pizarra and Zalea reaching altitudes of 155 [m] a.s.l. Smaller and local outcrops of marine clays can be found

from Pizarra to Álora at variable altitudes and decreasing in thickness. At Álora the marine clays are restricted to small channel fills of only a few metres thick at 151 [m] a.s.l. The most northern site with marine Pliocene sediments, marine sands containing shell fragments, is found a few kilometres north of Álora at around 180 [m] a.s.l.

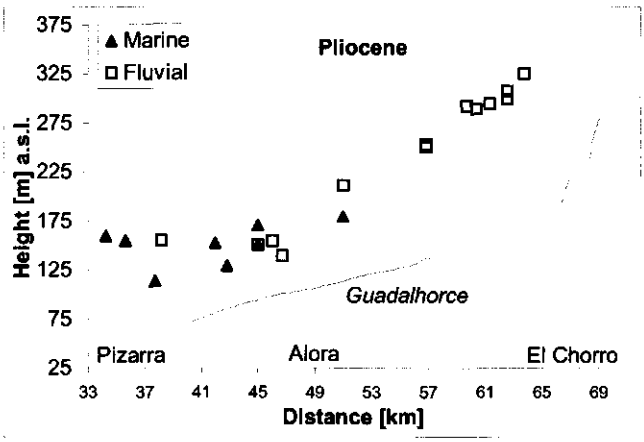

Fig. 2.6 Pliocene outcrops within the study area with their absolute heights above the present Guadalhorce river profile.

Pliocene fluvial sands and conglomerates are found as terrace remnants throughout the landscape. Layering of alternating coarse sands and poorly sorted conglomerates are common. The most important difference between the Pliocene conglomerates and older sediments mentioned before is the poor cementation and better developed layering. The deposits are between 20 to 50 [m] thick and are found at increasing altitudes to the north, up to 320 [m] a.s.l. south of El Chorro (Fig. 2.6).

South of Álora and Pizarra, we have found slightly different conglomerates as mentioned before (numbered locations 3 and 4 in Fig. 2.4). They consist of well cemented unsorted to poorly sorted, coarse to fine, mainly whitish silt matrix supported conglomerates with boulders up to 40 cm. No macrofossils were found. Layering is poor including sections of tens of metres without any layering or structure. These sediments are best described as mudflows.

These mudflow deposits are found in elongated lobes originating from the lower boundaries of the Tortonian outcrops (at around 300 [m] south of Álora and at 200 [m] near Pizarra), all the way down to the present level of the Guadalhorce river (around 100 [m] south of Álora and 50 [m] near Pizarra). On the highest topographical positions sometimes whole blocks of slumped and rotated Late Tortonian materials are incorporated. In the lower topographical positions layering is more common and indicates continuation even below the present Guadalhorce level. These mudflows are deposited on top of the basement rock, in this case Miocene marls and sandstones.

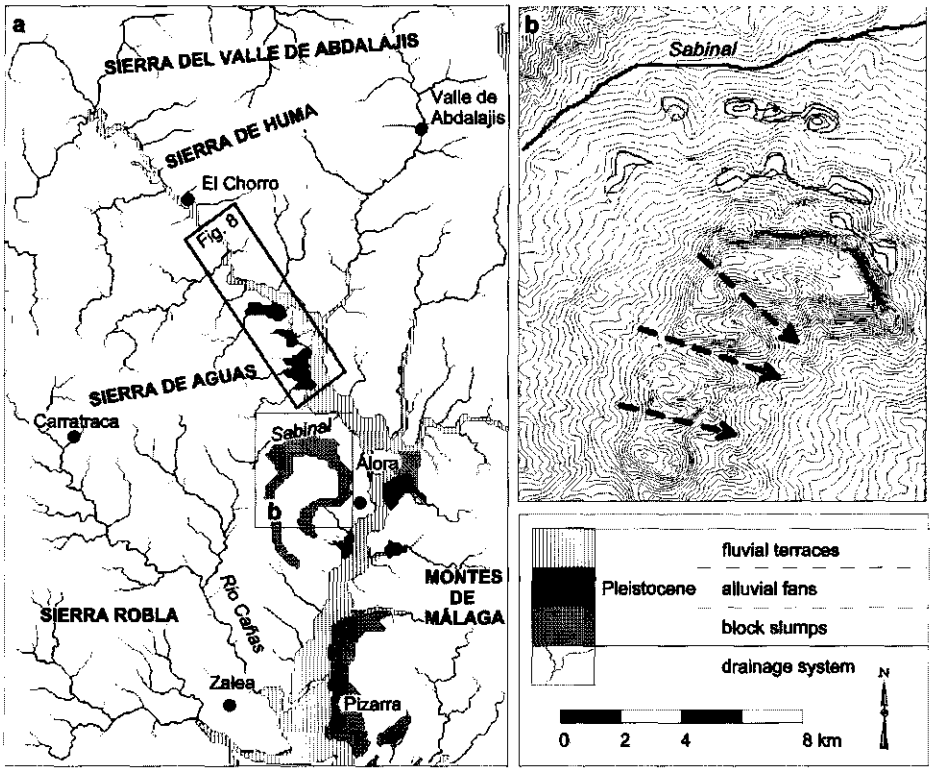

Fig. 2.7 Pleistocene deposits in the study area with a) geographical positions and important locations and b) overview of the Sabinal valley with block slumps and palaeo-drainage directions (contour line interval is 10 [m], highest point is 559 [m]).

2.3.4 Pleistocene

Pleistocene sedimentation in the Málaga basin has been mainly continental (López Garrido and Sanz de Galdeano, 1999). This holds also true for the study area where no marine deposits from the Pleistocene have been found (Fig. 2.7). The most important fluvial deposits are the alluvial plains of the Guadalhorce river with several terrace levels. Major tributary systems from the Sierra de Aguas and Montes de Málaga have left alluvial fan complexes interfingering with these terraces. Most of the fan complexes are severely dissected, sometimes more than 25 [m]. In Fig. 2.8 the fluvial terrace remnants can be observed along the present Guadalhorce river profile. A total of 7 levels have been recognised. These levels of Pleistocene terrace remnants are, contrary to those of the Pliocene deposits, all parallel to the current longitudinal profile of the Guadalhorce river suggesting a fluvial system in dynamic equilibrium with its controlling factors.

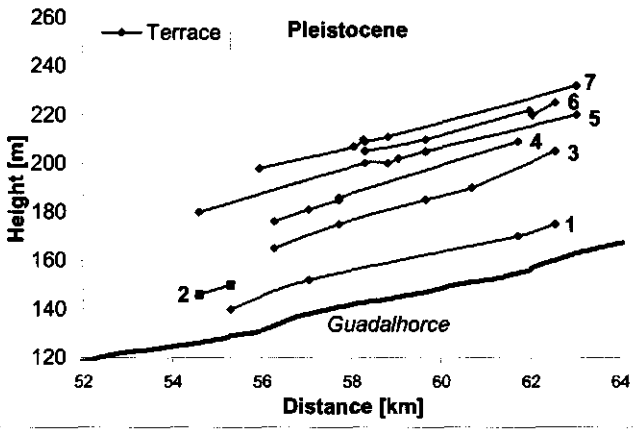

Fig. 2.8 Pleistocene terraces levels 1 to 7 for the area between Álora and El Chorro. Little squares are observation points (location is given in Fig. 2.7).

2.4 Discussion

2.4.1 Landscape evolution

The sediments from the Late Tortonian indicate shallow marine conditions dominated by strong marine currents in a relatively narrow sea strait. As opposed to Van der Meer (his Fig. 11, 1995) in this case a connection between the Atlantic Ocean and the Mediterranean sea. During this period in the Tortonian several connections between the Atlantic Ocean and the Mediterranean existed (Weijermars, 1991), which are reported in both the western (e.g. Serrano, 1979; Sanz de Galdeano and López Garrido, 1991; López Garrido and Sanz de Galdeano, 1999), and the eastern Betics (e.g. Fernández and Rodríguez Fernández, 1991; Wröbel and Michalzik, 1999). Probably the main cause of these connections was a eustatic sea level rise, but there was also a major influence exerted by local tectonic factors, such as dip-slip movement on NW-SE and NE-SW trending faults, and prolonged regional uplift of the Betic Cordilleras (Martín Algarra, 1987; López Garrido and Sanz de Galdeano, 1999).
In the present literature this Atlantic Mediterranean connection in the region of Álora is considered to be 5 to 10 km width. Especially in the areas with weaker lithologies the marine strait is considered to widen considerably, more or less following the contours of the Lower Miocene sediments (Fig. 4 in Sanz de Galdeano and López Garrido, 1991 as well as Fig. 4 in López Garrido and Sanz de Galdeano, 1999). This suggests a pre Tortonian Guadalhorce drainage system (terrestrial stage) more or less comparable to the present day system. However, no deposits of this stage have been found so far. In addition, the first sediments registered in the Late Tortonian are very coarse and angular, indicators of mountain building and emerging land. Altogether if we combine the idea of a narrow sea strait with the observations of the basal boundaries of the present day outcrops (channel forms in Fig. 2.4)

the actual strait could have been even more narrow (Fig. 2.10a). This could explain as far as preservation is concerned why the Tortonian is not found on top of the Early Miocene sandstone ridges southwest and northeast of Álora.

The Tortonian sedimentation ended with continued continental uplift in combination with a eustatic sea level drop, resulting in the closure of the connections between the Mediterranean and the Atlantic Ocean (López Garrido and Sanz de Galdeano, 1999). According to the eustatic sea level curve for the late Tortonian, this major regression started around 7 to 6.7 [Ma], at a maximum of +10 [m] a.s.l. (Haq et al., 1987; Savoye et al., 1993). These closures of all Atlantic Mediterranean connections by the aforementioned factors, together with climatic controls caused the Messinian Salinity Crisis (Krijgsman et al., 1999). This crisis implied a Mediterranean base level lowering of more than 1200 [m] (Hsu et al., 1973; Savoye et al., 1993). This drop in base level led to erosion of former coasts and severe incision of the river systems that drained into the Mediterranean basin (e.g. Clauzon, 1978). During this stage probably 90 % of the Tortonian sediments were removed from the study area.

In the Early Pliocene a marine transgression re-established the sea connection between the Atlantic Ocean and the Mediterranean through the strait of Gibraltar. As a result the Mediterranean filled very rapidly up to the Pliocene high stand of +80 [m] at 4.7 [Ma] (Haq et al., 1987; Savoye et al., 1993). These Pliocene materials filled the deeply incised Messinian relief rapidly by fan-delta systems depositing gravels, sands and more distal marls and clays. According to Weijermars (his Fig. 34, 1991) another connection existed through the Málaga basin, but we agree with other observations that this Pliocene marine transgression reached only until Álora (Sanz de Galdeano and López Garrido, 1991; López Garrido and Sanz de Galdeano, 1999). The Pliocene landscape reconstruction in Fig. 2.10c shows a several times narrower valley than in the Late Tortonian. An important detail is the Pliocene highstand reaching halfway up the area north of Álora. This is actually a few kilometres more inland than normally given in the literature (Sanz de Galdeano and López Garrido, 1991).

The first sediments attributed to the Pliocene in the study area are the conglomerates south of Álora and Pizarra. They are best described as mudflows and they are definitely the first sediments after the prolonged period of Messinian erosion. Firstly because Pliocene marine clays can be found overlying these mudflows on several locations. Secondly because these mudflow deposits reach below the present level of the Guadalhorce river and are directly overlying the basement topography. Summarising this means both mudflow deposits are younger than Late Tortonian and older than the marine Pliocene highstand deposits. Therefore, we have to place them at the Messinian-Pliocene boundary, in an environment of steep gradients, recovering climate (wetter) and with a deeply eroded central Guadalhorce valley.

The Pizarra mudflow originates from one of the major valleys within the Pizarra Tortonian outcrop. Just south of this deposit large slumped and rotated block of Tortonian sediments is situated a, which suggest a relation of large scale slumping of cemented blocks and the trigger of large quantities of unconsolidated materials. In other words the cementation of the Tortonian outcrops is restricted to the outer exposed surfaces and the process of cementation probably dates to the Messinian.

As mentioned in the previous paragraph, important features in the area are massive block mass movements. Especially around the Tortonian outcrops of Álora and Pizarra numerous large blocks have slumped into de valleys with some of them reaching hundreds of metres in size. These blocks consist of cemented Tortonian sediments (conglomerates, sands,

calcarenites) including the original sedimentary structures. Normally they have slumped backward with some rotation and slid down over considerable distances (up to 200 [m]). The Sabinal valley just north of the Tortonian Álora outcrop is the best example with more than ten blocks sliding down. They can easily be recognised on a detailed contour map (Fig. 2.7). The tops of the three lowest blocks in the Sabinal valley are all situated around 260 [m] a.s.l.
As can be observed the Pliocene marine deposits are situated at different heights in the present landscape, which range from 180 to 114 [m] a.s.l. There can be several reasons for the altitude distribution of these marine sediments: 1) different high stands (recorded for the Pliocene) and thus different ages of Pliocene marine terraces, 2) differential uplift (regional or along NW-SE and NE-SW faults), 3) erosion levels of the incising Guadalhorce during the consequent marine regressions or 4) different distal facies of the prolonged Pliocene highstand.
According to eustatic sea level curve by Haq et al. (1987) the next transgressions reached 25, 60 and 65 [m] lower than the oldest highstand. The altitudes found in the study area are within this reach. However, Pliocene marine sediments are found outside the study area in the west at 400 [m] (Alazoina) and going south and east towards Málaga between 100 and 50 [m] a.s.l. This indicates at least important regional uplift. Fault movements are considered less important in the study area, since marine sediments can be found at comparable altitudes on both sides of the supposed fault lines. At least several low marine outcrops are known to be topped with some fluvial material indicating former Guadalhorce terrace levels. Different distal facies are evident, comparing the succession from north to south at decreasing altitudes from sands with shelves to channel fill to extensive clay terraces.

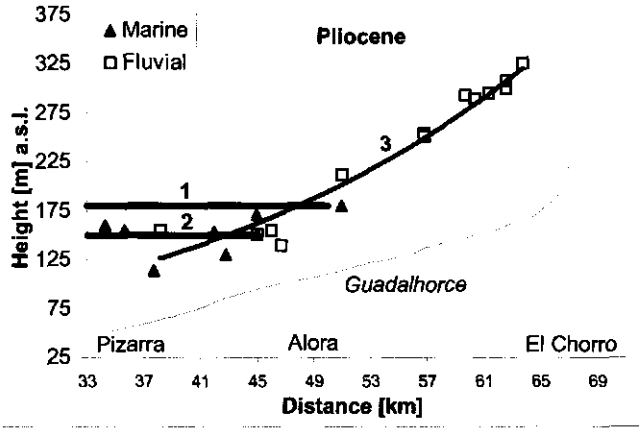

Fig. 2.9 Trend lines of sea level and river gradient for the Pliocene deposits.

In general the Pliocene sediments are considered as a shallowing upward sequence, with fine grained sands as an indication of an important regression in the Late Pliocene (Sanz de Galdeano and López Garrido, 1991; López Garrido and Sanz de Galdeano, 1999). However, these sands can be found at a height of 155 [m] a.s.l. in the south of the study area while the

highest Pliocene deposits found north of Álora are located at 180 [m] a.s.l. This matches quite well with the 4.7 [Ma] +80 [m] and the 3.2 [Ma] +55 [m] highstands (lines 1 and 2 in Fig. 2.9), suggesting no tectonic activity in the Álora to Pizarra area throughout the Lower and Middle Pliocene. On the other hand the trend-line for the Pliocene fluvial deposits shows a very steep gradient, which could be an indication of significant uplift of the Chorro area since the Pliocene (*line* 3 *in* Fig. 2.9).

Evidence suggests that for a long period during the Pliocene the palaeo-Guadalhorce was not able to incise significantly in addition to more lateral erosion. As a result most of the sediments of the Pliocene and earlier are removed by the Guadalhorce river and tributary systems. This lack of evidence of incision supports a scenario of relatively low uplift rates during that period. In addition, in this period the Sierra de Huma formed an important obstacle since the El Chorro canyon did not exist yet in its full extent. On the moment that the uplift of the area resumes the Guadalhorce cuts through the bedrock of the Sierra Huma (location 3 in Fig. 2.10f). In addition to the canyon itself also antecedent incised meanders north and south of the canyon, and several terrace levels (Fig. 2.8) indicate renewed uplift of the area.

As far as the Pleistocene terrace levels are concerned climate can provide the trigger for the various erosion and deposition phases but has no bearing on whether terrace staircases are formed. There has to be some kind of uplift. There are many theories on the causes for such uplift ranging from direct erosional isostasy to glacio- and hydro-isostasy. Some theories argue that glacio- and hydro-isostasy have a large spatial imprint as a result of crustal dynamics (Maddy et al., 2000). All isostasy theories are supported by the observation that when the climate oscillations increased during the Middle Pleistocene the uplift rates have also increased as witnessed by nice staircases registering each 100 [ka] climate cycle as a separate terrace. This tendency is clearly reconstructed in the Thames (Maddy 1997), Meuse/ Maas (Van den Berg, 1994), Somme (Antoine, 2000) and Allier (Veldkamp, 1992). Techniques to date calcrete formations in Pleistocene terraces could provide some information on the chronology (Kelly et al., 2000). At the south side of the Sierra de Mijas, 50 kilometres south of the study area travertines were dated back to 217 [ka] B.P. at a height of 430 [m] a.s.l. (Durán et al., 1988). Unfortunately calcretes have not yet been located nor analysed yet in the study area.

2.4.2 Development of the drainage system

Directly after the closure of the straits in the onset towards the Messinian the Late Tortonian sediments are supposed to have occupied an approximately horizontal flat valley system from Antequera to Málaga. This valley, filled with uncemented Late Tortonian deposits, continued to receive water and sediments from the surrounding higher relief and a new terrestrial drainage system started to form. Base level dropped progressively following the regressing sea, in this case the Atlantic to the north and the Mediterranean to the south. Probably slightly higher uplift rates in the External Zone triggered the early Guadalhorce at least from the Sierra de Huma in a southern direction. As a consequence rivers originating in the Sierra de Aguas, Montes de Málaga and other areas to the west and south joined the growing Guadalhorce river, which followed the regressing Mediterranean sea towards Málaga and the Alboran basin (Fig. 2.10a to d).

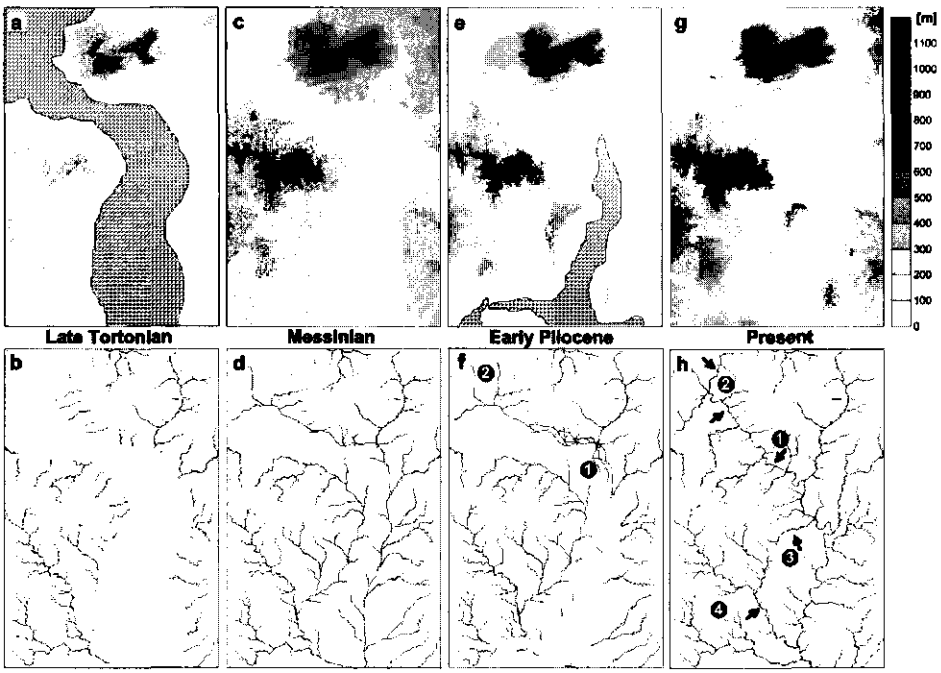

Fig. 2.10 Palaeo-geographical reconstructions and development of the drainage network in the study area from the Late Tortonian to present.

Because of the continued baselevel lowering, the early Guadalhorce started to incise. As a result all three outcrops present a palaeo-valley morphology at their tops with drainage patterns suggesting former connections with the surrounding high relief (e.g. Sierra de Aguas, Montes de Málaga), as can be seen for example at Álora (Fig. 2.7b). Erosion continued until the Pliocene highstand, and by that time the Guadalhorce valley south of Álora was excavated below the present level of the Guadalhorce river as can be seen at the toes of the Pizarra and Álora Pliocene mudflows (Figs. 2.10e and f).

The Pliocene fluvial deposits north of Álora indicate a palaeo-Guadalhorce more to the east than at present (location 1 in Figs. 2.10f and h). In this area a prominent sandstone ridge formed the Messinian western side of the valley, which was filled by the Pliocene deposits. Sedimentary structures in these deposits point to a braided river system (Fig. 2.10f). Question remains when the Guadalhorce river reached it present length. Somewhere between the Messinian and Pleistocene the Guadalhorce must have captured streams from the Antequera basin to the north (location 2 Figs. 2.10f and h). Comparing the Early Pliocene fluvial deposits at more than 300 [m] at El Chorro to 50 [m] at Pizarra and the steep trend-line of the Pliocene river gradient (Fig. 2.9) it seems possible that the Pliocene Guadalhorce was a much shorter river system (upper reach). At least the El Chorro canyon did not exist at it full extent.

During the Pleistocene major shifts in the drainage system took place. As mentioned in the previous section on locations 1 and 2 (Fig. 2.10f) as a consequence of uplift and possible capture events. In addition, to the south the removal of weaker lithologies of the Early

Miocene flysch plays an important role. For example the Álora Pliocene mudflow palaeo-currents indicate a direction where at present no Tortonian outcrops can be found. In this area the Cañas and Sabinal rivers are actively eroding the Early Miocene flysch (Fig. 2.4). Therefore these rivers must have developed after the Early Pliocene removing the Late Tortonian materials from this area (location 3 Fig. 2.10h). This is supported by the fact that Pliocene fluvial terrace remnants can be found along the eastern side of the Sierra Robla (Fig. 2.4) indicating a palaeo-Cañas a few kilometres to the west (location 4, Fig. 2.10h).

Table 2.1 Minimum and maximum uplift scenarios for the study area.

	S[a]	Time[b] [Ma]	Uplift Pizarra [m Ma^{-1}][c]	Álora [m Ma^{-1}][c]	El Chorro [m Ma^{-1}][c]
Pleistocene	1	0.7-1.64	68.2 (27.4)	68.2 (27.4)	100.0 (58.1)
Pliocene-Pleistocene	2	2.6-4.0	10.4 (2.2)	10.4 (2.2)	18.4 (10.2)
Pliocene	3	1.66-3.06	15.3 (4.5)	15.3 (4.5)	28.2 (17.4)
Tortonian-Messinian	4	2.0-2.3	239.1 (36.9)	239.1 (36.9)	239.1 (36.9)
Tortonian-Messinian	5	2.0-2.3	159.8 (11.2)	209.9 (14.8)	239.1 (36.9)

[a] scenarios mentioned in text
[b] duration of uplift
[c] +/- minimum maximum range

2.4.3 Regional uplift scenarios

From the geomorphological data presented so far, we can get an indication of uplift rates since the Late Tortonian for the study area. Several important markers in height, time and geographical position have been found, which help to limit different uplift scenarios (Table 2.1). These scenarios are defined by both stages in global eustatic sea level as incision of the Guadalhorce river, which clearly reflects increasing uplift from Pizarra towards El Chorro (see nickpoint at El Chorro in Fig. 2.2). Therefore resulting rates are minimum rates within the uncertainty on the temporal boundaries.

First, the youngest markers are the Pleistocene terraces of which the highest level is situated at 67 [m] a.s.l. above the present Guadalhorce at 1.64 [Ma]. These terraces are found north of Álora (see Fig. 2.7) and within the time frame towards the Pliocene higher uplift rates are possible in the El Chorro area. However, if these 7 levels of terraces are related to the glacial-interglacial cycles, then the result is an uplift of at least 67 [m] over the last 0.7 [Ma] (scenario 1 in Table 2.1).

Second, the highest Pliocene marine deposit in the area is located at 180 [m]. Taking into account the Early Pliocene sea level high stand of +80 [m] at around 4.7 [Ma] (Haq et al., 1987; Savoye et al., 1993), this would mean a total uplift, Pliocene and Pleistocene, of 100 [m] in this area. As a consequence around 33 [m] uplift is left for the Pliocene, taking into account around 67 [m] uplift for the Pleistocene. As mentioned in the previous section marine terrace levels could suggest very low tectonic activity between 4.7 [Ma] and 3.2 [Ma] highstands. In combination with the range of scenario 1 this results in 2 different scenarios of uplift until terrace formation in the Late Pleistocene (scenario 2) or uplift restricted to the Pliocene (scenario 3).

Third, the Tortonian deposition came to an end after the last highstand of +10 [m] before the Messinian at around 7 to 6.7 [Ma] ago (Haq et al., 1987; Savoye et al., 1993). This gives at least 552 [m] uplift (652 [m] minus 100 [m] for the Pliocene and Pleistocene) for the region, assuming that present differences in outcrop altitudes are due to erosion in the Early Messinian (scenario 4). However, this 100 [m] Pliocene Pleistocene uplift is restricted to the areas north of Álora between the Pleistocene terraces and the Pliocene outcrop. More to the north uplift rates could have been higher for the Pleistocene, reducing the possible uplift rates for the Tortonian Messinian period. An alternative scenario is assuming no significant erosion of the top layers of the outcrops, which implies differential uplift from 552 [m] in the Chorro area, 449 [m] in the Álora area and 342 [m] near Pizarra (scenario 5). A constraint is the global eustatic rise of +35 [m] at 5.5 [Ma] (Haq et al., 1987), which never reached the Mediterranean (Savoy et al., 1993). Therefore the El Chorro area must show uplift rates higher than 26.2 (+/- 2.9) [m Ma^{-1}].
The highest uplift rates are found in the Messinian, which agrees with the latest ideas on the important tectonic causes of the Messinian salinity crisis (Krijgsman et al. 1999). In addition, in the eastern Betics increased tectonic activity is reported for the end of the Miocene (e.g. Weijermars et al., 1985). In the study area the Pliocene seems a quieter period with uplift rates of at least a factor 10 lower while during the Pleistocene uplift increases again. For the Sierra Nevada area Sanz de Galdeano and López Garrido (1999) found the same temporal distribution of tectonic events. Although actual rates are several times larger with a mean of over 438 [m Ma^{-1}] since the beginning of the Tortonian. Uplift rates in the study area for the Plio-Pleistocene are slightly lower than those reported for the Sorbas basin in the Eastern Betics, which range from over 160 [m Ma^{-1}] in the Sierras to 80 [m Ma^{-1}] in the basin centre (Mather, 1991). Nevertheless in the study area a similar spatial distribution exists considering Álora and Pizarra to be situated towards the central part of the Málaga basin and El Chorro to the basin margins and Sierras.
As far as the Pleistocene terraces in the study area are concerned we see very comparable uplift rates associated with complete staircases ranging from 40–100 [m Ma^{-1}] within the Thames basin (Maddy et al., 2000), 50-60 [m Ma^{-1}]for the Somme (Antoine, 2000), 60 [m Ma^{-1}] for the Meuse/ Maas (Van den Berg, 1994) to 100 [m Ma^{-1}]for the Allier (Veldkamp, 1992). Model simulations of terrace formation have also clearly demonstrated a relationship between uplift rate and terrace preservation potential (Veldkamp and Van Dijke, 2000). In settings with slow uplift rates terraces are formed but are mostly subsequently eroded, while a rapidly uplifting setting prevents the formation of terraces. The possible interpretation for the Guadalhorce that each terrace is assumed to have registered each glacial/interglacial cycle, yield an average uplift rate of approximately 96 [m Ma^{-1}]. This is exactly in the range of uplift rate for maximal terrace preservation.

2.5 Conclusions

Late Tortonian sediments indicate the tectonic activity near the end of the Miocene. This mountain building in a marine environment combined with a narrow connection between the Atlantic and the Mediterranean results in complex deposits and structures. From the end of the Tortonian and during the Messinian a large portion of these Tortonian deposits were removed. The remnants are significantly uplifted during a period of tectonic activity.

Messinian incision of the Guadalhorce river system only reached inland to Álora probably because of a bedrock threshold. In addition, tributary river systems were not fully developed yet and probably the drainage area of the Guadalhorce was limited and influenced by the strong uplift in the Sierra Huma and El Chorro area.
During the Pliocene the upper part of the river valley started to develop. This took place in several stages indicating tectonic and climatic controls. In the second half of the Pleistocene the Guadalhorce river system must have incised fully into the Jurassic Limestone at El Chorro. Tectonic control is also evident form incised meanders before and after El Chorro.
Especially for older sediments we have to take into account that erosion and compaction causes minimal heights of the deposits. In addition, the temporal resolution is very variable. Therefore these are means and minimal rates. Calculations of minimum uplift rates for the study area during the Messinian range from 239-276 [m Ma^{-1}] for the El Chorro area to 160-239 [m Ma^{-1}] for the Pizarra area. In the Pliocene slower uplift rates have been found ranging from 10-15 [m Ma^{-1}]. However, in the Pleistocene tectonic activity increases again with uplift rates up to 100 [m Ma^{-1}].

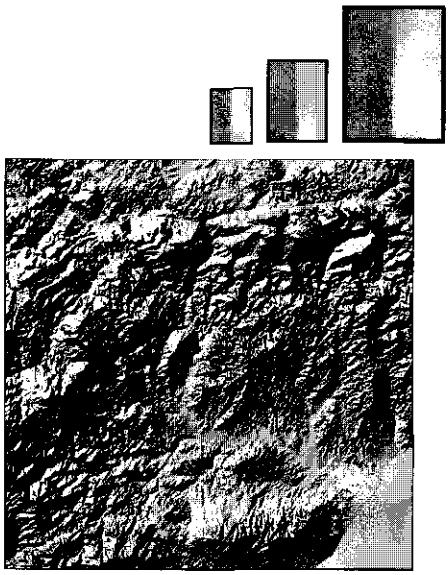

Chapter 3

Landscape Process Modelling

After investigating the geological background of the research area, this chapter describes the development and testing of a landscape process model. In contrast to the field based approach of the previous chapter, this chapter is rather experimental based and in search of a suitable modelling approach for landscape development. Many landscape models have been developed over the past decades, however there is relatively little known about handling the effects of changing spatial and temporal resolutions. Therefore, resolution effects remain a factor of uncertainty in many hydrological and geomorphological modelling approaches. In this chapter we present an experimental multi-scale study of landscape process modelling. An emphasis was laid on quantifying the effect of changing the spatial resolution upon modelling the processes of erosion and sedimentation. A simple single process model was constructed and equal boundary conditions were created. The use of artificial Digital Elevation Models (DEMs), i.e. straight and smooth slopes, eliminated the effects of landscape representation. Only variable factors were DEM resolution and the method of flow routing, both steepest descent and multiple flow directions. The experiments revealed an important dependency of modelled erosion and sedimentation rates on these main variables. The general trend is an increase of erosion predictions with coarser resolutions. An artificial mathematical overestimation of erosion and a realistic natural modelling effect of underestimating re-sedimentation cause this. Increasing the spatial extent eliminates the artificial effect while at the same time the realistic effect is enhanced. Both effects can be quantified and are expected to increase within natural landscapes. The modelling of landscape processes will benefit from integrating these types of results at different resolutions.

3.1 Introduction

Over the years numerous models related to landscape processes and their dynamics have been developed. These models vary in their main focus (e.g. geomorphological, hydrological) and

Based on: Schoorl, J.M., Sonneveld, M.P.W. & Veldkamp A., 2000. Three-dimensional landscape process modelling: the effect of DEM resolution. Earth Surface Processes and Landforms 25, 1025-1034.

the applied methodology (e.g. physical, empirical). Processes involved in landscape development are typically linked to certain spatial and temporal scales, which is caused by the non-linearity of landscape processes and the heterogeneity of the system (Beven, 1995), This imposes important restrictions and as a result the used focus and methodology are supposed to determine the validity of the solutions (Rodríguez-Iturbe et al., 1984). These restrictions are also referred to as scale effects and have led to interesting discussions especially in hydrological studies (e.g. Beven, 1995; Kalma and Sivapalan, 1995; Sposito, 1998).
At the core of a geomorphological model that can simulate dynamic landscape development we find the processes of erosion and sedimentation (e.g. Moore and Burch, 1986). We have to bear in mind that not all models consider the process of sedimentation or re-sedimentation. This relevance within a model can be called a scale effect and will depend on the applied spatial and temporal resolution as well as the extent (Dietrich and Montgomery, 1998). Taking into account that geomorphological processes operate at different spatial and temporal resolutions, a multi-scale modelling approach seems most appropriate to construct landscape process models. According to Beven (1995) the best approach is to start at coarser levels and follow a procedure of disaggregation. However, we strongly advocate a hierarchic multi-scale approach, because it will enable us to combine data from different scales in the calibration and validation exercises. In such an approach both scaling-up (aggregation) and scaling-down (disaggregation) enhance the integration and understanding of data and results from different resolutions. Nevertheless, we have to be sure that no new artificial scale effects are introduced by modelling landscape processes at different scales and related spatial and temporal resolutions. To avoid confusion on the meaning of scale we will restrict ourselves in this study to spatial resolution and temporal resolution (e.g. cell sizes, time steps) and spatial extent and temporal extent (e.g. total area, time span).
One of the key variables in many studies on geomorphological modelling over the last decades is the topography of the landscape represented by a Digital Elevation Model or DEM (e.g. Willgoose et al., 1991a; 1991b; Howard, 1994; Dietrich et al., 1995). As a result there exist a wide range of topographic attributes used in these models that can be computed by several techniques of terrain analysis (Moore et al., 1991). The numerical values of these attributes differ considerably with DEM resolution because of differences in representation of the landscape and the computational techniques (e.g. Quinn et al., 1991; Zhang and Montgomery, 1994; Wang and Yin, 1998; Yin and Wang, 1999). Nevertheless there is little known of the systematic effects of changing or improving resolution upon the results produced by current geomorphological models (Dietrich and Montgomery, 1998).
The objective of this chapter is to reveal and quantify the effect of DEM resolution upon modelling the processes of erosion and sedimentation, unbiased by landscape representations. To obtain comparable quantification of these effects we propose to use a simple model, capable of calculating equal amounts of erosion and sedimentation under standard conditions irrespective of DEM resolution. This simple model comprises key parameters and variables, which are easy to determine and remain valid at any resolution. Artificial DEMs are used with equal area and gradients to eliminate the effect of landscape representation. Once the effects are quantified for the model output under standard conditions we can continue the investigation on the effect of DEM resolution by changing other key parameters as flow routing and grid extent.

3.2 Methods

3.2.1 Basic concepts

This study has used a modelling approach called LAPSUS (LandscApe ProcesS modelling at mUlti dimensions and scaleS) and is based on early works of Kirkby (1971; 1978; 1986) and Foster and Meyer (1972; 1975). They assume the potential energy content of flowing water over the landscape surface as the driving force for sediment transport. Another important assumption is the use of the continuity equation for sediment movement, which states that the difference between sediment input and output equalises the net increase in storage. Assuming quasi steady state Foster and Meyer (1972; 1975) formulated down slope sediment transport continuity as:

$$-\frac{\partial z}{\partial t} = \frac{C - S}{h} \tag{3.1}$$

where z is elevation [m], t stands for [time], C is sediment transport capacity [m^2 $time^{-1}$], and S is the sediment transport rate [m^2 $time^{-1}$]. Term h under erosion conditions stands for detachment rate, while under sedimentation conditions it represents the settlement rate. To find elevation change δz over timestep δt we need to calculate the changes in the sediment transport rate δS.
These changes in the rate of transport are controlled by the transport capacity C, where an capacity excess will be filled by detachment of sediment (e.g. erosion, surface lower) and a capacity deficit will lower the amount of sediment in transport (e.g. sedimentation, surface higher). According to Foster and Meyer (1972; 1975), after integration, assuming that transport capacity and detachment or settlement capacity remain constant within one finite element, the rate of sediment in transport can be calculated as follows:

$$S = C + (S_0 - C) \cdot e^{-dx/h} \tag{3.2}$$

where the transport rate S [m^2 $time^{-1}$] over the length dx of a finite element is calculated as a function of transport capacity C [m^2 $time^{-1}$] and detachment rate or settlement rate h compared with the amount of sediment already in transport S_0 [m^2 $time^{-1}$]. Please note that S is expressed as soil volume/ unit grid width/ year. To convert to erosion or deposition rate in mass/area/year, S is divided by the grid length (dx) and multiplied by soil bulk density. Term h [m] refers to the transport capacity divided by the detachment capacity [m $time^{-1}$] (C/D) or to the transport capacity in proportion to the settlement capacity [-m $time^{-1}$] (C/T). Implementation of Eq. 3.2 will need expressions for transport capacity C, detachment capacity D and settlement capacity T. These capacities are calculated in this study as functions of discharge and slope (i.e. Kirkby, 1971; 1980; 1986; Willgoose, 1991a; 1991b; Montgomery and Foufoula-Georgiou, 1993) which gives:

$$C = \alpha \cdot Q^m \cdot \Lambda^n \tag{3.3}$$

where C is calculated as a function of discharge Q [m^2 $time^{-1}$] and slope tangent ($\delta z/\delta x$) Λ [-], m and n are constants (dummy variable α corrects the units). Assuming, amongst others, that

detachment and settlement capacity is proportional to a certain shear and that the drag coefficient is constant, we obtain:

$$D = K_{es} \cdot Q \cdot \Lambda \tag{3.4}$$

$$T = P_{es} \cdot Q \cdot \Lambda \tag{3.5}$$

where K_{es} is a lumped surface factor [m^{-1}] indicating the erodibility of the surface and P_{es} a similar factor indicating lumped sedimentation characteristics [m^{-1}]. Note that the erosion conditions for D or sedimentation conditions for T will result in opposite signs for the change in S and as a result also δz.

3.2.2 Model structure and flow routing

LAPSUS is based on a grid structure of square cells of equal size. Each cell presents a generalised part of the landscape that can comprise several unique characteristics like altitude, soils etc. The model structure has been designed to make optimal use of the simulation of both two-dimensional as three-dimensional characteristics added to the time dimension. In this way the model considers the evaluation of capacities as a two-dimensional process since we are only using gravitational force and water flow down slope within a finite element. However for the estimation and routing of the incoming and outgoing water and sediment fluxes, the model evaluates the results of surrounding grid cells within the whole three-dimensional landscape. The finite element methodology implies variable length but a unit width at different resolutions for each element.

We will both compare the effects of steepest descent and multiple flow directions for the routing of the runoff that will provide the estimates of Q in Eqs. 3.3 to 3.5. For many years the method of steepest descent has been widely used in standard hydrological and geomorphological models and GIS packages (e.g. Moore et al., 1991; Willgoose and Riley, 1998). Calculation of multiple flow directions is proposed as dividing the flow from a cell towards all down slope neighbours, using a certain weighting factor for each fraction (Freeman, 1991; Quinn et al., 1991; Holmgren, 1994) which leads to the following:

$$f_i = \frac{(\Lambda)_i^p}{\sum_{j=1}^{\max 8} (\Lambda)_j^p} \tag{3.6}$$

where fraction f_i of the amount of flow out of a cell in direction i, is equal to the difference in height or slope gradient Λ (tangent) in direction i powered by factor p, divided by the summation of Λ for all (never more than 8) down slope neighbours j powered by factor p.

3.3 Data

To simulate true effects of DEM resolution upon the processes of erosion and sedimentation we have constructed two types of artificial DEMs (Fig. 3.1). These DEMs are constructed in such a way that for each resolution we obtain a constant extent and constant slope angle. Five different spatial resolutions (1x1, 3x3, 9x9, 27x27 and 81x81 [m]) were compared for two different extents namely a hillslope and a catchment. The total amount of cells in each DEM

decreases with increasing spatial resolution, but always the spatial extent for the hillslopes amounts 6561 [m^2] compared with 78732 [m^2] for the catchments. The height differences result in slope gradients for all DEMs equal to a tangent of 0.08 (Λ in Eqs. 3.3 to 3.5).
To make sure that possible encountered effects are caused by resolution we need to create equal boundary and input conditions for every experiment. For our standard runs with a time step of a year we have used the following assumptions:

1. Fixed m (2.0) and n (2.0) exponents in Eq. 3.3 as if only wash is the dominant process (Kirkby, 1987).
2. Uniform rainfall in both amounts and intensity of 534 [mm] per year with a constant annual infiltration and evaporation of 63% (to calculate Q in Eqs. 3.3 to 3.5)
3. Uniform soil characteristics, depths and erodibility, K_{es} and P_{es} are 0.002 (Eqs. 3.4 and 3.5).
4. Exponent p of 4.0 (Eq. 3.6) for determining the fraction for the multiple flow directions (Holmgren, 1994).

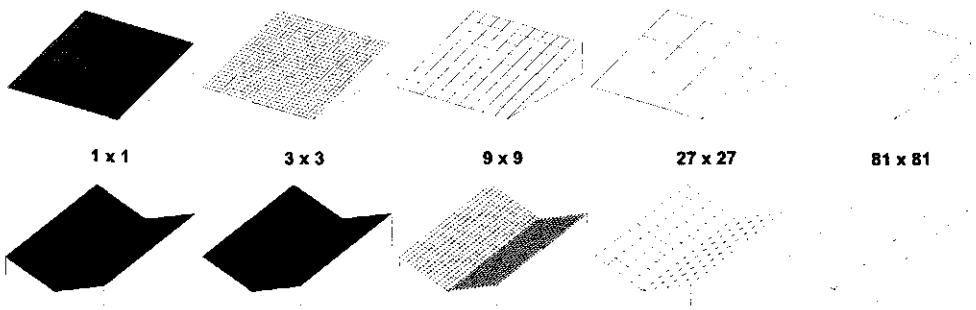

Fig. 3.1 The artificial DEMs used in this chapter at 1x1, 3x3, 9x9, 27x27 and 81x81 [m] resolution for artificial hillslopes (up) and catchments (down).

3.4 Results

Our first experiments were modelled for Hillslopes using the Steepest Descent method (HSD) for all 5 different resolutions. Resulting soil loss is given in Fig. 3.2, calculated from the sediment flux leaving the slope measured along the lower boundary. This graph shows a strong increasing soil loss with coarser resolutions. Total soil loss is almost doubled comparing the finest with the coarsest resolution with an increase of 97.5 percent. The results of applying the Multiple Flow routing upon the same straight hillslope (HMF) reveals a similar trend although the soil loss is slightly lower than the steepest descent results (lowest dotted line in Fig. 3.2). Note that our coarsest resolution (81x81 [m]) is comprised of only one single grid cell and therefore can not be modelled with multiple flow directions.

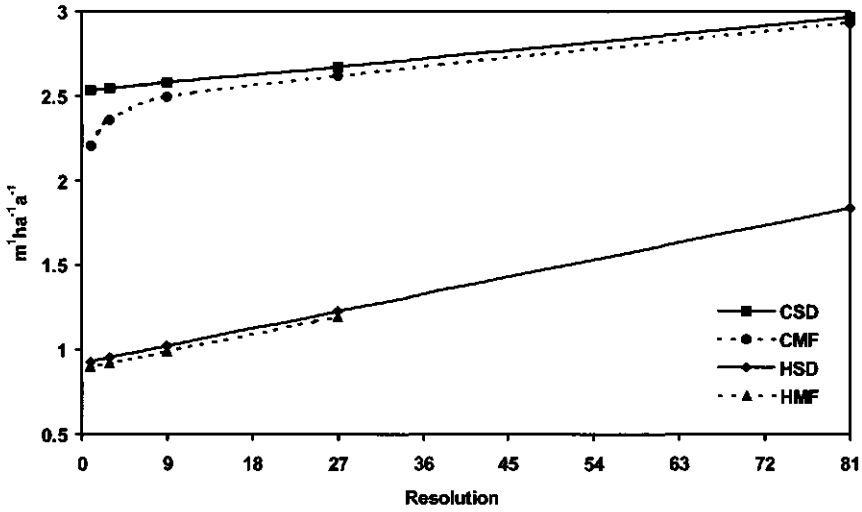

Fig. 3.2 Resulting soil loss at different resolutions for modelling Hillslopes with Steepest Descent (HSD), Hillslopes with Multiple Flow directions (HMF), Catchment with Steepest Descent (CSD) and Catchment with Multiple Flow directions (CMF).

These same experiments were repeated for the different catchment resolutions (examples in Fig. 3.1). The results given in Fig. 3.2 for Catchments with Steepest Descent (CSD) show again an increasing amount of soil leaving the system with coarser resolution. However, this increase of only 17 percent is less strong as on the hillslopes. For the Catchments with Multiple Flow directions (CMF) the results in Fig. 3.2 still show increasing soil losses with coarser resolution, but according to a logarithmic type of curve with the biggest differences at the finer resolutions. For all resolutions CMF shows lower amounts of soil loss than CSD. The relative increase of 33 percent for CMF from finest to coarsest resolution is less than for HSD but is more than CSD.

Differences between HSD and HMF are shown in Fig. 3.3 and range from a 3.3 percent decrease for the finest resolution (1x1 [m]) to 2.2 percent decrease for the coarsest resolution (27x27 [m]). The differences in Fig. 3.3 between CSD and CMF range from 13 percent decrease for the finest resolution to 0.95 percent decrease for the coarsest resolution (81x81 [m]). Total amounts of (re-)sedimentation for slopes and catchments are given in Fig. 3.4. Only the line of CMF is visible since during the hillslope and CSD simulations not a single re-sedimentation event was calculated.

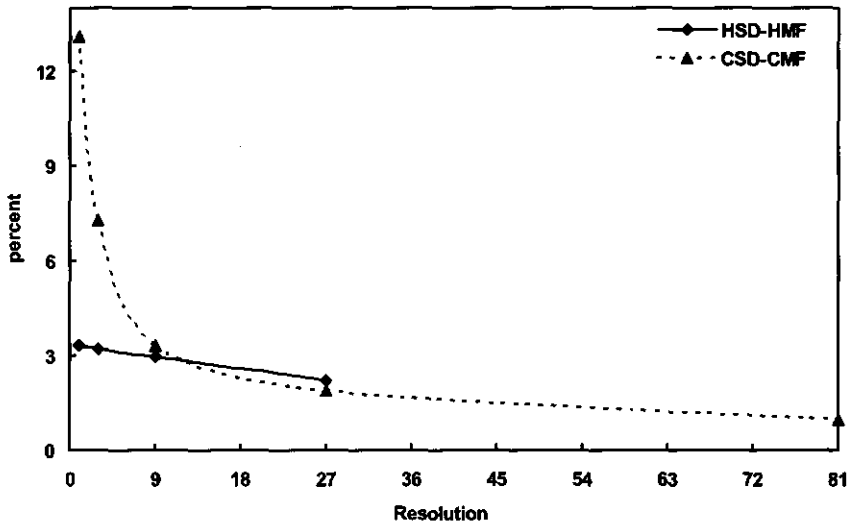

Fig. 3.3 Comparison of hillslope and catchment cases as percent decrease comparing Steepest Descent and Multiple Flow directions for Hillslopes (HSD-HMF) and Catchments (CSD-CMF)

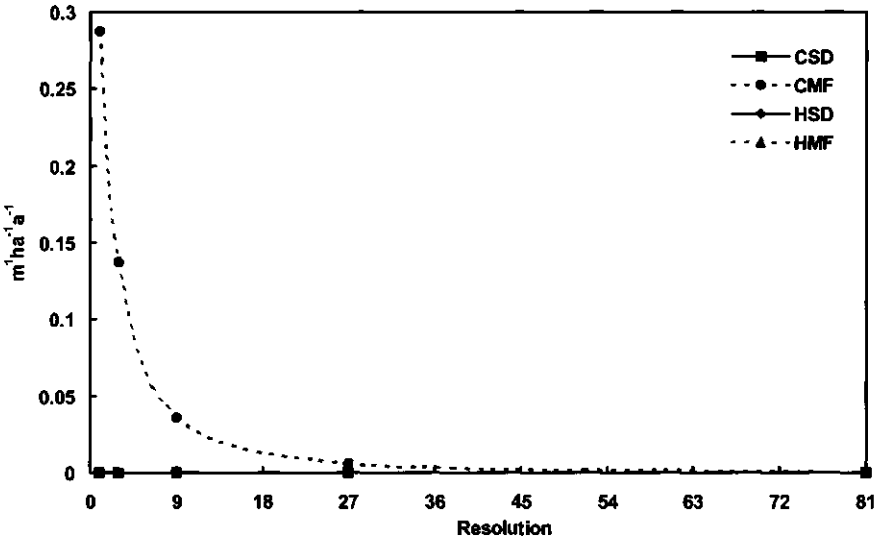

Fig. 3.4 Simulated re-sedimentation for the hillslopes and catchments.

3.5 Discussion

In general we have to consider the simplicity of this single process modelling approach as a tool to reveal the effects of changing resolutions. We are aware of the fact that more sophisticated models exist, especially on finer temporal resolutions. These models often include separate procedures for example for detachment by raindrops, interception, infiltration, soil surface conditions etc. However, by excluding or considering constant these kinds of components we create the boundary conditions for this experimental study. Furthermore, the artificial DEMs in this study should exclude landscape representation effects as changing slope angles and drainage areas with different resolutions (e.g. Zhang and Montgomery, 1994; Garbrecht and Martz,1994; Braun et al., 1997). It was expected with one single formula and all parameters constant, except for resolution, that we would find equal amounts of erosion and re-sedimentation for all hillslope simulations and equal amounts for all catchment simulations.

3.5.1 Resolution and erosion predictions

In contradiction to what we had expected the general trend for all simulations (HSD, HMF, CSD and CMF) is an increase of erosion with coarser resolutions. Already the first experiments with HSD revealed the strongest effects. A logical explanation would be local re-sedimentation, but during HSD simulation there was not one single event of re-sedimentation calculated (Fig. 3.4). Since all parameters were exactly the same, the answers had to be found in the calculated capacities of transport and detachment. In fact the major difference is found in the number of calculations in the downslope direction namely 81 for the 1x1 [m] resolution as opposed to only 1 for the 81x81 [m] resolution. In this downslope direction the only variable in our experiments was the discharge, as a function of the total surface of each single cell and the resolution dx length in Eq. 3.2. As a result also the capacities of transport and detachment both vary along the hillslope and especially in comparison with the different resolutions.

This model behaviour has been tested for HSD simulations by varying the K_{es} factor. High K_{es} values indicate transport limited conditions and low K_{es} values indicate detachment limited conditions. Fig. 3.5a shows the model behaviour for the different resolutions. Under detachment limited conditions, K_{es} lower than 0.01, the parallel lines for different resolutions indicate a systematic overestimation of sediment transport and resulting soil loss. Using the number of calculations compared with resolution dx implies the following correction:

$$\mathrm{Corr} = \frac{\mathrm{n} \cdot \mathrm{dx} + \mathrm{dx}}{n \cdot dx} \tag{3.7}$$

where n is the number of calculations or steps down slope and dx resolution length. Thus, for detachment limited conditions we actually correct one extra resolution length. The suggested correction factor will have to be adapted for those K_{es} values larger than 0.01 in the transition towards transport limited erosion (see Fig. 3.5b). When the hillslope is sufficiently long and the resolution sufficiently fine this correction becomes virtually negligible, since the number of calculations n is one of the main variables in Eq. 3.7.

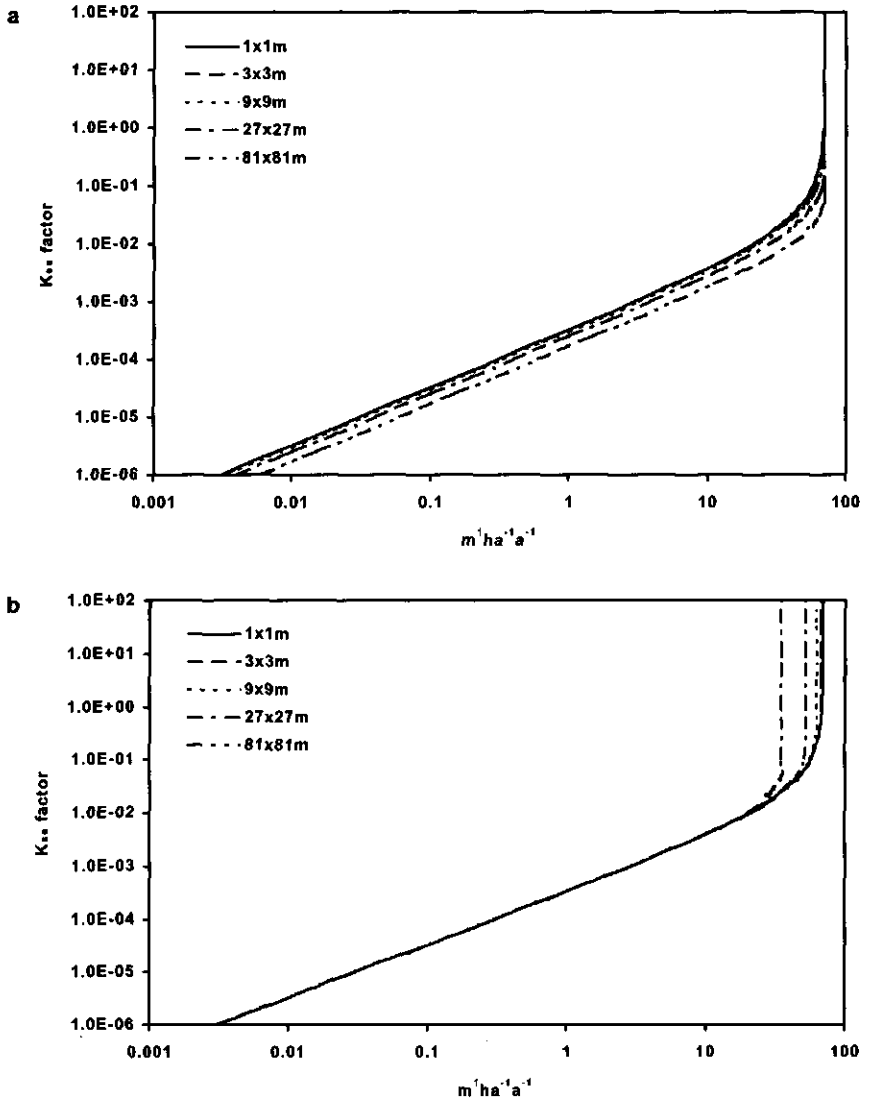

Fig. 3.5 Total soil loss for the five resolutions on HSD as a function of a varying K_{es} factor for (a) original data and (b) after applying the correction factor.

Thus, with increasing our spatial extent the difference caused by the *dx* resolution length will decrease. This is clearly demonstrated when we increase our spatial extent from our hillslopes to our catchments. The resolution effect decreases from 97.5 percent (HSD case) to 17 percent in the CSD case. As far as the absolute differences are concerned it is obvious that the

hillslope length is more dominant than surface area. Some examples are shown in Table 3.1, where in spite of a constant slope gradient and extent (drainage area), the sediment fluxes increase with increasing slope length and grid size. Thus, the absolute increase of total soil loss comparing HSD with CSD is the result of the increased extent and the increased slope length from 81 [m] (hillslope) to 121,5 [m] (catchment).

Table 3.1 Examples of the influence of effective slope length upon sediment fluxes modelled with steepest descent for the CSD case and two hillslopes (H243 and H324).

	Extent	Slope Length	Output per resolution [m ha^{-1}a^{-1}]				
	[m^2]	[m]	1x1	3x3	9x9	27x27	81x81
CSD	78732	121.5	2.53	2.54	2.58	2.67	2.97
H243	78732	243	2.77	2.79	2.86	3.06	3.68
H324	78732	324	3.69	3.71	3.78	3.98	4.59

Variation of the K_{es} factor defines the amount of the sediment detached in the simulated area, which is equal to the amount of net erosion or total soil loss (Fig. 3.4). In our basic approach the K_{es} factor is the only knob for calibrating real-world situations. For example using different K_{es} factors for different soils or lithology or as a function of land use (Dietrich et al., 1995). We have to keep in mind however that wherever the K_{es} factor is lumping many surface properties, the factor is also subjected to influences of changes in resolution, gradient of slope and discharges. This explains the wide range and variety of K_{es} factors found around the world from USLE type approaches on experimental plots (Torri et al., 1997). The more spatial or temporal resolution sensitive parameters are incorporated, the more calibration steps are needed. This is reported for a comparable hydrological example of intensive parameter calibration for different case studies using the TOPMODEL approach (Beven, 1997).

3.5.2 Resolution and flow routing

Differences found between HSD and HMF are a direct result of implementing multiple flow directions. This way of routing facilitates the mimicking of diverging characteristics of water flow over surfaces (Quinn et al., 1991). Every grid cell will divide its flow among his lower neighbours. In doing so the former steepest descent neighbour will receive less water, which will lower the calculated transport capacity and detachment capacity in that steepest direction. Convexities and concavities in the shape of the sloping surface enhance this effect (Holmgren, 1994). Nevertheless, in spite of our artificial straight slope, the effect is still noticeable in Fig. 3.2. Thus, the effect of multiple flow routing will decrease with coarser resolutions. This is a different effect than that of enhancing re-sedimentation, which is discussed in the next section.

3.5.3 Resolution and re-sedimentation predictions

Of all experiments the CMF case showed the most drastic differences in total soil loss as a result of changing resolutions and flow routing. Local re-sedimentation in the catchment accounts for an exponential decrease in soil loss with finer resolutions (see Fig. 3.4). The multiple flow direction routing is directly responsible for these re-sedimentation events. Finer resolutions show to be more affected by this process because there are more different ways of routing possible. In this case the effect is especially enhanced in the headwater positions in the catchments, where different water flow paths will meet. These different flows are all

partly filled with sediment and especially in these positions a new equilibrium will have to be formed depending on the local discharge and slope gradient of this channel. If, in these positions, there is an excess of sediment in transport as a function of the discharge and slope gradient the sediment will be deposited. Moore and Burch (1986), describing differences between final sediment output and internal erosion and deposition events reported a similar effect.

3.6 Concluding remarks

This experimental study examined the effects of DEM resolution upon modelling the processes of erosion and sedimentation in the context of landscape development. Five different resolutions were tested on a 6561 [m^2] hillslope and on a 78732 [m^2] catchment. Instead of predicting only two amounts of erosion for these two different extents, we have found different outcomes for all simulations. As a result twenty soil loss rates have been calculated from similar areas with completely identical model procedures, boundaries, and parameters.

We clearly saw that changing the DEM resolution influenced the outcomes of our simple landscape process model. In general there are two different effects we have observed in our scaling experiment of coarsening resolutions. First, the over prediction of erosion, a resolution and extent related scale effect caused by K_{es} dependent artificial calculation errors. Secondly, the underestimation of re-sedimentation, a more realistic and natural scale effect related to erosion rate and re-sedimentation events that are more plausible to occur in a fine grid using multiple flow routing. The latter is therefore a more realistic representation of the real world processes than steepest decent and coarse grids.

As far as the first more artificial effect is concerned a systematic correction can be necessary, depending on the K_{es} magnitude and total extent of the DEM. This is especially relevant for lower K_{es} values used in modelling detachment limited hillslope processes, where the effective length over the hillslope where detachment takes place becomes the dominant factor. However, higher K_{es} values do not require specific correction in this modelling approach. Because under transport limited conditions the only dominant factor becomes the transport capacity as function of discharge Q and slope gradient.

The second realistic effect of underestimating re-sedimentation can be considered as one of the main scale effects found in erosion studies. Many examples are known of overestimation of erosion rates in coarse resolution studies and the introduction of sediment delivery ratios. A tempting solution for this scale effect can be tested with our approach. Namely to quantify re-sedimentation rates for representative fine resolution areas and to integrate these results at coarser resolutions.

Finally we can conclude that it is possible to model landscape processes within a multi-scale framework by changing the DEM resolutions. It is important however, that the extent of the landscape and its relief characteristics are realistically represented by the used DEM. By using information of for example re-sedimentation rates from finer resolutions we can simulate more realistic landscape development for larger areas and coarser resolutions.

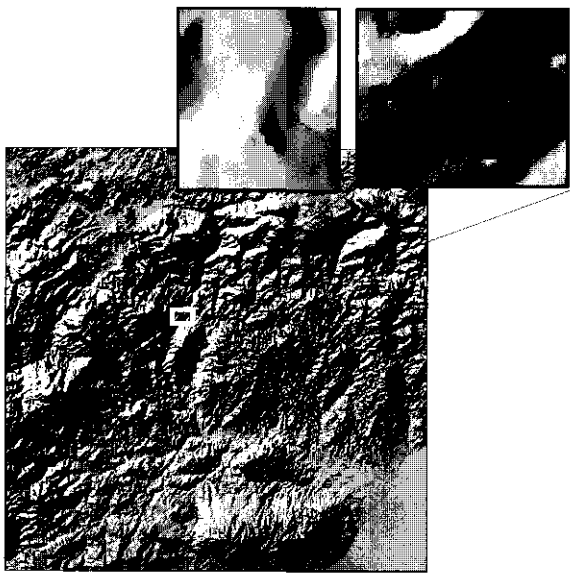

Chapter 4

Monitoring Long Term Soil Redistribution

This chapter investigates the possibility within the research area to monitor actual soil redistribution rates in the field. Consequently concentrations in the soil of anthropogenic and natural radionuclides have been investigated to assess the applicability of the ^{137}Cs technique in an area of typical Mediterranean steep slopes. This technique can be used to estimate net soil redistribution rates but its potentials in areas with shallow and stony soils on hard rock lithology have not been evaluated so far. In this chapter the radionuclide concentrations are discussed in relation to other soil properties, lithology and slope position in a Mediterranean environment. Both natural Potassium-40 (^{40}K), Uranium-238 (^{238}U), Thorium-232 (^{232}Th) and anthropogenic Caesium-137 (^{137}Cs) radionuclides have been determined in samples taken along slope transects on soils developed on serpentinite and gneiss lithologies. In addition to the radionuclide concentrations also parameters such as slope position, slope angle, aspect, soil depth, surface stone cover, moss, litter, vegetation cover, soil crust, stone content and bulk density have been estimated.
All natural radionuclides ^{40}K, ^{238}U, ^{232}Th show significant higher concentrations in the gneiss than in the serpentinite soils. As opposed to the ^{137}Cs concentration, which is found significantly higher in the serpentinite soils, for the reference profiles probably because of the difference in clay mineralogy. The exponential decreasing depth distribution of ^{137}Cs and its homogeneous spatial distribution emphasise the applicability of the ^{137}Cs technique in this ecosystem. The ^{137}Cs inventory and concentration are in agreement with the expectations according to the soil erosion and degradation indicators measured. Surfaces with erosion or degradation signs (higher bulk density, shallow soils or surface crust development) show lower ^{137}Cs concentrations and protected surfaces by vegetation show higher ^{137}Cs inventories. The distribution of ^{137}Cs along the slopes can be explained to a high extend within existing conceptual models. The gneiss slopes show a zonation of four to five areas of differential erosion/ accumulation processes corresponding with more regularised slopes. The

---

Based on: Schoorl, J.M., Boix Fayos, C., De Meijer, R.J., Van der Graaf, E.R. & Veldkamp, A., 2002. The ^{137}Cs technique on steep Mediterranean slopes (Part I): analysing the effects of lithology and slope position.

serpentinites show more erosion areas with less accumulation downslope as an example of a more unstable slope type.

4.1 Introduction

Over the past few decades the so-called ^{137}Cs technique has been applied in many environments to determine net soil redistribution rates (e.g. Martz and de Jong, 1987; Ritchie and McHenry, 1990; Walling and Quine, 1990). This technique overcomes many of the common problems encountered in monitoring erosion dynamics at field and landscape scale and is applicable for medium long term (30 to 40 years) soil redistribution estimates (e.g. Walling and Quine, 1992; Chappell et al., 1998). In this technique the anthropogenic radionuclide Caesium-137 (^{137}Cs) is used as a sediment tracer from upland erosion studies, to catchment sediment budgets, to depositional areas in colluvial positions, river terraces, lakes and deltas (e.g. Ritchie and McHenry, 1990; Walling and Quine, 1991).
Important assumptions of the ^{137}Cs technique are: (i) a spatially uniform deposition within a climatic zone and (ii) immediate fixation to the clay fraction, which results in redistribution associated with soil particles (e.g. Ritchie and McHenry, 1990; Walling and Quine, 1990; Chappell, 1999). Before the measured radionuclide concentrations can be related to quantitative rates of erosion or deposition, these assumptions of the ^{137}Cs technique have to be evaluated. For example the exponential decreasing depth distribution within a undisturbed reference soil profile can be influenced by original fallout concentrations and rainfall distribution, soil properties (clay mineralogy, pH, organic matter content) and bioturbation (e.g. Livens and Loveland, 1988; Isaksson and Erlandsson, 1998; Baeza et al, 2001; Tyler et al., 2001). In case of sloping cultivated areas, in addition to overland flow driven soil redistribution, profile distributions will be influenced by tillage practises (e.g. Zhang et al., 1998; Quine, 1999).
Dominant factors in the context of a soil are the climatology, lithology and the landscape. Highly inter-related they determine the weathering of parent material, soil formation, soil gain or soil loss and so on. These are also the most important parameters in the redistribution of the soil associated ^{137}Cs. So far only a few studies address the issue of the soil context and lithology (Pennock et al., 1995; Kachanoski and Carter, 1999). Furthermore, in the analysing procedures of soil samples both anthropogenic and natural radionuclides can be measured. However, only a few authors take these natural radionuclides into consideration despite of their potential to further explain radionuclide profile distribution (VandenBygaart et al., 1999). Moreover many interesting studies investigating the amounts of radionuclides in the environment tend to underestimate the context of the soil and landscape (Karahan and Bayulken, 2000; Rubio Montero and Martín Sánchęz, 2001). This soil context may therefore become highly significant in Mediterranean environments, for example the role of soil texture, soil depth and parent material on available quantities of both anthropogenic and natural radionuclides (Kiss et al., 1988).
Especially for the Mediterranean area the limited soil depth, stoniness, steep dissected topography and different parent materials could hamper a successful implication of the ^{137}Cs technique (Chappell, 1999). Studies using the ^{137}Cs technique in Mediterranean ecosystems mainly focus on the estimation of net soil loss and were carried out on intermediate slopes (Navas and Walling, 1992; Quine et al., 1994; Navas et al., 1997; Porto et al., 2001; Kosmas et al., 2001). It remains unclear if this technique can be applied to more extreme conditions

very frequently found in Mediterranean landscapes, such as shallow soils, high stone content and steep slopes (> 20-35°).
This chapter summarises the first part of an investigation where the ^{137}Cs technique was used to model soil redistribution in a Mediterranean landscape. This first part focuses on the feasibility of the technique and the exploration of the ^{137}Cs data, their analysis and significance in relation to important environmental factors such as soil context, lithology and slope morphology. The second part (Chapter 5) investigates the erosion rates and soil redistribution patterns derived from ^{137}Cs data in relation to the calibration of a landscape evolution model.
Thus, the objectives of this chapter are (i) to test the applicability of the ^{137}Cs technique on steep slopes and shallow stony soils under Mediterranean environmental conditions, (ii) to verify the influence of lithology on both anthropogenic and natural radionuclides and, finally, (iii) to explore the relationships between ^{137}Cs and soil properties, indicators of soil degradation and slope position.

4.2 Materials and methods

4.2.1 Study area

For the detailed slope to catchment scale study of this chapter (see also Fig. 1.2), two sample areas have been chosen comprising two different lithologies in an area just north of Álora on the slopes of the Sierra de Aguas (Fig. 4.1). As mentioned in previous chapters this region has a summer dry Mediterranean climate (Csa) with decreasing precipitation from west to east. The area around Álora shows a mean annual temperature of 17.5°C and receives a mean yearly rainfall of 534 [mm], mainly from October to April.

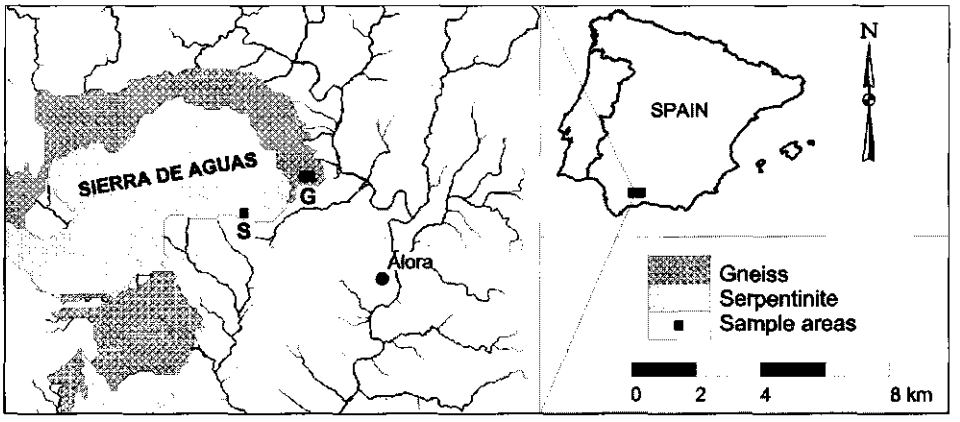

Fig. 4.1 Sample area location in the research area, the sampled lithologies in the Sierra de Aguas are gneiss (G) and serpentinite (S).

The first sample area (G in Fig. 4.1) is located in a small catchment on garnet gneiss bedrock, while the second sample area (S in Fig. 4.1) is a typical ultramaffic peridotite/ serpentinite hilltop. The lithological transition between these parent materials is rather sharp (within several metres). Both lithologies stem from the Alpine Orogeny in the Tertiary, when fluid mantle material, forming a peridotite massif, intruded into the slates and schists deposits in this area (Sanz de Galdeano, 1990). The garnet gneiss was formed by contact metamorphosis of these slates and schists. Furthermore water uptake converted large parts of the peridotite into serpentinite (Acosta et al., 1997).
Both lithologies show a steep dissected topography with general slope angles from 25 to 35 degrees. Soils in the studied areas range from Leptosols, Regosols to Cambisols (FAO, 1988; Ruiz et al., 1993). In general more Leptosols are found in the serpentinite area where bare rock outcrops are also common in the steeper and unstable areas. Soil depths in the serpentinite soils range from 12 to 32 [cm]. Average stone cover on the surface is 85 [%], average gravimetric stone content is 39 [%] and average matrix bulk density is 1.2 [g cm^{-3}]. The serpentinite soils under semi-natural vegetation show silty-clay to sandy-loam textures with clays high in smectite and low in vermiculite and kaolinite. In the gneiss area soils are slightly deeper (between 17 and 56 [cm] deep) and less coarse and show clay-loam to sandy-loam textures with clays high in kaolinite and low in illite and smectite. They show an average surface stone cover of 36 [%], a stone content of 19 [%] and an average matrix bulk density of 1.6 [g cm^{-3}].

4.2.2 Sampling strategy

In both sample areas 3 reference profiles were selected (SAR 1 to 3 and GR 1 to 3). All reference sites were located on isolated hilltops, in an area of no erosion (Table 4.1, Fig. 4.2). The topography of the area together with human factors complicate the selection of reference locations. Therefore, it was considered necessary to locate more than one reference profile for each lithology to assure the representativeness of the reference data. These profiles allow the study of the undisturbed profile distribution of the radionuclides. Reference profiles have been sampled following standard procedures (Walling and Quine, 1990) with a 20 [cm] diameter core sampler with depth increments of 4 [cm] until the bedrock or saprolite was reached.

Table 4.1 Details of the sampling strategy with the number of gneiss reference samples (GR), gneiss bulk samples (GCB), serpentinite reference samples (SAR) and serpentinite bulk samples (SAB).

	Volume	Surface	Gneiss		Serpentinite	
	[cm^3]	[cm^2]	Sites	Samples[b]	Sites	Samples[b]
Reference profiles	1256.6	314.2	3	22 (GR)	3	16 (SAR)
Bulk transects	[a]	50.3	4	26 (GCB)	4	20 (SAB)
Total			7	48	7	36

[a] variable volumes since depths have been sampled until bedrock or saprolite
[b] sample coding used in the text given between brackets

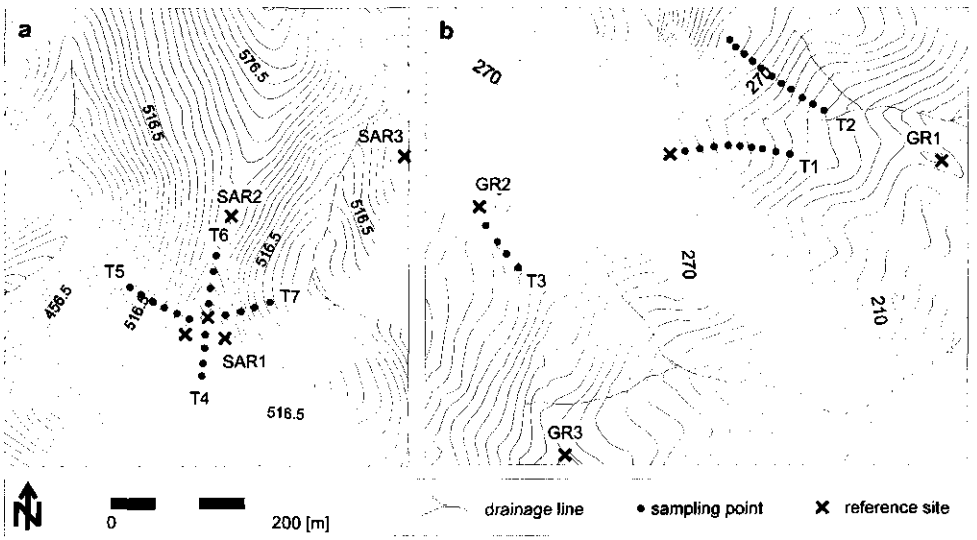

Fig. 4.2 DEM of the sample areas with a contour line interval of 5 [m] and transect locations in the Sierra de Aguas just north of Álora for a) serpentinite slope transects (SAB) T4 to T7 and references profiles SAR 1 to 3 and b) on gneiss slope transects (GCB) T1 to T3 and reference profiles GR 1 to 3.

Furthermore in each sample area series of bulk samples along slopes were taken with a 8 [cm] diameter core sampler of 45 [cm] length, until the bedrock or 45 [cm] soil depth was reached (SAB and GCB samples). These bulk samples were taken in catenas directed downslope with equal slope length increments. In some of these catenas also crest and upslope areas have been sampled, which can be used also as a reference inventory. In the field a description of the soil surface was made at each sampling point including: slope angle, slope position, aspect, soil depth, vegetation cover, surface stone cover, position and average size of the stones, rock outcrops, moss cover, lichens and the presence and thickness of soil crust. In the laboratory after sieving and weighting also the stone content of the bulk samples (stoniness), the percentage of soil matrix, and the bulk density of the soil with and without stones was determined for each sampling point. In total 46 bulk samples and 6 reference profiles with 38 samples at different depths were taken (see Table 4.1).

To determine the radionuclides concentration samples were air-dried, hand disaggregated and sieved through a 2 [mm] mesh. Thereafter the samples were sealed and placed in 1 [dm^3] Marinelli beakers and stored for at least three weeks to obtain approximate secular equilibrium between ^{226}Ra and ^{222}Rn. The samples were analysed on a Hyper-Pure Germanium gamma-ray detector in a low background setup. Activities of ^{238}U were determined from the decay of ^{214}Pb (295 and 352 [keV] gamma-rays) and ^{214}Bi (609, 1120 and 1764 [keV] gamma-rays). ^{232}Th activity was calculated from the intensity of gamma-rays from the decay products ^{218}Tl, ^{212}Pb, ^{212}Bi and ^{228}Ac. For the ^{40}K and ^{137}Cs activity the gamma-rays of 1461 [keV] and 662 [keV] were used, respectively. All activities were corrected for background radiation and self-absorption. Typical counting times for gamma

emission were between $10^4 - 10^5$ [s], with mean analytical precision decreasing rapidly with minor quantities.
As indicators of the anthropogenic radionuclide ^{137}Cs, concentration within the sampled soil [Bq kg^{-1}] and inventory activity of the sampled surface [mBq cm^{-2}] have been used. The concentration gives a very good indication of the degree of absorption and immobilisation of the radionuclide by the soil particles. The inventory takes into account the area and the bulk density of the soil, thus incorporating the structure of the soil body into the indicator.

4.2.3 Data analysis

The data were analysed with three different statistical approaches. Consequently, the potential relationships between the measured radionuclides (both concentration activity and inventory surface activity), soil and landscape properties, soil cover characteristics and slope position were investigated.
Straight forward *Correlation matrixes* were calculated between the measured radionuclides (concentration and inventory activity) and other soil properties (percentage of stone content, soil bulk density with and without stones and soil depth), soil cover characteristics (percentage of vegetation cover, stone cover, moss, litter and crust) and some characteristic of the sampling position (morphological position on the slope, expected ^{137}Cs content according to the slope position, aspect and slope angle). Some of these variables have been occasionally used as indicators of soil erosion and degradation processes (Boix Fayos et al., 2001; Rubio and Bochet, 1998). A measure of the association between these indicators helps to understand the relationships between soil characteristics and soil movement.
Principal Component Analysis was used to reorganise the data set along a new data set of independent orthogonal axes and identifying groups of related variables. The variables used as input for this analysis have to be un-correlated, so in that sense some variables from the original data matrix used for other statistical analysis (correlation matrix for instance) could not be used in this analysis. Furthermore the Varimax normalised rotation was applied to normalise the factor loadings (raw factor loadings divided by the square roots of the respective communalities). This rotation is aimed at maximising the variances in the columns of the matrix of normalised factor loadings. The Kaiser criterion was applied to select the number of factors, only factors with eigenvalues higher than 1 were retained.
Finally a *Cluster analysis* was carried out to identify diagnostic groups within the set of samples by a simple classification method. The joining or tree clustering method uses the dissimilarities or distances between objects when forming the clusters. These distances can be based on a single dimension or multiple dimensions. In this case the Euclidean distance was used, which is the geometric distance in the multidimensional space.
The linkage or amalgamation rule is based in Ward's method. This method is distinct from all other methods because it uses an analysis of variance approach to evaluate the distances between clusters. In short, this method attempts to minimise the Sum of Squares (SS) of any two (hypothetical) clusters that can be formed at each step.

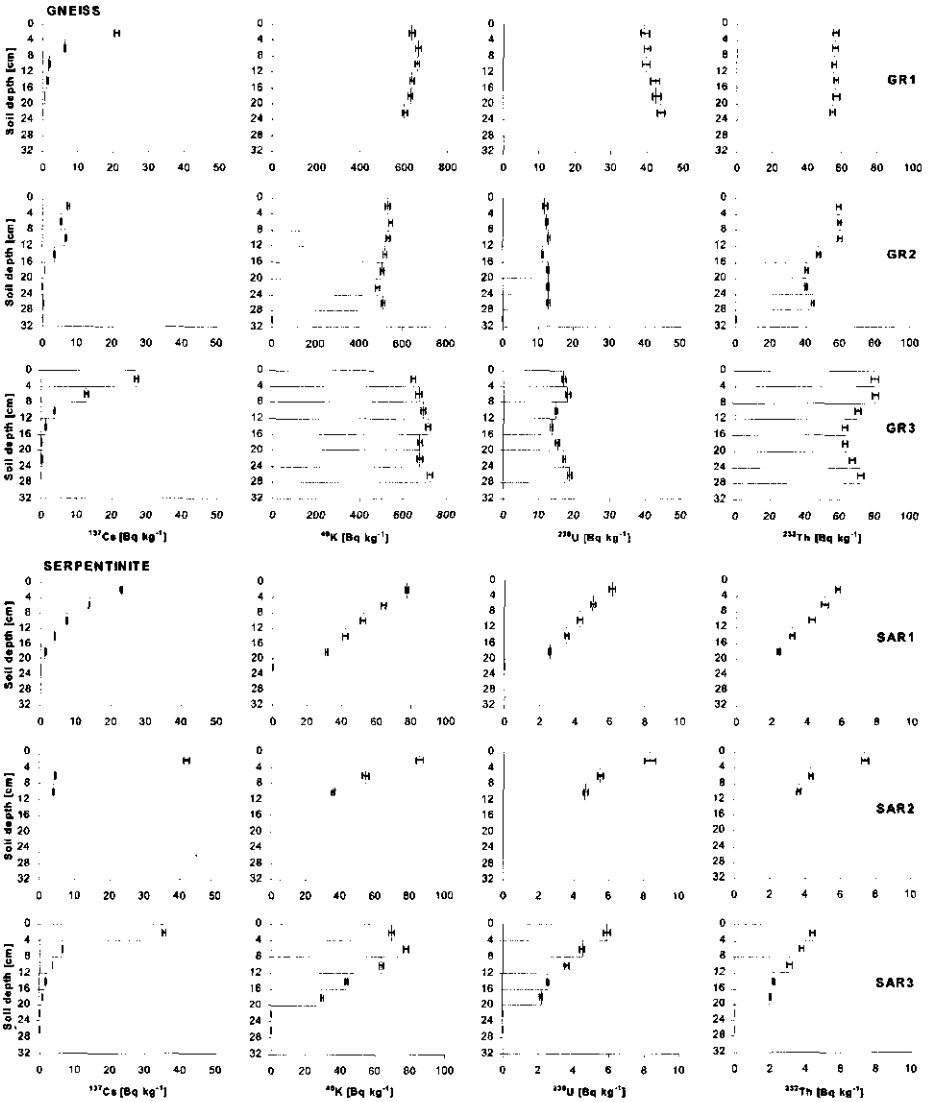

Fig. 4.3 Radionuclide concentrations for the six reference profiles with from left to right ^{137}Cs, ^{40}K, ^{238}U and ^{232}Th and from top to bottom the gneiss profiles GR1, GR2 and GR3 and the serpentinite profiles SAR1, SAR2 and SAR3. Error bars indicate measurement precision.

4.3 Results and discussion

4.3.1 Influence of lithology on ^{137}Cs content and natural radionuclides

In Fig. 4.3 the radionuclide concentration profiles are given for all reference locations. In general the concentrations of the anthropogenic ^{137}Cs decreases rapidly with depth as generally expected. Below a depth of 28 [cm] into the soil no significant ^{137}Cs concentrations were found. Typically 90 [%] of all ^{137}Cs can be found in the first 12 [cm] of soil. Profile GR2 deviates from the other reference locations by the absence of a surface ^{137}Cs peak.

It can be noticed that at the surface the ^{137}Cs concentrations at the serpentinites are somewhat higher than at the gneiss locations. Consequently, calculating and fitting a exponential curve through the data from both lithologies could result in slightly different parameters. A possible reason for this could be that gneiss soils are rich in kaolin clay that is reported to have a very low level of adsorption (Livens and Loveland, 1988). This can be seen in the lower concentration of ^{137}Cs in the gneiss soils compared to the serpentinite soils where kaolin minerals are present in much lower concentrations. However, the depth decreasing distribution pattern of the ^{137}Cs concentrations in gneiss and serpentinite are similar (Fig. 4.3). In addition, comparing total mean values for the reference profiles on both lithologies the results are statistically similar. This agreement supports the hypothesis of a homogeneous surface deposition of ^{137}Cs and strengthens the assumption that ^{137}Cs can be used for erosion and redistribution of soils.

Comparing all samples Fig. 4.4 illustrates the average, standard deviation and standard error of the radionuclides measured on gneiss and serpentinite soils. In addition, a single-way ANOVA test was performed to check if there were statistical significant differences between soil properties and the radionuclide content according to the gneiss or serpentinite lithology for all samples (Table 4.2).

Table 4.2 Comparing measured radionuclides and soil characteristics between lithologies. Mean values and effects of the ANOVA test (N=52).

Variables	Gneiss[a]	Serpentinite[a]	F-test	p-level
Surface stones [%]	52.7	85.8	28.97	0.000
Moss [%]	0	8.7	3.31	0.075
Litter [%]	13.3	72.4	83.06	0.000
Stones in soil [%]	20.4	41.2	71.71	0.000
BD[b] (+ stones) [g m^{-3}]	1.6	1.4	21.61	0.000
BD[b] Matrix [g m^{-3}]	1.3	0.8	108.83	0.000
Crust [mm]	3.2	0.4	11.81	0.001
^{137}Cs [Bq kg^{-1}]	3.2	10.1	35.85	0.000
^{137}Cs [mBq cm^{-2}]	140.0	170.8	1.37	0.247
^{40}K [Bq kg^{-1}]	505.0	68.6	635.02	0.000
^{238}U [Bq kg^{-1}]	20.9	8.0	86.37	0.000
^{232}Th [Bq kg^{-1}]	56.22	6.49	448.84	0.000

[a] Average values
[b] Bulk Density

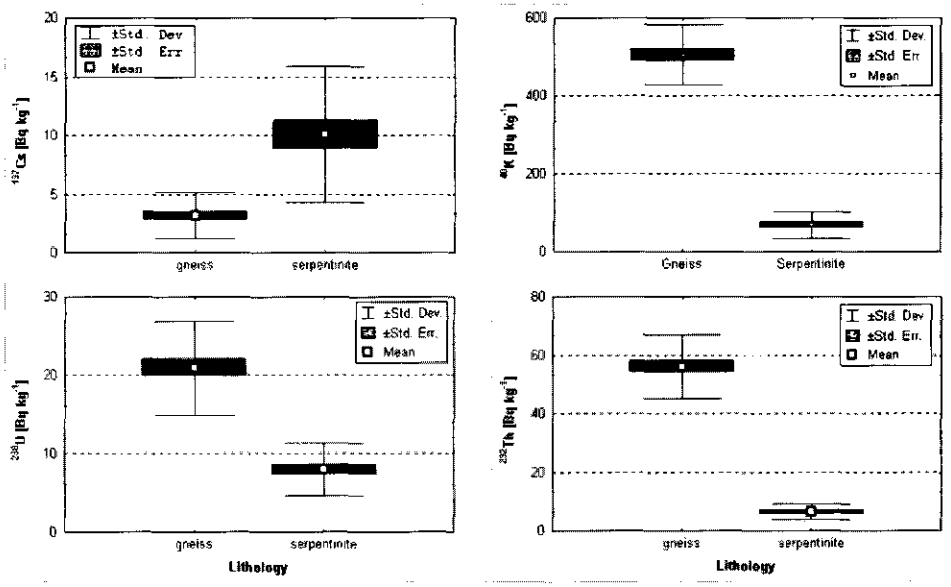

Fig. 4.4 Mean, standard deviation and standard errors of the concentrations of the radionuclides ^{137}Cs, ^{40}K, ^{238}U, ^{232}Th (N=85) on gneiss and serpentinite lithologies.

Analysing the results of Fig. 4.4 and Table 4.2, statistically significant differences between gneiss and serpentinite soils were found in all the measured variables except for ^{137}Cs inventory (surface activity). Considering the other measured parameters surface stoniness, litter, moss and stoniness into the soil are significantly higher in the serpentinite soils, while gneiss soils show higher bulk densities and more crust development. The large difference between the lithologies for the anthropogenic ^{137}Cs radionuclide concentrations for all samples in Fig 4.4, clearly indicates an increased loss of ^{137}Cs for the gneiss areas as compared to the serpentinite area. As can be observed for the natural radionuclides there are three marked differences (see Figs. 4.3 and 4.4):

1. The radionuclide concentrations in gneiss are an order of magnitude higher than in the serpentinite.
2. Whilst in gneiss the concentrations hardly vary with depth, in serpentinite the concentrations decrease with increasing depth.
3. In serpentinite the U/Th ratio is about 1, in gneiss about 0.3.

The first and third observation reflects the general difference between metamorphic and ultramaffic rocks in content of natural radionuclides and is related to their differences in geochemistry. The second observation suggests a clear relationship with soil forming factors and weathering conditions of which clay content and clay type are the dominant resultants (Livens and Loveland, 1988; VandenBygaart et al., 1999). Due to the different dominant chemical components in the parent material in the study area the gneiss soils show kaolinite

as the dominant clay mineral, while the serpentinite soils show more smectite as the dominant clay mineral (Wedepohl, 1978).
Furthermore the direct influence of lithology on the measured natural radionuclides (^{40}K, ^{238}U and ^{232}Th) is far more important than on the anthropogenic ^{137}Cs. Mean activity values in the gneiss area for the radionuclides ^{40}K, ^{238}U and ^{232}Th (614, 22 and 59 [Bq kg^{-1}] respectively) are a factor 10 higher than those for the serpentinite area (56, 5 and 4 [Bq kg^{-1}] respectively). Comparing other locations and lithologies, the soils in the gneiss area are rather high in ^{40}K and ^{232}Th compared with results from other areas around Istanbul, Turkey (342, 21 and 37 [Bq kg^{-1}] respectively, Karahan and Bayulken, 2000) and results from Saskatchewan, Canada (480, 19 and 8 [Bq kg^{-1}] respectively, Kiss et al., 1988). However, the soils in the serpentinite area are again extremely low compared to all other natural radionuclide concentrations.

4.3.2 Relations between ^{137}Cs, soil properties and soil coverage

A correlation-matrix between the total ^{137}Cs content indicators of the sample (inventory surface activity and concentration activity), the natural radionuclides concentrations and other soil characteristics measured at the same sampling points has been calculated (Table 4.3). The ^{137}Cs concentration seems to be a much more sensitive indicator than the ^{137}Cs inventory activity, showing a higher number of significant relationships with other soil characteristics. The strongest positive correlations have been found between ^{137}Cs concentration and litter, indicating stable positions, and between concentration and stoniness of the soil.

Table 4.3 Correlation matrix between measured radionuclides concentrations (anthropogenic ^{137}Cs concentration, ^{137}Cs inventory activity, natural radionuclides ^{40}K, ^{238}U and ^{232}Th) and other soil parameters (N=52).

	^{137}Cs concentration [Bq kg^{-1}]	^{137}Cs inventory [mBq cm^{-2}]	^{40}K concentration [Bq kg^{-1}]	^{238}U concentration [Bq kg^{-1}]	^{232}Th concentration [Bq kg^{-1}]
Slope position	0.13	0.00	-0.23	**-0.32***	-0.17
Expected value	-0.07	-0.04	0.00	-0.05	0.03
Slope [°]	0.02	0.02	0.05	0.18	0.05
Aspect [°]	0.12	0.12	-0.18	-0.05	-0.12
Stone cover [%]	**0.40****	0.06	**-0.60*****	**-0.32***	**-0.58*****
Vegetation [%]	0.16	**0.27***	0.04	-0.07	0.05
Moss [%]	-0.04	-0.03	-0.26	-0.18	-0.23
Soil crust [mm]	**-0.37****	-0.07	**0.30***	**0.29***	**0.41****
Litter [%]	**0.63*****	0.24	**-0.77*****	**-0.72*****	**-0.75*****
BD[a] +stones [g cm^{-3}]	**-0.35***	0.19	**0.52*****	0.23	**0.65*****
BD[a] matrix [g cm^{-3}]	**-0.59*****	-0.01	**0.76*****	**0.50*****	**0.82*****
Soil depth [cm]	**-0.47*****	0.04	**0.52*****	**0.40*****	**0.58*****
Stones [%]	**0.60*****	0.17	**-0.70*****	**-0.54*****	**-0.68*****

[a] Bulk Density
Significance levels:
*= $p<0.05$
**=$p<0.005$
***=$p<0.001$

A negative relation between ^{137}Cs concentration and soil depth appears. The concentration of ^{137}Cs decreases with increasing soil depth. Soil bulk density and soil crust are also negatively associated with ^{137}Cs concentration, indicating that in more eroded or degraded soils (high bulk density, extended soil crust) ^{137}Cs have been washed away or moved out. The only significant relationship of ^{137}Cs inventory is with the vegetation cover, a positive association between these two parameters appear. When the soil is more protected against erosion higher values of ^{137}Cs concentration or inventory appear. Natural radionuclides can be easily distinguished from the anthropogenic one because they show completely opposite relationships. In this way all the natural radionuclides show positive relationships with soil crust, bulk density and soil depth, and negative associations with stone cover, stone content and litter cover.

The concentration of ^{137}Cs is found positively associated with the stone content. With increasing stoniness of the soil, higher concentrations of ^{137}Cs can be found. Similar results have been reported also by Lu and Higgit (2000). This strong correlation is an indicator of the depth dependent and rapid adsorption of ^{137}Cs within the soil matrix and the limited vertical displacement. The same amount of ^{137}Cs was deposited as in other surfaces but when less soil matrix for adsorption is available, the amount of adsorbed ^{137}Cs per unit mass of soil matrix becomes higher.

The associations shown by the correlation matrix between some soil properties and concentration and inventory of ^{137}Cs indicate that the behaviour of ^{137}Cs is in agreement with the expectations according to the measured soil erosion and degradation indicators. Surfaces with erosion or degradation signs like higher bulk density, limiting soil depth and surface crust development show lower ^{137}Cs activities. These are exactly the signs that are frequently used as degradation indicators (Mouat et al., 1992; Stolte, 1997). As a consequence the more stable surfaces protected by vegetation or litter show higher ^{137}Cs activities, indicating areas where less erosion is expected or where sediment is trapped (Nicolau et al., 1996; López Bermúdez et al., 1998, Kosmas et al., 2000).

To better understand the variance and the contributions of the various variables, the data were subjected to a Principal Component Analysis. The results indicate that there are some combinations of variables explaining a relatively high percentage of the total variation between the samples. From the 6 extracted components 4 have been selected because they have Eigenvalues higher than 1 (Table 4.4). The rationale for this is that a component with an Eigenvalue less than 1 accounts for less of the total variance than any of the original variables. The factor loadings can be found in Table 4.5.

Table 4.4 Eigenvalues and variance from the Principal Component Analysis.

	Eigenvalue	Total variance [%]	Cumulative Eigenvalue	Cumulative variance [%]
Factor 1	6.0	40.1	6.0	40.1
Factor 2	2.2	14.7	8.2	54.9
Factor 3	1.7	11.1	9.9	65.9
Factor 4	1.3	8.6	11.2	74.6

These selected first 4 components (Tables 4.4 and 4.5) together explain about 75 [%] of the variance. The first and strongest component (explaining 40.1 [%] of the variance) is referring

to the soil structure and a lithological factor. It is mainly a combination of the stoniness in the soil, the soil bulk density and the litter cover, on one hand; and the natural radionuclides on the other hand. The second component refers to the morphological position of the soil sample on the slope because it is a combination of the slope position and the slope angle. This second component explains 14.7 [%] of the variance. The third is an erosion-degradation component because it is a combination of vegetation and crust variables and explains 11.1 [%] of the variance. The fourth component is dominated by the inventory surface activity of ^{137}Cs and explains about 8.6 [%] of the variance.

Table 4.5 Factor loadings (Varimax normalised) of the Principal Component Analysis.

	Factor 1	Factor 2	Factor 3	Factor 4
Aspect [°]	0.163	0.693	0.044	-0.154
Slope position	0.217	**-0.781**	0.291	0.032
Slope angle [°]	0.000	**0.890**	0.115	0.093
BD matrix [$gc^{1}m^{-3}$]	**-0.866**	-0.065	-0.275	-0.027
Stones [%]	**0.803**	0.152	0.365	-0.051
Soil depth [cm]	**-0.723**	0.136	-0.176	-0.359
Vegetation [%]	0.157	-0.169	**0.737**	-0.347
Stones [%]	0.690	0.272	0.054	0.343
Moss [%]	0.317	-0.305	-0.586	0.114
Litter [%]	**0.754**	-0.140	0.086	-0.417
Crust [mm]	-0.465	0.132	**-0.736**	-0.189
^{137}Cs inventory	0.082	0.133	0.164	**-0.731**
^{40}K concentration	**-0.931**	0.055	0.110	0.210
^{238}U concentration	**-0.784**	0.229	0.056	0.410
^{232}Th concentration	**-0.941**	0.013	0.071	0.050
Expl.Var	5.751	2.234	1.827	1.376
Prp.Totl	0.383	0.149	0.122	0.092

Marked loadings (bold) are >0.07

4.3.3 Soil redistribution processes and slope morphology

The variables which explain mainly the first four components of the PCA (except for the natural radionuclides) in the previous section, have been used as input to reorganise the set of samples in clusters using the Ward's classification method. These variables were: stoniness [%], bulk density of the soil matrix [g cm^{-3}], litter [%], slope position, slope angle [°], soil depth [cm], vegetation [%] and inventory of ^{137}Cs [mBq cm^{-2}]. By comparing the inventory activity of samples with the reference level for the area a qualitative estimate of soil redistribution can be made. Samples above this reference level indicate soil gain, samples under this reference level indicate soil loss.

The basic lithology classification was kept to perform a more clear analysis of the ^{137}Cs distribution along the different slope transects. Two cluster analysis were conducted, one for the samples taken on gneiss lithology and the other one for the samples taken on serpentinite lithology. Figs. 4.5 and 4.6 show the results of the classification for the gneiss and the serpentines slopes, respectively. An interpretation of the resulting groups from the cluster

classification has been performed taking into account the distribution of the samples along the slopes and the ^{137}Cs content of the samples (gain or loss).

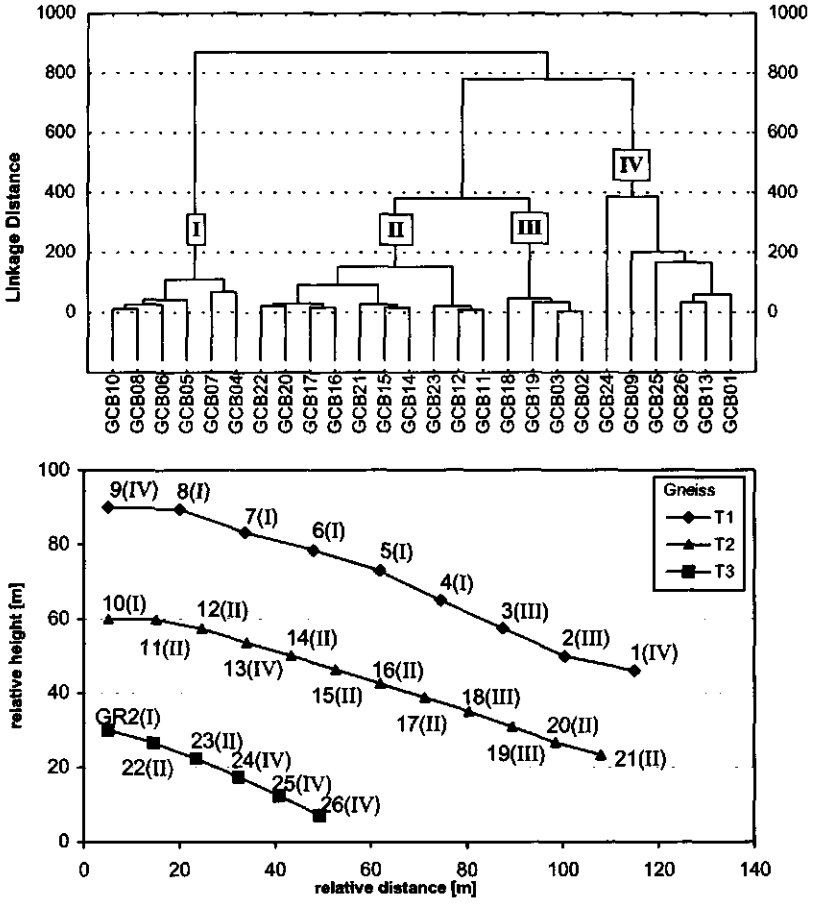

Fig. 4.5 Classification of the soil samples (cluster analysis, upper graph) and location of the samples and the identified groups on the gneiss slopes (lower graph).

For the gneiss slopes four main groups of samples can be distinguished. Without going into detail about the actual erosion or sedimentation rates, the groups have been related to positions on the slopes where processes of ^{137}Cs or soil loss (erosion) and ^{137}Cs or soil accumulation (sedimentation) take place (Fig. 4.5). Group I corresponds with soil loss areas located at the medium slope in convex areas (samples 5, 6 and 8 of transect 1; sample 10 of transect 2), there is a subgroup within group I and this is formed by samples 4 and 7 of transect 1 that correspond to slight concave slope positions where a slight soil accumulation takes place, acting as buffer areas. Group II contains areas of slight soil loss in more straight segments of the slope (samples 11, 12, 14, 15, 16, 17, 20, 21 of transect 2; samples 22 and 23

of transect 3). Group III (samples 18, 19 of transect 2; samples 3 and 2 of transect 1) contains samples located in areas with severe soil loss downslope in slight convex segments with steep slope gradients. Finally Group IV is formed by accumulation areas located downslope and not eroded surfaces upslope (sample 1 and 9 in transect 1; sample 13 in transect 2; samples 24, 25 and 26 in transect 3).

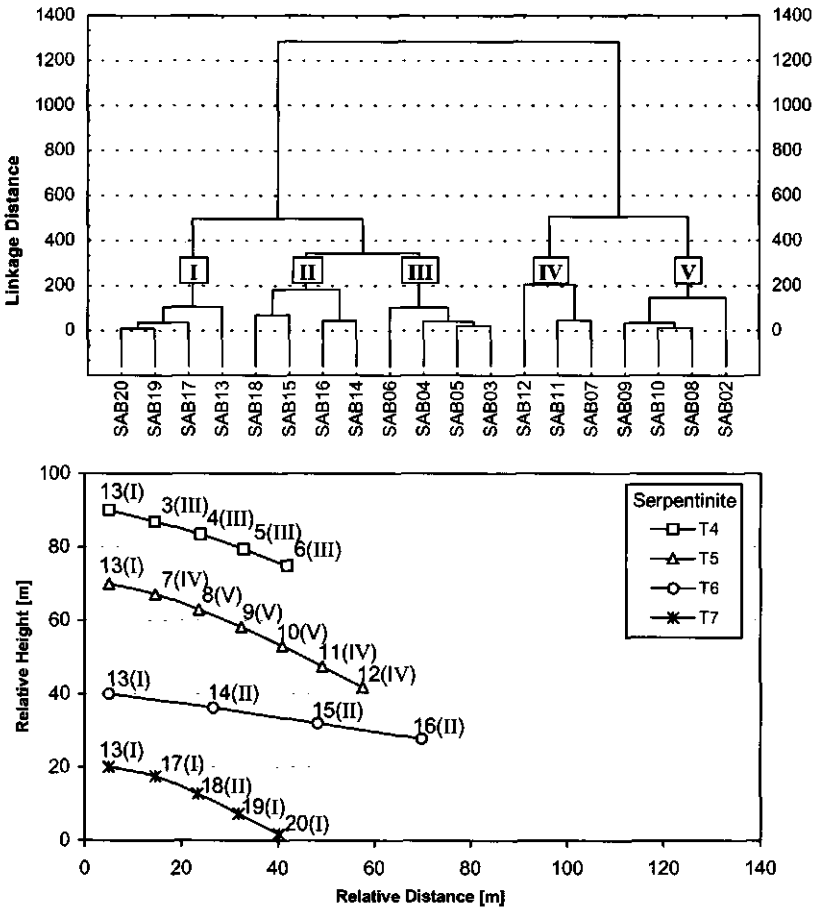

Fig. 4.6 Classification of the soil samples (cluster analysis, upper graph) and location of the samples and the identified groups on the serpentinite slopes (lower graph).

For the slopes on serpentines 5 major groups have been identified (Fig. 4.6). Group I, areas of no loss or slight accumulation of soil and ^{137}Cs, located upslope transect 7 and downslope of transect 4, respectively (samples 20, 19, 17, 13). Group II, area of slight soil loss located at medium-down slope positions of transects 6 and 7 (samples 14, 15, 16, 18). Group III, areas of medium soil loss at transect 4 mainly (samples 3, 4, 5, 6). Group IV, areas of high accumulation of soil and ^{137}Cs , downslope transect 5 and upslope before the erosion area

begins in the same transect (samples 12, 11, 7). Finally group V containing areas of severe soil ^{137}Cs loss at midslope positions of transect 5 (samples 8, 9, 10).
At the catchment scale the ^{137}Cs technique is demonstrated to be an effective method of estimating soil redistribution revealing high correlations with topographical elements. Martz and Jong (1987) found that even when topographical-morphological classes seem not to differ very much one from another, it is still possible to distinguish between depositional (main channels and upland depressions) and erosional classes (small channels, crests and level sites). At the slope scale a high variability of ^{137}Cs distribution is usually found, however the conceptual model of ^{137}Cs distribution along a hillslope, first established by Campbell et al. (1982) and later revised and adapted by Loughran et al. (1989) explains satisfactorily the theoretical processes of soil redistribution at slope scale.
The distribution of ^{137}Cs along the slopes of this study can be at a high extend explained within the conceptual model of Loughran et al. (1989), transects 1 and 2 (gneiss slopes) fit quite good this model. Other variations on this model concerning the sequence of erosion and accumulation processes are mainly due to the different lithologies and slope length. Nevertheless, the studied slopes can be classified in four types according to the present-day condition of soil redistribution, from upslope to downslope: (i) Slopes with a non-erosion area/medium erosion area: short slopes on serpentinites lithology (transects 4 and 6); (ii) Slopes with a non-erosion area/slight erosion/ accumulation area: these are short slopes both on serpentinite and gneiss lithology (transects 3 and 7); (iii) Slopes with non-erosion area/severe erosion/ high accumulation area: these are short slopes on serpentines lithology (transect 5); (iv) Slopes with non-erosion area/medium erosion area with slight accumulation processes in depressions/ a severe erosion area/ an accumulation area: this sequence appears in longer and more regularised slopes on gneiss lithology (transects 1 and 2).

4.4 Conclusions

Except for profile GR2 the soil profile depth distributions of the anthropogenic ^{137}Cs isotopes show the typical exponential decrease with soil depth, which is indicative for undisturbed reference profiles. This suggests that indeed no soil management has taken place and that there are neglectable influences of pedogenic processes and bioturbation in the reference and bulk profiles of the research area (VandenBygaart et al., 1999; Tyler et al., 2001). In contrast to the natural radionuclides the exponential decrease with depth into the soil of ^{137}Cs and its homogeneous distribution emphasises the applicability of the ^{137}Cs technique in this typical Mediterranean environment, in spite of the limited soil depth, hard rock lithology and steep slopes.
The ^{137}Cs method to estimate soil redistribution seems to have an important potential of application even for very steep Mediterranean slopes characterised by shallow and stony soils. Field sampling techniques must be adapted to the characteristics of these slopes and special attention must be given to the determination of parameters like stone content and bulk density. A limitation of the technique is the high difficulty of finding reference sampling sites due to the high level of human disturbance on the Mediterranean landscapes, nevertheless taking as many reference profiles as possible is recommended to assure representativeness.
All together, the strongly parent material dependent characteristics of the radionuclides emphasises the importance of the soil context. While studying environmental effects of fallout and radiation, including soil surveys and topographical data will enhance accuracy and

significance. Unfortunately this full soil context is sometimes underestimated in these types of environmental studies (Karahan and Bayulken, 2000; Rubio Montero and Martín Sánchez, 2001).

The results with respect to the morphological position along the hillslope of erosion and accumulation areas have been interpreted in the framework of existing conceptual models with satisfactory results. This validates the use of this technique for estimating soil redistribution in this type of environment. The relationships between anthropogenic and natural radionuclides and other soil cover characteristics have been established. Erosion and degradation symptoms at the scale of soil profile were associated with lower concentrations of ^{137}Cs.

Comparing different lithologies reveal significant differences in the concentrations of the natural radionuclides, smaller differences are found for the concentrations of the anthropogenic radionuclide. However, for the surface activity of ^{137}Cs no significant differences have been found. The source of parent material and therefore different soil forming factors, clay mineralogy and type of weathering are marking the difference in the natural radionuclides. The lack of significant difference in the inventory surface activity of ^{137}Cs indicates homogeneous deposition over the area, justifying the applicability of the ^{137}Cs technique to estimate soil redistribution in this Mediterranean environment.

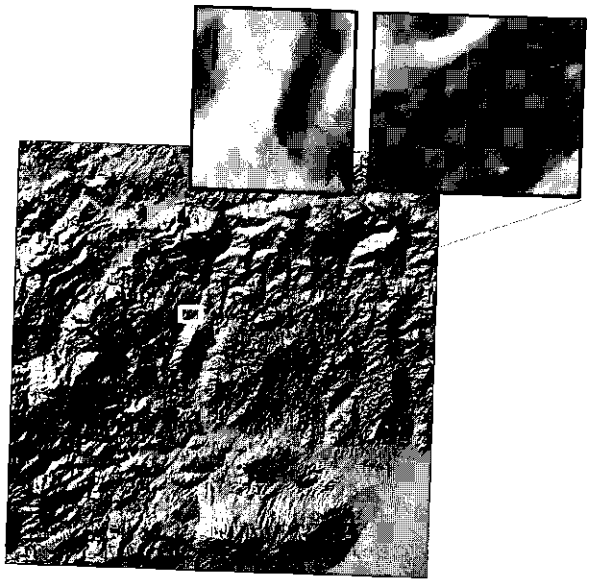

Chapter 5

Landscape Evolution Model Calibration

As mentioned in the previous chapter, over the past years the Caesium-137 (^{137}Cs) technique has been successfully applied in numerous environments all over the world. This technique is using the world-wide distribution of the anthropogenic ^{137}Cs radionuclide and its redistribution associated with soil particles as an effective estimation of net soil-loss rates. In contrast to numerous studies on deep, often cultivated, clay soils with gentle to intermediate slopes, typical Mediterranean shallow stony soils on steep slopes have received almost no attention thus far. In this chapter, the landscape evolution over the past 37 years has been evaluated using the ^{137}Cs technique for two lithological different areas in the Álora research area. In soils on gneiss and serpentinite bedrock several transects have been selected on steep slopes up to 35 degrees with mean soil depths ranging from 37 to 24 [cm] for gneiss and serpentinite respectively. Estimating net soil redistribution rates from radionuclide distributions depends on the calculation of the local area reference inventory and the applied calibration technique. Several methods have been tested and final results were found to differ considerably. After careful parameter selection, the resulting net soil redistribution estimates for the different transects have been compared with simulations of a simple landscape evolution model, resulting in different possible scenarios of erosional response. Total net soil-loss for the research area range from 2.3 ±0.25 [t $ha^{-1}a^{-1}$] to 69.1 ±7.8 [t $ha^{-1}a^{-1}$] for serpentinite and gneiss slopes respectively. Differences in total slope sediment budgets as well as differences along the transects reveal influences of landscape representation and land use. In this case the impact of tillage translocation and resulting erosion rates are far more important than possible parent material induced differences. However, comparing the two sampled areas not only net rates but spatial patterns as well reveal important differences in distribution over the landscape of net erosion and net sedimentation zones.

Based on: Schoorl, J.M., Veldkamp, A., Boix Fayos, C., van der Graaf, E.R. & de Meijer, R.J., 2002. The ^{137}Cs technique on steep Mediterranean slopes (Part II): landscape evolution and model calibration.

5.1 Introduction

Soil redistribution is a common feature in sloping landscapes under both natural and agricultural conditions. Over the years, many studies have intended to quantify soil redistribution rates over various temporal and spatial scales. Overcoming the difficulties of monitoring soil redistribution in extended areas, the ^{137}Cs technique has the potential to evaluate both erosion and deposition over a period of decades (e.g. Ritchie and McHenry, 1990; Walling and Quine, 1990; 1991; 1992).

One of the important uncertainties of the ^{137}Cs technique is the translation of the measured inventory activities into quantitative erosion and deposition rates. Over the years many relationships have been tested. In general, several investigations have been dealing with agricultural fields where ^{137}Cs is found to be mixed into the plough-layer (e.g. Zhang et al., 1990; Walling and Quine, 1991; Kachanoski, 1993). As a consequence to evaluate net soil redistribution, in addition to soil transport by water, also tillage erosion needs to be taken into consideration (e.g. Poesen et al., 1997; Quine, 1999). Furthermore, as net soil-loss seems to be dominant in many field, slope and catchment studies, no deposition calibration techniques have been used (Zhang et al., 1998; Kachanoski and Carter, 1999; Nagle et al., 2000). Studies that did take deposition in cultivated areas into consideration often make use of the equal mixing of ^{137}Cs into the depositional layer (e.g. Martz and de Jong, 1987; 1991; Bussaca, 1993; Sutherland, 1998).

Because of this focus on agricultural landscapes, there are fewer studies taking into account (semi-) natural conditions. In natural landscapes the decreasing ^{137}Cs depth distribution in the soil shows a characteristic exponential profile, concentrating the ^{137}Cs near the surface (Zhang et al., 1990). Therefore, depending on which part of the soil profile is eroded a loss of a certain amount of ^{137}Cs quantifies the amount of erosion for natural conditions, this means that an equal amount of ^{137}Cs loss corresponds to considerably less erosion for agricultural conditions. Again several authors report only net soil-loss with no need for deposition calibration techniques (e.g. Loughran et al., 1990). Those who did take deposition into consideration are dealing with the uncertain labelling of the sediments, including dust deposition (e.g. Chappell, 1999).

The assumption that the original fallout build up in the soil profile is the same for level reference sites and (steep) sloping positions is subjected to discussion. For both cultivated and uncultivated slope positions this means no significant redistribution of ^{137}Cs during the fall out build up from the 50's to the 70's, especially not around 1963 (Walling and Quine, 1992). The wetter the research area the more likely it will become that soil redistribution could have taken place. However, in semi-arid to sub-humid Mediterranean Spain the assumption seems justified. Anyway for studies involving cultivated land this assumption becomes less important using the plough-layer mixing models (Martz and De Jong, 1991; Sutherland, 1998; Zhang et al., 1998).

Calibration techniques concerning deposition face the problem of the unknown ^{137}Cs labelling of the deposited material (Yang et al., 1998). ^{137}Cs concentrations vary considerably depending on which part of the upslope profile is eroded, especially when the upslope sources of the sediments are undisturbed natural exponential profiles. Sedimentation in an area of extreme converging water and sediment flows can mean deposition of sediments with a high concentration of ^{137}Cs from several surrounding locations. In such a case a 100 [%] increase in ^{137}Cs represents only a few [cm] of soil gain. This as opposed to the situation where the deposited sediment is coming from one and the same location, which can give a 100 [%]

increase of ^{137}Cs only if the source profile is completely eroded (normally more than 20 [cm]).
Soil redistribution in cultivated areas is often evaluated using the cultivation layer / plough-layer mixing models (Sutherland, 1998; Zhang et al. 1998). These models incorporate in case of erosion the unlabeled soil into the yearly plough-layer. However, uncertainty remains in cases where the plough depth is considerably less then the layer containing the ^{137}Cs for example with chisel or duckfoot ploughs in stony soils on steep slopes. Another disadvantage is that to estimate net sedimentation rates Sutherland (1998) uses the thickness of the ^{137}Cs layer. This approach requires again depth depended radionuclide analyses at each sample point, which increase the number of (costly) analysis as compared to bulk samples used in this study. Martz and De Jong (1991) use for both cultivated and natural profiles a plough-layer mixing model. For natural positions with exponential profile distributions this means underestimating erosion rates compared with exponential methods.
Before even starting to use calibration techniques, the most important assumption of the ^{137}Cs technique is the local uniform distribution of the fallout. Therefore the establishment of a reliable fallout baseline in a study area, also called the reference inventory, is essential for the quantification of the ^{137}Cs redistribution (Walling and Quine, 1992). In general this reference inventory has to be sampled within the chosen research area in stable undisturbed locations, where since the beginning of the fallout in the 1950's no significant loss or gain of soil has taken place. However, these locations are often difficult to identify within a certain area, mainly because of the constantly changing topography and human disturbances (Quine et al., 1994; Chappell, 1999). As a result the reference inventory in many studies is based on only a single reference soil profile, which is not a statistically sound basis (Sutherland, 1998). Furthermore, uneroded reference locations are often limited to very small areas. Especially on isolated hill tops in Mediterranean upland areas, the effective area (zero slope, no erosion) is too small and often allows only one single sampling profile (Sutherland, 1996).
Despite the potentials of the ^{137}Cs technique to assess soil erosion and redistribution in any environment (Walling and Quine, 1990), relatively few ^{137}Cs studies are reported for the south of Europe and the Iberian Peninsula. Fortunately recent work in the Mediterranean region has shown the potentials of the ^{137}Cs technique in Greece and Italy (Kosmas et al., 2001; Porto et al., 2001). Concerning the Iberian Peninsula some work has been done in the north and middle of Spain for both soil erosion and redistribution assessments (e.g. Navas and Walling, 1992; Quine et al., 1994; Navas et al., 1997). However, on quantification of ^{137}Cs related soil redistribution in semi-natural environments in the south of Spain, so far, no reports could be found.
The objective of this chapter is to analyse the applicability of the ^{137}Cs technique to calibrate landscape evolution modelling in a Mediterranean steep slope and shallow soil environment. In this case the slope transect data of ^{137}Cs distribution is translated into amounts of soil redistribution (erosion and deposition) for different parent materials and land use. Comparing these ^{137}Cs redistribution results with the modelling of the same transect provides information on model behaviour and possible limitations.

5.2 Materials and methods

5.2.1 Study area

The research area is situated close the village of Álora in the middle of the research area. In the Sierra de Aguas just north of Álora two sample areas were chosen in two different lithologies (Fig. 5.1). The sample areas are located on an isolated serpentinite hill top covered by semi-natural vegetation and in a small catchment on garnet gneiss bedrock with olive orchards on several slopes. A Digital Elevation Model (DEM) with a resolution of 7.5 [m] has been extracted from aerial photographs (Fig. 5.1).

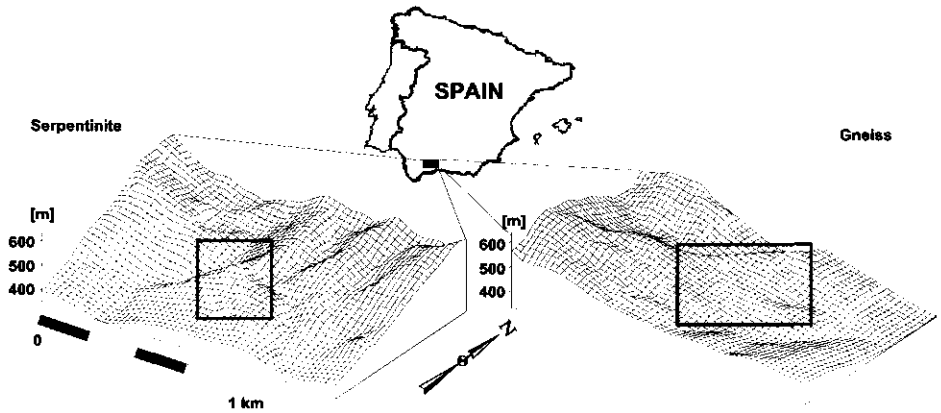

Fig. 5.1 Topographic overview of the two sample areas on the serpentinite and gneiss lithology.

As mentioned before in previous chapters, the area around Álora has a summer dry Mediterranean climate (Csa) with a mean annual temperature of 17.5°C and a mean yearly rainfall of 534 [mm], mainly in the period from October to April. However, in the Mediterranean region, annual rainfall is often variable. Historical records show that mean annual rainfall varies roughly between 250 and 1050 [mm] over the past fifty years (Fig. 5.2). In the research area the year of maximum bomb testing and thus fallout (1963) is also a year with relatively enhanced rainfall.

5.2.2 Reference inventory and bulk ^{137}Cs sampling

In the research area 9 reference profiles and 7 transects were sampled, following standard procedures (see paragraph 4.2.1, Chapter 4). All together a total of 86 samples were analysed. For the 9 reference sites 6 profiles (3 in each lithology) were sampled with 4 [cm] depth increments until the bedrock or saprolite was encountered. The rest of the samples in reference sites and along the transects were taken as a single bulk sample until 45 [cm] of depth, or until the bedrock or saprolite was reached.

The sample areas are located in an area of steeply dissected topography. Slope profiles are typical convex with slope lengths from 50 to 150 [m] ending in v-shaped channels or gullies

with hardly any sediment in storage. Mean soil depth ranges from 37 to 24 [cm] and stoniness from 19 to 38 [%] for gneiss and serpentinite slopes, respectively. Slope angles in the sampled areas range between 15 and 30 degrees for the gneiss transects and up to 35 degrees for the serpentinite transects. Slope profiles are given in Fig. 5.3, with 3 transects sampled in the gneiss and 4 transects in the serpentinite area. The transects were sampled with effective slope length intervals of 10 [m] (T1, T3, T4, T5 and T7), 15 [m] (T2) and 22 [m] (T6). Total sampled slope lengths were mainly constrained by road cuts or other human activity.

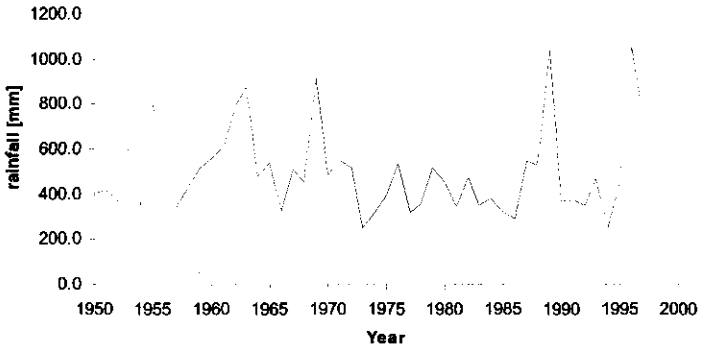

Fig. 5.2 Annual rainfall data for the last 50 years at Álora Estacion, situated in the middle of the research area.

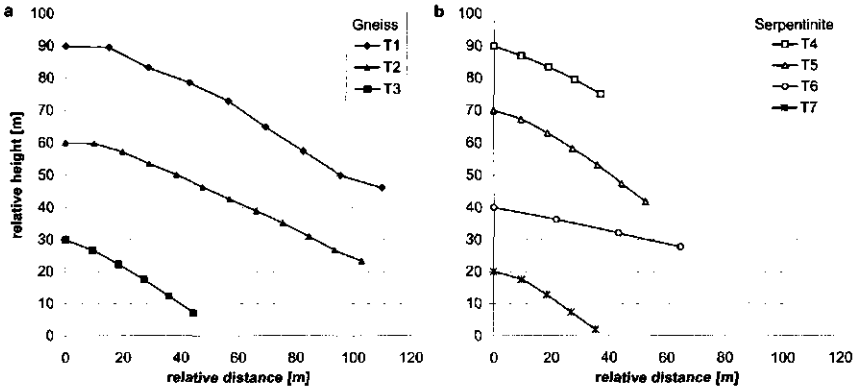

Fig. 5.3 Slope profiles of sampled transects for a) gneiss T1 to T3 and b) serpentinite T4 to T7.

5.2.3 Soil redistribution modelling with ^{137}Cs

To calculate the net soil flux along the transects in the study area the distributions of the ^{137}Cs inventories have been evaluated using two different models. The first model is based on the

exponential decreasing profile distribution of ^{137}Cs in natural soils (uncultivated) and belongs to the group of profile distribution models (Walling and Quine, 1990). The second model is based on the evenly mixture of ^{137}Cs in the plough-layer of cultivated areas and belongs to the group of mass balance models (Walling and Quine, 1990).
Assuming that the maximum rate of ^{137}Cs deposition occurred in 1963, soil-loss has been calculated for the natural soils in our uncultivated serpentinite sample area using the following calibration procedure (Zhang et al., 1990; Chappell et al., 1998):

$$R_e = 100 \cdot Bd \cdot \frac{\left(b - \left(LN\left(\frac{Y-a}{d}\right)\right)\right)}{c \cdot y} \tag{5.1}$$

where R_e stands for net annual soil-loss [t $ha^{-1}a^{-1}$], Bd soil bulk density [kg m^{-3}], Y the total ^{137}Cs inventory of the sample point [mBq cm^{-2}], y numbers of years between 1963 and year of sampling [a], under the assumption that the parameters a [mBq cm^{-2}], b [-] and c [m^{-1}] and d [mBq cm^{-2}] are known from the exponential growth curve simulating the cumulative ^{137}Cs activity X_h [mBq cm^{-2}] against depth into the soil h_{sd} [cm] for all samples at undisturbed reference sites:

$$X_h = a + d \cdot e^{(b - c \cdot h_{sd})} \tag{5.2}$$

For the gneiss area soil-loss has been calculated using a calibration procedure developed for cultivated areas assuming that the ^{137}Cs is mixed into the plough-layer (Zhang et al., 1990; Zhang et al., 1998):

$$R_e = -10 \cdot H \cdot Bd \cdot \left(1 - \left(\frac{Y}{X_{ref}}\right)^{\frac{1}{y}}\right) \tag{5.3}$$

where R_e, Bd, n and Y are the same as above, H is the depth of the plough-layer [m] and X_{ref} the total reference inventory for the study area [mBq cm^{-2}]. All of the above described models were adequately tested in different regions of the world (e.g. Zhang et al., 1990; Chappell et al., 1998; Zhang et al., 1998; Chappell, 1999; Porto et al., 2001).

5.2.4 Runoff based soil redistribution modelling

The results of the ^{137}Cs soil flux modelling have been compared with a simple landscape evolution model LAPSUS (see Chapter 3). This model is a basic surface erosion model for Digital Elevation Models (DEMs) and is based on the continuity equation for sediment movement (Eq. 3.1). LAPSUS evaluates the sediment transport rate (Eq. 3.2) by calculating the transport capacity of water as a function of runoff and slope gradient (Eq. 3.3). When the capacity is higher than the actual transport rate, this capacity is filled by the detachment of soil particles from the soil surface (Eq. 3.4). Detachment is highly dependent on the erodibility K_{es} [m^{-1}] of the surface and consequently causes lowering of the surface or erosion. When the actual transport rate exceeds the local capacity, for example because of lower

gradients, then the surplus of sediment in transport will be deposited by a settlement function causing a higher surface or sedimentation (Eq. 3.5).
The routing of the overland flow and the resulting model calculations are done comparing the Steepest Descent method (SD) with a Multiple Flow (MF) algorithm (Eq. 3.6) to allow for a better representation of divergent properties of the convex topography (e.g. Freeman, 1991; Quinn et al., 1991; Holmgren, 1994). A DEM with a resolution of 7.5 [m] was used in this study for both lithologies. In addition to the topographical potentials, main input parameters have been annual infiltration and evaporation losses (starting from 73 [%]) related to soil depth [m], annual precipitation (534 [mm a^{-1}]) and parent material (local bulk densities between 863-2263 [kg m^{-3}]).

5.2.5 Tillage soil redistribution modelling

For the gneiss area also tillage erosion will have to be taken into consideration, since transects T1 and T2 are situated in an olive orchard. Common tillage practises in these typical Mediterranean areas consist of passing a duckfoot chisel plough by a tracked tractor to control weeds (competing for water) and enhance infiltration (Poesen et al., 1997; Gomez et al., 1999; Quine et al., 1999).
Net downslope soil flux per tillage operation S_{till} [kg m^{-1}] can be calculated with a diffusion–type equation assuming a linear relationship between soil flux and slope tangent (e.g. Govers et al., 1994):

$$S_{till} = k_{sf} \cdot \Lambda \tag{5.4}$$

where k_{sf} is the soil flux coefficient [kg m^{-1}] along the slope and Λ the slope tangent [m m^{-1}]. The soil flux coefficient k_{sf} for the study area was derived following the experiments by Poesen et al. (1997) and Quine et al. (1999):

$$k_{sf} = k_{td} \cdot Bd \cdot H \tag{5.5}$$

where k_{td} is the tillage displacement coefficient [m], Bd soil bulk density [kg m^{-3}] and H is the depth of the plough-layer [m]. Since experimental data on tillage erosion for the study area was lacking, the k_{td} was calibrated and compared with the data provided by Poesen et al. (1997) and Quine et al. (1999). The experimental design, slope characteristics and soil properties in their study area compare well with the case study presented here.

5.3 Results and discussion

5.3.1 Reference inventory

In Fig. 5.4, the ^{137}Cs surface activities are given for all reference profiles with depth increments of 4 [cm]. Measured concentrations [Bq kg^{-1}] have been converted into activities per unit area [mBq cm^{-2}] by multiplying the concentration with the total sample weight <2 [mm] (so without stones) and dividing by the sampled surface. In general, the profile distribution of ^{137}Cs follows the general assumptions of the ^{137}Cs technique. High ^{137}Cs activities are found in the topsoil layers, decreasing rapidly with increasing soil depth. Deeper

than 28 [cm] into the soil no significant quantities of ^{137}Cs were found. Typically 90 [%] of all ^{137}Cs can be found in the first 12 [cm] of soil. Comparing all profiles GR2 shows the weakest typical profile distribution.

Establishing a reliable reference inventory for the study area is crucial for any further interpretations or evaluation (Sutherland, 1996). Unfortunately there are some major constraints in establishing this reference inventory by sampling in a research area. First undisturbed reference sites will have to be available. Topography and human interference often hamper establishing one or more profiles inside or near the research area, especially with the land use history of the Mediterranean area (e.g. Le Houerou, 2000). Even when several reference profiles are available, the spatial variability can be considerable (Fig. 5.4). Finally, in literature different methods have been used to extract the exponential distribution from the samples of the reference profiles. (Chappell et al., 1998; Porto et al., 2001; Walling and Quine, 1990; Yang et al., 1998).

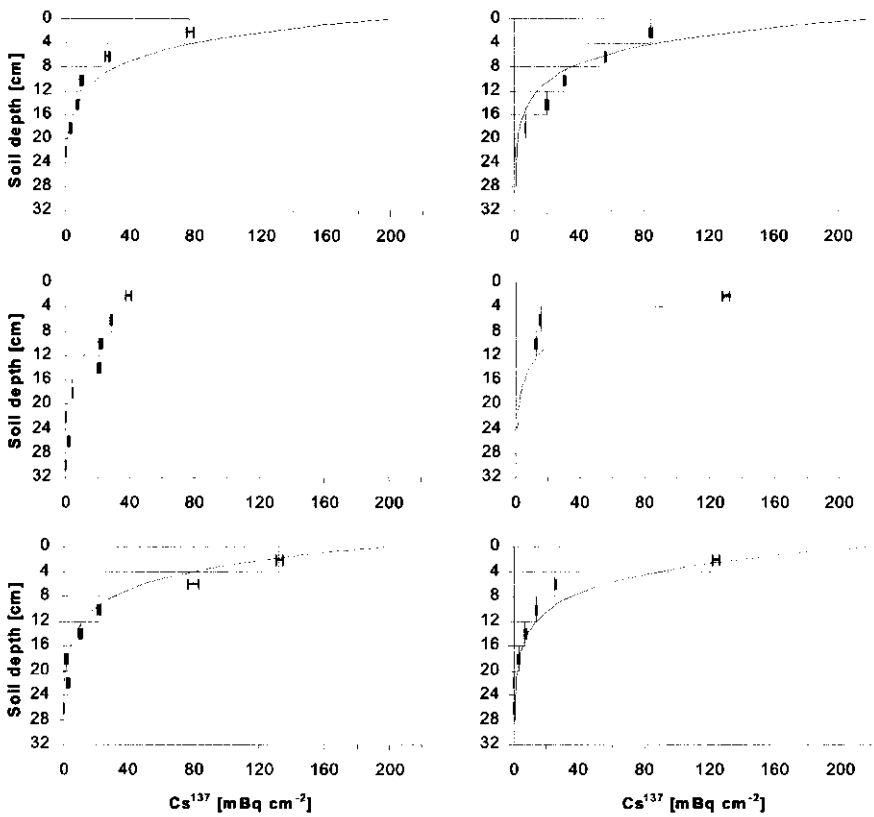

Fig. 5.4 Soil depth distribution of ^{137}Cs activities at reference profiles (error bars indicating measuring precision) with a) GR1, b) GR2, c) GR3, d) SAR1, e) SAR2 and f) SAR3. An exponential model fit combining the data of the 3 profiles is given for both gneiss and serpentinite.

For all reference samples (Fig. 5.4) and for each lithology a reference inventory has been determined by fitting an exponential model (Eq. 5.2) to the measured concentrations or activities at each soil depth (Table 5.1). First, different methods have been tested: (i) ID inventory surface activity [mBq cm^{-2}] against depth [cm] (Yang et al., 1998), (ii) CD concentration [Bq kg^{-1}] against depth [cm] (Chappell et al., 1998), (iii) CMD concentration [Bq kg^{-1}] against mass depth [kg cm^{-2}] (Porto et al., 2001) and (iiii) ICD cumulative inventory [mBq cm^{-2}] against depth [cm] (Walling and Quine, 1990). Secondly different sample sizes have been tested separating the lithologies and removing the weakest profiles

Table 5.1 Exponential curve fitting for activity and concentration depth distributions with different methods using *N* samples.

	Method	*N*	r^2	X_{ref} [a]	*a*	*B*	*c*
All samples	ID	41	0.93	238 ±29	5.0	5.45	-0.41
All samples	CD	41	0.88	249 ±36	1.4	4.34	-0.54
All samples	CMD	41	0.84	179 ±13	0.9	4.01	-0.38
All samples	ICD	41	0.89	194 ±18	0.2	5.27	-0.24
Gneiss	ICD	23	0.86	177 ±23	-1.2	5.19	-0.19
Serpentinite	ICD	18	0.92	207 ±14	1.1	5.32	-0.27
All samples[b c]	ICD	33	0.92	210 ±13	-0.3	5.35	-0.23
Gneiss[b]	ICD	18	0.98	198 ±24	-0.9	5.29	-0.23
Serpentinite[c]	ICD	15	0.97	219 ±14	0.23	5.39	-0.23

[a] in [mBq cm^{-2}] with standard error
[b] without profile GR2
[c] without profile SAR2

The different curve fitting procedures in Table 5.1 show that the explained variance is increasing when separating the two lithologies and removing the weakest profiles in terms of exponential depth distribution (GR2 and SAR2). In addition to the effect of removing these profiles this apparent increasing explanation is also enhanced by the decreasing *N* sample size. When using only one of the profiles, as in many studies, fit's can go up to 99 [%] (Chappell et al., 1998; Porto et al., 2001). This as opposed to Sutherland (1998), who suggested that there is a minimum number of samples needed to prevent over or under estimation, although uncertainties remain due to the influence of spatial variability combined with local variability of different depth samples.
The results in Table 5.1 also demonstrate clearly the importance of a good determination of the reference inventory since the different solutions for the mean area activity vary from 177 ±23 to 249 ±36 [mBq cm^{-2}] influencing directly the calibration rates and threshold between erosion and deposition. In addition to the reference inventory, the shape coefficient of the exponential curve (factor *c*) also plays a crucial role in the determination of soil redistribution rates. In Fig. 5.5 is given an example of the variation of soil redistribution rates using the Zhang et al. (1990) model of Eq. 5.1 by introducing the different solutions of Table 5.1. Absolute differences are increasing considerably with increasing soil redistribution rates. For example, a sample with a ^{137}Cs inventory of 50 [mBq cm^{-2}] shows soil loss rates in Fig. 5.5 ranging from 6 to 14 [t $ha^{-1}a^{-1}$].

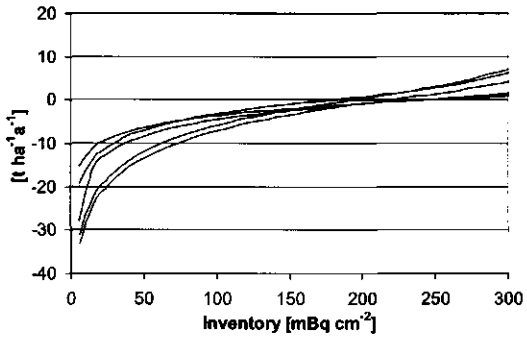

Fig. 5.5 Example of soil redistribution rates for the different methods of fitting an exponential curve and the resulting differences in shape factor.

Analysing the previous section the best fit models (last two rows in Table 5.1) have been used for the rest of this paper. In the first place because the removed profile GR2 is clearly disturbed and does not show the natural exponential decrease (Fig. 5.4) while removed profile SAR2 is too shallow with only 12 [cm] of effective soil depth. Secondly because statistical analysis have clearly suggested differences in various soil and slope properties between the lithologies as for example the ^{137}Cs concentration (see Chapter 4). Both reference inventories, 198 ±24 and 219 ±14 [mBq cm^{-2}] for gneiss and serpentinite respectively, are comparable to other inventories found in the northern hemisphere not influenced by the Chernobyl accident (e.g. Walling and Quine, 1990; Zhang et al., 1998; Porto et al., 2001). These reference levels for both lithologies have been plotted as dotted lines in Fig. 5.5. Compared with the reference found by Quine et al. (1994) in a semi-arid region in Spain our reference inventory is slightly higher because of the wetter climate in our study area. The resulting shape coefficient c of 0.23 is the same as used by Zhang et al. (1990) representing a steeper and shallower profile distribution than the 0.16/0.093 of Chappell et al. (1998) and the 0.14 of Porto et al. (2001).

5.3.2 Measured ^{137}Cs redistribution

In Fig. 5.6, the ^{137}Cs inventory activities [mBq cm^{-2}] are given for all samples in the different transects. For the gneiss area, only 3 out of 27 samples are showing inventory activities significantly above the reference level indicating deposition of sediment of which GCB 9 was actually an undisturbed reference location and GCB 24 shows an extremely high inventory. The serpentinite area shows only one sample more with significant inventory activities above the reference level indicating deposition of soil and ^{137}Cs for 4 out of 19 samples. Sample SAR 13 is considered to be situated in an undisturbed reference location and was repeated in Fig. 5.6 since it was the starting point of all transects (see also Fig. 5.3). The mean inventory activity for the gneiss area is 140 ±19 [mBq cm^{-2}] as opposed to 171 ±17 [mBq cm^{-2}] for the serpentinite area. When considering only eroding profiles the mean inventory drops to 96 ±10 and 121 ±10 [mBq cm^{-2}] while for profiles with deposition the mean inventory is 278 ±41 and 265 ±21 [mBq cm^{-2}], for the gneiss and serpentinite area, respectively.

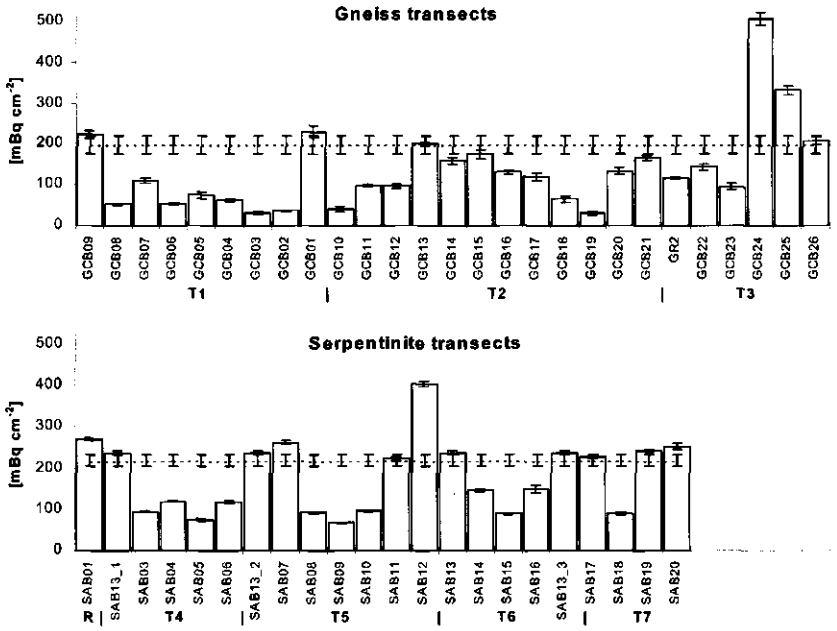

Fig. 5.6 Measured ^{137}Cs activities in the bulk samples for the transects T1 to T7 in the gneiss and serpentinite sample areas. GCB9, SAB01 and SAB13 are actually undisturbed reference profiles. Measurement significance given by error bars. Reference levels for both areas are given as dotted lines with standard deviation as second error bar.

5.3.3 Modelling soil redistribution

First of all the ^{137}Cs inventory activities where translated into net soil redistribution rates. For the undisturbed semi-natural profiles of the serpentinite sample area Eq. 5.1 was used, including local sample *Bd* [kg m^{-3}], an exponential curve shape factor *c* of 0.23 [mBq cm^{-3}] (see Table 5.1) and an X_{ref} of 219 ±14 [mBq cm^{-2}]. The cultivated soils of the gneiss area were evaluated using Eq. 5.3, with also local sample *Bd*, a plough-layer *H* of 0.16 [m] and an X_{ref} of 198 ±24 [mBq cm^{-2}]. All samples where taken and analysed during a short period in the same year (2000) so no correction for differential decay is needed. For the 37 year period the resulting net annual soil redistribution rates are presented in Figs. 5.7 and 5.8 (Cs-mod).

To calibrate the LAPSUS model two different simulations have been performed, starting with the undisturbed semi-natural slopes of the serpentinite. To obtain an indication of the possible rates the total soil redistribution budgets have been calculated for each slope transect and both the lowest total output (-2.3 ±0.25 [t $ha^{-1}a^{-1}$] at T7) and the highest total output (-8.9 ±0.24 [t $ha^{-1}a^{-1}$] at T4) have been evaluated (Table 5.2). The first simulation used a low K_{es} value giving catena averaged net sediment outputs similar to T7. The second run used a higher K_{es} value increasing the net sediment output until the same levels as T4 were reached.

Table 5.2 Serpentinite transects mean soil-loss and percentage deviation from the ^{137}Cs model comparing the ^{137}Cs and LAPSUS models for different K_{es} values.

	^{137}Cs model	LAPSUS			
		K_{es} ($7.4\ 10^{-5}$ [m^{-1}])		K_{es} ($3.8\ 10^{-4}$ [m^{-1}])	
	[t $ha^{-1}a^{-1}$]	[t $ha^{-1}a^{-1}$]	[%]	[t $ha^{-1}a^{-1}$]	[%]
T4	-8.9 ±0.24	-2.1	-76.7	-8.9	-
T5	-4.3 ±0.26	-3.4	-20.1	-14.9	249.1
T6	-5.6 ±0.26	-0.6	-89.7	-2.5	-56.4
T7	-2.3 ±0.25	-2.3	-	-11.2	403.4

In Fig. 5.7 a comparison is presented of modelling soil redistribution with the ^{137}Cs technique (Eq. 5.1) and the LAPSUS model for the undisturbed natural slopes of the serpentinite sample area using a high K_{es} factor (to match T4) and a low K_{es} factor (to match T7). In addition, different flow routing procedures have been applied (see Chapter 3, Eq. 3.6) to allow for more divergent properties, Multiple Flow (MF), as opposed to using the Steepest Descent (SD). In general the slope profiles extracted from the DEM compare well with the ones measured in the field. However, results differ considerably in total sediment output from the slopes comparing both K_{es} scenarios (Table 5.2). Comparing individual sample points, even though the trends of increasing and decreasing erosion are similar, net quantities of soil redistribution differ for the ^{137}Cs model and LAPSUS simulation (Fig. 5.7). In general the MF simulations are slightly better than the SD simulations. Considering these trends T7 reveals the weakest relation.

The same as for the serpentinite also for the cultivated gneiss transects different scenarios have been tested. A test run on T3 showed that modelling only water erosion using the K_{es} factor from the serpentinite area is not sufficient (see lower T3 graph in Fig. 5.8). Tillage erosion has to be included and in this case both transects T1 and T2 have been used to calibrate the model outputs resulting in a high and a low k_{sf} value (see Eq. 5.4 and 5.5, Table 5.3). Again for each transect the net soil redistribution output budget has been used to calibrate the LAPSUS model (see Table 5.3). In Fig. 5.8 is presented the resulting net soil redistribution for both scenarios along the gneiss transects.

Table 5.3 Gneiss transects mean soil-loss and percentage deviation from the ^{137}Cs model comparing the ^{137}Cs and LAPSUS models for different k_{sf} values.

	^{137}Cs model	LAPSUS			
		k_{sf} (49.5 [kg m^{-1}])		k_{sf} (138.2 [kg m^{-1}])	
	[t $ha^{-1}a^{-1}$]	[t $ha^{-1}a^{-1}$]	[%]	[t $ha^{-1}a^{-1}$]	[%]
T1	-69.1 ±7.8	-26.6	-60.1	-69.1	-
T2	-40.7 ±8.1	-40.7	-	-109.2	168.2
T3	1.4 ±9.1	240.9	>>>[a]	-19.1[b]	<<<[a]

[a] out of proportion
[b] water erosion only

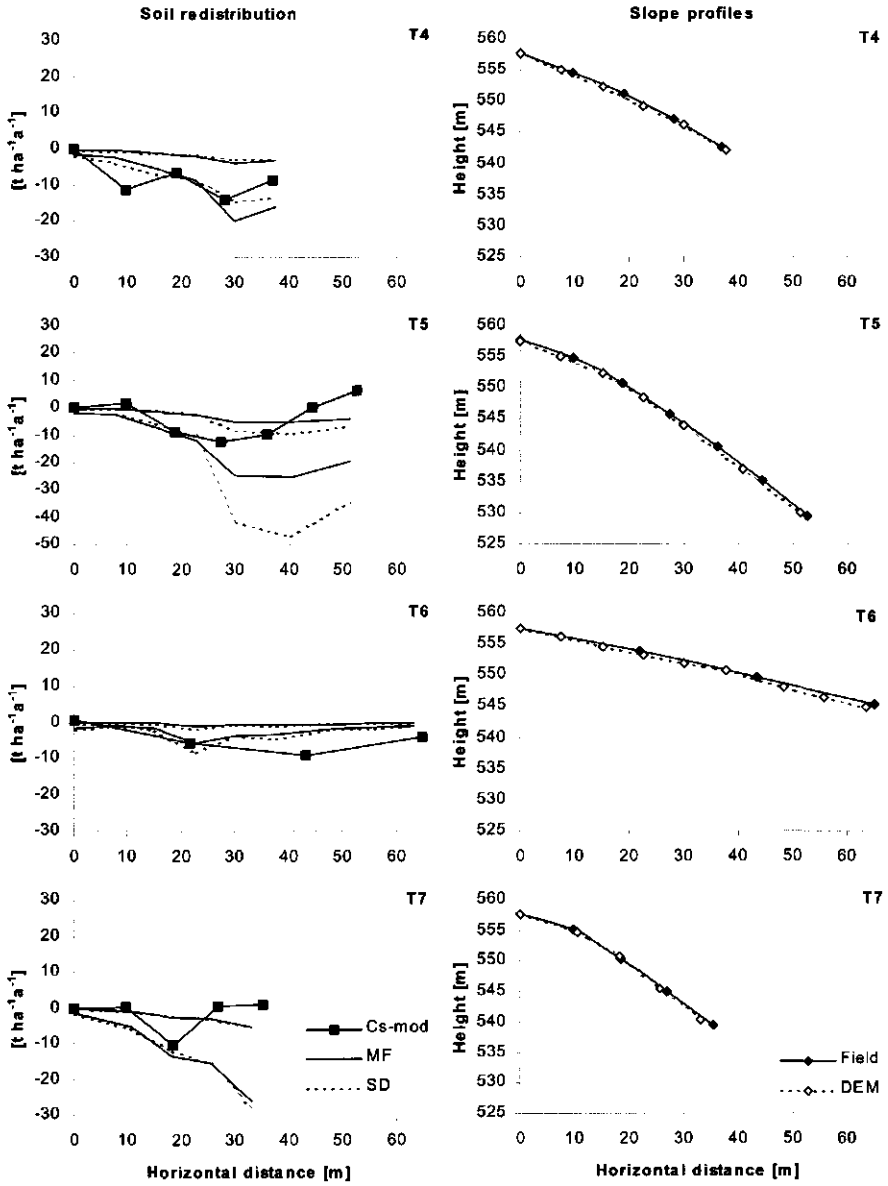

Fig. 5.7 Comparing the net soil redistribution results from the field ^{137}Cs technique (Cs-mod) with the LAPSUS model along the natural serpentinite transects T4 to T7 for different K_{es} values (left), on the right a comparison of the transects slope profiles measured in the field and extracted from the DEM.

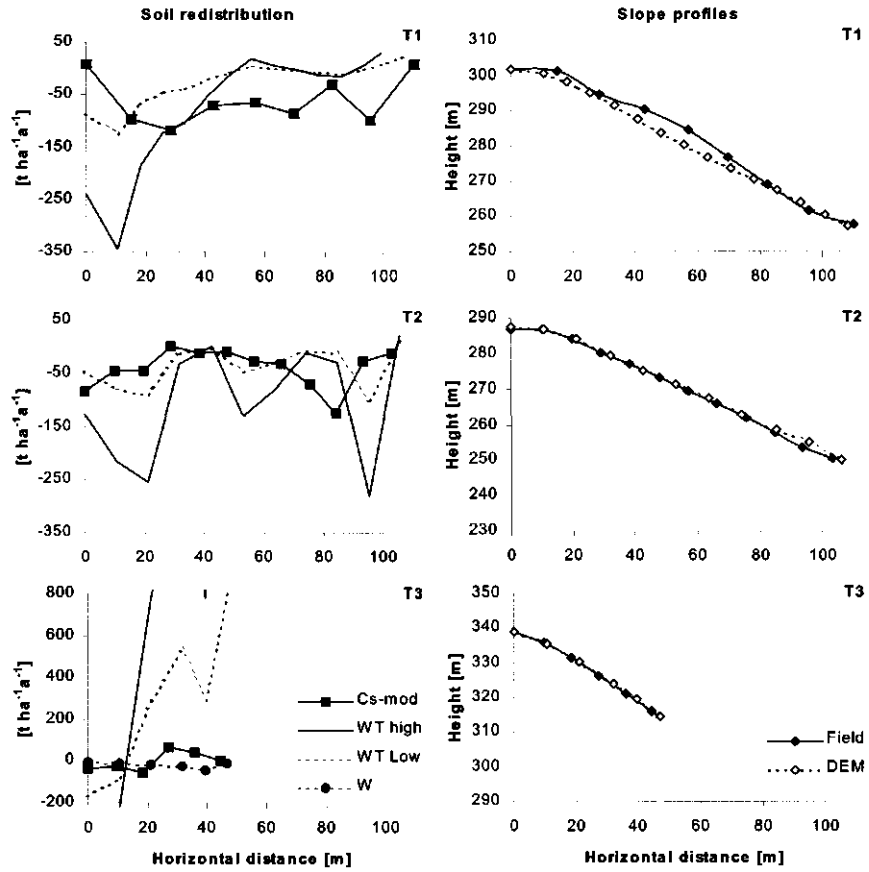

Fig. 5.8 Comparing the net soil redistribution results from the field ^{137}Cs technique (Cs-mod) with the LAPSUS model water erosion (W) and including tillage erosion (WT) along the gneiss transects T1 to T3 (left) and a comparison of the transects slope profiles measured in the field and extracted from the DEM (right).

In general, overlooking the Figs. 5.5 to 5.8 the number of sample points indicating deposition is remarkable, especially for those under natural conditions. Especially because of the time span of 37 years on steep slopes, net soil loss would be expected dominant and net depositional areas on the slopes to be limited. Consequently, in the majority of comparable studies only soil loss and net erosion is reported dominant (e.g. Zhang et al., 1998; Porto et al., 2001). However, the study area reveals typical climatological conditions of the Mediterranean environment. This implies that normally only the extreme events cause functioning of the whole drainage system (De Ploey et al., 1991). In addition, Mediterranean slopes are known to show complicated patterns of runoff generation and reinfiltration within several meters of slope length (Nicolau et al., 1996; Bergkamp, 1998).

The results of the ^{137}Cs calibrated soil redistribution for the natural slopes of the serpentinite area resulted in modelling both a low and a high K_{es} scenario. Which one of the scenarios is more realistic or whether the actual K_{es} lies somewhere in between the estimated values (Table 5.2) is difficult to estimate. Clearly, the model underestimates differences in local runoff and infiltration generation patterns, which cause resedimentation on the slope. This could be the result of the resolution and precision of the used DEM. Although transect gradients seem comparable (Fig. 5.7) this does not necessarily have to be the case for the neighbouring altitudes of grid points, influencing the diverging and converging properties of the DEM and as a result the extracted transect. The found differences could also be an indication that different K_{es} values are valid and needed for the different transects, since these K_{es} factors combine by definition numerous local soil surface characteristics such as roughness, crust etc.

In the gneiss area the modelling of T1 and T2 have resulted in different tillage soil flux coefficients (k_{sf}). These k_{sf} values between 138.2 and 49.5 [kg m^{-1}] are low compared to values given by Quine et al. (1999) but compare well to values given for contour ploughing by Poesen et al. (1997) and Lobb et al. (1995) respectively, although the latter is reported for mouldboard ploughing. However, the k_{sf} values for this study represent actually the average annual tillage erosion over the simulated period of 37 years, while values given in literature often represent a single tillage pass during an experiment. Consequently, the differences between T1 and T2 could have been caused by differences in the number of tillage operations on these slopes. Farmers in the area are known to till less in dry years and when prices are low (De Graaf and Eppink, 1999). Since the land management history for the specific transects is unknown, uncertainties remain about exactly how much tillage operations have been performed in these 37 years and when for example the duckfoot chisel plough by a tracked tractor has replaced conventional (less eroding) techniques.

A second factor of uncertainty in comparing tillage soil fluxes from literature and this study is the used procedure to simulate tillage. Tillage is simulated in LAPSUS using multiple flow directions to allow for a better representation of diverging and converging properties of the topography. The same as for flowing water, the use of multiple flow directions implements longer paths of transport, decreasing tangents and decreasing effective erosion (Chapter 3; Schoorl et al., 2000).

Looking at the soil redistribution patterns along the slope the differences in gneiss transect T1 can clearly be explained by the poor precision of the DEM in that place (Fig. 5.8). The top-section of T1 is missing the flatter area measured in the field therefore overestimating considerably tillage erosion in this top-section. Mid-slope of T1 the DEM is missing the convexity of the field, the resulting straight slope reduces tillage translocation, and as a result, the model simulates a clear underestimation of tillage erosion. Of all the gneiss transects, T2 reveals the best results, following at least more or less the trends along the slope. Again local differences along the transect are due to small differences in the profile gradients.

In Fig. 5.9 an example is given of the spatial impact of soil redistribution for the highest eroding LAPSUS scenarios (MF), separating net erosion and net sedimentation in the two sample areas. Spatial patterns for the (semi-)natural serpentinite slopes reveal common patterns of increasing erosion downslope, in the channels and in areas of converging water flows (more potential water flowing, increasing capacity to transport sediment). The sedimentation patterns are similar to the erosion patterns, although less elevated and almost zero at the divides, simply because there have to be first sediment in transport before it can be

deposited in areas of decreasing capacity. This as opposed to the patterns in the cultivated gneiss area, where both erosion and sedimentation reveal severe movement of soil even on the divides. The highest rates of soil redistribution in the gneiss area can be found in the mid-slope areas and on the edges of the steeper gully walls, where the steepest gradients can be found. In addition, tillage erosion is dominant in the convex slope areas (often upslope), while deposition is dominant in concave areas (down slope near the valley floor).

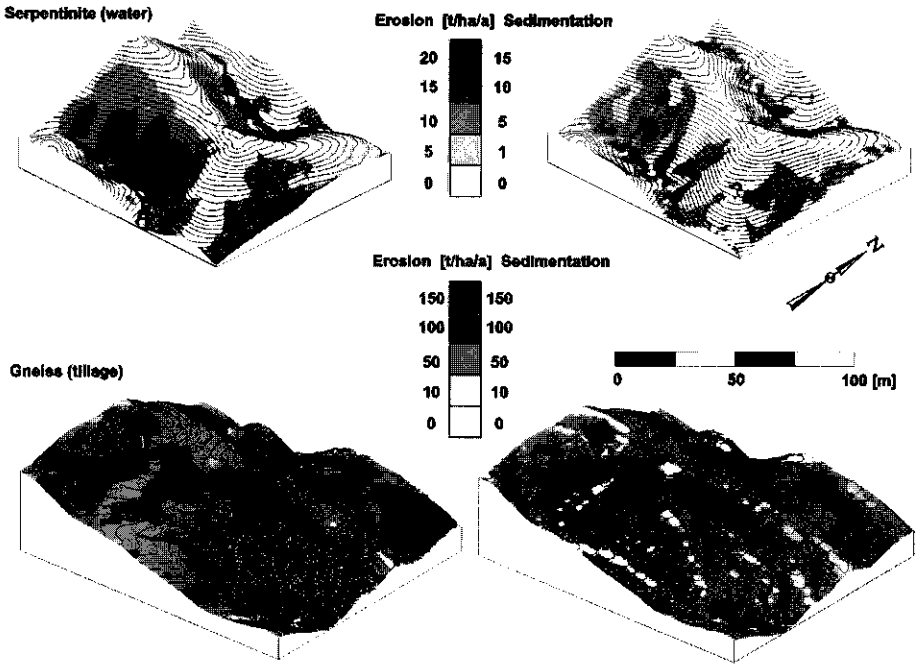

Fig. 5.9 Examples of LAPSUS simulations giving erosion patterns (on the left) and sedimentation patterns (on the right) for the serpentinite area (only water erosion) and the gneiss area (tillage and water erosion).

Comparing the natural transects of the serpentinite sample area with the cultivated gneiss area, the mean net soil-loss increases by almost a factor 10. In this case, land use and land management cause these differences, since in the gneiss area the lacking vegetation cover and tillage operations are the dominant factors of erosion. These dominant human factors obscure the natural effects of different parent material and the disturbances of T3 make this transect unsuitable for comparisons with the natural serpentinite transects. Pennock et al. (1995) also found significant difference between net soil-loss and parent material, although less extreme (12 to 30 [t ha^{-1} a^{-1}]) than in this study (2 to 69 [t ha^{-1} a^{-1}]) due to shorter slope lengths and lower slope angles.

5.4 Conclusions

As part of the ^{137}Cs technique the determination of the reference inventory for a study area is an important input for any calibration model and should not be underestimated. In addition to climate (e.g. rainfall), also the lithology should be taken into consideration, since the undisturbed exponential profile depends on parent material characteristics but also soil depth, stoniness and bulk density. Furthermore, different methods of extracting the exponential curve from the data reveal significant differences.

For the slope data, DEM resolution and sampling strategy used in this study, calibrating the total net soil redistribution from slopes and catchments seem more feasible than local slope patterns comparing field point data with spatial modelling. The main source of uncertainty is the representation of the landscape and its diverging and converging properties. Therefore, the DEM resolution and precision is an important factor in modelling landscape evolution. Furthermore, increasing the spatial resolution of the ^{137}Cs derived soil redistribution rates would enhance the possibilities of calibrating the different erosional response between transects and lithologies. Especially the future application of continuous measurements techniques for entire slopes and catchments could provide the necessary spatial input.

Differences in parent material influence important soil properties such as clay content and bulk density. These soil properties enhance the differences in net soil redistribution estimates since the their influences are incorporated in many of the local reference inventory estimates and soil redistribution calibration formula. However, the impact of human factors such as tillage and management are far more important and obscure the natural differences in erosional response. Furthermore, the spatial impact of water erosion and tillage erosion are very different. Whereas slope length and converging water flows enhance water erosion down slope and into the channels and gullies, tillage erosion is dominated by the change in local gradient showing net erosion in convex areas over the whole slope while net accumulation takes place in concave areas down slope.

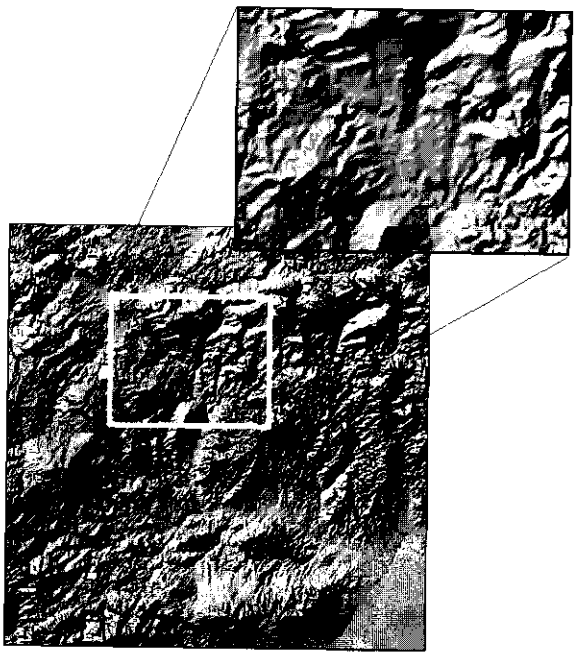

Chapter 6

Dynamic Landscape

In this chapter, the LAPSUS model is applied at the landscape level, aiming at the coarser level of multiple catchments over a period of ten years. Soil suitability assessments for land use plannung are commonly based on on-site specific topographic, soil and climatic characteristics, and are often neglecting the effects of physical landscape processes by water. However, soil science is gradually evolving from the one-dimensional profile view towards the three-dimensional landscape context. Furthermore, the spatial and temporal resolution of the landscape level requires specific input data and modelling procedures. Existing studies aiming at the landscape level often are data driven approaches operating at detailed resolutions of seconds and hours for single slopes or catchments. In this chapter LAPSUS simulations are focussed on the effects of soil and water redistribution within a landscape (run-on, runoff, erosion and sedimentation) on soil water availability. By means of four scenarios with increasing complexity, patterns of soil loss and sediment deposition are simulated and resultant effects of water routing, soil depth and erodibility on water availability are evaluated for all scenarios. The model operates in the landscape context using annual time steps and both on-site effects (local changes in terms of boundary conditions) and off-site effects (caused by changes elsewhere) were accounted for. Different approaches for surface runoff routing have a major influence on the magnitude and spatial patterns of soil redistribution. Also initial conditions such as soil depth, parent material characteristics and parent material dependent erodibility have spatial impacts upon soil erosion and sedimentation within the landscape. Locally decreasing water storage capacity (on-site) may cause increased runoff and erosion at lower positions in the landscape (off-site). Localised soil redistribution can cause significant changes in actual soil depth and indirectly affect related total amounts of available soil water. The changing patterns of soil redistribution for the different scenarios are both related to modelling techniques as well as to the implemented boundary conditions. This study indicates that at the landscape scale spatial variability in for

Based on: Schoorl, J.M., Veldkamp A. and Bouma J., 2002. Modelling water and soil redistribution in a dynamic landscape context. Soil Science Society of American Journal.

example soil properties is inherent to both the complexity of the landscape (parent material) and on-site and off-site effects of controlling processes.

6.1 Introduction

In addition to for example yield data and distance to markets, soil suitability assessments or land evaluations are often based on available soil survey data, because soils do not occur in random patterns in a landscape but, rather, in recognisable patterns governed by the soil forming factors (e.g. Buol et al., 1989; Bouma, 1999). Such spatial patterns are shown on maps of different scales and soils are usually described by representative profile descriptions. Traditionally, soil suitability assessments and land evaluation is largely based on the soil profile data (e.g. FAO, 1976). This profile based one-dimensional view has governed soil science for many years. However, soil science is gradually evolving towards the three-dimensional landscape context (Jacob and Nordt, 1991). Consequently an increasing number of studies is directed at the slope and catchment level (e.g. Beven et al., 1984; Nearing et al, 1989; Gessler et al., 2000). Nevertheless, the detailed spatial and temporal resolutions of such studies hamper the implementation at higher landscape levels such as multiple catchments on varying lithologies.

Landscapes are the result of and shaped by a set of interrelated and non-linear processes (Milne, 1991). These processes all show specific impacts in space and time. In most landscapes, water and soil redistribution (erosion and sedimentation) are the main processes that cause a logical self-organisation of relief, soils and ecosystems (Holling, 1992; Rigon et al., 1994). The main effect of these landscape processes is that they connect soil pedons in specific ways such as topo-sequences and catenas, causing changes in soil properties (from soil depth to available water) to have both on- and off-site effects. On-site effects are considered locally forced changing conditions (e.g. reduced infiltration by crust forming, erosion), while off-site effects are the result of changed conditions elsewhere. However, these off-site effects within landscapes such as deposition, changes in run-on or even land use have been mostly neglected in land evaluations and other agricultural research (Fresco, 1995; Veldkamp et al., 2001). In contrast with current procedures, land use suitabilities should also be evaluated for both on-site and off-site effects. While creating simulation scenarios, average rainfall data can be used for each land unit while major differences in water input may occur due to runoff and run-on. Also aspect, slope gradient and wind direction may result in different impacts of radiation, evaporation and temperature upon available water, factors that are not commonly expressed in simulation models of land evaluation. Furthermore, relevant time scales should be considered ranging from a growing season for annuals (<1 year) up to multiple decades (>10 to 100 years) for perennials and natural vegetation.

Aside from soil properties, soil redistribution (e.g. erosion and sedimentation) is considered an important reason for each landscape element to have its own specific productivity (Hall and Olson, 1991). Consequently, similar soils in different landscape positions may have different productivity potentials. The resulting landscape processes can have large impacts in sloping areas, which is well known from various erosion studies (Lal, 1997). These studies, however, mainly focus on the erosion aspects of the landscape processes while deposition can have an equally large impact. Payton and Shishira (1994) published an well-illustrated example including both aspects of erosion and deposition for Tanzania. They demonstrated how within one century a good productive district turned into a marginal area with very

limited productivity, illustrating the effects of erosion and sedimentation along a soil catena. Productive soils were either eroded or buried as a result of mis-management of arable land. A similar example for a less sloping and drier environment in Niger is described by Bromley et al. (1997).

Evaluating land use systems thus requires a combined on- and off-site approach in such a way that not only soil processes at the pedon level, but also three-dimensional landscape processes are taken into account. Such an approach should aim at exploring natural soil and landscape processes in such a way that desirable land use can lead to continuing productivity without reducing soil quality. This aim will require a landscape approach focusing not only on evaluating pedon characteristics but also on introducing landscape components. To meet the aim of 'landscape evaluation', studies integrating on- and off-site impacts of land use for both short and long time-spans are required (e.g. Pennock and van Kessel, 1997; Schoorl and Veldkamp, 2001).

Ideally, the results of these landscape-scale studies should be used in a dynamic landscape modelling approach to gain more insight in the complex functioning of ecosystems and soils at the landscape scale (Gessler et al., 2000). Furthermore these types of studies should include not only agricultural production systems but also many non-agricultural land uses as well. There are many sophisticated hydrological and geomorphological models available (e.g. Beven et al., 1984; Nearing et al, 1989) but they all require high temporal (up to seconds) and spatial (slope segment) resolution of the input data and are therefore unsuitable for the proposed soil landscape suitability assessment.

This chapter will describe a simple modelling approach to integrate three-dimensional landscape processes with one-dimensional soil processes, based on readily available soil survey data. Thus, it is intended to provide a new dimension to soil survey interpretations that currently do not consider the multi-dimensional landscape context. Examples of scenario building will show the impact and unexpected effects of this annual integration over a period of ten years at the multi-catchment level. Model simulations will allow assessments of current and possible water and soil redistribution for on-site effects (local changes in terms of boundary conditions) and off-site effects (caused by changes elsewhere) within the landscape.

6.2 Materials and methods

6.2.1 Study area

A study area of about 239 [km^2] has been selected in the Guadalhorce River basin with a range in altitudes from 100 to 1200 [m] (Fig. 6.1). The area is situated near the village of Álora (longitude 04-41-57W, latitude 36-49-10) in the province of Málaga, southern Spain and was selected because of its lithological diversity and resulting soils. General climate is summer dry Mediterranean with a mean annual temperature of 17.5°C and mean annual rainfall of 534 [mm], mainly from October to April (Álora Estación). This landscape is composed by geological units and soil units as shown in Fig. 6.1b (Ruiz et al., 1993).

Comparing Figs. 6.1a and 6.1b it is clear that steeper areas (high contour density) reflect more resistant parent material like in the north east limestone (LM), the central western zone serpentinite (SP), molasse (MO) and gneiss (GN) and the south east corner phylites (PL). The less steeper areas (less contour density) can be found from the southwest to the northeast marls (MA). Finally, in the middle an almost flat area can be recognised of river terraces (RI).

This same broad geological outline and the resulting soils of the area are reflected in the simplified soil depth map (Fig. 6.1c). This map has been developed by field survey of the dominant land units, geo-referenced sampling and spatial interpolation. The main criteria to discern land units such as terraces, footslopes, hills, upland area etc. have been the parent material and topographic position (Wielemaker et al., 2001).

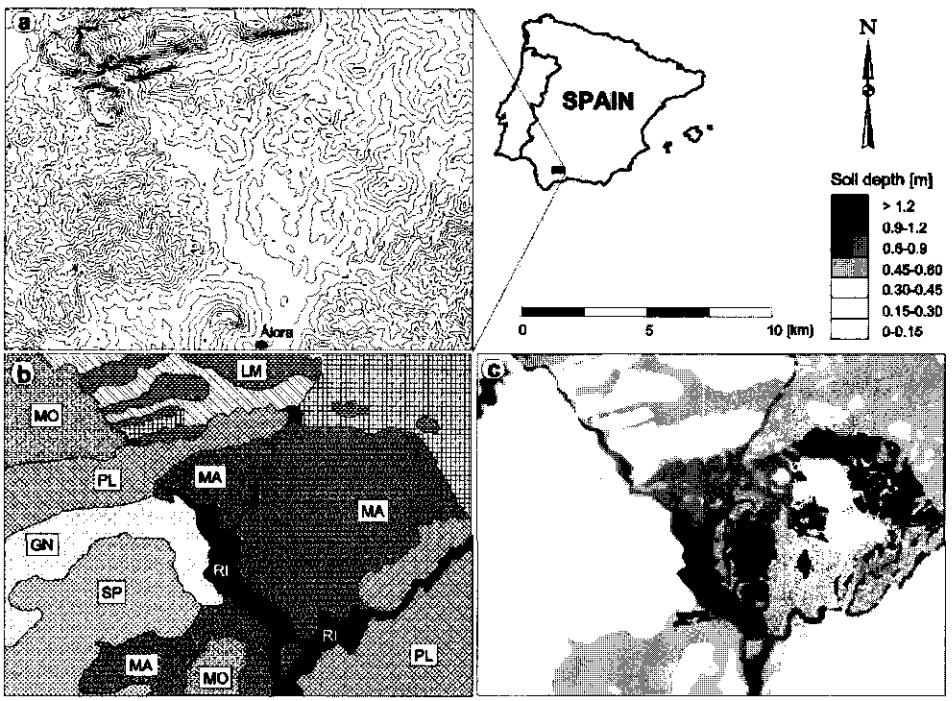

Fig. 6.1 Study area in the lower Guadalhorce River basin with (a) DEM of the area, contour line interval is 50 [m], (b) major soil units according to parent material: river terraces (RI), gneiss (GN), molasse (MO), marls (MA), limestone (LM), phylites (PL) and serpentinite (SP), and (c) initial soil depth map.

6.2.2 Modelling

Topography, represented by a Digital Elevation Model (DEM), is the driving force behind the geomorphic processes. This readily available DEM has been processed from 20 meter contour lines by interpolation to a raster map according to x, y and z with a grid cell resolution of 100 [m] (SGE, 1997). With this resolution the study area is divided in a raster of 132 rows by 181 columns. Because of the relevant temporal resolution for this study of 1 to 10 years and the spatial resolution up to multiple catchments the LAPSUS model was used (Chapter 3, Schoorl et al., 2000). Consequently, input data and resulting modelling structures were implemented at

an annual basis. LAPSUS is a finite element model and uses sediment transport equations based on early works of Kirkby (1971) and Foster and Meyer (1972, 1975) on the continuity equation for sediment movement (Chapter 3, Eq. 3.1).
In this way this approach simulates net annual soil redistribution by mimicking one average yearly event to shape the landscape. Therefore, annual sediment transport rates (Eq. 3.2) are driven by the topographical potentials imposed upon the runoff water, taking into account annual infiltration and evaporation losses by using the amount of net annual runoff reaching the main drainage system. Total amount of annual runoff water and the downslope gradient determine transport capacity (Eq. 3.3). When this transport capacity is higher than the actual sediment transport rate, the sediment in transport can be increased by detachment implying erosion (Eq. 3.4). The rate of detachment is controlled by the K_{es} factor, which stands for the erodibility of the soil surface (e.g. Beven and Kirkby, 1979; Kirkby, 1987). By definition this K_{es} factor incorporates many properties of the soil surface including crusting and land use. This factor should not be confused with the Universal Soil Loss Equation (Wischmeier and Smith, 1958) erodibility factor K. Nevertheless both factors comprise numerous local surface characteristics and resulting variability is considerable (Torri et al., 1997). When the sediment transport rate becomes higher than the transport capacity because of decreasing gradients in slope or discharge, the excess of sediment is deposited by sedimentation taking into account the settlement factor P_{es} (Eq. 3.5).
Runoff routing is simulated with both steepest descent and multiple flow directions. The steepest descent flow routing divides the runoff towards one single cell with the steepest gradient and is also called the D8 method (Moore et al., 1991). This as opposed to multiple flow directions of Holmgren (1994) where in case of multiple downslope neighbours a weighted fraction of the collected run-on in a grid cell is divided over all lower neighbours (Eq. 3.6). The same weighted division then applies for calculation and evaluation of the sediment transport rates (Eq. 3.2) since water routing and evaluation of the transport rates and capacities are performed simultaneously. This means processing on the moment that the water balance is known, which enhances the diverging and converging properties of the landscape (Schoorl et al., 2000).
Available water for crop growth is an important land quality within the dynamic landscape context. Factors determining available water for different soil units are e.g. texture, bulk density, organic matter and effective soil depth which are related to the effective rooting depth of the crop considered. Local on-site processes can cause considerable differences in net decreasing or increasing soil water (Bouma and Droogers, 1999). However, since our focus is on the influence of the landscape, we have chosen in this study to define available water for any soil unit as the difference in water content between -10 [kPa] and -1500 [kPa] and as a function of the effective soil depth (see Fig. 6.1c). The on- and off-site effects on soil water are reflected through changes in soil depth due to erosion and sedimentation.

6.2.3 Input parameters and scenarios

In addition to the topographical potentials of the DEM, precipitation is the principal input parameter. The spatial and temporal distribution of rainfall in this Mediterranean area is highly variable (Pardo Iguzquiza, 1998; Renschler et al., 1999). For example mean annual rainfall ranged from 248 [mm] in 1994 to 1052 [mm] in 1996 at Álora Estación. However, since we want to demonstrate the spatial impact of slope and soil related landscape sensitivities we assume constant mean annual rainfall for all scenarios, neglecting these

effects of climate variation. The effect of altitude on annual rainfall amounts was calculated following the linear regression (r^2 of 0.63) established by Pardo Iguzquiza (1998) giving annual rainfall R_a [m] at altitude a [m] as:

$$R_a = 0.402 + 5.27 \cdot 10^{-4} a \qquad (6.1)$$

The mean annual rainwater retention and evaporation loss in this region is approximately 75% of the precipitation, based on measured mean annual discharges in various tributaries in the Guadalhorce River basin, leaving 25% of the annual rainfall as run-off (e.g. CHS, 1974). Since land use in the region is related to the parent material, effects of different land uses are considered constant in both time and space to allow for specific evaluation of the main scenario parameters. We formulated four scenarios (A to D) with increasing topographic and soil related complexity. The last scenario (D) is considered as the most realistic one (Table 6.1). The simulation period was 10 years with a time step of 1 year, resulting in a yearly update of the input parameters such as soil depth, topography and available water storage capacity.

Scenario A is the baseline condition for all experiments, showing only few landscape dynamics, as implied by the aforementioned inputs. All soil related parameters are assumed uniform and constant, soil depth is set at 2 [m], storage capacity at 0.132 [m]. The K_{es} and P_{es} factors are calibrated on a standard value for the whole area, giving soil losses comparable with other studies in this region (e.g. Poesen and Hooke, 1997; Renschler et al., 1999). The calculations of the transport rate and the distribution of the collected run-on are made by routing the runoff towards the steepest downslope (SD) neighbour cell (Moore et al., 1991).

Scenario B introduces the first step towards a more dynamic landscape concept by applying the multiple flow (MF) direction algorithm (Eq. 3.6) to all parameters of scenario A. The weight factor p of Eq. 3.6 is set at 4.0 for the topography in the research area following the experiments of Holmgren (1994). This scenario will introduce the diverging properties of the topography, since the grid cell size of 100 [m] in this study is far below the effective (mean) slope length in the research area of over 400 [m], resulting in a sufficient number of grids representing the slope.

Scenario C implements the initial soil depths of Fig. 6.1c. As a result every grid cell has its own separate capacity for annual infiltration and storage. Due to storage limits, shallower soils will generate more runoff than other areas with deeper soils. As a result within (sub-) catchments redistribution of the runoff will take place. We calibrated the model by adjusting the infiltration loss so that the total mean annual runoff leaving the catchments and sub-catchments equals to the previous scenarios.

Scenario D, finally provides different K_{es} (erodibility of the surface) factors for each soil type. A simple relationship is used in assigning lower K_{es} values to the more resistant parent materials in relation to their actual soil depth. Data on different K_{es} factors were aggregated from qualitative field observations, bulk density and literature review on different parent materials (e.g. Kosmas et al., 1997; Cerdá, 1999; Romero Diaz et al., 1999). Following the major soil units of Fig. 6.1b, final K_{es} factors used in this study ranged between 1.10^{-5} and 3.10^{-5} [m^{-1}] (Table 6.1).

Table 6.1 Main scenario input parameters for water routing, soil depth and erodibility.

	Duration [a]	Timestep [a]	Routing	Soil depth [m]	K_{es} factor[§] [m^{-1}]
Scenario A	10	1	SD[†]	2.0	2.10^{-5}
Scenario B	10	1	MF[‡]	2.0	2.10^{-5}
Scenario C	10	1	MF	0.1 – 1.2	2.10^{-5}
Scenario D	10	1	MF	0.1 – 1.2	1.10^{-5} - 3.10^{-5}

[†]steepest descent
[‡]multiple flow direction
[§]sedimentation factor P_{es} equals erodibility factor K_{es}

6.3 Results and discussion

6.3.1 Water redistribution

The run-off pattern of scenario A is presented in Fig. 6.2a. It shows a typical pattern generated by many of the standard modeling approaches and Geographical Information Systems (GIS) using a steepest descent flow routing (Moore et al., 1991). The central channel in the middle of the graph collects most of the runoff and transports the water out of the area at the lower middle (south) boundary. Note that the total runoff does not change as a result of different routing algorithms in scenario B as long as the annual precipitation, evaporation and infiltration balance remains the same. However, the pattern inside sub-catchments does change considerably going from scenario A to B (Fig. 6.2b) because of the effects of more divergent routing. These changes, after implementing the multiple flow direction algorithm of Eq. 3.6 in scenario B, can be found on both the slopes and in the channels of the sub-catchments. In general the water is allowed to diverge more on the irregular and convex slopes, increasing the length of the flow paths and narrowing the water divide (compare Figs. 6.2c and d). As a result in upland areas less water is flowing directly towards the upper parts of the channels although the total discharge from each catchment does not change (Desmet and Govers, 1996; Tarboton, 1997).

Resulting differences in runoff comparing scenario A and B to scenarios C (Fig. 6.2e) are directly related to the effects of different soil depths, allowing less or more water to be stored and infiltrated. In this way these imposed scenario conditions cause the shallow soil areas (e.g. soils on limestones, serpentinites) to generate more runoff, while areas with deeper soils (e.g. soils on marls) generated less runoff which is consistent with field measurements (van Wesemael et al., 2000). When only considering scenarios C and D the initial runoff patterns will not have any influence since they will be the same for each scenario. However, after the first time step of one year, erosion and sedimentation patterns started to change initial soil depths and topography throughout the area differently for each of the scenarios. As a result after the first year during the next time step runoff patterns started to change as well between scenarios. This implies that when analysing terrain attributes from a DEM (e.g. Boer et al., 1996; Tucker et al., 2001), such attributes need to be evaluated for each step in time of the model.

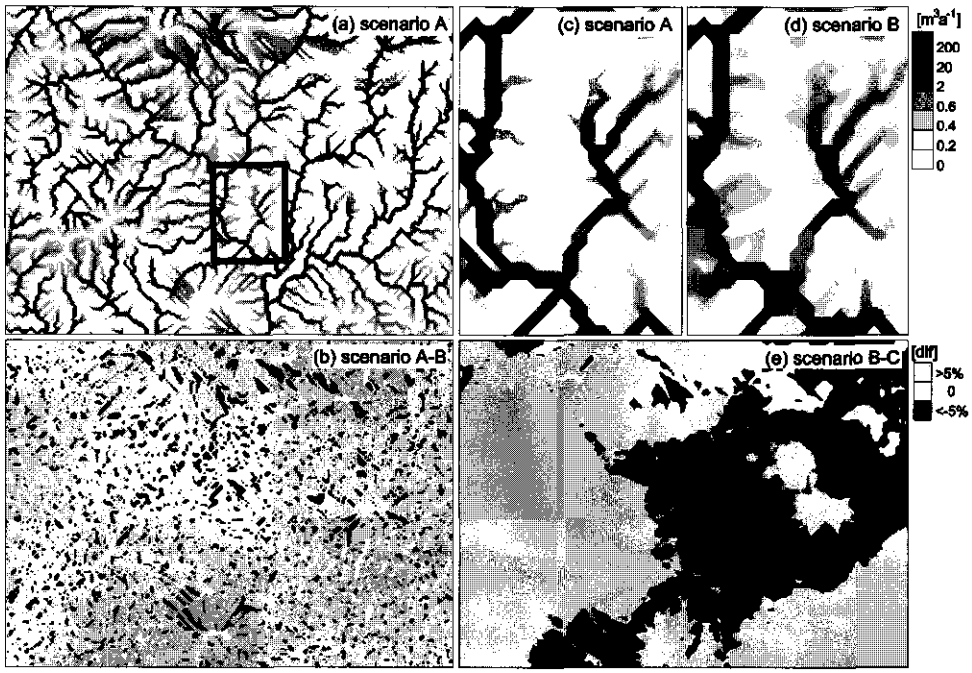

Fig. 6.2 Water redistribution with (a) runoff patterns of annual rainfall excess under standard scenario A conditions, (b) changes in runoff between scenario A and B using MF instead of SD, (c) detailed area indicated in (a) with SD, (d) detailed area with MF and (e) changes in runoff between scenario C and D.

6.3.2 Soil redistribution

An example of erosion and sedimentation patterns for scenario D is plotted in Fig. 6.3. In general lower erosion rates are situated on low gradient slopes, especially near the center of the study area. Higher erosion rates can be found along the major tributary channels (high discharges) and, for example, on some steep slopes in the north of the study area (Fig. 6.3a). Sedimentation in the landscape is located on the longer slopes and valley bottoms of the area (Fig. 6.3b). Higher sedimentation rates can be found mainly in the central river terrace area where tributary channels lose their energy in the flatter river plain. This can also locally happen in the tributary channel itself because of changes in channel gradient and lateral sediment budgets.

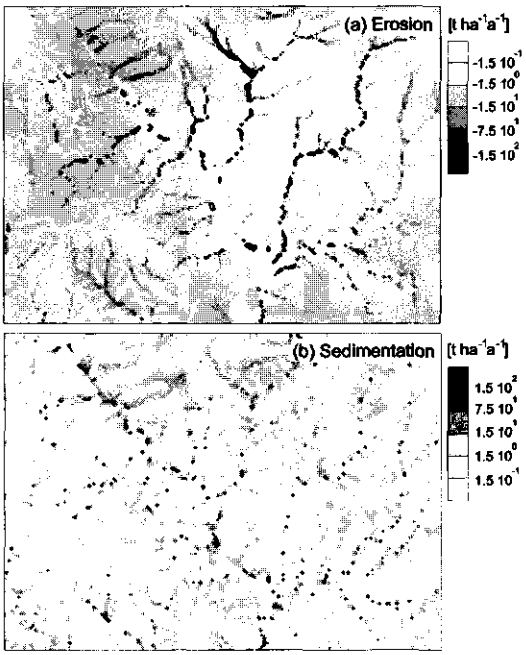

Fig. 6.3 Example of annual soil redistribution in the landscape for scenario D (a) erosion and (b) sedimentation.

In Table 6.2 simulation results for the different scenarios are presented with mean erosion and sedimentation rates and net soil loss for the whole area. In general, erosion rates are dominant over the sedimentation rates although both react differently to the implemented scenarios. In this case erosion rates increase some 8%, while sedimentation rates increase up to 64% after introducing landscape dynamics (scenario D). Comparing all scenarios, the largest changes occur for erosion from scenario B to C, indicating the effect of increasing runoff rates on steep slopes with shallow soils. Implementing the multiple flow directions resulted in the largest changes in sedimentation rates between scenario A and B. This is clearly an effect of increasing flow directions and therefore lowering the dominant down slope flow gradient and increasing the lengths of flow paths (Schoorl et al., 2000).

Table 6.2 Mean annual soil redistribution rates in metric tons per hectare and percentages of change between scenarios.

Scenario	Erosion				Sedimentation				Net soil loss
	[t ha^{-1}a^{-1}]	%A	%B	%C	[t ha^{-1}a^{-1}]	%A	%B	%C	[t ha^{-1}a^{-1}]
A	-8.1	-	-	-	1.2	-	-	-	-6.9
B	-8.4	4	-	-	2.1	71	-	-	-6.3
C	-9.3	14	10	-	2.2	73	1	-	-7.1
D	-8.8	8	4	-5	2.0	64	-4	-5	-6.7

To find out where these changes occur in our study area, we have plotted differences larger than 5% in maps of both erosion (Figs. 6.4a to 6.4d) and sedimentation (Figs. 6.5a to 6.5d) between different scenarios. Figure 6.4a shows the shifting erosion patterns from scenario A to B. Changes occur randomly over the whole area more or less consistent with the shifting of the drainage patterns indicated in Fig. 6.2b, stressing the importance of flow routing algorithms used in modeling (e.g. Quinn et al., 1991; Desmet and Govers, 1996; Tarboton, 1997; Yin and Wang, 1999). Sedimentation patterns in Fig. 6.5a show the dominant increase related to the improved simulation of divergent properties of the landscape.
Introducing initial soil depths from scenario B to C (Fig. 6.4b) shows a general trend of larger areas with more erosion (the higher areas of Fig. 6.1) and the lower areas with less erosion. As indicated above this is the effect of the shallower soils on the steeper slopes that cause more runoff and generate more streampower. An unexpected effect is that not only soil units as whole are affected by increased or decreased erosion, the off-site effects also influence areas located down stream. For example increased erosion is found especially along major tributary channels (Fig. 6.4b) and increased sedimentation is found in the central river area (Fig. 6.5b). Sedimentation shows on-site effects on local spots with isolated increased sedimentation rates due to the excessive sediment delivered to these locations and changes in channel gradients (Fig. 6.3b).

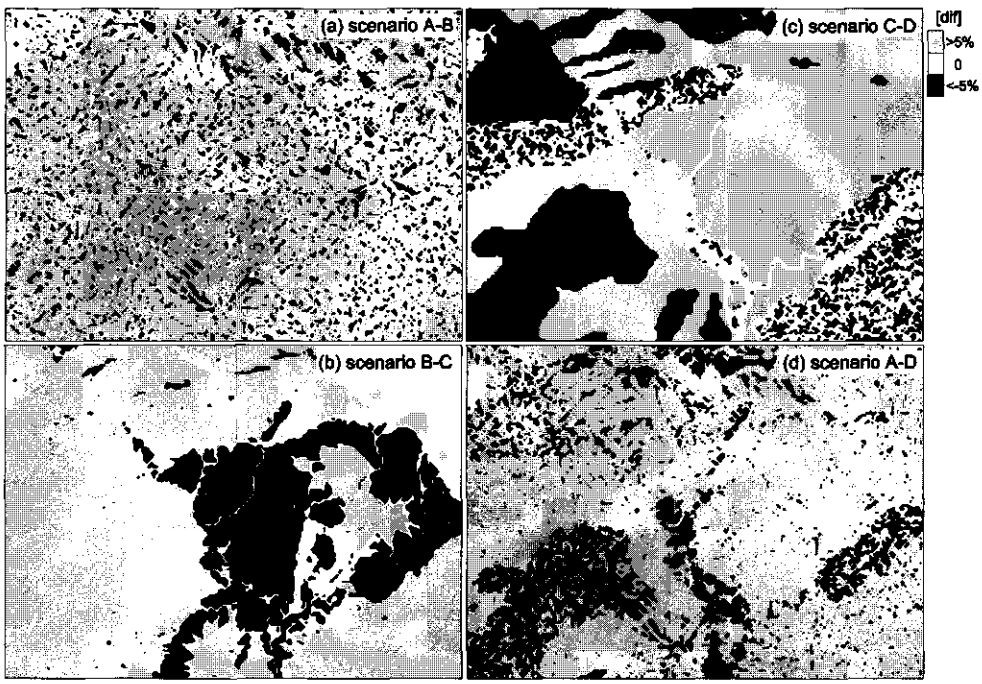

Fig. 6.4 Changes in soil erosion patterns, shown with 5% decreasing or increasing threshold for (a) scenario A to B, (b) scenario B to C, (c) scenario C to D and (d) total change from scenario A to D.

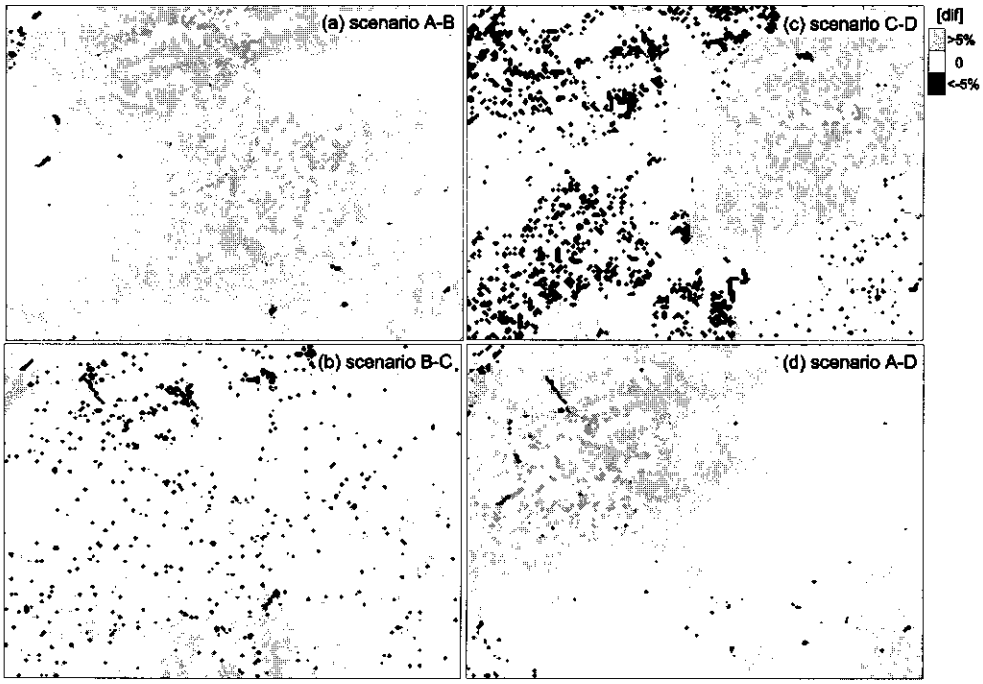

Fig. 6.5 Changes in sedimentation patterns, shown with 5% decreasing or increasing threshold for (a) scenario A to B, (b) scenario B to C, (c) scenario C to D and (d) total change from scenario A to D.

Patterns of change after implementation of different K_{es} factors, which represent mainly the erodibility of the parent material, are shown in Figs. 6.4c and 6.5c. This case represents the opposite effect than in Fig. 6.4b. Lower areas show increased erosion while the higher areas reveal less erosion (Fig. 6.4c). In addition, sedimentation decreases although not for the soil unit as a whole but much more segregated on the slopes (Fig. 6.5c). This is the effect of the softer and more erodible parent materials on lower positions in the landscape, while harder parent materials including bedrock are situated in the higher elevated areas. Therefore, when less soil material can be detached upslope, it causes less soil to be re-deposited on the lower slope positions.

Finally the maps of Figs. 6.4d and 6.5d show the cumulative results of changes from scenario A to D, implementing the most dynamic scenario in our simulations. Although areas of increased erosion dominate in Fig. 6.4d, this effect is compensated by increased sedimentation in the river terrace area (Fig. 6.5d) and decreased erosion in the upland areas giving the same net soil loss for both scenarios (Table 6.2). Thus, without spatial explicit information about true on-site and off-site effects, general indications of changing erosion or sedimentation rates remain difficult to interpret. Still, with adequate field data the present methodology offers the possibility to locate and quantify these landscape processes. For example with the ^{137}Cs-technique (Walling and Quine, 1990) which can provide landscape wide soil redistribution data at the adequate temporal resolution (years and decades).

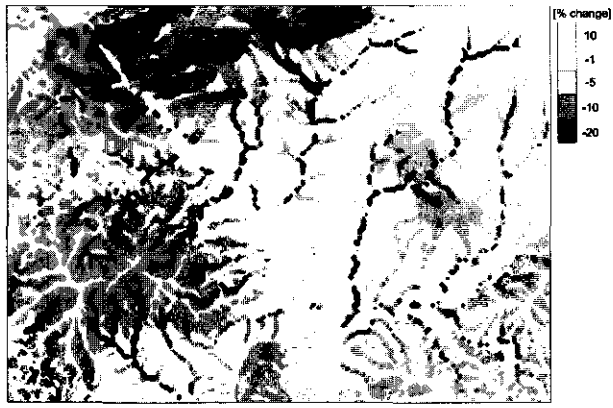

Fig. 6.6 Changes in available water storage capacity for scenario D compared with scenario A.

6.3.3 Available soil water

Spatial distribution of changes in available water (AW) in the study area for this chapter is presented in Fig. 6.6 for scenario D. The majority of areas with a decreasing AW are located in the north and along tributary channels especially in the gneiss (GN) and serpentinite (SP) area. Here the shallow soils are more prone to soil loss, as opposed to increases in AW of more than 10% in the central river valley. To illustrate the effects of our scenarios, 4 major soil units were chosen comprising different parent materials (Table 6.3). Since the AW is related to effective soil depth, we have only considered scenarios C and D here.

Table 6.3 Initial mean soil depth, available water (AW) as percentage of soil volume, AW mean amounts for initial soil depths and changes in AW and soil loss after 10 years of simulation for the study region and landscape units.

	Initial			Simulation			
	Soil depth	AW		Scenario C		Scenario D	
†	[m]	% vol	[mm]	ΔAW [mm]	Soil loss‡ [t ha^{-1}a^{-1}]	ΔAW [mm]	Soil loss‡ [t ha^{-1}a^{-1}]
Region	0.35	-	-	-	-7.1	-	-6.7
RI	0.96	0.146	139.6	1.36	14.9	1.7	15.1
MA	0.54	0.118	63.5	-0.51	-4.8	-0.79	-8.9
MO	0.13	0.102	13.4	-0.43	-5.6	-0.31	-2.9
GN	0.19	0.073	13.7	-0.58	-10.7	-0.63	-9.2
GNup	0.14	0.073	10.4	-0.11	-1.7	-0.06	-0.9
GNmv	0.17	0.073	12.3	-0.21	-3.5	-0.23	-3.8
GNmc	0.18	0.073	13.4	-0.3	-5.0	-0.33	-5.5
GNdo	0.24	0.073	17.5	-6.53	-108.7	-6.21	-103.1

†RI river terraces, MA marl, MO molasse, GN gneiss, GNup gneiss catena upslope, GNmv midslope convex, GNmc midslope concave and GNdo downslope.

‡Soil loss: negative value means erosion, positive value means deposition

Comparing different lithologies under scenario C (Table 6.3), gneiss (GN) shows greater soil and AW losses, the latter up to 0.6 mm, while the molasse (MO) and marls (MA) show less soil and AW losses than the mean regional soil loss rates (e.g. soil loss is erosion plus sedimentation, see Table 6.2), indicating an increased net soil loss from these areas. Under scenario D, however, soil and AW losses are increased for the marl area (MA) and decreased for the molasse (MO). At the river terrace area (RI) very high sedimentation rates, or a net soil and AW gain were found under both scenarios C and D.
Again these trends indicate that within a dynamic landscape, different soil units attribute in their own way to the overall picture. For example the soil AW increases in the river terrace area where soils are already deep and well developed (Table 6.3). Since this area already has more than 100 mm available water for vegetation these changes will not be significant. This is in contrast, however, with other areas such as serpentinites and gneiss that are loosing valuable topsoil and AW. These decreases can be serious, if the soil depth drops below the threshold for vegetation growth (e.g. Kosmas et al., 2000).
This study indicates that each soil unit should be taken into consideration in the landscape context. Comparing for example molasse (MO) and marl (MA), the latter unit has much deeper soils and is therefore less sensitive to a small change (Table 6.3). In this case the gneiss area (GN) is most vulnerable with shallow soils and high erosion rates. Consequently, the mean AW is likely to be depleted rapidly. Although the loss of AW seems hardly serious as it appears only to be a few percent, we have to consider that these values are the means of the entire area and the local variability can be detrimental at some sensitive locations.
A selected catena in the gneiss area is also presented in Table 6.3. In this case, the up-slope area shows low rates of change (GNup), with an AW loss of 0.1 mm. Here run-on from other areas is not important and only local factors affect soil loss. Data in Table 6.3 show significant differences between concave (GNmc) and convex (GNmv) mid-slope positions. Concave positions receive more run-on, which increases the local transport capacity and therefore show higher soil losses. The down-slope position is associated with an active eroding channel since soil and AW losses are extremely high, the latter more than 6.5 mm.
Differences among the different scenarios are closely linked to on-site and off-site effects. Under scenario D, the up-slope position shows a decreased on-site erosion and AW (Table 6.3). Consequently, the off-site effect is that at both mid-slope positions, there is more soil and AW losses (0.02 - 0.03 mm) because the transport capacities are not completely used upslope. These kinds of patterns on the concave and convex slope positions are also found by Gessler et al. (2000) for soil properties such as soil Carbon and soil bulk density. Even though their study is much more quantitative and more detailed, this shows that within a dynamic model a coarser resolution does not necessarily mean loss of information.

6.4 Conclusions

At the landscape scale, different spatial inherent properties and physical processes can contribute to the changing run-on, run-off, erosion, and sedimentation patterns. In this study we distinguish four major effects causing these changing patterns: 1) the differences in generation of run-on and run-off from different flow-routing algorithms; 2) the effect of changing infiltration patterns associated with initial soil depth; 3) the effect of soil erodibility; 4) the changing soil depths and topography during simulation. The first and last effects are more related to modeling techniques, while the other two effects have to do with the

implemented boundary conditions. However, they all imply both on-site and off-site effects in the landscape and different impacts for erosion and for re-sedimentation. Realistic modeling of processes in dynamic landscapes should at least include these effects.
When discussing and evaluating effects of soil redistribution one should always consider the landscape context. A net soil loss from a watershed does not reveal important spatial variation and implications. Erosion can become critical in one area while other areas can benefit from the net sedimentation. In the case of available soil water, it is important to know the interplay of soil depth, storage and infiltration at the soil profile level, and run-on and run-off, slope and parent material in their specific position in the landscape. Therefore, soil profile, catena or hillslope investigations will have to be combined into usable data for landscape analysis on the higher aggregation levels as discussed in this paper. Since quantitative data are difficult to obtain (by existing measuring techniques) and as a consequence calibration and validation are hampered on coarser spatial and temporal scales, the use of scenarios and modeling can provide a spatially explicit background for qualitative evaluation.

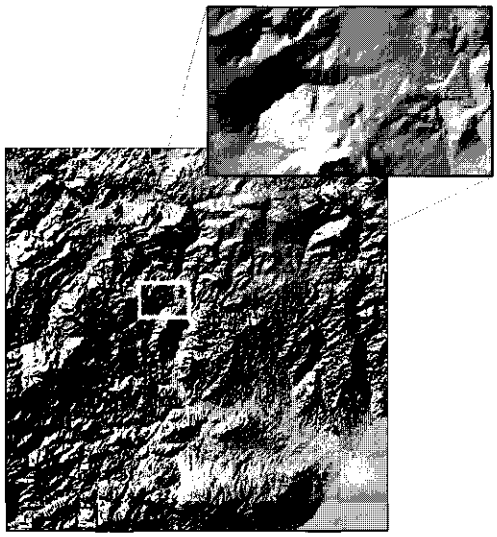

Chapter 7

Linking Landscape Process Modelling and Land Use

In this chapter the single process landscape evolution model LAPSUS, developed in Chapter 3, is used to explore the impacts of land use changes on landscape and soil properties. Examples are shown of both on-site as well as off-site effects of land use change and the influence of different pathways of change in the study area of this thesis. In this area the main land use consists of citrus, olive/almond, wheat, semi-natural vegetation and a rest-group (bare, river beds, urban). For a period of 10 years LAPSUS calculates soil redistribution (erosion and sedimentation) for different scenarios of input parameters. These inputs are a DEM (e.g. slope lengths and angles), precipitation, soil erodibility, and land use related infiltration. For each scenario different assumptions are made on the direction and rate of land use change. As an example the effects of abandonment of olive orchards are demonstrated, simulating both a fast and gradual change for a period of 10 years. Each scenario produces different spatial and temporal patterns of total amounts of erosion and sedimentation throughout the landscape. Consequently potential land use related parameters like soil depth, infiltration and flooding risk change significantly too. The scenario of an abrupt change produces the highest erosion rates, compared to the gradual change scenario and the baseline scenario. However, because of the multi dimensional characteristics of the landscape not only the area suffering from land use changes is affected. Increasing erosion and runoff rates from upstream-located olive orchards have an impact on down slope local run-on, erosion and sedimentation rates. In this case the citrus orchards situated in the valley bottom locally suffer damages from re-sedimentation events but benefit from the increase in run-on water and nutrients. Thus, the off-site effects from an exogenous driven change in land use (EC subsidies) might trigger endogenous land use changes in adjacent areas.

Based on: Schoorl, J.M. & Veldkamp, A., 2001. Linking land use and landscape process modelling: a case study for the Álora region (South Spain). Agriculture, Ecosystems and Environment 85, 281-292.

7.1 Introduction

It is well known that changing land use affects on-site landscape properties, for example soil degradation and increased erosion after deforestation. Processes causing these effects operate in all types of landscape, although they are not always that evident and show lower rates when there is a continuous vegetation cover. Landscapes are considered multi-dimensional with vertical (on-site) and horizontal (off-site) properties and processes. The most dynamic interactions between agro-ecosystems and landscapes involve water-related processes. Water as precipitation is partly intercepted, evaporated and taken up by vegetation after which the remaining water is released into the landscape by infiltration or runoff. This migrating water has the potential to change a landscape by weathering (infiltrated water), erosion (runoff) and sedimentation (run-on). These landscape-changing processes are thus directly influenced by the existing agro-ecosystems by water uptake or by slowing down the surface water, therefore stimulating infiltration. Land use has thus an effect on landscape processes, which, in turn, determine soil properties. If we consider a temporal scale of one year to one century we can focus our attention on erosion and sedimentation since weathering processes can safely be ignored.

7.1.1 On- and Off-site effects of land use

Land use change can affect soil properties in the landscape context, either in a positive or negative way. Deforestation, for example, will almost always negatively affect soil properties. In most cases this leads to short-term soil productivity loss (Veldkamp and Bouma, in press). The conversion of forest to grasslands and permanent crops such as plantations usually leads to less degradation after several years because these systems allow the soil to recover to some extent. Conversion from forest or grassland to arable lands is the worst scenario in terms of soil productivity and quality (e.g. Dick, 1992, Caravaca et al., 1999).
However, we have to keep in mind that these changes take place in a landscape context where landscape processes on-site often cause unintended off-site effects in sloping areas. For example a decrease of the infiltration for one land use can lead to on-site increased erosion and runoff rates. Consequently for other land uses in areas down slope this can cause an increased sediment delivery, an increase in water availability or even more erosion because of the increased runoff (Bathurst et al., 1996).

7.1.2 Dynamic landscape concept

Threshold effects are other typical aspects of landscape processes. Since the non-linear landscape processes tend to self-organise into stable domains they do not immediately respond to a shift in one or a few of its many controlling factors. When many controlling factors are changing or if their magnitude of change is very large, the whole system will reorganise itself into a new stable domain (Milne, 1991). Such reorganisations often happen suddenly and are viewed as catastrophic events. An apparent small change in one of its controlling variables, like a precipitation event, may trigger such a catastrophic event. It is as if the system is pushed over a threshold (Holling, 1992). It can take years of small events and changes in the landscape to bring it to the brink of such a reorganisation. Examples of such catastrophic events are abrupt land use changes like abandonment, landslides, mudflows, large erosion and deposition events, but also fire, pests and diseases represent natural effects of ecosystem reorganisation. For example forest fires in the Mediterranean, in addition to

changing the vegetation, can alter soil properties like clay content, aggregate stability and water retention capacity (Boix Fayos, 1997). Again within the landscape context this will not only affect on-site but will also have off-site impacts.

7.1.3 Mediterranean land use changes

In addition to the intense deforestation since roman times, land use has changed significantly in the Mediterranean region in the last decades (e.g. Le Houerou, 2000). Imeson et al (1998) mention several key processes such as on the one hand population growth and development of industry, tourism and modern irrigated agriculture and on the other hand land abandonment in marginal areas because of economic and environmental factors. Since the founding of the European Community a third factor can be added namely the influence of European Community directed policies. Their main influence consists of subsidies and price controls. For example for olive orchards the current OCM (Community organisation of the olive oil market) implements intervention mechanisms to guarantee income levels, to modernise the production process and to stabilise prices and production. In recent years changes in these policies, market demands and available technology have triggered important transformations in olive tree cropping in southern Spain (Rallo Romero, 1998; De Graaf and Eppink, 1999).
The objective of this chapter is to reveal the effects of two different land use change scenarios upon the spatial and temporal distribution of landscape shaping processes. The single process surface erosion model LAPSUS of Chapter 3 is used to simulate changing erosion and sedimentation patterns within the landscape represented by a digital elevation model (DEM). The main land use related parameters incorporated in this study are infiltration, soil depth and erodibility. Both on-site and off-site effects for two scenarios of abandonment of olive orchards are exemplified and demonstrated.

7.2 Materials and methods

7.2.1 Geo-referenced base-line information

A Digital Elevation Model (DEM) with a spatial resolution of 25 [m] is the starting point for our grid based case study. For this uni-scale experiment we have chosen a detailed section just north of Álora of 17.12 [km^2] (Fig. 7.1). With a resolution of 25 [m] on an area extent of 5.35 by 3.2 km we obtain a grid of 128 rows by 214 columns (total 27392 grids). The relief for the study area shows altitudes ranging from 100 to 625 [m] above sea level.
Fieldwork, aerial photographs, satellite images and expert knowledge provide the basis for building the base-line maps for the study area. The main land use can be divided into 5 major classes (Fig. 7.2) namely 11 [%] annuals (wheat *Triticum aestivum*, chickpea *Cicer europea*), 26 [%] citrus (orange *Citrus sinensis*, lemon *Citrus limon*), 39 [%] olive (*Olea europea*) with some almond (*Prunus dulcis*), 19 [%] semi-natural vegetation (matoral and forest) and 5 [%] rest group (urban, bare, riverbed).
Soil types and properties of the area are described by Ruiz et al. (1993) and comprise typical catenas for semi-arid to sub-humid areas. Parent material and tillage practises have resulted in stony soils especially under olive and almonds. These soils are tilled several times a year, depending on the rainfall, to control weeds and improve infiltration (e.g. Poesen et al., 1997; Quine et al., 1999). Extensive fieldwork (soil description, sampling and depth measurements)

provided the resulting soil depth map (Fig. 7.1), which represents clearly the underlying geology, slope gradients and topographical position (De Bruin and Stein, 1998).

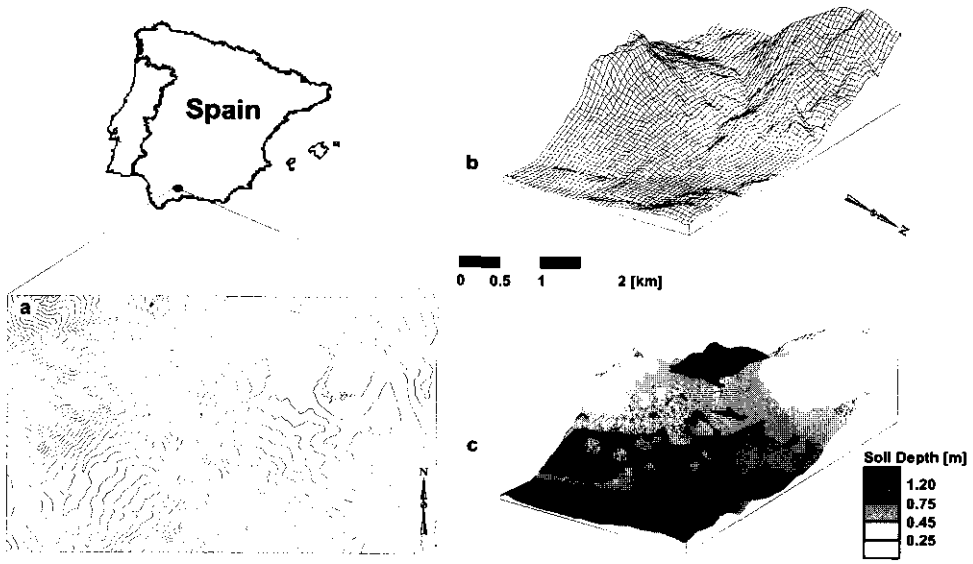

Fig. 7.1 Location of the study area in southern Spain including (a) the 20m contour line map, (b) the DEM and (c) the soil depth from deeper than 1.50m (shaded black) to less than 0.30 [m] (shaded white).

7.2.2 Landscape process modelling

For the calculation of the landscape dynamics the LAPSUS model is used (see Chapter 3). The LAPSUS model evaluates the rates of sediment transport (Eq. 3.2) by calculating the transport capacity of water flowing down slope from one gridcell to another as a function of the discharge and the gradient of the slope (Eq. 3.3). Surplus of capacity is filled by the detachment of sediment, which depends on the erodibility K_{es} [m^{-1}] of the surface (Eq. 3.4). This detachment of sediment provokes lowering of the surface or erosion. However, when the rate of sediment in transport exceeds the local capacity, for example because of lower gradients, the surplus of sediment in transport will be deposited by a settlement function causing a higher surface or sedimentation (Eq. 3.5). The routing of the overland flow and the resulting model calculations are done with a multiple flow algorithm (Eq. 3.6) to allow for a better representation of divergent properties of the convex topography (e.g. Freeman, 1991, Quinn et al., 1991, Holmgren, 1994). Our modelling framework was tested elaborately for the effects of changing flow algorithms, spatial resolution and temporal resolution (see Chapter 3). LAPSUS was only validated for its base scenario by field observations, it displays erosion and sedimentation patterns which match closely with real world erosion and sedimentation patterns at the same spatial resolution (25 by 25 [m]).

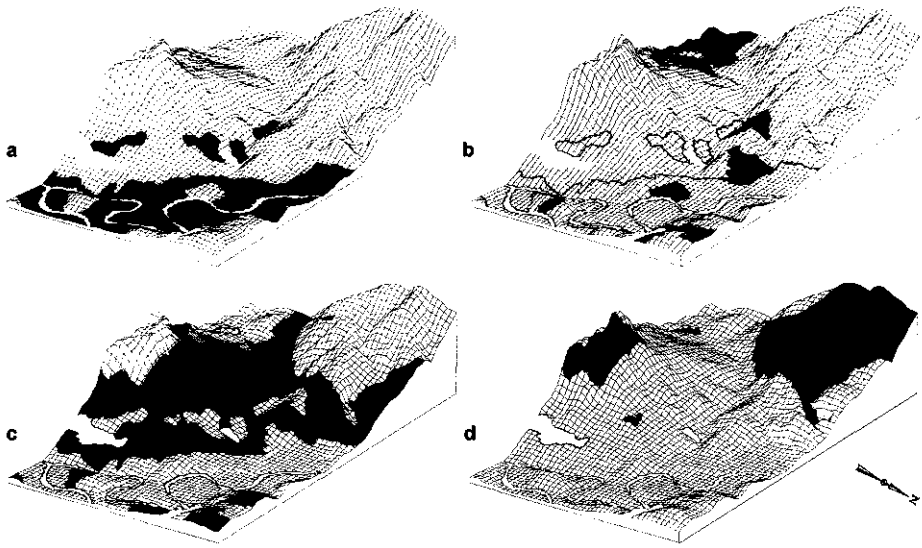

Fig. 7.2 Main land use in the case study area shaded black for (a) citrus, (b) annuals, (c) olive and (d) semi-natural vegetation with the rest group in white.

Table 7.1 Scenario input parameters depending on parent material and land use: surface erodibility (K_{es}), water retention capacity (AWC), surface erodibility factor (EF) and infiltration factor (IF).

	Parent material		Land use		
	K_{es} [m^{-1}][a]	AWC [$m^3\ m^{-3}$][b]		EF [-][a]	IF [-][a]
Colluvium	$7{\cdot}4\ 10^{-6}$	0·161	Citrus	0·5	1·0
Marls	$11{\cdot}1\ 10^{-6}$	0·105	Annuals	1·3	1·2
Sand/ gravel	$7{\cdot}4\ 10^{-6}$	0·151	Olive A	0·75	1·5
Schist	$6{\cdot}7\ 10^{-6}$	0·135	Olive B	1·5	0·75
Gneiss	$5{\cdot}2\ 10^{-6}$	0·066	Olive C	1·5/ 0·75	0·75/ 1·5
Conglomerate	$3{\cdot}7\ 10^{-6}$	0·055	Semi-natural	1·2	0·75
Serpentinite	$2{\cdot}2\ 10^{-6}$	0·044	rest	0·01	0

Olive A, B and C indicate the different scenarios

[a] literature/ model calibration

[b] reference profiles

7.2.3 Case study scenarios

Main input parameters for the grid-based LAPSUS model are the topographical potentials (slope gradients) from our DEM and the evaluation of the rainfall surplus that will generate the overland flow. Within each gridcell of 25 by 25 [m] we assume uniform conditions for all parameters involved. The model will evaluate all considered parameters on an annual basis

for a total run time of 10 years. For the scenarios given annual rainfall of 534 mm is considered to be constant over time and uniform over space, thus neglecting for example regional topographical effects.
The current situation is reflected in base scenario A (Table 7.1), which assumes that infiltration and erodibility depend on land use and underlying soil properties (e.g. Bonachela et al. 1999; Cerdá, 1999). Indicative values given in Table 7.1 are compiled from fieldwork, literature and model calibration (e.g. Nicolau et al., 1996; Kosmas et al., 1997; Oostwoud-Wijdenes et al., 1997; Vanderlinden et al., 1998). As a result the infiltration (I) for each grid cell is calculated as follows:

$$I = IF \cdot AWC \cdot d_s \tag{7.1}$$

where I is a function of soil depth [m^1] (d_s), water retention capacity [m^3 m^{-3}] (AWC) and management practises [-] (IF). Detachment of surface particles D [m^2 / s] depends on:

$$D = K_{es} \cdot EF \cdot Q \cdot \Lambda \tag{7.2}$$

where K_{es} is the erodibility of the parent material [m^{-1}], EF a surface management factor [-], Q is discharge [m^3 / s] and Λ the height difference or slope [-].
Scenarios B and C are two simple examples of the links between the different components of the system by implying an abandonment of olive orchards in this area. This could happen for example as a result of changing EC policies and subsidising systems (e.g. Rallo Romero, 1998, de Graaf and Eppink, 1999). The assumption is that for the 5 to 10 year simulation period infiltration decreases while the erodibility and runoff increase upon abandonment because of crusting and compaction of the soil (e.g. Boix Fayos et al., 1998; Renschler et al., 1999; Lasanta et al., 2000), poor regeneration of vegetation (e.g. Ruecker et al., 1998; Lasanta et al, 2000) and the lack of tillage practises (Gomez et al., 1999). In this case the scenario B uses an abrupt change of abandoning of all orchards within one year (see olive B parameters in Table 7.1), while scenario C implies a gradual annual change over 10 years of taking the olive orchards out of production. In this case the highest and steepest fields first, after 10 years the same values as for scenario B are reached.

7.2.4 Flooding risk

To evaluate the effects of changing land use we will use a simple indicator of flooding risk. For this case study the yearly flooding risk for each grid cell is calculated as a function of the distance to a channel, the discharge within that channel and the height difference with the channel bed.

7.3 Results

While presenting and discussing the outcomes of the simulated scenarios we have to take into account the different temporal and spatial levels used in this section and in Figs. 7.3 to 7.6. These temporal levels vary from cumulative 10 year means (Fig. 7.3 and 7.5) to yearly rates (Fig. 7.4 and 7.6) and spatially from grid level (amounts in Fig. 7.3 and 7.6) to land use units (Fig. 7.4 and 7.5) to total area (patterns of Fig. 7.3 and 7.6, and graphs of Fig. 7.4a and 7.5a).

Local erosion and sedimentation rates for each gridcell and their spatial distribution are presented in Fig. 7.3 for each scenario. Local erosion rates throughout the area for the 10 year period varied from 0 to more than 300 [t $ha^{-1}a^{-1}$], with means of 1.3, 2.2 and 1.7 [t $ha^{-1}a^{-1}$] for scenario A, B and C respectively. In general erosion rates are clearly higher in down slope areas, on the steeper slopes and in areas where the runoff is concentrated in channels. Sedimentation is mainly concentrated within specific points in the main channels and on the transition from the steep slopes to the more flat areas in the central valley. Sedimentation rates varied from 0 to more than 1.5 [t $ha^{-1}a^{-1}$].
The calculated annual amounts of erosion for the three scenarios in metric tons per hectare are given for the area as a whole in Fig. 7.4a and for the main land use types in Figs. 7.4b to 7.4f. Note the different scaling of the y-axis for Figs. 7.4a and 7.4b while comparing the amounts. Under baseline conditions (scenario A) areas under semi-natural vegetation show the highest erosion rates followed by annuals and olive just above the mean rates for the whole area. Citrus and the rest group show much lower erosion rates. In general for scenario B all erosion rates are higher except for semi-natural vegetation and the rest group. The highest erosion rates are found in the olive area, which cause also a major increase in the mean total amounts. Also the annuals and citrus show an increase in erosion rates resulting in even higher erosion rates for the annuals than semi-natural vegetation. Finally the general trend for scenario C is a gradual non-linear increase of erosion rates during simulation. For the area under olive this increase is slightly exponential, while for annuals the increase in erosion rates is less halfway the simulation. Exceptions are again semi-natural vegetation and the rest group, which hardly show any changes.

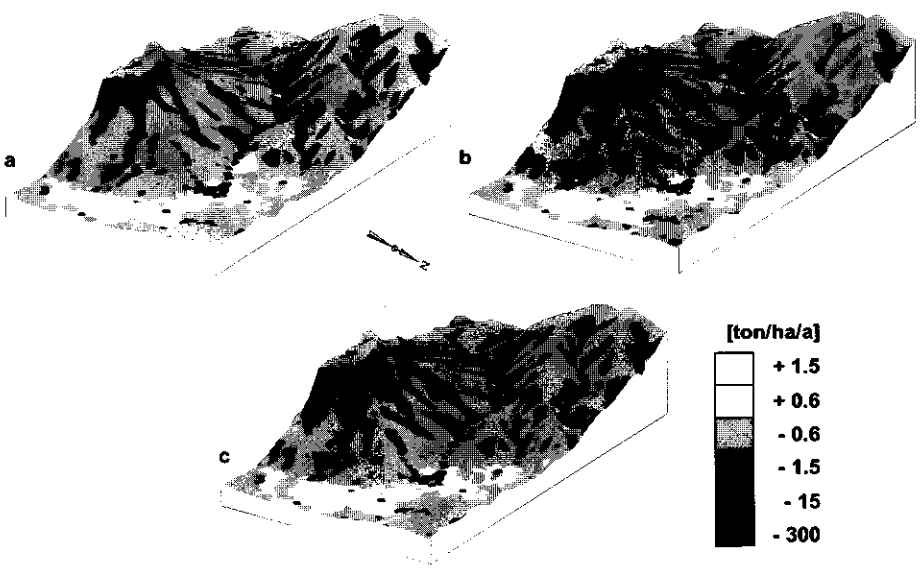

Fig. 7.3 Spatial distribution for the 10 year simulation period of total erosion (negative values) and sedimentation (positive values) for (a) scenario A, (b) scenario B and (c) scenario C.

Total cumulative amounts of sedimentation in metric tons per hectare are given for the whole area in Fig. 7.5a and per land use in Figs. 7.5b to 7.5f for the 10 year simulation period. Note the different scaling of the amounts for the rest group showing almost four times higher amounts of sedimentation than the other land uses. All land uses show an increase in re-sedimentation, except for the areas under semi-natural vegetation, giving a total increase going from scenario A to B of 71.9 [%] and from A to C of 7.3 [%]. As a rule the smallest amounts of re-sedimentation are found in the areas under annuals and semi-natural vegetation. Citrus and olive show larger amounts of re-sedimentation. While semi-natural vegetation does not show any effect of changing scenarios, olive shows the strongest increase of re-sedimentation quantities for scenario B and C of 159.6 [%] and 9.9[%] respectively. Followed by citrus (53.1 and 8.1 [%]) and annuals (16.8 and 4.9 [%]).

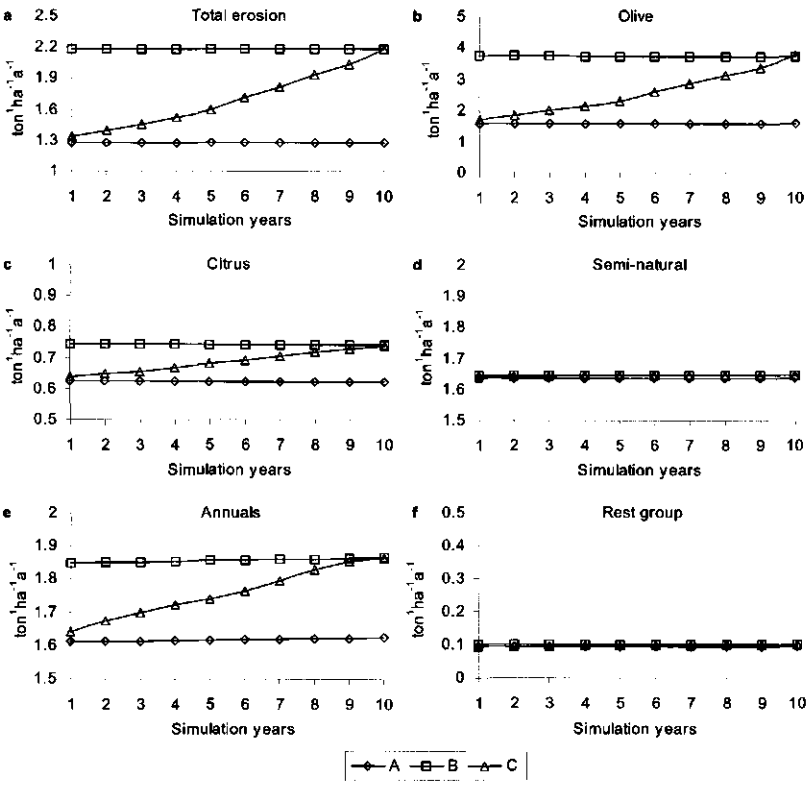

Fig. 7.4 Simulation of annual erosion for the scenarios A, B and C for (a) whole case study area, (b) olive, (c) citrus, (d) semi-natural vegetation, (e) annuals and (f) rest group. Note the different scaling of the y-axis for (a) and (b).

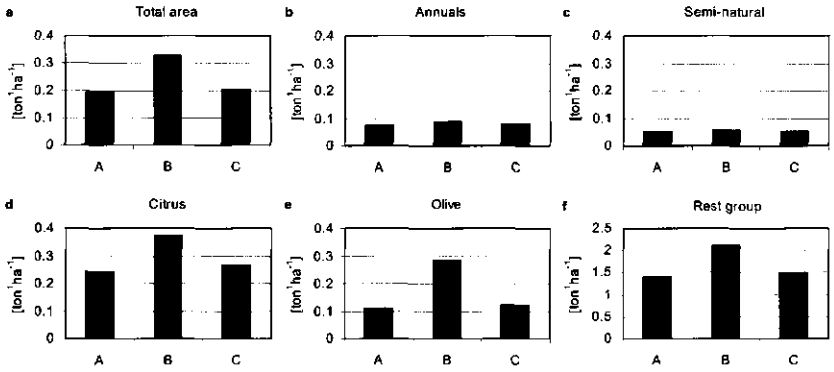

Fig. 7.5 Cumulative sedimentation for the simulated period and scenarios in metric tons per hectare for (a) whole case study area, (b) annuals, (c) semi-natural vegetation, (d) citrus, (e) olive and (f) rest group. Note the different scaling of the y-axis for the rest group.

7.4 Discussion

In this case study only a limited number of parameters have been used, which makes the model relatively sensitive to these inputs. Also not taken into account is the temporal variation of these parameters with the changing soil depths or vegetation regeneration. However, changing soil depths do affect the runoff during the simulation, which is one of the major variables in calculating the transport capacity and detachment capacity (Q in Eq. 7.2). The influence of vegetation regeneration is considered minimal for the 5 to 10 year simulation period (Ruecker et al., 1998, Lasanta et al., 2000) and the effect of no tillage will dominate the infiltration characteristics (Gomez et al., 1999). Nevertheless together with the temporal resolution of 1 to 10 years this provides a simple and realistic example of an easy to adapt scenario driven comparison at the landscape level. For example the K_{es} factor (Table 7.1), in our case study, aggregates many surface characteristics (including tillage and crusting) at a large spatial resolution. Although our K_{es} factor not comparable by definition, the variability in these type of factors is high even under standardised conditions as is clear from numerous K-factors found in USLE related studies (e.g. Torri et al., 1997).

7.4.1 Case study area general impression

Although at first sight, the overall impression of the erosion and sedimentation rates in Fig. 7.3 seem not to differ very much between scenarios, when concerning the patterns within the landscape we can see the different influence of the scenarios within the land use units. Not the unit as a whole, but certain confined areas react more than other areas do (Puigdefabregas et al., 1998). These main patterns are determined by the underlying topography and the resulting drainage network, while the actual rates and impact of the erosion and sedimentation are determined by the parent material and land use (e.g. Cerdá, 1998; 1999). Comparing the spatial distribution for the three scenarios shows the impact of the olive abandonment especially in the mid-slope areas where the largest changes in the erosion and sedimentation

patterns can be found. However, also without any land use change (scenario A), the landscape will still be altered by the natural processes of landscape evolution.

7.4.2 On-site land use effects

In spite of the general trends during the simulation for scenarios A and B and increasing erosion rates for scenario C, the actual rates for each land use differ considerably (Fig. 7.4 and 7.5). They range from almost 3.7 [t $ha^{-1}a^{-1}$] for olive in scenario B to less than 0.62 [t $ha^{-1}a^{-1}$] for citrus under baseline conditions. The same holds true for the re-sedimentation as mentioned in the previous paragraph although there the citrus shows the highest and the annuals show the lowest rates.

Erosion rates for olive in this case study are moderately high compared to rates given by Poesen and Hooke (1997). However their data was compiled from different land uses, slope gradients and parent materials on small scale plot studies without major channels and gullies. Romero Diaz et al. (1999) give some differences in erosional response between olive and abandoned fields in the Mediterranean but their abandoned fields do not originate from olive orchards. In addition, erosion studies mentioned by Kosmas et al. (1997) show almost no erosion for olive in Greece because of management practises (no tillage, dense undergrowth). The question remains whether this example from Greece would be a possible scenario for the degraded environment of south Spain (Ruecker et al., 1998, Gomez et al., 1999, Lasanta et al., 2000). On the other hand our erosion rates seem low compared to rates found at the field level for olive orchards by Laguna and Giraldez (1990), indicating the potentials of many years of tillage erosion. Their results could indicate a slight underestimation of tillage erosion in our initial K_{es} factor for the scenarios, although important parameters at the landscape level as slope gradient, slope length, parent material and stoniness are different for the Álora region.

Since the topographical potentials move the water and sediments down slope, only areas down slope of olive areas will be affected. As a consequence the citrus area, located in the valley floor, reveals the largest impact followed by the annuals. Semi-natural vegetation however is hardly affected by the scenarios because most of the as semi-natural vegetation classified areas are located in the landscape upslope of the olive fields. An exception to the general erosion and re-sedimentation rates is the rest group because of the fact that for urban areas and the riverbed the erodibility K_{es} was set to 0.

7.4.3 Off-site effects: flooding risk

Comparing scenarios A with B and C it was to be expected that olive would reveal an increased erosion since the scenario directly alters the input parameters for infiltration and especially erodibility. Of course this increase is not uniform and visualisation of the patterns in the three-dimensional landscape show the important relationship with the main parameters as slope length, slope angle and discharge. Nevertheless, the input parameters for the other land uses did not change, so the encountered differences (see Fig. 7.4 and Fig. 7.5) are a direct off-site result of changes in our dynamic landscape. In this case the increased erosion, the decreasing soil depth and decreasing infiltration of the areas under olive provoke an increasing runoff and sediment in transport into the other areas.

An example of this off-site effect is given in Fig. 7.6 where a simple evaluation is given for the risk of flooding. First of all the areas in Fig. 7.6a which are most prone to flooding also are the most affected ones by the off-site effects of the scenarios in Figs. 7.6b and 7.6c. The mid-slope on-site changes in the olive orchards trigger increased flooding in the whole valley

area where no olive orchards can be found. Increasing amounts of runoff from the slopes are diverged into the channels, which continue to collect all extra runoff until the river is reached and the water leaves the case study area. Especially vulnerable areas are the sharp river bends, inner terraces and the alluvial fan area where the catchment drains into the central river valley. In our case study all these areas are used for citrus, which consequently have suffered flood damages in the past.

7.4.4 Pathway of change

As shown in the previous sections, when considering the pathway of change, the total impact of scenario B is much higher than scenario C. This holds true for erosion rates, re-sedimentation and flooding. However, the different responses comparing B and C are not linear. Accumulating the effects over the 10 year period suggests that gradual change of scenario C causes 53 [%] less erosion and even 90 [%] less re-sedimentation. Apparently the threshold effect of a sudden land use change in scenario B triggers slightly more erosion and much more re-sedimentation than the gradual change of scenario C.

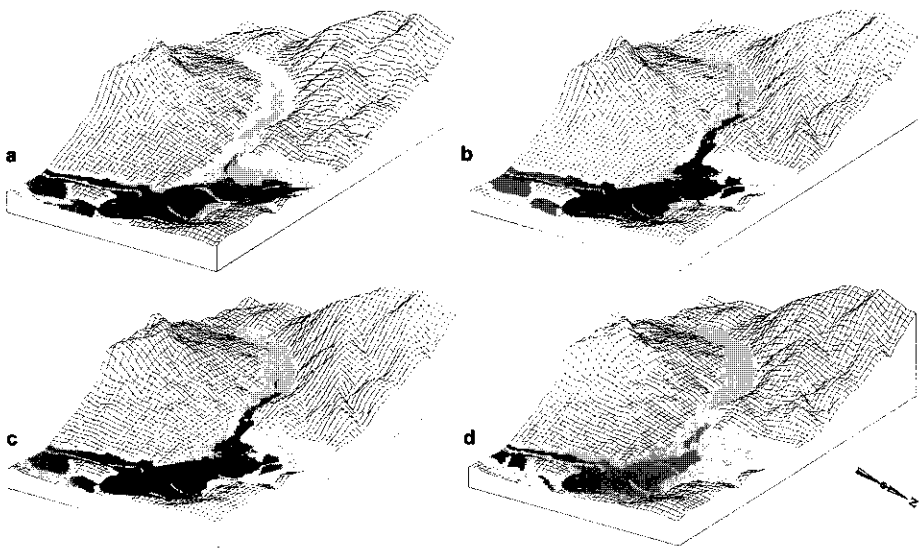

Fig. 7.6 Flooding maps for (a) the first time step T=1 (valid for both A and C scenario), (b) increase for the last time step T=10 of scenario B, (c) increase for the last time step T=10 of scenario C and (d) increase for the fifth timestep T=5 of scenario C. White (low) to black (high) grey scale indicates increasing flooding.

However, the increased flooding risk map of Fig. 7.6b for scenario B is relatively stable for every single simulation year, since the most important flooding factor is the discharge. This is in strong contrast with scenario C where the flooding maps of Fig. 7.6c and 7.6d change considerably (after 10 and 5 years of simulation respectively) since every year there are less

olive orchards left and more runoff and erosion is generated. As a result the final flooding map of scenario C in our last simulation year in Fig. 7.6c resembles to and shows a similar impact as Fig. 7.6b. Even in the case of a gradual change scenario C if we do not alter the consequences of the simulated land use change by conservation measures or stimulating vegetation regeneration (e.g. De Graaf and Eppink, 1999, Lasanta et al., 2000) the final result, as far as annual erosion rates and increased runoff are concerned, are similar for both scenarios.

7.5 Conclusions

In this case study we demonstrated that in the landscape system the on-site consequences of land use change can result in major off-site effects. Of major importance for the impact of changes in land use is the position of a certain land use within the landscape. Concerning the simulated landscape processes the most important changing rates as a consequence of a land use change are runoff, run-on, infiltration, erosion and re-sedimentation. These changes occur both on-site as off-site of the land use under change. Changes in upland areas will influence both mid-slope and downslope areas. On the other hand upland areas receive initially less water than mid-slope areas and the impact will be less intensive. In addition, the effects will not be limited to the case study area alone. For example the increased runoff and sediment transport will eventually enter and possibly alter the down stream part of the whole river drainage system.

In our scenario examples we have simulated the impact of changes in landscape processes originated from changes in olive orchards. These orchards are mainly situated on mid-slope positions and as a result the on-site changes show off-site consequences for areas located down slope and in the valley floor. Future European policies on olive oil production can proof the significance of scenarios on olive field abandonment as an example of the impact of one land use change upon the landscape and other land uses. Implications of these types of changes in policies for subsidising crops can have serious influences on the biophysical landscape and the agro-ecological system as a whole.

These scenarios have also clearly demonstrated the dynamic interactions between land use and erosion/sedimentation. Especially the off-site effect might trigger unintended side effects. The significant increase of sedimentation on the valley bottom might hamper the citrus growth or destroy citrus plantations. Thus the decision to change the olive land use might indirectly drive a change in the citrus. This is a clear example of the feedback mechanisms of land use change. An exogenous driven change in land use (EC olive subsidies) might trigger endogenous land use changes in the citrus due to the off-site effects of the olive abandonment.

The model presented in this paper can be used as a tool to explore possible effects of certain land use changes within a dynamic landscape context. All type of changes affecting the infiltration and erodibility can be evaluated within the model, including management practises. Also the other way around, the effect of changes in landscape dynamics upon land use can be evaluated, for example variations in precipitation. The current model is far from complete since it only calculates effects of water erosion and re-sedimentation. Other relevant regional processes like land sliding, slumping and related mass movements are not included. Nevertheless, despite these limitations the model is able to catch overall landscape system dynamics quite well.

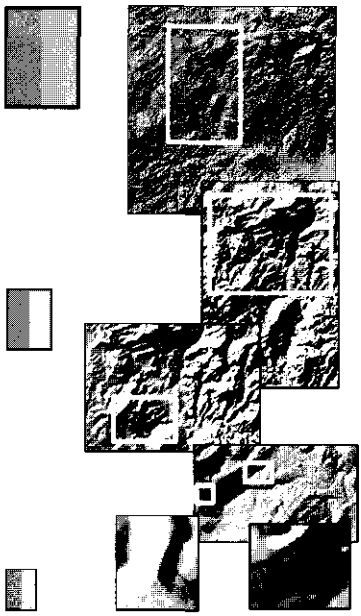

Chapter 8

Synthesis

This final chapter will address the most important issues of this thesis to synthesise the implications and to indicate possible improvements and future research. As has become clear from the previous sections, this study is necessarily made at different spatial and temporal levels within the landscape. Such an approach implies consideration of spatial and temporal resolution-extension related topics. Therefore, the level of observation needs to be specified and placed in the context of its boundaries and limitations. Especially where coarse resolution seems automatically related to large areas and long-term processes as opposed to fine resolution in small areas with short-term processes. However, this is not necessarily always the case and maybe the most interesting field of investigation are those areas where different scale levels interchange. The first part of this chapter will be dedicated to the more technical aspects of the applied models in this thesis. The second part comprises the coupling and integration of the results from the different chapters and the final part will discuss the possibilities of future research.

8.1 Landscape and the use of models and DEMs

8.1.1 Modelling techniques

In general specific technical details seldom are available for existing modelling techniques of which TOPMODEL is one of the exceptions (Beven, 1997). Nevertheless, even when these models are extensively described and tested the actual source code and modelling techniques often remain a blackbox. Also most existing models are event based and require large amounts of high resolution temporal and spatial data. However, one could argue whether these event based catchment models address the valid processes for annual landscape development. Therefore, the development of a simple landscape evolution model seemed justified. Consequently, the development of LAPSUS provided many insights on technical modelling aspects, including calculation errors. Certainly it provided the model developer with control on every parameter, calculation step and simulation outcome (see Appendix).
One of the major assumptions within this thesis is the validity of the LAPSUS model at the landscape-annual scale. The underlying theory of the potential energy content of flowing water over a landscape surface and the continuity equation for sediment movement are rather process based. Stretching the temporal and spatial scales of these actual processes from

seconds or hours per centimetre towards annual rates per hectare goes against the human perception and challenges the theoretical and physical background. However, a model is by definition a strong simplification of reality and actual conditions. Therefore, the assumption that every year a certain amount of water flows over a surface and causes a certain amount of sediment in transport seems also justified. Furthermore a model is only a tool to calculate and visualise the modeller's perception of the geomorphological response of a particular system (Beven, 1997). Consequently in this thesis, the system under consideration was the landscape and net annual effects were mimicked with one single time step.

Considering the spatial components, the LAPSUS model is a process based model using finite elements to simulate soil redistribution by flowing water over a length of surface. The question is how long and how wide can this finite element become? With the assumption that as long as the simulated length and corresponding gradient represent a slope segment, any size could be valid. Examples from hydrological modelling have shown spatial resolutions from 2 to 120 [m] (Beven, 1997). Although natural slopes rarely exceed a few hundred meters, even with grid sizes of more than 1 km the general gradients (potentials) within the landscape can be modelled. Of course, this includes a certain amount of abstraction and the physical basis is weakened (Kirkby et al., 1996). However, if model results can be calibrated concerning quantities and spatial patterns the modeller's goal can be satisfied. From Chapter 3 it has become clear that the LAPSUS model results can be compared for changing resolutions. Consequently instead of the validation of the theoretical base of the LAPSUS model, the main concern becomes the representation of the landscape such as DEM quality, resolution and extension.

The temporal components of the LAPSUS model are a compromise between the spatial resolution of interest and the applied process based lumped parameters. Considering response time and geomorphic equilibrium of systems, relevant time scales vary between hours and decades, even thousands of years (Howard, 1982). Nevertheless, in contrast to spatial resolution, many authors allow significantly less scaling of the temporal components. In addition to the spatial resolution for TOPMODEL discussed in the previous section, an example of this apparent spatial-temporal contradiction is the flooding simulation of the Meuse basin at a spatial resolution of 1 [km] grids for a temporal resolution of 15 minutes (De Roo et al., 2000). In this example, evidently, the spatial components of key processes were generalised extensively while the process rates were still quite detailed.

One of the technical modelling aspects used in the LAPSUS model is the neighbour technique (see *i* and *j* loops of the model source code in the Appendix). During the calculation cycle the grids are processed in the order at which boundary conditions become available. Therefore the model actually starts to process first those grids that have no possibility of run-on, i.e. that have no higher neighbours. These grids can only be found on the ridges and the divides throughout the landscape. Therefore, the model exhibits a natural behaviour of processing the grids following actually the direction of the running water. After processing and evaluating the sediment transport rates, the running water with sediment in transport is then divided using a multiple flow algorithm; all the lower neighbours receive a certain weighted fraction of the flowing water. Technically speaking the model is checking constantly in so called "loops" whether all higher neighbours have been processed and which lower neighbours will receive the water and sediment in transport. Consequently the model mimics a natural behaviour of water and sediment fluxes in the landscape, as opposed to working with overlays of discharge maps and DEMs.

8.1.2 DEMs

In this thesis the landscape is represented by a Digital Elevation Model (DEM), which is a digital array (raster) of longitude z, latitude y and elevation z of varying resolutions. DEMs can be processed by various techniques: (i) digitising contour-lines from topographic maps (which normally are processed from stereo aerial photographs), (ii) survey techniques (laser theodolites, remote sensing), (iii) direct digital processing of aerial photographs or orthophotos. Furthermore, once the contour lines and spot height points have been extracted, different interpolation techniques can be used to provide the final raster (roughly from triangulation to kriging). Important aspects of a DEM are the extension (area covered, slope, catchment, basin etc.), resolution (size of a single cell) and precision (quality ± [cm] or [m]), which are all spatial entities.

Ideally DEMs would represent large extensions of fine resolution grids, since larger grids hamper the simulation of for example ridges, channels and rivers. Although calculation speed and memory restrictions of computer based modelling have improved considerably over the years, the availability or production of fine resolution DEMs is still restricted. Nevertheless, depending on the level of observation and simulation not always the most detailed DEM is needed to represent adequately the landscape (e.g. Thompson et al., 2001). As long as the landscape features of interest such as for example slope length, slope angle or curvature are sufficiently modelled, the DEM resolution can be easily 100 [m]. Except from the resolution, the precision or quality of a DEM is rarely investigated, which can have an important influence on hydrological or geomorphological simulation results (Wise, 2000).

However, even before assessing DEM quality there are common problems encountered when processing DEMs: sinks and flats. Sinks are locations in the DEM that are surrounded only by higher neighbouring grids, in other words when calculating overland flow areas of only water accumulation without any outlet. Flats are areas of exactly the same altitude without any gradient, again difficult to imagine in natural landscape where zero gradients hardly exist. The problem with these features is that they can have a natural or an artificial origin. Possible natural sinks are dolines, subsiding basins, inter-dunal areas or depressions in till plains. Natural flats can be salt plains or standing water bodies such as lakes and reservoirs.

The artificial sinks and flats originate from the applied interpolation technique and from DEM resolution or precision. Most problems arise in areas with small gradients such as valley bottoms and alluvial plains. For example a common error in triangulation is interpolation across breaklines such as terraces or river channels. Any triangle calculated during triangulation should always include this lineation or channel in one of its sides, preventing that crossing triangles can be formed. Resolution can be a problem with incised channels smaller than the grid size, where the grid cell is assigned the height of the river bank instead of the channel. Precision is one of the major causes for artificial flats, for example if the precision is ±1 [m] and the gradient of an alluvial plain is 0.1 over 100 [m] than several grids will be assigned the same height.

Most of standard GIS packages have procedures to fill sinks until the same height is reached as the outlet or spill, thus, creating a new flat area. Depending on where this spill is located, the source of the DEM and the DEM resolution this can become quite an extensive area (Wise, 2000). Flat areas in these packages are then forced to drain in the direction of the spill, forcing a steepest descent and often "fishbone" drainage structure. However, filling sink areas is only the simplest solution and therefore arbitrary. For example locating and lowering the area of the spill could implicate less grids to be adapted but is technically more difficult. In

addition, the solution of draining flat areas towards a spill is geomorphological speaking not always the best solution. For example a flat area in a DEM along a river channel could be a river terrace, which will not drain perpendicular or directly towards the channel but will originally have more or less the same gradient as the river bed and drain parallel to the river channel. Unfortunately these possible improved solutions are not yet available in any standard GIS package.
Whether the sinks and flats are problematic or not is highly related to the type of modelling and the way in which the DEM is implemented. Standard procedures using the DEM only for the topographic gradients, aspect, curvature etc. will hardly be affected. More hydrological directed approaches such as watershed delineation, flow direction and flowaccumulation at least need removal of sinks. In the case of more geomorphological oriented applications such as LAPSUS, both artificial sinks and flat areas need to be removed. In the first place because the use of multiple flow directions to simulate diverging properties of topography is equally important on slopes as on river terraces, alluvial fans and deltaic areas. Effectively areas of zero height difference can hardly be found in nature. In the second place because these areas are important zones of sedimentation and a model driven by topographic gradients will simply not do anything in zero slope areas.

8.2 Landscape evolution and coupling of results at different scales

8.2.1 Landscape evolution and land use

The present day topography and organisation of the landscape in the research area is the logical result of the past twenty million years of landscape evolution. A general structure of mountain ranges and basins (pull apart type) controlled by major fault systems becomes clear from even the simplest contour line map. The highest mountain ranges consist of the more resistant limestones and serpentinites, the lower mountain ranges comprise the older Paleozoic schists and phylites, while the basins have been filled with more easily erodible flysch materials from the Tertiary. The interplay of erosion, uplift, climate and sea level changes have further shaped the landscape, from the tabular mountains of Tortonian marine conglomerates, Pliocene marine terraces and fluvial deposits to Pleistocene alluvial fans, river terraces and mass movements in the lowest positions of the landscape. This same logical distribution can be found for the resulting soils and the general land use of the region. The mountainous areas, high altitudes, difficult to access, with steep slopes and shallow soils are left under semi-natural vegetation, some reforestation and occasionally grazing. The intermediate sloping areas of the old metamorphic Paleozoic rocks show somewhat deeper soils, are assessable from the central valley systems and are mainly used for olive and almond orchards. The former flysch basins contain large areas with marls, intermediate slopes (not too steep) and deep clayey soils which are used for the growth of cereals because of the vertic properties of the marl soils. Finally the river terrace area, almost flat with deep soils is used for irrigated citrus.
The result is a logical relation between geology and land use, which is clearly visible from aerial photos or satellite images. However, modern technology and socio-economic developments are starting to disturb this general picture. For example, the use of drip irrigation is increasing considerably within the area. For the traditional citrus fields in the river terrace area this means no significant change where drip irrigation can save water and

improve crop performance. However, these systems are also increasingly applied in the areas with olive and almond orchards, implying a major change in management practises such as tillage. Consequently, changes in hydrologic and geomorphic behaviour both on-site as off-site can be expected (see Chapter 7). The same holds true for the marl area where the past few years several farmers have transformed their traditional cereal fields into drip irrigated orchards. By maintaining a constant water supply, the soil remains wet and the vertic properties of these marl soils are eliminated and the root system can survive. However, what happens when the water supply can not be maintained in very dry years or because of changing policies on water redistribution for urban purposes. In addition these areas are very vulnerable for landsliding triggered by severe rainfall in the rain season, irrigation systems will increase the antecedent moisture conditions and increase landslide risks.
Even though the case study area presents some remarkable examples of palaeo-landscape preservation, such as the undeformed uplifted remnants of marine conglomerates and sands from the Late Miocene and marine terraces from the Early Pliocene, several hiatus can be identified that influence the uncertainty of tectonic uplift rates. Therefore, to evaluate tectonic rates, both spatial and temporal resolution of the observations determine the validity of the results. Nevertheless, according to the geological evidence in this case study area the final present day uplift rates range between 40-100 [m Ma^{-1}], which equals 0.04 to 0.1 [mm a^{-1}]. Although slightly lower and depending on the bulk density of the sediment, these rates are in the same order of magnitude as the measured net erosion rates in Chapters 4 and 5 for natural slopes in the serpentinite study area of the Sierra de Aguas namely 0.1 to 0.5 [mm a^{-1}] or 2 to 8 [t $ha^{-1}a^{-1}$]. This suggests a link of the spatial-temporal resolution of geological landscape evolution and actual natural landscape development. Especially when comparing these same rates with net erosion rates of the cultivated areas in the gneiss area. The erosion rates of 40 to 70 [t $ha^{-1}a^{-1}$] or 24 to 43 [mm a^{-1}] indicate a factor 10 or more increase of soil redistribution, demonstrating the enormous impact of human induced landscape evolution and land use change. Although recent studies indicate that after abandonment soil surface characteristics and properties recover considerably (Martínez Fernández et al., 1995), the consequences of permanent loss of soil depth and the recovery rate of the geomorphic equilibrium remain uncertain.

8.2.2 Soil redistribution

Modelling landscape development involves the simulation of processes of erosion and (re-)sedimentation throughout the landscape. From literature reviews often the "multi-scale lapsus" of landscape becomes apparent in the discussion and presentation of modelling results. A simple statement of a certain erosion rate without indicating the temporal and spatial constraints and domains, hampers the correct interpretation of such results. Depending on land use, lithology and topography, net soil loss rates differ from location to location, as well as from plot, slope, catchment to multiple-catchments. From chapters 4 to 7 it has become clear that there are many ways of presenting and discussing soil redistribution rates.
For most slope and plot studies net soil loss have been found dominant at the annual or longer resolution. The same holds true for the landscape development at the geological time scale when considering uplifting areas. This as opposed to the landscape context of years and decades where both erosion as well as sedimentation have to be taken into consideration. The LAPSUS results of the research area in the chapters 5 to 7 indicate clearly different areas of sedimentation at different resolutions. Consequently, in the landscape context acceptable net

regional soil loss rates are just an average, concealing the areas of serious soil loss as well as areas of sedimentation.
Especially in the Mediterranean area the issue of soil redistribution is highly related to important factors as parent material, soil depth, vegetation and runoff generation. Within the landscape context this means that changing conditions in one area of the landscape can influence conditions elsewhere. For example land use change, abandonment or vegetation regeneration can alter infiltration, runoff generation and erodibility. These type of on-site changes can have major consequences for down slope and downstream located areas in terms of changes in run-on and amounts of sediment in transport reaching these areas.
Soil redistribution patterns differ considerably between natural and cultivated areas, or in other words between overland flow and tillage erosion. While overland flow is dominated by the capacity of the running water in terms of gradient and amount, tillage is mainly dominated by the gradient in combination with depth and direction of labour. The latter is more sensitive to changing gradients, since on a straight slope net soil translocation will be zero (input is the same as output), while erosion is dominant in convex positions (including upslope) and sedimentation dominant in concave positions (often downslope). This as opposed to water erosion that will increase always down slope and in areas of converging water flows but remains highly dependent on availability and erodibility of transportable material. Consequently, the most important difference in addition to the actual rates is the impact of tillage erosion directly starting from the water divides and normally unlimited supply of transportable material.

8.2.3 Sustainability

The "multi-scale lapsus" of landscape becomes evident as well when discussing issues of sustainability in the research area. For the sustainable development of the use of land in the Álora region, this implies understanding of the specific geological and climatological conditions in relation to the present landscape. Necessarily the multiple temporal and spatial levels of key processes, including their extension and resolution, have to be taken into consideration. However, there are not many signs of any dialog of policy makers and earth scientists in this region.
For example, in the arable sector the distribution of the limited water supplies is an important issue. Annual or inter-annual temporal variability of precipitation as well as long term development of climate change influence possible demand for and availability of water. In addition, choices have to be made between irrigated crops or tourist industry. If economic development or policies (from local to the international EC level) increase the marginality of present land use than, as stated in Chapter 7, the abandonment of land or land use change possibly implies both on-site as off-site effects. With such a scenario the Álora area could face increased erosion risk in upland areas and increased flooding risk in the alluvial areas.
At this moment urban land development should also consider the geological and climatological constraints of the research area. Local authorities should be encouraged not to allow building in landslide prone areas such as the Miocene flysch marls and to prevent construction of houses in flood plains. Maybe the worst example in the area is the construction over the past years of an industrial complex at the distal area of an alluvial fan. Unfortunately all these examples can be found at this moment in the research area. The future will learn whether the spatial-temporal expectations and planning of such projects will

interfere with the temporal and spatial resolution of the geological evolution of landscape development.

8.3 Future Research

Following the classical paradigm of a scientific investigation these four years of research have raised just as many questions as have been answered. In addition, from the previous sections it becomes clear that still many improvements are possible in modelling landscape development at different spatial and temporal resolutions-extensions. In the following paragraphs some of these new questions and improvements are discussed as ground for future research.

8.3.1 DEM preparation

An important input for LAPSUS, as for any other spatial explicit landscape process model, is the representation of the landscape by a DEM. As discussed in one of the previous sections, these DEMs often include typical errors such as artificial sinks and flat areas. Especially when these DEMs are used to simulate geomorphologic processes, the standard procedures in GIS packages to solve these errors can influence the geomorphic behaviour. Therefore, when preparing DEMs new standard cleaning procedures for sinks and flats have to be developed from a geomorphological point of view. Such procedures should implement removal of sinks by adapting the least number of grids possible and tilting of flat areas using geomorphological criteria.

8.3.2 Landscape processes

LAPSUS so far is only simulating sheet and wash erosion on the slopes as dominant landscape forming processes on the applied temporal and spatial resolution of this research. In other areas with for example different lithology, land use or topography other processes such as splash erosion (short term), river incision (long term), soil creep (diffusive) or landslides (catastrophic) could become more important. To avoid underestimation of the landscape process rates in different areas these kind of processes should be included into the model. Further investigation for example could focus on the capability of LAPSUS to capture these kind of processes by adjusting the m and n exponents and the general K_{es} factor (see Chapter 3, Eq. 3.3).

8.3.3 Continuing the multi-scale experiments

The experiments of Chapter 3 with artificial DEMs are indicating different resolution effects. This is only one example of many artificial and natural scale effects that can be found in landscape process modelling. Investigating some of these effects on real DEMs is partly done in Chapter 6 and 7. However, the real challenge is to develop a multi-scale modelling approach that can simulate the essential processes on their optimal resolution-extension level. For example key slope processes can be modelled in a small detailed part of the catchment and resulting data on erodibility can be extrapolated over the rest of the watershed under the same boundary conditions. Consequently such a multi-scale approach should function also the other way around where for example constraints on climatological inputs or land use change for a whole region should be disaggregated into applicable inputs for catchment or slope simulations

8.3.4 ^{137}Cs continuous measurement

One of the major constraints of the ^{137}Cs technique as described in this thesis is the number of samples and the sampling strategy. For an exploratory investigation, sampling along transects as has been done in Chapters 4 and 5 results sufficient to obtain indicative rates. However, to improve the spatial component of the ^{137}Cs derived soil redistribution rates, increasing the number of samples and sampling in a grid structure would improve considerably the validity of the estimated spatial patterns of soil redistribution. Furthermore, technological advances constantly improve the equipment and methodology for detecting radionuclides and thus ^{137}Cs in the environment. Recent developments in this field are the continuous measuring devises, which can be used on land, in the sea and in the air. Such continuous measurements at the landscape level could provide maps of ^{137}Cs distribution, and thus soil redistribution, for entire slopes and catchments. This would eliminate the spatial extrapolation of point measurements along transects and grids. Providing that the obtained accuracy is sufficient these continuous measurements could be easily applied upon different lithologies in search of the parent material dependent erodibility factors.

8.3.5 Further coupling with land use change modelling

Analysing the results of Chapter 7 it becomes clear that the implementation of land use change scenarios can have an important impact upon the spatial distribution and rates of landscape processes both on-site as off-site from the area under change. However, this relation between land use change and landscape processes is dynamic and reversible, consequently the impact of landscape processes can cause land use change. For example when agricultural areas suffer depletion of valuable (top-)soil and nutrients, which can cause cultivation of a certain crop biophysically or economically unfeasible. Further coupling of land use and landscape process modelling therefore seems justified, especially with the application of sophisticated land use change models that can handle the multi-scale spatial, temporal, biophysical and socio-economic key factors. An example of dynamic land use change modelling at different spatial and temporal levels is the CLUE-framework (The Conversion of Land Use and its Effects, Veldkamp and Fresco, 1996a; 1996b). Most applications of CLUE until now use rather static biophysical driving factors. An integration of CLUE and LAPSUS would increase considerably the possibilities of simulating and predicting land use change in relation to actual landscape processes (Veldkamp et al., 2001).

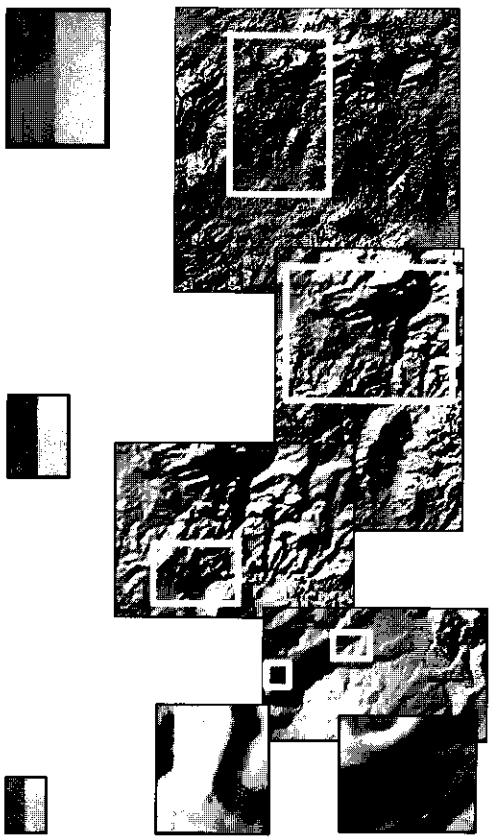

References

Acosta, A., Pereira, M.D., Shaw, D.M. and Bea, F., 1997. Serpentinizacion de la Peridotita de Ronda (Cordillera Betics) por la interacción con fluidos ricos en volátiles: comportamiento del B. Revista de la Sociedad Geológica de España 10, 301-308.

Alcamo, J., 1994. IMAGE 2.0 Integrated modeling of global climate change. Kluwer Academic Publishers, Dordrecht, NL, pp 75.

Ansted, D.T., 1859. On the geology of Málaga and the southern part of Andalucía. Quarterly Journal of the Geological Society of London XV, 597-601.

Antoine, P., Lautridou, J.P. and Laurent, M., 2000. Long-term fluvial archives in NW France: response of the Seine and Somme rivers to tectonic movements, climatic variations and sea level changes. Geomorphology 33, 183-207.

Baeza, A., Paniagua, J., Rufo, M., Guillen, J. and Sterling, A., 2001. Seasonal variations in radionuclide transfer in a Mediterranean grazing-land ecosystem. Journal of Environmental Radioactivity 55, 283-302.

Bathurst, J.C., Kilsby, C. and White, S., 1996. Modelling the impact of climate change and land use change on basin hydrology and soil erosion in Mediterranean Europe. In: Brandt, C.J. and Thornes, J.B. (Eds.), Mediterranean Desertification and Land Use. John Wiley & Sons, Ltd., Chichester. pp 355-387.

Bergkamp, G., 1998. A hierarchical view of the interactions of runoff and infiltration with vegetation and microtopography in semiarid shrublands. Catena 33, 201-220.

Beven, K.J., 1995. Linking parameters across scales: subgrid parameterizations and scale dependent hydrological models. Hydrological Processes 9, 507-525.

Beven, K.J., 1997. TOPMODEL: A critique. Hydrological Processes 11, 1069-1085.

Beven, K.J. and Kirkby, M.J., 1979. A physically based, variable contributing area model of basin hydrology. Hydrological Sciences Bulletin 24, 43-69.

Beven, K.J., Kirkby, M.J., Schoffield, N. and Tagg, A., 1984. Testing a physically based flood forecasting model (TOPMODEL) for three UK catchments. Journal of Hydrology 69, 119-143.

Biermann, C., 1995. The Betic Cordilleras (SE Spain), Anatomy of a dualistic collision-type orogenic belt. Geologie en Mijnbouw 74, 167-182.

Boer, M.M., Del Barrio, G. and Puigdefabregas, J., 1996. Mapping soil depth classes in dry Mediterranean areas using terrain attributes derived from a digital elevation model. Geoderma 72, 99-118.

Boix Fayos, C., 1997. The roles of texture and structure in the water retention capacity of burnt Mediterranean soils with varying rainfall. Catena 31, 219-236.

Boix Fayos, C., Calvo Cases, A., Imeson, A.C. and Soriano Soto, M.D., 2001. Influence of soil properties on the aggregation of some Mediterranean soils and the use of aggregate size and stability as land degradation indicators. Catena 44, 47-67.

Boix Fayos, C., Calvo Cases, A., Imeson, A.C., Soriano Soto, M.D. and Tiemessen, I.R., 1998. Spatial and short-term temporal variations in runoff, soil aggregation and other soil properties along a Mediterranean climatological gradient. Catena 33, 123-138.

Bonachela, S., Orgaz, F., Villalobos, F.J. and Fereres, E., 1999. Measurement and simulation of evaporation from soil in olive orchards. Irrigation Science 18, 205-211.

Bouma, J., 1997. Long-term characterization: monitoring and modeling. In: Lal, R., Blum, W.H., Valentine, C. and Stewart, B.A. (Eds.), Advances in Soil Science: Methods for assessment of soil degradation. CRC press, Boca Raton, New York. pp 337-358.

Bouma, J., 1999. Land evaluation for landscape units. In: Summer, M.E. (Ed.), Handbook of Soil Science. CRC-Press, Florida. pp 393-412.

Bouma, J., Booltink, H.W.G. and Stein, A., 1996. Reliability of soil data and risk assessment of data applications. Soil Science Society of America 47, 63-79.

Bouma, J. and Droogers, P., 1999. Comparing different methods for estimating the soil moisture supply capacity of a soil serie subjected to different types of management. Geoderma 92, 185-197.

Braun, P., Molnar, T. and Kleeberg, H.B., 1997. The problem of scaling in grid-related hydrological process modelling. Hydrological Processes 11, 1219-1239.

Bridgland, D.R., 2000. River terrace systems in north-west Europe: an archive of environmental change, uplift and early human occupation. Quaternary Science Reviews 19, 1293-1303.

Bromley, J., Brouwer, J., Barker, A.P., Gaze, S.R. and Valentin, C., 1997. The role of surface water redistribution in an area of patterned vegetation in a semi-arid environment, south-west Niger. Journal of Hydrology 198, 1-29.

Buol, S.W., Hole, F.D. and Cracken, R.J., 1989. Soil genesis and classification. Iowa State University Press, Ames, IA, pp 233.

Busacca, A.J., Cook, C.A. and Mulla, D.J., 1993. Comparing landscape - scale estimation of soil erosion in the Palouse using ^{137}Cs and RUSLE. Journal of Soil and Water Conservation 48, 361-367.

Campbell, B.L., Loughran, R.J. and Elliott, G.L., 1982. Caesium-137 as an indicator of geomorphic processes in a drainage basin system. Australian Geographical Studies 20, 49-64.

Caravaca, F., Lax, A. and Albaladejo, J., 1999. Organic matter, nutrient contents and cation exchange capacity in fine fractions from semi-arid calcareous soils. Geoderma 93, 161-176.

Cerdá, A., 1998. The influence of geomorphological position and vegetation cover on the erosional and hydrological processes on a Mediterranean hillslope. Hydrological Processes 12, 661-671.

Cerdá, A., 1999. Parent material and vegetation affect soil erosion in Eastern Spain. Soil Science Society of America Journal 63, 362-368.

Chappell, A., 1999. The limitations of using ^{137}Cs for estimating soil redistribution in semi-arid environments. Geomorphology 29, 135-152.

Chappell, A., Warren, A., Oliver, M.A. and Charlton, M., 1998. The utility of ^{137}Cs for measuring soil redistribution rates in southwest Niger. Geoderma 81, 313-337.

Chappell, A., Warren, A., Taylor, N. and Charlton, M., 1998. Soil flux (loss and gain) in southwestern Niger and its agricultural impact. Land Degradation & Development 9, 295-310.

CHS, 1974. Presa de Guadalhorce - Guadalteba, Confederación Hidrográfica del Sur de España. Ministerio de Obras Publicas, Dirección General de Obras Hidráulicas, Málaga, pp 36.

Clauzon, G., 1978. The Messinian Var canyon (Provence, southern France) -paleographic implications. Marine Geology 27, 231-246.

Coulthard, T.J., Macklin, M.G. and Kirkby, M.J., 2001. Modelling the impacts of different flood magnitudes and frequencies on catchment evolution. In: Maddy, D., Macklin, M.G. and

Woodward, J.C. (Eds.), River basin sediment systems: archives of environmental change. A.A. Balkema Publishers, Lisse, Abingdon, Exton, Tokyo. pp 285-503.

De Bakker, H., 1995. Veertig jaar bodemkartering 1943-1983 - introductie van bodemkundige concepten. In: Buurman, P. and Sevink, J. (Eds.), Van bodemkaart tot informatiesysteem. Wageningen Pers, Wageningen, Netherlands. pp 18-27.

De Bruin, S., 2000. Predicting the aerial extent of land-cover types using classified imagery and geostatistics. Remote Sensing of Environment 74, 387-396.

De Bruin, S. and Gorte, B.G.H., 2000. Probabilistic image classification using geological map units applied to land-cover change detection. International Journal of Remote Sensing 21 (12), 2389-2402.

De Bruin, S. and Stein, A., 1998. Soil-landscape modelling using fuzzy c-means clustering attribute data derived from a Digital Elevation Model (DEM). Geoderma 83, 17-33.

De Bruin, S., Wielemaker, W.G. and Molenaar, M., 1999. Formalisation of soil - landscape knowledge through interactive hierarchical disaggregation. Geoderma 91, 151-172.

De Graaf, J. and Eppink, L.A.A.J., 1999. Olive oil production and soil conservation in southern Spain in relation to EU subsidy policies. Land Use Policy 16, 259-267.

De Ploey, J., Kirkby, M.J. and Ahnert, F., 1991. Hillslope erosion by rainstorms: A magnitude-frequency analysis. Earth Surface Processes and Landforms 16, 399-409.

De Roo, A.P.J., Wesseling, C.G. and Van Deursen, W.P.A., 2000. Physically based river basin modelling within a GIS: the LISFLOOD model. Hydrological Processes 14, 1981-1992.

Desmet, P.J.J. and Govers, G., 1996. Algorithms to route flow over digital landscapes: a comparison and their implications for predicting ephemeral gullies. Geomorphologie: Relief, Processus, Environnement nr. 3, 41-50.

Dick, R.P., 1992. A review: long term effects of agricultural systems on soil biochemical and microbial parameters. Agriculture, Ecosystems and Environment 40, 25-36.

Dietrich, W.E. and Montgomery, D.R., 1998. Hillslopes, channels, and landscape scale. In: Sposito, G. (Ed.), Scale dependence and scale invariance in hydrology. Cambridge University Press, Cambridge UK. pp 30-60.

Dietrich, W.E., Reiss, R., Hsu, M. and Montgomery, D.R., 1995. A process-based model for colluvial soil depth and shallow landsliding using digital elevation data. In: Kalma, J.D. and Sivapalan, M. (Eds.), Scale issues in Hydrological Modelling. John Wiley & Sons, New York. pp 141-158.

Droogers, P. and Bouma, J., 1997. Soil survey input in exploratory modeling of sustainable soil management practises. Soil Science Society of America Journal 61, 1704-1710.

Durán, J.J., Grun, R. and Soria, J.M., 1988. Edad de las formaciones travertinicas del flanco meridional de la Sierra de Mijas (provincia de Málaga, Cordilleras Beticas. Geogaceta 5, 61-63.

Ehlers, J., 1996. Quaternary and Glacial Geology. John Wiley & Sons, Chichester, UK, pp 578.

FAO, 1976. A framework for land evaluation. FAO, Rome, pp 37.

FAO, 1988. FAO/ Unesco soil map of the world, revised legend. World resources report 60, FAO, Rome. 1989 Reprinted as technical paper 20, ISRIC Wageningen, pp 138.

FAO, 1992. The Den Bosch Declaration and agenda for action on sustainable agriculture and rural development. Report of the FAO/Netherlands conference on agriculture and the environment. 's-Hertogenbosch, The Netherlands, 15-19 April 1991. FAO, Rome, Italy, pp 55.

Felix, R., 1995. Bodemkartering voor 1943 het geologisch perspectief. In: Buurman, P. and Sevink, J. (Eds.), Van bodemkaart tot informatiesysteem. Wageningen Pers, Wageningen, Netherlands. pp 1-17.

Fernández, J. and Rodríguez Fernández, J., 1991. Facies evolution of nearshore marine clastic deposits during the Tortonian transgression - Granada Basin, Betic Cordilleras, Spain. Sedimentary Geology 71, 5-21.

Foster, G.R. and Meyer, L.D., 1972. A closed-form soil erosion equation for upland areas. In: Shen, H.W. (Ed.), Sedimentation: symposium to honour professor H.A. Einstein. Colorado State University, Fort Collins, Colorado. pp 12.1-12.19.

Foster, G.R. and Meyer, L.D., 1975. Mathematical simulation of upland erosion by fundamental erosion mechanics. In: Anonymous (Ed.), Present and perspective technology for predicting sediment yields and sources. Proceedings Sediment Yield Workshop, Oxford 1972. United States Department of Agriculture, Washington D.C.. pp 190-207.

Freeman, T.G., 1991. Calculating catchment area with divergent flow based on a regular grid. Computers & Geosciences 17, 413-422.

Fresco, L.O., 1995. Agro-ecological knowledge at different scales. In: Bouma, J. and a.n. (Eds.), Eco-regional approaches for sustainable land use and food production. Kluwer Academic Publishers, Dordrecht. pp 133-141.

Garbrecht, J. and Martz, L.W., 1994. Grid size dependency of parameters extracted from digital elevation models. Computers & Geosciences 20, 85-87.

Gessler, P.E., Chadwick, O.A., Chamran, F., Althouse, L. and Holmes, K., 2000. Modeling soil - landscape and ecosystem properties using terrain attributes. Soil Science Society of America Journal 64, 2046-2056.

Gomez, J.A., Giraldez, J.V., Pastor, M. and Fereres, E., 1999. Effects of tillage method on soil physical properties infiltration and yield in an olive orchard. Soil & Tillage Research 52, 167-175.

Govers, G., Vandaele, K., Desmet, P.J.J., Poesen, J. and Bunte, K., 1994. The role of tillage in soil redistribution on hillslopes. European Journal of Soil Science 45, 469-478.

Hall, G.F. and Olson, C.G., 1991. Predicting variability of soils from landscape models. In: Anonymous (Ed.), Spatial variabilities of soils and landforms. SSSA Special Publication no. 28, pp 9-24.

Haq, B.U., Hardenbol, J. and Vail, P.R., 1987. Chronology of fluctuating sea levels since the Triassic. Science 235, 1156-1166.

Harvey, A.M., Silva, P.G., Mather, A.E., Goy, J.L., Stokes, M. and Zazo, C., 1999. The impact of Quaternary sea level and climatic change on coastal alluvial fans in the Cabo de Gata ranges, southeast Spain. Geomorphology 28, 1-22.

Holling, C.S., 1992. Cross-scale morphology, geometry and dynamics of ecosystems. Ecological Monographs 62, 447-502.

Holmgren, P., 1994. Multiple flow direction algorithms for runoff modelling in grid based elevation models: an empirical evaluation. Hydrological Processes 8, 327-334.

Howard, A.D., 1982. Equilibrium and time scales in geomorphology: application to sand-bed alluvial streams. Earth Surface Processes and Landforms 7, 305-325.

Howard, A.D., 1994. A detachment-limited model of drainage basin evolution. Water Resources Research 30, 2261-2285.

Hsu, K.J., Ryan, W.B.F. and Cita, M.B., 1973. Late Miocene desiccation of the Mediterranean. Nature 242, 240-244.

Imeson, A.C., Cammeraat, L.H. and Prinsen, H., 1998. A conceptual approach for evaluating the storage and release of contaminants derived from process based land degradation studies: an example from the Guadalentin basin, Southeast Spain. Agriculture, Ecosystems and Environment 67, 223-237.

Instituto Geológico y Minero de España (IGME), 1978. Mapa geológico de España, Escala 1: 50000, Hoja Álora 1052 (16-44). IGME, Madrid

Instituto Tecnológico GeoMinero de España (ITGE), 1990. Mapa geológico de España, Escala 1: 50000, Hoja Ardales 1038 (16-43). ITGE Madrid

Isaksson, M. and Erlandsson, B., 1998. Models for the vertical migration of ^{137}Cs in the ground - A field study. Journal of Environmental Radioactivity 41, 163-182.

Jacob, J.S. and Nordt, L.C., 1991. Soil and landscape evolution: a paradigm for pedology. Soil Science Society of America Journal 55, 1194-1194.

Jímenez, A.P., Braga, J.C. and Martín, J.M., 1991. Oyster distribution in the Upper Tortonian of the Almanzora Corridor (Almeria, S.E. Spain). Geobios 24, 725-734.

Kachanoski, R.G., 1993. Estimating soil loss from changes in soil cesium-137. Canadian Journal of Soil Science 73, 629-632.

Kachanoski, R.G. and Carter, M.R., 1999. Landscape position and soil redistribution under three soil types and land use practises in Prince Edward Island. Soil & Tillage Research 51, 211-217.

Kalma, J.D. and Sivapalan, M., 1995. Scale issues in hydrological modelling. Wiley, Chishester, pp 589.

Karahan, G. and Bayulken, A., 2000. Assessment of gamma dose rates around Istanbul (Turkey). Journal of Environmental Radioactivity 47, 213-221.

Kelly, M., Black, S. and Rowan, J.S., 2000. A calcrete-based U/Th chronology for landform evolution in the Sorbas basin, southeast Spain. Quaternary Science Reviews 19, 995-1010.

Kirkby, M.J., 1971. Hillslope process-response models based on the continuity equation. In: Brunsden, D. (Ed.), Slopes, forms and processes. Inst. of Brit. Geographers, Spec. Pub., pp 15-30.

Kirkby, M.J., 1978. Implications for sediment transport. In: Kirkby, M.J. (Ed.), Hillslope hydrology. Jon Wiley & Sons. Ltd., Chichester, UK. pp 325-363.

Kirkby, M.J., 1986. A two-dimensional simulation model for slope and stream evolution. In: Abrahams, A.D. (Ed.), Hillslope processes. Allen & Unwin, Inc., Winchester, Mass., USA. pp 203-222.

Kirkby, M.J., 1987. Modelling some influences of soil erosion, landslides and valley gradient on drainage density and hollow development. Catena Supplement 10, 1-44.

Kirkby, M.J., Imeson, A.C., Bergkamp, G. and Cammeraat, L.H., 1996. Scaling up processes and models from the field plot to the watershed and regional areas. Journal of Soil and Water Conservation 51 (5), 391-396.

Kiss, J.J., de Jong, E. and Bettany, J.R., 1988. The distribution of natural radionuclides in native soils of southern Saskatchewan, Canada. Journal of Environmental Quality 17, 437-445.

Kosmas, C., Danalatos, N.G., Cammeraat, L.H., Chabart, M., Diamantopoulos, J., Farand, R., Gutierrez, L., Jacob, A., Marques, H., Martínez Fernández, J., Mizara, A., Moustakas, N., Nicolau, J.M., Oliveros, C., Pinna, G., Puddu, R., Puigdefabregas, J., Roxo, M., Simao, A., Stamou, G. et al. 1997. The effect of land use on runoff and soil erosion rates under Mediterranean conditions. Catena 29, 45-59.

Kosmas, C., Gerontidis, S., Marathianou, M., Detsis, B., Zafiriou, T., Van Muysen, W., Govers, G., Quine, T.A. and Vanoost, K., 2001. The effects of tillage displaced soil on soil properties and wheat biomass. Soil & Tillage Research 58, 31-44.

Kosmas, C., Danalatos, N.G. and Gerontidis, S., 2000. The effect of land parameters on vegetation performance and degree of erosion under Mediterranean conditions. Catena 40, 3-17.

Kosmas, C., Gerontidis, S. and Marathianou, M., 2000. The effects of land use change on soils and vegetation cover over various lithological formations on Lesvos (Greece). Catena 40, 51-68.

Krijgsman, W., Hilgen, F.J., Raffi, I., Sierro, F.J. and Wilson, D.S., 1999. Chronology, causes and progression of the Messinian salinity crisis. Nature 400, 652-655.

Laguna, A. and Giraldez, J.V., 1990. Soil erosion under conventional management systems of olive tree culture. In: Anonymous (Ed.), Proceedings of the Seminar on Interaction between agricultural systems and soil conservation in the Mediterranean belt, September 4 - 8, 1990. European Society for Soil Conservation, Oeiras, Portugal. pp 94-101.

Lal, R., 1997. Agronomic impact of soil degradation. In: Lal, R., Blum, W.H., Valentine, C. and Stewart, B.A. (Eds.), Advances in Soil Science: Methods for assessment of soil degradation. CRC press, Boca Raton, New York. pp 459-473.

Lark, R.M. and Beckett, P.H.T., 1998. A geostatistical descriptor of the spatial distribution of soil classes, and its use in predicting the purity of possible soil map units. Geoderma 83, 243-267.

Lasanta, T., Garcia Ruiz, J.M., Perez Rontome, C. and Sancho Marcen, C., 2000. Runoff and sediment yield in a semi-arid environment: the effect of land management after farmland abandonment. Catena 38, 265-278.

Le Houerou, H.N., 2000. Restoration and rehabilitation of arid and semi-arid Mediterranean ecosystems in north Africa and west Asia: A review. Arid Soil Research and Rehabilitation 14, 3-14.

Livens, F.R. and Loveland, P.J., 1988. The influence of soil properties on the environmental mobility of caesium in Cumbria. Soil Use & Management 4, 69-75.

Lobb, D.A., Kachanoski, R.G. and Miller, M.H., 1995. Tillage translocation and tillage erosion on shoulder slope landscape position measured using ^{137}Cs as a tracer. Canadian Journal of Soil Science 75, 211-218.

López Bermúdez, F., Romero Díaz, A. and Martínez Fernández, J., 1998. Vegetation and soil erosion under a semi-arid Mediterranean climate: a case study from Murcia (Spain). Geomorphology 24, 51-58.

López Garrido, A.C. and Sanz de Galdeano, C., 1991. La comunicación en el Tortoniense entre el Atlántico y el mediterráneo por la cuenca del Guadalhorce (Málaga). 1er Congr. Esp. Terciario. Vic. Barcelona. 190-193.

López Garrido, A.C. and Sanz de Galdeano, C., 1999. Neogene sedimentation and tectonic-eustatic control of the Málaga Basin, South Spain. Journal of Petroleum Geology 22, 81-96.

Loughran, R.J., Campbell, B.L., Elliott, G.L., Cummings, D. and Shelly, D.J., 1989. A caesium-137 sediment hillslope model with tests from south-eastern Australia. Zeitschrift fur Geomorphologie N. F. 33, 235-250.

Loughran, R.J., Campbell, B.L., Elliott, G.L. and Shelly, D.J., 1990. Determination of the rate of sheet erosion on grazing land using caesium-137. Applied Geography 10, 125-133.

Lu, X.X. and Higgitt, D.L., 2000. Estimating erosion rates on sloping agricultural land in the Yangtze Three Gorges, China, from caesium-137 measurements. Catena 39, 33-51.

Maddy, D., 1997. Uplift driven valley incision and river terrace formation in Southern England. Journal of Quaternary Science 12, 539-545.

Maddy, D., Bridgland, D.R. and Green, C.P., 2000. Crustal uplift in southern England: evidence from river terrace records. Geomorphology 33, 167-181.

Margulis, H., 1954. Aux sources de la pedologie (Dokoutchaiev - Sibirtzev). Ecole Nationale Superieure Agronomique de Toulouse , Toulouse, FR, pp 85.

Martín Algarra, A., 1987. Evolución geológica alpina del contacto entre las Zonas Internas y las Zonas Externas de la Cordillera Betica. Unpublished Ph.D. Thesis Departamento de Geología, Universidad de Granada, Spain, pp 1171.

Martínez Fernández, J., López Bermúdez, F. and Romero Díaz, A., 1995. Land use and soil - vegetation relationships in a Mediterranean ecosystem: El Ardal, Murcia, Spain. Catena 25, 153-167.

Martz, L.W. and de Jong, E., 1987. Using Cesium-137 to assess the variability of net soil erosion and its association with topography in a Canadian prairie landscape. Catena 14, 439-451.

Martz, L.W. and de Jong, E., 1991. Using Cesium-137 and landform classification to develop a net soil erosion budget for a small Canadian prairie watershed. Catena 18, 289-308.

Mather, A.E., 1991. Late Caenozoic drainage evolution of the Sorbas Basin, Southeast Spain. Ph.D. Thesis, University of Liverpool, UK, pp 276.

Mather, A.E., 1993. Basin inversion: some consequences for drainage evolution and alluvial architecture. Sedimentology 40, 1069-1089.

Mather, A.E., 2000. Impact of headwater river capture on alluvial system development: an example from the Plio-Pleistocene of the Sorbas Basin, SE Spain. Journal of the Geological Society, London 157, 957-966.

Milne, B.T., 1991. Heterogenity as a multi-scale characteristic of landscapes. In: Kolasa, J. and Pickett, S.T.A. (Eds.), Ecological heterogenity. Ecological studies 86. Springer Verlag, pp 69-84.

Milne, G., 1936. Normal erosion as a factor in soil profile development. Nature 138, 548-549.

Montgomery, D.R. and Foufoula Georgiou, E., 1993. Channel network source representation using digital elevation models. Water Resources Research 29, 3925-3934.

Moore, I.D. and Burch, G.J., 1986. Modelling erosion and deposition: topographic effects. Transactions, American Society of Agricultural Engineers 29, 1624-1640.

Moore, I.D., Grayson, R.B. and Ladson, A.R., 1991. Digital terrain modelling; A review of hydrological, geomorphological and biological applications. Hydrological Processes 5, 3-30.

Morgan, R.P.C., Quinton, J.N. and Rickson, R.J., 1994. Modelling methodology for soil erosion assessment and soil conservation design: the EUROSEM approach. Outlook on Agriculture 23, 5-9.

Mouat, D.A., Fox, C.A. and Rose, M.R., 1992. Ecological indicator strategy for monitoring arid ecosystems. In: McKenzie, D.H., Hyatt, E.D. and McDonald, J.V. (Eds.), Ecological indicators. Volume I. Elsevier Applied Science, London, UK. pp 717-737.

Nagle, G.N., Lassoie, J.P., Fahey, T.J. and McIntyre, S.C., 2000. The use of caesium-137 to estimate agricultural erosion on steep slopes in a tropical watershed. Hydrological Processes 14, 957-969.

Navas, A., García Ruiz, J.M., Machin, J., Lasanta, T., Valero, B., Walling, D.E. and Quine, T.A., 1997. Soil erosion on dry farming land in two changing environments of the central Ebro Valley, Spain. In: Anonymous (Ed.), Human impact on erosion and sedimentation (Proceedings of Rabat Symposium S6 April 1997). IAHS Publ. no. 245, pp 13-20.

Navas, A. and Walling, D.E., 1992. Using caesium-137 to assess sediment movement on slopes in a semi-arid upland environment in Spain. In: Walling, D.E., Davies, T.R. and Hasholt, B. (Eds.), Erosion, Debris flows and environment in Mountain Regions (Proceedings of the Chengdu Symposium July 1992). IAHS Publ. no. 209, pp 129-138.

Nearing, M.A., Foster, G.R., Lane, L.J. and Finckner, S.C., 1989. A process-based soil erosion model for USDA Water Erosion Prediction Project technology. Transactions, American Society of Agricultural Engineers 32, 1587-1593.

Nicolau, J.M., Sole-Benet, A., Puigdefabregas, J. and Gutierrez, L., 1996. Effects of soil and vegetation on runoff along a catena in semi-arid Spain. Geomorphology 14, 297-309.

Pardo Iguzquiza, E., 1998. Comparison of geostatistical methods for estimating the areal average climatological rainfall mean using data on precipitation and topography. International Journal of Climatology 18, 1031-1047.

Park, S.J., McSweeney, K. and Lowery, B., 2001. Identification of the spatial distribution of soils using a process - based terrain characterization. Geoderma 103, 249-272.

Payton, R.W. and Shishira, E.K., 1994. Effects of soil erosion and sedimentation on land quality defining pedogenetic baselines in the Kondoa district of Tanzania. In: Syers, J.K. and Rimmer, D.L. (Eds.), Soil science and sustainable land management in the tropics. CAB International, Wallingford, UK. pp 235-247.

Pennock, D.J., Lemmen, D.S. and de Jong, E., 1995. Cesium-137 measured erosion rates for soils of five parent-material groups in southwestern Saskatchewan. Canadian Journal of Soil Science 75, 205-210.

Pennock, D.J. and van Kessel, C., 1997. Effect of agricultural and of clear-cut forest harvest on landscape-scale soil organic carbon storage in Saskatchewan. Canadian Journal of Soil Science 77, 211-218.

Poesen, J., van Wesemael, B., Govers, G., Martínez Fernández, J., Desmet, P.J.J., Vandaele, K., Quine, T.A. and Degraer, G., 1997. Patterns of rock fragment cover generated by tillage erosion. Geomorphology 18, 183-197.

Poesen, J.W.A. and Hooke, J.M., 1997. Erosion, flooding and channel management in Mediterranean environments of southern Europe. Progress in Physical Geography 21, 157-199.

Porto, P., Walling, D.E. and Ferro, V., 2001. Validating the use of caesium-137 measurements to estimate soil erosion rates in a small drainage basin in Calabria, Southern Italy. Journal of Hydrology 248, 93-108.

Puigdefabregas, J., Del Barrio, G., Boer, M.M., Gutierrez, L. and Sole, A., 1998. Differential responses of hillslope and channel elements to rainfall events in a semi-arid area. Geomorphology 23, 337-351.

Pulleman, M.M., Bouma, J., van Essen, E.A. and Meijles, E.W., 2000. Soil organic matter content as a function of different land use history. Soil Science Society of America Journal 64, 689-693.

Quine, T.A., 1999. Use of caesium-137 data for validation of spatially distributed erosion models: the implications of tillage erosion. Catena 37, 415-430.

Quine, T.A., Govers, G., Poesen, J., Walling, D.E., van Wesemael, B. and Martínez Fernández, J., 1999. Fine-earth translocation by tillage in stony soils in the Guadalentin, south-east Spain: an investigation using caesium-134. Soil & Tillage Research 51, 279-301.

Quine, T.A., Navas, A., Walling, D.E. and Machin, J., 1994. Soil erosion and redistribution on cultivated and uncultivated land near Las Bardenas in the central Ebro river basin, Spain. Land Degradation and Rehabilitation 5, 41-55.

Quinn, P., Beven, K.J., Chevallier, P. and Planchon, O., 1991. The prediction of hillslope flow paths for distributed hydrological modelling using Digital Terrain Models. Hydrological Processes 5, 59-79.

Rallo Romero, L., 1998. Sistemas fruticolas de secano: el olivar. In: Jímenez Dias, R.M. and Lamo de Espinosa, J. (Eds.), Agricultura Sostenible. Ediciones Mundi-Prensa, Madrid. pp 471-487.

Renschler, C.S., Mannaerts, C. and Diekkrüger, B., 1999. Evaluating spatial and temporal variability in soil erosion risk, rainfall erosivity and soil loss ratios in Andalusia, Spain. Catena 34, 209-225.

Rigon, R., Rinaldo, A. and Rodríguez Iturbe, I., 1994. On landscape self-organisation. Journal of Geophysical Research 99, 11971-11993.

Ritchie, J.C. and McHenry, J.R., 1990. Application of radioactive fallout cesium-137 for measuring soil erosion and sediment accumulation rates and patterns. Journal of Environmental Quality 19, 215-233.

Rodríguez Iturbe, I., Gupta, V.K. and Waymire, E., 1984. Scale considerations in the modelling of temporal rainfall. Water Resources Research 20, 1611-1619.

Romero Diaz, A., Cammeraat, L.H., Vacca, A. and Kosmas, C., 1999. Soil erosion at three experimental sites in the Mediterranean. Earth Surface Processes and Landforms 24, 1243-1256.

Rubio Montero, P. and Marín Sanchez, A., 2001. Plutonium contamination from accidental release or simply fallout: study of soils at Palomares (Spain). Journal of Environmental Radioactivity 55, 157-165.

Rubio, J.L. and Bochet, E., 1998. Desertification indicators as diagnosis criteria for desertification risk assessment in Europe. Journal of Arid Environments 39, 113-120.

Ruecker, G., Schad, P., Alcubilla, M.M. and Ferrer, C., 1998. Natural regeneration of degraded soils and site changes on abandoned agricultural terraces in Mediterranean Spain. Land Degradation & Development 9, 179-188.

Ruiz, J.A., Ortega, E., Sierra, C., Saura, I., Asensio, C., Roca, A. and Iriarte, A., 1993. Proyecto LUCDEME: mapa de suelos escala 1: 100.000, Alora-1052. ICONA, Granada, pp 76.

Saldaña, A., Stein, A. and Zinck, J.A., 1998. Spatial variability of soil properties at different scales within three terraces of the Henares River (Spain). Catena 33, 139-153.

Sanz de Galdeano, C., 1990. Geologic evolution of the Betic Cordilleras in the Western Mediterranean, Miocene to the present. Tectonophysics 172, 107-119.

Sanz de Galdeano, C. and López Garrido, A.C., 1991. Tectonic evolution of the Málaga Basin (Betic Cordillera). Regional implications. Geodinamica Acta 5, 173-186.

Sanz de Galdeano, C. and López Garrido, A.C., 1999. Nature and impact of Neotectonic deformation in the western Sierra Nevada (Spain). Geomorphology 30, 259-272.

Sanz de Galdeano, C., Serrano, F., López Garrido, A.C. and Martín Perez, J.A., 1993. Palaeogeography of the Late Aquitanian-Early Burdigalian basin in the western Betic internal zone. Geobios 26, 43-55.

Savoye, B., Piper, D.J.W. and Droz, L., 1993. Plio-Pleistocene evolution of the Var deep-sea fan off the French Riviera. Marine and Petroleum Geology 10, 550-571.

Schoorl, J.M., Sonneveld, M.P.W. and Veldkamp, A., 2000. Three-dimensional landscape process modelling: the effect of DEM resolution. Earth Surface Processes and Landforms 25, 1025-1034.

Schoorl, J.M. and Veldkamp, A., 2000. Multi-scale landscape process modelling in the Lower Guadalhorce Basin (Spain). In: Anonymous (Ed.), Book of Abstracts: Vijfde Nederlandse Aardwetenschappelijke Congres, Veldhoven 20 en 21 April 2000. NAC V, Veldhoven. pp 3.28.

Schoorl, J.M. and Veldkamp, A., 2001. Linking land use and landscape process modelling: a case study for the Alora region (South Spain). Agriculture, Ecosystems and Environment 85, 281-292.

Schoorl, J.M., Boix Fayos, C., de Meijer, R.J., van der Graaf, E.R. and Veldkamp, A., 2002a. The ^{137}Cs technique on steep Mediterranean slopes (Part 1): analysing effects of lithology and slope position. Catena in prep.

Schoorl, J.M., Veldkamp, A., Boix Fayos, C., van der Graaf, E.R. and de Meijer, R.J., 2002b. The ^{137}Cs technique on steep Mediterranean slopes (Part 2): landscape evolution and model calibration. Catena in prep.

Schoorl, J.M., Veldkamp, A. and Bouma, J., 2002c. Modelling water and soil redistribution in a dynamic landscape context.. Soil Science Society of America Journal in press.

Schoorl, J.M., Veldkamp, A., van den Berg van Saparoea, R.M., Buurman, P. and Wielemaker, W.G., 2000. Late-Cenozoic landscape development: the lower Guadalhorce valley. In: Anonymous (Ed.), Book of Abstracts: Vijfde Nederlandse Aardwetenschappelijke Congres, Veldhoven 20 en 21 April 2000. NAC V, Veldhoven. pp 3.29.

Schoorl, N. 1901. Verbindingen van suikers met urea. Proefschrift, Universiteit van Amsterdam. pp 107.

Schulze, R., 2000. Transcending scales of space and time in impact studies of climate change on agrohydrological responses. Agriculture, Ecosystems and Environment 82, 185-212.

Serrano, F., 1979. Los foraminiferos planctonicos del Mioceno Superior de la cuenca de Ronda y su comparación con los de otras áreas de las Cordilleras Beticas. Unpublished Ph.D. Thesis, Departamento de Geología, Universidad de Málaga, Spain, pp 247.

SGE, 1997. Cartografía Digital, MDT 25, uf23, uf24, uf33, uf34. Servicio Geográfico del Ejercito, Madrid

Sibirtzev, N., 1897. Étude des sols de la Russie. In: Bittner, A. (Ed.), Mémoires présentés à 7me session congrès géologique international, 1897, St. Pétersbourg. Petersburg, USSR.

Sposito, G., 1989. The Chemistry of Soils. Oxford University Press, New York, Oxford UK, pp 277.

Sposito, G., 1998. Scale dependence and scale invariance in hydrology. Cambridge University Press, Cambridge UK, pp 425.

Stokes, M. and Mather, A.E., 2000. Response of Plio-Pleistocene alluvial systems to tectonically induced base-level changes, Vera Basin, SE Spain. Journal of the Geological Society, London 157, 303-316.

Stolte, J., Ritsema, C.J. and De Roo, A.P.J., 1997. Effects of crust and cracks on simulated catchment discharge and soil loss. Journal of Hydrology 195, 279-290.

Sutherland, R.A., 1996. Caesium-137 soil sampling and inventory variability in reference locations: a literature survey. Hydrological Processes 10, 43-53.

Sutherland, R.A., 1998. The potential for reference site resampling in estimating sediment redistribution and assessing landscape stability by the caesium-137 method. Hydrological Processes 21, 995-1007.

Takken, I., Govers, G., Steegen, A., Nachtergaele, J. and Guerif, J., 2001. The prediction of runoff flow directions on tilled fields. Journal of Hydrology 248, 1-13.

Talling, P.J., 1998. How and where do incised valleys form if sea level remains above the shelf edge. Geology 26, 87-90.

Tarboton, D.G., 1997. A new method for the determination of flow directions and upslope areas in grid digital elevation models. Water Resources Research 33, 309-319.

Thompson, J.A., Bell, J.C. and Butler, C.A., 2001. Digital elevation model resolution: effects on terrain attribute calculation and quantitative soil - landscape modelling. Geoderma 100, 67-89.

Torri, D., Poesen, J.W.A. and Borselli, L., 1997. Predictability and uncertainty of the soil erodibility factor using a global dataset. Catena 31, 1-22.

Tucker, G.E., Catani, F., Rinaldo, A. and Bras, R.L., 2001. Statistical analysis of drainage density from digital terrain data. Geomorphology 36, 187-202.

Turner II, B.L., Skole, D., Sanderson, S., Fischer, G., Fresco, L.O. and Leemans, R., 1995. Land-use and land-cover change. Science/ research plan. IGBP Report No. 35, HDP Report No. 7. IGBP, HDP, Stockholm, Geneva, pp 132.

Tyler, A.N., Carter, S., Davidson, D.A., Long, D.J. and Tipping, R., 2001. The extent and significance of bioturbation on ^{137}Cs distributions in upland soils. Catena 43, 81-90.

USDA, 1999. Soil Taxonomy: a basic system of soil classification for making and interpreting soil surveys. U.S. Government Printing Office, Wasinghton D.C. USA, pp 869.

Van den Berg, M.W., 1994. Neotectonics of the Roer Valley rift system: Style and rate of crustal deformation inferred from syn-tectonic sedimentation. Geologie en Mijnbouw 73, 143-156.

Van der Meer, F., 1995. Triassic-Miocene paleogeography and basin evolution of the Subbetic Zone between Ronda and Málaga, Spain. Geologie en Mijnbouw 74, 43-63.

Van Diepen, C.A., Wolf, J., Van Keulen, H. and Rappoldt, C., 1989. WOFOST: a simulation model of crop production. Soil Use & Management 5, 16-24.

van Loon, A.J., 2000. Towards the geological past. Earth Science Reviews 51, 203-209.

van Loon, A.J., 2001. Changing the face of the Earth. Earth Science Reviews 52, 371-379.

van Wesemael, B., Mulligan, M. and Poesen, J., 2000. Spatial patterns of soil water balance on intensively cultivated hillslopes in a semi-arid environment: the impact of rock fragments and soil thickness. Hydrological Processes 14, 1811-1828.

VandenBygaart, A.J., Protz, R. and McCabe, D.C., 1999. Distribution of natural radionuclides and ^{137}Cs in soils of southwestern Ontario. Canadian Journal of Soil Science 79, 161-171.

Vanderlinden, K., Gabriels, D. and Giraldez, J.V., 1998. Evaluation of infiltration measurements under olive trees in Cordoba. Soil & Tillage Research 48, 303-315.

Veldkamp, A., 1992. A 3-D model of quaternary terrace development, simulations of terrace stratigraphy and valley asymmetry: a case study for the Allier terraces (Limagne, France). Earth Surface Processes and Landforms 17, 487-500.

Veldkamp, A. and Bouma, J., 2000. Soils and land use change. In: Alloway, B. and Gregory, P.J. (Eds.), The Soils Handbook. Blackwell Science, in press.

Veldkamp, A. and Fresco, L.O., 1996a. CLUE-CR: an integrated multi-scale model to simulate land use change scenarios in Costa Rica. Ecological Modelling 91, 231-248.

Veldkamp, A. and Fresco, L.O., 1996b. CLUE: a conceptual model to study the conversion of land use and its effects. Ecological Modelling 85, 253-270.

Veldkamp, A., Kok, K., De Koning, G.H.J., Schoorl, J.M., Sonneveld, M.P.W. and Verburg, P.H., 2001. Multi-scale system approaches in agronomic research at the landscape level. Soil & Tillage Research 58, 129-140.

Veldkamp, A. and Tebbens, L.A., 2001. Registration of abrupt climate changes within fluvial systems: insights from numerical modelling experiments. Global and Planetary Change 28, 129-144.

Veldkamp, A. and Van Dijke, J.J., 2000. Simulating internal and external controls on fluvial terrace stratigraphy: a qualitative comparison with the Maas record. Geomorphology 33, 225-236.

Walling, D.E. and He, Q., 1999. Improved models for estimating soil erosion rates from Cesium-137 measurements. Journal of Environmental Quality 28, 611-622.

Walling, D.E. and Quine, T.A., 1990. Calibration of Caesium-137 measurements to provide quantitative erosion rate data. Land Degradation and Rehabilitation 2, 161-175.

Walling, D.E. and Quine, T.A., 1991. Use of ^{137}Cs measurements to investigate soil erosion on arable fields in the UK: potential applications and limitations. Journal of Soil Science 42, 147-165.

Walling, D.E. and Quine, T.A., 1992. The use of caesium-137 measurements in soil erosion surveys. In: Bogen, J., Walling, D.E. and Day, T.J. (Eds.), Erosion and Sediment Transport Monitoring Programmes in River Basins (Proceedings of the Oslo Symposium, August 1992). IAHS Publication no. 210, pp 143-153.

Wang, X. and Yin, Z., 1998. A comparison of drainage networks derived from digital elevation models at two scales. Journal of Hydrology 210, 221-241.

Wedepohl, K.H., 1978. Handbook of geochemistry. Springer-Verlag, Berlin, Heidelberg, New York,

Weijermars, R., 1991. Geology and tectonics of the Betic Zone, SE Spain. Earth Science Reviews 31, 153-236.

Weijermars, R., Roep, T.B., Van den Eeckhout, B., Postma, G. and Kleverlaan, K., 1985. Uplift history of a Betic fold nappe inferred from Neogene - Quaternary sedimentation and tectonics (in the Sierra Alhamilla and Almeria, Sorbas and Tabernas Basin of the Betic Cordilleras, SE Spain). Geologie en Mijnbouw 64, 397-411.

Wielemaker, W.G., de Bruin, S., Epema, G.F. and Veldkamp, A., 2001. Significance and application of the multi-hierarchical landsystem in soil mapping. Catena 43, 15-34.

Willgoose, G., Bras, R.L. and Rodríguez Iturbe, I., 1991a. A coupled channel network growth and hillslope evolution model. Water Resources Research 27, 1671-1684.

Willgoose, G., Bras, R.L. and Rodríguez Iturbe, I., 1991b. Results from a new model of river basin evolution. Earth Surface Processes and Landforms 16, 237-254.

Willgoose, G. and Riley, S., 1998. The long-term stability of engineered landforms of the ranger uranium mine, Northern Territory, Australia: applications of a catchment evolution model. Earth Surface Processes and Landforms 23, 237-259.

Wischmeier, W.H. and Smith, D.D., 1958. Rainfall energy and its relationship to soil loss. Transactions, American Geophysical Union 39, 285-291.

Wood, J., 1996. The geomorphological characterisation of digital elevation models. Department of Geography, University of Leicester, Leicester, UK,

Wröbel, F. and Michalzik, D., 1999. Facies successions in the pre-evaporitic Late Miocene of the Lorca Basin, SE Spain. Sedimentary Geology 127, 171-191.

Yang, H., Chang, Q., Du, M., Minami, K. and Hatta, T., 1998. Quantitative model of soil erosion rates using ^{137}Cs for uncultivated soil. Soil Science 163 (3), 248-257.

Yin, Z. and Wang, X., 1999. A cross-scale comparison of drainage basin characteristics derived from digital elevation models. Earth Surface Processes and Landforms 24, 557-562.

Zhang, W. and Montgomery, D.R., 1994. Digital elevation model grid size, landscape representation, and hydrologic simulations. Water Resources Research 30, 1019-1028.

Zhang, X., Higgitt, D.L. and Walling, D.E., 1990. A preliminary assessment of the potential for using caesium-137 to estimate rates of soil erosion in the Loess Plateau of China. Hydrological Sciences Journal des Sciences Hydrologiques 35, 243-252.

Zhang, X., Quine, T.A. and Walling, D.E., 1998. Soil erosion rates on sloping cultivated land on the Loess Plateau near Ansai, Shaanxi Province, China: an investigation using ^{137}Cs and rill measurements. Hydrological Processes 12, 171-189.

Summary

"Addressing the Multi-scale Lapsus of Landscape" with the sub-title *"Multi-scale landscape process modelling to support sustainable land use: A case study for the Lower Guadalhorce valley South Spain"* focuses on the role of landscape as the main driving factor behind many geo-environmental processes at different temporal and spatial levels. LAPSUS[7] is the name of the geomorphological model developed in this study and at the same time it is taken, with a certain degree of freedom, as a reference to the underestimated importance of landscape as cause and result of geomorphological processes.

The **main objective** of this research is to investigate the role of the landscape at different spatial and temporal levels (extension and resolution) in geomorphological processes, focussing on the sustainability of land use within a representative Mediterranean landscape. Landscape is defined in terms of genesis, geomorphology, lithology/ soil, land cover, land use, and even land management (human factor).

The **research area** chosen for this study is located in the south of Spain, surrounding the village of Álora, in the central Guadalhorce river basin in the province of Málaga, Andalucía (Fig. 1.1). The area has a mean annual temperature of 17.5 °C and receives a mean yearly rainfall of 534 [mm], distributed mainly from October to April. This research area was selected as representative for a wide variety of Mediterranean environmental conditions in terms of a complex geological history resulting in a spatial diversification over short distances of morphology, lithology and active landscape processes ranging from tectonics, land use changes to land degradation.

The study is directed, from the beginning to the end, at different spatial and temporal extensions-resolutions, studying different landscape processes within their specific spatial and temporal boundaries (Fig. 1.2). The first step in this investigation is the understanding of the evolution of the landscape and the geological background of the research area (spatial extension 10^2 [km^2], temporal extension 10^7 [a], temporal resolution 10^4 to 10^5 [a], Chapter 2). The second step is the development of a multi-scale landscape process model LAPSUS, valid at different spatial and temporal resolutions (spatial extension 10^3 to 10^5 [m^2], spatial resolution from 1 to 81 [m], Chapter 3). The third step comprises the actual measurement of net soil redistribution rates at the landscape level using the ^{137}Cs technique. First, the applicability of this technique under the current Mediterranean conditions of the research area

[7] LandscApe ProcesS modelling at mUltidimensions and Scales

is evaluated (spatial extension 10^3 to 10^5 [m^2] Chapter 4). Secondly, net ^{137}Cs derived soil redistribution rates on the temporal resolution of years and decades is simulated and the monitored erosion and sedimentation patterns are compared with the possibilities of the LAPSUS model (spatial resolution 7.5 [m], Chapter 5). The fourth step is the evaluation of the soil-landscape context at the multi-catchment or basin scale with special attention to the effects of soil redistribution upon water availability for vegetation (spatial extension 10^2 [km^2], Chapter 6). The fifth step is the integration of landscape process modelling and changes in land use to evaluate on-site and off-site effects (spatial extension 10 [km^2], spatial resolution 25 [m], temporal extension 10 [a], temporal resolution 1 [a], Chapter 7). As a final step a synthesis of results, comments and evaluation of the research is done (Chapter 8).

Landscape evolution from a geological perspective. Landscape evolution is the result of a variety of geomorphological processes and their controls in time. Tectonics, climate and sea level fluctuations have mainly controlled landscape evolution in the research area. Data is obtained and analysed from the Upper Miocene to present (Chapter 2). Consequently, geomorphological reconstructions are made using sedimentary evidence such as marine and fluvial deposits, as well as erosional evidence such as terrain form and longitudinal profile analysis. These reconstructions add information and constraints to the uplift history and landscape development of the research area. Main sedimentation phases are the Late Tortonian, Early Pliocene and Pleistocene. Important erosional hiatus are found for the Middle Miocene, Messinian and Late Pliocene to Early Pleistocene. Concerning the palaeo-landscape, this resulted in a relative large and elongated Tortonian marine valley filled up with complex sedimentary structures. Next a prolonged stage of erosion of these deposits and incision of the major valley system took place during the Messinian. In the Pliocene a short palaeo-Guadalhorce, in a narrow and much smaller valley existed, partly filled with marine sediments combined with prograding fan delta complexes. During the Pleistocene a wider and larger incising river system resulted in rearrangements of the drainage network (Fig. 2.10). Evaluating the uplift history of the area, the tectonic activity was relatively higher during the Tortonian-Messinian and Late Pleistocene, while it was lower during the Pliocene. Relative uplift rates for the study area range between 160-276 [m Ma^{-1}] in the Messinian, 10-15 [m Ma^{-1}] in the Pliocene to 40-100 [m Ma^{-1}] during the Pleistocene (Table 2.1).

Multi-scale landscape process modelling. Once the geological background is understood, the development and testing of a landscape process model is undertaken (Chapter 3). Since resolution effects remain a factor of uncertainty in many hydrological and geomorphological modelling approaches, an experimental multi-scale study of landscape process modelling is presented, with emphasis on quantifying the effect of changing the spatial resolution upon modelling the processes of erosion and sedimentation (Fig. 3.1). A simple single process model is constructed and equal boundary conditions are created. The use of artificial DEMs eliminates the possible effects of landscape representation. Consequently, the only variable factors are DEM resolution and the method of flow routing, both steepest descent and multiple flow directions. An important dependency of modelled erosion and sedimentation rates on these main variables is found. The general trend is an increase of erosion predictions with coarser resolutions (Figs. 3.2 and 3.3). An artificial mathematical overestimation of erosion and a realistic natural modelling effect of underestimating re-sedimentation cause this. Increasing the spatial extent eliminates the artificial effect while at the same time the realistic effect is enhanced. Both effects can be quantified and are expected to increase within natural

landscapes. The modelling of landscape processes will benefit from integrating these types of results at different resolutions.

The use of the ^{137}Cs technique in a Mediterranean environment. The ^{137}Cs technique has been used in all sorts of environments all over the world to estimate net soil redistribution rates. However, its potentials in areas with shallow and stony soils on hard rock lithology remain unclear. Concentrations in the soil of artificial and natural radionuclides are investigated to assess the applicability of this technique in the study area as a mean to estimate soil redistribution (Chapter 4) and to calibrate the LAPSUS model (Chapter 5). The radionuclide concentrations vary in relation to lithology: natural radionuclides such as Potassium-40 (^{40}K), Uranium-238 (^{238}U) and Thorium-232 (^{232}Th) show significant higher concentrations in the gneiss than in the serpentinite soils for both reference profiles as all other samples. This as opposed to the artificial radionuclide Caesium-137 (^{137}Cs), which is found significantly higher in the serpentinite soils, for the reference profiles probably because of the difference in clay mineralogy and for the transect samples because of difference in soil distribution. The exponential decrease of ^{137}Cs with soil depth and its homogeneous spatial distribution emphasise the applicability of the ^{137}Cs technique in this type of Mediterranean environments. The spatial distribution of the ^{137}Cs inventory and concentration are in agreement with the soil erosion and degradation indicators measured in the field. Surfaces with erosion or degradation features (higher bulk density, shallow soils or surface crust development) show lower ^{137}Cs concentrations and inventories, while protected surfaces by vegetation show higher ^{137}Cs concentrations and inventories. The distribution of ^{137}Cs along the slopes can be explained within existing conceptual models. In this way the serpentinite and gneiss slopes are classified in four models according to the present soil redistribution and the detection of erosion and deposition areas (Fig. 4.5 and 4.6).

Furthermore the landscape evolution over the past 37 years is evaluated. Estimating net soil redistribution rates from radionuclide distributions depend on the calculation of the local area reference inventory and the applied calibration technique (Fig. 5.5). The resulting net soil redistribution estimates are compared with simulations of the LAPSUS model. Total net soil loss for the research area ranges from 2 to 69 [t $ha^{-1}a^{-1}$] for serpentinite and gneiss slopes respectively (Table 5.2, Fig. 5.7, Table 5.3, Fig. 5.8). Differences in total slope sediment budgets as well as differences along the transects reveal influences of landscape representation and land use. In this case the impact of tillage erosion is far more important than possible parent material induced differences.

Dynamic landscape, soil and water redistribution. Soil suitability assessments for land use purposes are commonly based on on-site specific topographic, soil and climatic characteristics, often neglecting the effects of physical landscape processes by water. The LAPSUS model is applied, including the effects of soil and water redistribution within the landscape (run-on, runoff, erosion and sedimentation) on soil water availability (Chapter 6). The approach focuses at the coarser level of multiple catchments over a period of ten years. By means of four scenarios with increasing complexity (Table 6.1), patterns of soil loss and sediment deposition are simulated and resultant effects of water routing, soil depth and erodibility on water availability are evaluated (Figs. 6.2 to 6.6). The model operates in the landscape context using annual time steps and both on-site effects (local changes in terms of boundary conditions) and off-site effects (caused by changes elsewhere) are accounted for. Different approaches for surface runoff routing have a major influence on the magnitude and spatial patterns of water and soil redistribution within the landscape, as well as initial

conditions such as soil depth, parent material characteristics and erodibility. Locally decreasing water storage capacity (on-site) may cause increased runoff and erosion at lower positions in the landscape (off-site). Apparent acceptable mean regional soil loss rates, often include local soil redistribution rates that cause significant changes in actual soil depth, indirectly affecting related total amounts of available soil water.

Linking landscape process modelling and land use change. LAPSUS is also used to explore the impacts of land use changes scenarios on landscape development (Chapter 7). For a period of 10 years LAPSUS calculates soil redistribution (erosion and sedimentation) for three scenarios (Table 7.1). Main inputs are a DEM, precipitation and land use related infiltration and erodibility. Examples are shown of both on-site as well as off-site effects of land use change and the influence of different pathways of change. Each scenario produces different spatial and temporal patterns of total amounts of erosion and sedimentation throughout the landscape (Fig. 7.3). Consequently, potential land use related parameters like soil depth, infiltration and flooding risk (Fig. 7.6) change significantly too. The scenario of an abrupt change produces the highest erosion rates, compared to the gradual change scenario and the baseline scenario (Fig. 7.4). However, because of the multi-dimensional characteristics of the landscape not only the area suffering from land use change is affected. Increasing erosion and runoff rates from upstream-located olive orchards have an impact on downstream local run-on, erosion and sedimentation rates. In this case the citrus orchards situated in the valley bottom locally suffer damages from re-sedimentation events but benefit from the increase in run-on water and nutrients (Fig. 7.5).

Synthesising, the landscape was studied at different levels of temporal and spatial extensions and resolutions. Consequently it is not easy to link the results of the processes understood at those different levels, however the abstraction of some findings can give some direction: according to the geological evidence in this case study area the final present day uplift rates range between 0.07 to 0.1 [mm a^{-1}]. These rates are in the same order of magnitude as the net erosion rates for natural slopes measured with the ^{137}Cs technique. This suggests a link of the spatial temporal resolution of geological landscape evolution and actual natural landscape development. At the same time the cultivated areas on gneiss lithology indicate a factor 10 or more increase of soil redistribution, demonstrating the enormous impact of human induced landscape evolution and land use change.

LAPSUS has been developed as a single process landscape evolution model, based on the potential energy content of flowing water over a landscape surface and the continuity equation for sediment movement, operating at the landscape-annual scale. The temporal components of the model are a compromise between the spatial resolution of interest and the applied process based lumped parameters. It also can be used at different grid sizes. It has shown quite reasonable results for simulating erosion/accumulation rates at slope, subcatchment and catchment scale, introducing the effect of different lithologies and land uses. This simplification of the reality and the isolation of the influence of different factors in the landscape evolution can help to understand the on-site and off-site effects of land use changes on the landscape and the impact on the sustainability development of the region.

Resumen

Este estudio con el título *"Sobre las distintas escalas del Lapsus del paisaje"* y el subtítulo *"Modelización de los procesos del paisaje a diferentes escalas como apoyo al uso sostenible del suelo: caso de estudio del valle bajo del Guadalhorce, Sur de España"* se centra en el papel del paisaje como principal factor conductor a partir del cual tienen lugar distintos procesos geo-ambientales a diferentes niveles espaciales y temporales. LAPSUS[8] es el nombre del modelo geomorfológico desarrollado en esta investigación y al mismo tiempo se utiliza, con un cierto grado de libertad, como un juego de palabras que hace referencia a la subestimada importancia del paisaje como causa y resultado de procesos geomórficos.

El principal objetivo del trabajo consiste en investigar el papel del paisaje a distintos niveles espaciales y temporales (extensión y resolución) en los procesos geomórficos, poniendo especial atención a la sostenibilidad del uso del suelo en un paisaje representativo de montaña media Mediterránea. El paisaje se define en términos de génesis, geomorfología, litología, suelos, cobertura superficial, uso del suelo e incluso gestión del mismo (factor humano).

El área de estudio se ubica en el Sur de España, en los alrededores de la localidad de Álora, cuenca baja del río Guadalhorce en la provincia de Málaga, Andalucía (Fig. 1.1). El área goza de una temperatura media anual de 17,5° y recibe una precipitación media anual de 534 mm, distribuida principalmente de Octubre a Abril. Esta zona de estudio fue seleccionada como representativa de una amplia variedad de condiciones, teniendo en cuenta la compleja historia geológica del área, que resulta en una amplia diversidad espacial de morfologías, litologías y procesos activos del paisaje en una corta distancia desde tectónicos, pasando por cambios de usos del suelo hasta procesos de degradación del mismo.

El estudio se aborda, desde el principio hasta el final, a distintas extensiones y resoluciones espaciales y temporales, cambiando de escala espacio-temporal según lo requiera el proceso del paisaje estudiado. La Figura 1.2 esquematiza los cambios de escala en el enfoque de los temas que se han ido alternando a lo largo de todo el estudio.

El primer paso en la investigación es la caracterización y entendimiento de la evolución del paisaje y de los antecedentes geológicos del área (extensión espacial 10^2 km^2, extensión temporal 10^7 a, resolución temporal de 10^4 a 10^5 a, Capítulo 2). El segundo paso consiste en el desarrollo de un modelo del paisaje a diferentes escalas, LAPSUS, válido asimismo a diferentes resoluciones espaciales y temporales (extensión espacial de 10^3 a 10^5 m^2,

[8] Acrónimo de LanscApe ProcesS modelling at mUltidimensions and Scales.

resolución espacial de 1 a 81 m, Capítulo 3). El tercer paso comprende la medida actual de las tasas netas de redistribución de suelo usando la técnica del isótopo radioactivo ^{137}Cs. Para ello se evalúa, en primer lugar, la aplicabilidad de esta técnica en las presentes condiciones ambientales mediterráneas del área de estudio (extensión espacial de 10^3 a 10^5 m^2, Capítulo 4). En segundo lugar, se simulan tasas de redistribución de suelo basadas en los valores netos de ^{137}Cs con resolución temporal de años y décadas. Los patrones de erosión y sedimentación resultantes se comparan con los resultados obtenidos con el modelo LAPSUS (resolución espacial 7.5 m, Capítulo 5). El cuarto paso evalúa los efectos de la redistribución de suelo sobre la disponibilidad de agua en el contexto paisaje-suelos a nivel de cuenca (extensión espacial 10^2 km^2, Capítulo 6). En el quinto paso se añade el factor uso del suelo a la modelización de los procesos del paisaje, con el fin de evaluar los efectos *on-site* y *off-site* como consecuencia de cambios en los usos del mismo (extensión espacial 10 km^2, resolución espacial 25 m, extensión temporal 10 a, resolución temporal 1 a, Capítulo 7). Finalmente se realiza una pequeña síntesis de resultados, comentarios y evaluación de la investigación realizada (Capítulo 8).

La evolución del paisaje desde una perspectiva geológica. La evolución del paisaje es el resultado de una variedad de procesos geomórficos y de sus controles en el tiempo. La tectónica, el clima y las fluctuaciones del nivel marino han controlado principalmente la evolución del paisaje en el área de estudio. Consecuentemente, las reconstrucciones geomórficas se realizan utilizando evidencias sedimentológicas tales como depósitos fluviales y marinos, así como evidencias erosivas como las formas del paisaje y análisis de perfiles longitudinales. La reconstrucción paleogeográfica se centra en el período de tiempo comprendido entre Mioceno Superior hasta nuestros días (Capítulo 2). Las principales fases de sedimentación datan de finales del Tortoniense, de principios del Plioceno y del Pleistoceno. En el Pleistoceno Medio, en el Mesiniense, a finales del Plioceno y principios del Pleistoceno aparecen importantes vacíos en la información sedimentológica. En lo que respecta al paleopaisaje reconstruido, éste resulta en un valle marino de edad Tortoniense, relativamente grande y alargado, relleno con complejas estructuras sedimentarias. Durante el Mesiniense tuvo lugar un estadio prolongado de erosión e incisión del valle. En el Plioceno un pequeño paleo-Guadalhorce existió, en un valle mucho más pequeño y estrecho, parcialmente relleno con sedimentos marinos en combinación con complejos de abanicos deltaicos progradantes. Durante el Pleistoceno un sistema de incisión fluvial mucho más amplio dio lugar a una reorganización de la red de drenaje. Al evaluar la historia de levantamiento del área se encuentra que la actividad tectónica fue alta durante el Tortoniense, el Mesiniense y el Pleistoceno Superior, mientras que durante el Plioceno la actividad tectónica parece haber sido mucho menor. Las tasas relativas de levantamiento para la zona de estudio oscilan entre 160-276 mMa^{-1} en el Mesiniense, 10-15 mMa^{-1} en el Plioceno a 40-100 mMa^{-1} durante el Pleistoceno (Tabla 2.1).

Modelización de los procesos del paisaje a diferentes escalas. Una vez entendidos los antecedentes geológicos del área, se lleva a cabo el desarrollo y prueba de un modelo de procesos del paisaje (Capítulo 3). Los efectos de la resolución constituyen un factor de incertidumbre en muchos modelos hidrológicos y geomorfológicos, así pues se aborda un estudio experimental de modelización a diferentes escalas poniendo especial atención en la cuantificación del efecto del cambio de la resolución espacial sobre la modelización de procesos de erosión y sedimentación (Fig. 3.1). De este modo se construye un modelo de flujo superficial (LAPSUS) y se toman iguales condiciones de partida. El uso de un MDT artificial

elimina los posibles efectos de la representación del paisaje. Consecuentemente los únicos factores variables son la resolución del MDT y los sistemas de dirección del flujo, utilizando tanto el sistema de descenso a la celda más baja como el sistema de direcciones múltiples de flujo. Se encuentra que las tasas de erosión y sedimentación modelizadas dependen enormemente de estas variables. La tendencia general es un incremento de la tasa de erosión estimada a mayores resoluciones (Fig. 3.2 y 3.3). Una sobrestimación matemática de la erosión y una subestimación en los modelos de la re-sedimentación natural causan este efecto. El incremento de la extensión espacial elimina el efecto artificial mientras que al mismo tiempo el efecto realista mejora. Ambos efectos pueden ser cuantificados y se espera su incremento al utilizarse en la simulación paisajes naturales. La modelización de los procesos del paisaje podría verse enormemente beneficiada si se integraran estos tipos de resultados a diferentes resoluciones.

El uso de la técnica del ^{137}Cs en ambientes mediterráneos. La técnica del ^{137}Cs se ha usado en todo tipo de ambientes para la estimación de las tasas netas de redistribución de suelo. Sin embargo su potencial sobre suelos poco profundos y pedregosos desarrollados sobre litologías duras se encuentra poco definido. En este trabajo se investigan las concentraciones en el suelo de isótopos radioactivos, naturales y artificiales, con el objetivo de evaluar la aplicabilidad de esta técnica en el área de estudio como medio para estimar la redistribución del suelo (Capítulo 4) y para calibrar el modelo LAPSUS (Capítulo 5). Las concentraciones de isótopos radioactivos varían en función de la litología, los isótopos naturales tales como Potasio-40 (^{40}K), Uranio-238 (^{238}U) y Torio-232 (^{232}Th) se muestran en mayor concentración en el gneis que en los suelos de serpentinitas, en contraste con el isótopo artificial Cesio-137 (^{137}Cs) que aparece en mayor concentración en los suelos de serpentinitas, probablemente debido a la diferencia en la mineralogía de arcillas. La distribución espacial del inventario y la concentración del ^{137}Cs están en concordancia con los indicadores de erosión y degradación de suelo estimados. Superficies con señales de erosión o degradación muestran concentraciones e inventarios más bajos de ^{137}Cs, mientras que superficies protegidas por la vegetación muestran concentraciones e inventarios más elevados de ^{137}Cs. La distribución de ^{137}Cs a lo largo de las laderas puede ser explicada dentro de los modelos conceptuales existentes. En este sentido las laderas de serpentinitas y gneis se pueden clasificar en cuatro modelos según la distribución actual de suelo que presentan y la detección de áreas de erosión y deposición.

Además se evalúa la evolución del paisaje en los últimos 37 años calibrando LAPSUS con los resultados de redistribución de suelo derivados de la técnica del ^{137}Cs. La estimación de las tasas netas de redistribución de suelo a partir de la distribución de isótopos radioactivos depende del cálculo del inventario de referencia local y del sistema de calibración aplicado (Fig. 5.5). Las tasas resultantes de redistribución de suelo estimadas se comparan con los resultados de las simulaciones de LAPSUS. La pérdida neta total de suelo para el área de investigación oscila desde 2 a 69 [t $ha^{-1}a^{-1}$] para las serpentinitas y para los gneis respectivamente (Tabla 5.2, Fig. 5.7, Tabla 5.3, Fig. 5.8). Las diferencias en el balance total de sedimentos a escala de ladera así como las diferencias a lo largo de transectos revelan las influencias de la representación del paisaje y los usos del suelo. En este caso el impacto del laboreo sobre la erosión es mucho más importante que la influencia de la litología.

La dinámica del paisaje, redistribución de suelo y agua. La evaluación del uso adecuado del suelo se basa principalmente en las características topográficas, edáficas y climáticas de la zona en concreto, a menudo ignorando los efectos de los procesos hidrológicos en el paisaje.

El modelo LAPSUS se aplica incluyendo los efectos de la redistribución de suelo y agua dentro del paisaje (simulando procesos de escorrentía erosión y sedimentación) sobre la disponibilidad de agua (Capítulo 6). El problema se aproxima desde una resolución mayor de cuencas múltiples sobre un período de 10 años. Utilizando cuatro escenarios a lo largo de los cuales se va incrementando la complejidad (Tabla 6.1), se simulan los patrones de pérdida de suelo y sedimentación y se evalúan los efectos resultantes de profundidad del suelo, distribución de flujos y erodibilidad sobre la disponibilidad de agua (Fig. 6.2, 6.3, 6.4, 6.5, y 6.6). El modelo opera en el contexto del paisaje utilizando incrementos de tiempo anuales, efectos *on-site* (cambiando las condiciones locales de partida) y *off-site* (causados por los cambios en otras partes de la cuenca). Las diferentes aproximaciones al sistema de redirección del flujo de agua ejercen una gran influencia sobre la magnitud y los patrones espaciales de redistribución de suelo. También las condiciones iniciales de profundidad del suelo y características de la roca madre ejercen gran influencia espacial sobre la redistribución de suelo en el paisaje. Localmente el descenso de la capacidad de almacenamiento de agua (*on-site*) puede causar incrementos de la escorrentía y la erosión en las posiciones más bajas del paisaje (*off-site*). Tasas medias regionales de pérdida de suelo aparentemente razonables, incluyen a menudo tasas de redistribución locales de suelo que causan cambios significativos en la profundidad del mismo, afectando indirectamente a la cantidad de agua disponible.

Conexión entre los procesos del paisaje y los cambios de uso del suelo. El modelo LAPSUS se utiliza también como herramienta para explorar el impacto de distintos escenarios con cambios en los usos del suelo en el desarrollo del paisaje (Capítulo7). Para un período de 10 años LAPSUS calcula la redistribución de suelo (erosión y sedimentación) para distintos escenarios propuestos (Tabla 7.1). Las principales entradas para el modelo son el MDT, la precipitación, la infiltración y la erodibilidad relacionadas con el uso específico del suelo. Se muestran ejemplos con efectos *on-site* y *off-site* de cambios de usos del suelo y la influencia de las distintas tendencias de cambio. Cada escenario produce diferentes patrones espaciales y temporales de erosión y sedimentación (Fig. 7.3). Como resultado, parámetros relacionados con el uso del suelo como profundidad del mismo, infiltración y riesgo de inundación (Fig. 7.6) cambian también significativamente. El escenario en el cual se introduce un cambio abrupto produce las mayores tasas de erosión comparado con el escenario donde se introduce un cambio gradual y el escenario base (Fig. 7.4). Sin embargo, debido a las características multidimensionales del paisaje, no sólo el área que sufre directamente el cambio de uso del suelo se encuentra afectada. El incremento de la erosión y las tasas de escorrentía de los campos de olivos de la parte alta de la cuenca produce un impacto en las tasas de escorrentía, erosión y sedimentación en la parte baja de la misma. En este caso los campos de cítricos ubicados en la base del valle sufren localmente daños debido a los efectos de la resedimentación pero se benefician de la mayor disponibilidad de agua y nutrientes (Fig. 7.5).

A modo de **síntesis** se puede decir que el estudio del paisaje ha sido abordado a diferentes niveles, haciendo alusión a distintas resoluciones y extensiones tanto espaciales como temporales. Como consecuencia no es fácil enlazar los resultados de los procesos entendidos a tan variadas escalas, sin embargo es necesario un intento de conceptualización de resultados: según la evidencia geológica en esta área de estudio, las tasas de levantamiento actual oscilan entre 0.07 a 0.1 mma^{-1}. Estas tasas se encuentran en el mismo orden de magnitud que las tasas de erosión neta medidas para laderas naturales con la técnica del ^{137}Cs. Esto sugiere una conexión entre la resolución espacio-temporal de la evolución geológica y la evolución actual natural del paisaje. Al mismo tiempo las áreas cultivadas y asentadas sobre gneises indican un

factor 10 o más de incremento de la redistribución del suelo, demostrando el enorme impacto de las actividades humanas y los cambios de uso del suelo sobre la evolución del paisaje.
LAPSUS se concibe como un modelo de evolución del paisaje sobre un proceso único (escorrentía superficial), basado en el contenido de energía potencial del flujo de agua superficial y la ecuación de continuidad para el movimiento de sedimentos, operando a una escala anual. Los componentes temporales del modelo constituyen un compromiso entre una resolución espacial determinada y los parámetros agrupados del proceso aplicado. Se puede utilizar también aplicando distintas resoluciones espaciales. El modelo ha mostrado resultados bastante razonables para las distintas tasas de erosión/acumulación simuladas a nivel de ladera, subcuenca y cuenca, introduciendo el efecto de las distintas litologías y usos del suelo. La simplificación de la realidad y el aislamiento de la influencia de los distintos factores en la evolución del paisaje puede ayudar a comprender los efectos *on-site* y *of-site* de los cambios del uso del suelo y su impacto en el desarrollo sostenible de la zona.

Samenvatting

Dit proefschrift *"een verhandeling over de lapsus van het landschap op verschillende schaal niveaus"* met als ondertitel *"het modeleren van processen in het landschap op meerdere schaal niveaus ter ondersteuning van duurzaam landgebruik: een studie in de benedenstroomse Guadalhorce vallei in het zuiden van Spanje"* richt zich op de rol van het landschap als de belangrijkste sturende factor voor vele geo-ecologische processen op verschillende temporele en ruimtelijke niveaus. LAPSUS[9] is de naam van het geomorfologische model dat voor dit proefschrift ontwikkeld is terwijl het tegelijkertijd, met een zekere graad van vrijheid, refereert aan de regelmatig onderschatte rol van het landschap als oorzaak en gevolg van de belangrijkste geo-ecologische processen met betrekking tot duurzaam landgebruik.

De **hoofd doelstelling** van deze studie is het onderzoeken van de rol van het landschap in geomorfologische en bodemkundige processen op verschillende ruimtelijke en temporele niveaus (zowel extensie als resolutie), met speciale aandacht voor de duurzame ontwikkeling van landgebruik in een representatief Mediterraan landschap. De term landschap is een zeer breed begrip en kan gedefinieerd worden in het kader van ontstaanswijze, geomorfologie, lithologie en bodem, land bedekking, land gebruik en zelfs de menselijke factor management.

Het **onderzoeksgebied** voor deze studie is gesitueerd in het zuiden van Spanje, midden in het stroomgebied van de Guadalhorce, in de omgeving van Álora, provincie van Málaga, Andalusie (zie Figuur 1.1). Het gebied heeft een gemiddelde jaar temperatuur van 17.5 graden Celsius en een gemiddelde jaarlijkse neerslag van 534 millimeter die voornamelijk valt in de winter tussen oktober en april. Deze condities in het onderzoeksgebied zijn representatief voor de mediterrane omgeving. Dit gebied is geselecteerd op grond van zijn complexe geologische geschiedenis met daardoor een grote verscheidenheid over betrekkelijke korte afstanden aan morfologie, lithologie en actieve landschapsprocessen variërend van tektoniek, veranderingen in landgebruik tot bodemerosie en sedimentatie.

Processen in het landschap zijn schaal afhankelijk zowel in de tijd (temporeel) als in de ruimte. Verder hebben deze processen een bepaalde omvang, duur of bereik (extensie) en een snelheid, grootte of eenheid (resolutie). De hoofdstukken in dit proefschrift zijn van begin tot einde gericht op de verschillende ruimtelijke en temporele extensies en resoluties van processen in het landschap (Figuur 1.2). De eerste stap in dit onderzoek is het begrijpen van

[9] acroniem voor Landschap proces modeleren op meerdere schaal niveaus en dimensies (LandscApe ProcesS modelling at mUltidimensions and Scales)

de vormingsgeschiedenis van het landschap en haar geologische achtergrond in het studie gebied (ruimtelijke extensie 10^2 km^2, temporele extensie 10^7 jaar, temporele resolutie 10^4 tot 10^5 jaar, Hoofdstuk 2). De tweede stap in dit onderzoek was het ontwikkelen van een model (LAPSUS) voor het simuleren van processen in het landschap dat gebruikt kan worden op meerdere schaal niveaus (ruimtelijke extensie 10^3 tot 10^5 m^2, ruimtelijke resolutie van 1 tot 81 m, Hoofdstuk 3). De derde stap omvatte het eigenlijke meten van netto bodemherverdeling op landschapsniveau met behulp van de Cesium techniek. Als eerste is de toepasbaarheid van deze techniek geëvalueerd voor de typische mediterrane omstandigheden in het onderzoeksgebied (ruimtelijke extensie 10^3 tot 10^5 m^2, Hoofdstuk 4). Daarna is de netto bodem herverdeling berekend met de Cesium techniek voor een geldige temporele resolutie van jaren tot decennia en de resulterende erosie en sedimentatie patronen zijn vergeleken met de mogelijkheden van het LAPSUS model (ruimtelijke resolutie 7.5 m, Hoofdstuk 5). De vierde stap in deze studie was het evalueren van de bodem landschap relaties op het niveau van een uitgestrekt stroomgebied met speciale aandacht voor het effect van bodemherverdeling op de beschikbaarheid van water voor gewassen (ruimtelijke extensie 10^2 km^2, Hoofdstuk 6). De vijfde stap is de integratie van het modeleren van processen in het landschap en de veranderingen in landgebruik om zowel lokale effecten als niet-lokale indirecte effecten te kunnen evalueren (ruimtelijke extensie 10 km^2, ruimtelijke resolutie 25 m, temporal extensie 10 jaar, temporal resolutie 1 jaar, Hoofdstuk 7). De laatste stap is een synthese van de resultaten en een evaluatie van het onderzoek (Hoofdstuk 8).

De evolutie van het landschap vanuit een geologisch perspectief. Het landschap onstaat door een scala van geomorfologische processen en hun controles in de tijd. Fluctuaties in tektoniek, klimaat en zeespiegel zijn de voornaamste actoren in de evolutie van het landschap in het studiegebied. Gegevens zijn verzameld en geanalyseerd vanaf het Boven Mioceen tot heden (Hoofdstuk 2). Hierdoor was het mogelijk om een geomorfologische reconstructie van het gebied te maken zowel op basis van fluviatiele en mariene sedimenten als ook op basis van erosieve kenmerken in het landschap zoals de morfologie en gradiënt ontwikkeling. Deze reconstructies dragen bij tot het verklaren van de opheffings geschiedenis en ontwikkeling van het landschap in het studie gebied. Belangrijke sedimentaire fases zijn gevonden in het Laat Tortonien, Vroeg Plioceen en Pleistoceen. Belangrijke erosieve hiaten komen voor in het Midden Mioceen, Messinien en Laat Plioceen tot Vroeg Pleistoceen. Dit betekent met betrekking tot het paleo-landschap, dat in het Tortonien een relatief lange maar nauwe zeestraat bestond in een recent opgeheven landschap. Deze zeestraat is opgevuld met complexe sedimentaire structuren. Gedurende het Messinien is de zee uit het gebied verdwenen en was er een langdurige periode van erosie van de Tortonien sedimenten en de insnijding van het huidige hoofddal systeem kwam tot stand. Door een ingrijpende zeespiegel stijging gedurende het Plioceen bestond er een aanzienlijk korter en minder uitgebreid oer Guadalhorce rivier systeem met in het benedenstroomse deel meerdere delta systemen en afzetting van mariene sedimenten. In het Pleistoceen ontstaat er een meer uitgebreid rivier systeem dat zich over het algemeen insnijd en zorgt voor meerdere herschikkingen van het drainage patroon (Figuren 2.10). Voor de geschiedenis van opheffing betekent dit: (i) relatief hogere ophef snelheden gedurende het Tortonien, Messinien en het Laat Pleistoceen en (ii) relatief lage opheffingssnelheden tijdens het Plioceen en Vroeg Pleistoceen. Deze relatieve ophef snelheden variëren tussen de 160-276 m Ma^{-1} voor het Messinien, 10-15 m Ma^{-1} voor het Plioceen tot 40-100 m Ma^{-1} gedurende het Pleistoceen (Tabel 2.1).

Het modeleren van landschapsprocessen op meerdere schaal niveaus. Na het bestuderen van de geologische achtergrond van het onderzoeksgebied, is er een begin gemaakt met het ontwikkelen en testen van een model dat de landschapvormende processen kan modeleren. Resolutie effecten blijven een factor van onzekerheid in de meeste hydrologische en geomorfologische modellen. Daarom is er een experimenteel landschapsmodel voor meerdere schaal niveaus getest waarbij de nadruk lag op het kwantificeren van de effecten van resolutie veranderingen op de bodem herverdelings-processen (Figuur 3.1). Een simpel proces model is ontwikkeld en tijdens de experimenten zijn alle invoer en rand voorwaarden gelijk gehouden. Het gevolg was dat de resolutie van het digitale hoogte model (DEM) en de methode van waterherverdeling als enige variabele factoren overbleven. Waterherverdeling in een DEM kan namelijk berekend worden met alleen de steilste, laagst gelegen omringende cel of via meerdere lager gelegen cellen. Tijdens deze experimenten zijn belangrijke verbanden gevonden tussen de variabele factoren als DEM resolutie en waterherverdelingsmethode en de erosie en sedimentatie processen. De algemeen gevonden trend is een toename van erosie wanneer er grovere resoluties gebruikt worden (Figuren 3.2 en 3.3). De oorzaak van deze trend is een mathematische overschatting van erosie en een realistisch modeleer effect met betrekking tot het onderschatten van sedimentatie. Het vergroten van de oppervlakte (extensie) van het te modeleren gebied verkleinen deze kunstmatige mathematische effecten maar vergroten het realistische effect. Beiden effecten zijn te kwantificeren en verwacht wordt dat deze effecten zullen toenemen wanneer DEMs van natuurlijke landschappen gebruikt gaan worden. De resultaten van deze experimenten en het kwantificeren van dit soort schaal effecten zullen het uiteindelijke modeleren van processen in het landschap op verschillende schaal niveaus ten goede komen.

De Cesium techniek in een mediterrane omgeving. Tot nu toe is de Cesium techniek voor het schatten van bodemherverdelingsnelheden toegepast in veel verschillende omgevingen over de gehele wereld. Echter, de toepasbaarheid van deze techniek in ondiepe en stenige bodems is nauwelijks onderzocht. Daarom zijn de concentraties in de bodem van zowel antropogene als natuurlijke radionucleïden onderzocht om de toepasbaarheid van de Cesium techniek in het onderzoeksgebied te bepalen met betrekking tot verschillende moedermaterialen (Hoofdstuk 4) en het bepalen van bodem herverdeling voor het kalibreren van het LAPSUS model (Hoofdstuk 5). De concentraties van de radionucleïden zijn afhankelijk van de lithologie: de natuurlijke radionucleïden zoals Kalium-40 (^{40}K), Uranium-238 (^{238}U) and Torium-232 (^{232}Th) vertonen significant hogere concentraties in de gneis bodems dan in de serpentiniet bodems zowel voor de referentie profielen als voor alle monsters bij elkaar. Dit in tegenstelling tot de antropogene radionucleïde Cesium-137 (^{137}Cs) welke significant hogere concentraties vertonen in serpentiniet bodems. De sterk exponentiële afname van ^{137}Cs met bodem diepte in alle referentie profielen en de homogene ruimtelijke distributie benadrukken de bruikbaarheid van de ^{137}Cs techniek in dit soort Mediterrane omgevingen. Bodemoppervlaktes met degradatie verschijnselen (zoals een hogere bulk dichtheid, ondiepe bodems of korst ontwikkeling) vertonen lagere ^{137}Cs concentraties, terwijl de stabielere en door vegetatie beschermde bodems hogere ^{137}Cs concentraties vertonen. De ruimtelijke verdeling van ^{137}Cs over de helling kan verklaard worden binnen de bestaande conceptuele modellen. Als gevolg hiervan zijn de serpentiniet en gneis bodems geclassificeerd op basis van de huidige bodem herverdeling en het onderscheiden van helling segmenten met erosie of sedimentatie (Figuren 4.5 en 4.6).

Vervolgens zijn de proces snelheden en de vorming van het landschap over de laatste decennia geëvalueerd. Het schatten van netto snelheden van bodemherverdeling aan de hand van radionucleïde distributies hangt af van de bepaling van de lokale referentie inventarisatie en de toegepaste ijk-methode (Figuur 5.5). De uiteindelijke netto snelheden van bodemherverdeling zijn vergeleken met de uitkomsten van LAPSUS simulaties. Totale netto bodemherverdelingen in het studie gebied variëren van 2 tot 69 ton $ha^{-1}a^{-1}$ voor de serpentiniet en gneis hellingen, respectievelijk (Tabel 5.2, Figuur 5.7, Tabel 5.3, Figuur 5.8). De verschillen in bodemverlies tussen de hellingen en binnen de transecten onthullen de invloeden van zowel landgebruik als de hoogte representatie van het landschap (DEM). In ieder geval zijn in het studiegebied de gevolgen van ploeg erosie veel belangrijker dan die van verschillen in het moedermateriaal.

Dynamisch landschap, bodem en water herverdeling. Bodemgeschiktheidsstudies voor landgebruikplanning worden vaak gebaseerd op lokale bodem en klimaat karakteristieken. Vaak worden hierbij de schaal effecten van actuele processen in het landschap genegeerd. Het LAPSUS model is toegepast om de effecten van bodem en water herverdeling in het landschap op de bodemwaterbeschikbaarheid voor gewassen te simuleren (hoofdstuk 6). Deze benadering legt de nadruk op het niveau van meerdere vanggebieden tegelijk over een periode van tien jaar. Door middel van vier scenarios met toenemende complexiteit (Tabel 6.1) zijn patronen van bodemerosie en hersedimentatie gesimuleerd, met speciale aandacht voor de gevolgen van waterherverdeling, bodem dieptes en erosie gevoeligheid op de waterbeschikbaarheid voor gewassen (Figuren 6.2 t/m 6.6). Het model simuleert met tijdstappen van een jaar en beschouwt zowel lokale effecten (on-site, plaatsgebonden en randvoorwaarden) als niet lokale effecten (off-site, veroorzaakt door veranderingen van buitenaf). Het gebruik van verschillende methoden voor het verdelen van oppervlakkige afstroming, alsook initiële condities zoals bodemdiepte, lithologische karakteristieken en erosiegevoeligheid hebben een belangrijke invloed op de hoeveelheid en de ruimtelijke patronen van bodemherverdeling in het landschap. Een afnemende water opslag capaciteit in de bodem op een bepaalde plaats kan leiden tot een toename van afstromend water en kan daardoor zowel lokaal meer erosie veroorzaken alsook op lager gelegen plaatsen in het landschap. Op het eerste gezicht aanvaardbare regionale erosie snelheden zijn slechts een gemiddelde en kunnen erosie snelheden negeren of uitmiddelen die op bepaalde locaties wel degelijk een significante afname kunnen veroorzaken van bodem diepte en daardoor hoeveelheid beschikbaar water voor gewassen.

Het koppelen van het modeleren van processen in het landschap en veranderingen in landgebruik. Het LAPSUS model is ook gebruikt om het effect te onderzoeken van veranderingen in landgebruik op de ontwikkeling van het landschap (Hoofdstuk 7). LAPSUS heeft met verschillende scenarios voor een periode van 10 jaar de bodem herverdeling berekend (zowel erosie als sedimentatie). De belangrijkste invoer gegevens waren een digitaal hoogte model (DEM), neerslag en landgebruik gerelateerde infiltratie en erosie gevoeligheid (Tabel 7.1). Dit heeft een aantal voorbeelden opgeleverd van lokale en niet-lokale effecten van landgebruikverandering en de invloed van verschillende temporele trajecten. Elk scenario produceert verschillende ruimtelijke en temporele patronen en dus hoeveelheden van erosie en sedimentatie in het landschap (Figuur 7.3). Dit heeft als gevolg dat ook de aan landgebruik gerelateerde parameters zoals bodemdiepte, infiltratie en overstromingsgevaar (Figuur 7.6) significant veranderen. Het scenario van een plotselinge landgebruikverandering veroorzaakt de hoogste erosie snelheden, in vergelijking met de geleidelijke verandering en de baseline

scenarios (Figuur 7.4). Echter door het multi dimensionale karakter van het landschap wordt niet alleen het gebied dat met de landgebruikveranderingen te maken heeft getroffen. In dit geval hebben toenemende hoeveelheden erosie en afstromend water van boven aan de helling en bovenstrooms gelegen olijf boomgaarden een belangrijke invloed op de hoeveelheid erosie, sedimentatie en afstromend water beneden aan de helling en in benedenstrooms gelegen gebieden. Hierdoor kunnen de in het dal gelegen citrus velden lokaal schade ondervinden van overstromingen, erosie en sedimentatie maar ook profiteren van de verhoogde aanvoer van water en nutriënten (Figuur 7.5).

Synthese. Het landschap is onderzocht op verschillende ruimtelijke en temporele extensies en resoluties. Door het werken met modellen vergt de koppeling van de resultaten van deze verschillende processen enige vorm van abstractie. Volgens de geologische aanwijzingen en interpretaties in het studiegebied liggen bijvoorbeeld de huidige opheffingssnelheden tussen de 0.07 en 0.1 mm a^{-1}. Deze snelheden zijn in dezelfde orde van grootte als de gemeten netto erosie snelheden voor natuurlijke gebieden met de ^{137}Cs techniek. Dit suggereert dat er een verband bestaat tussen de ruimtelijke en temporele resolutie van de geologische landschapsontwikkeling en de actuele bodem herverdelingsprocessen in natuurlijke gebieden. Tegelijkertijd vertonen de gecultiveerde hellingen een toename van erosie met een factor 10 of meer, wat de enorme invloed aangeeft van door de mens veroorzaakte landschap evolutie en landgebruikverandering.

LAPSUS is ontwikkeld als een eenvoudig landschap evolutie model, gebaseerd op de potentiële energie van stromend water over het landoppervlak en de continuiteits-vergelijking van sediment beweging op jaar basis. The temporele componenten van het model zijn een compromis tussen de beoogde ruimtelijke resolutie en de toegepaste proces parameters. Het model kan gebruikt worden voor verschillende resoluties. Het vertoont aannemelijke resultaten van erosie en sedimentatie snelheden op de schaal van helling, vanggebied tot stroomgebied waar effecten van lithologie en landgebruik worden geïntroduceerd. Deze vereenvoudiging van de werkelijkheid en de isolatie van verschillende invloeden van factoren in de ontwikkeling van het landschap kan behulpzaam zijn bij het begrijpen van de lokale en niet-lokale effecten van landgebruikveranderingen op het landschap en kan daarmee een belangrijke bijdrage leveren aan de duurzame ontwikkeling van de regio.

Curriculum Vitae

Jeroen Machiel Schoorl was born on the 11th of January 1969 in Arnhem (Gelderland, The Netherlands). He grew up in Hank on the boarders of the Biesbosch (Noord-Brabant) digging holes, constructing rafts, playing in pop-bands, repairing old Puch mopeds and even managed to finish his secondary education (VWO) at the Dongemond College in Raamsdonksveer in 1988. This same year he started his study Physical Geography at the Laboratory of Physical Geography and Soil Science at the University of Amsterdam. In 1994, he graduated as a Physical Geographer in the subjects of genetic geomorphology, erosion studies, soil inventorisation and land evaluation.

After a year and a half of freewheeling, which meant working from the production line to Archaeological GIS specialist and from flume construction worker to secretary, he started in March 1996 as researcher and daily manager of the NRP project "Multi-scale Land Use Modelling" a project at the former Agronomy department of Wageningen University, directed by Prof. Dr. Ir. L.O. Fresco as part of the international LUCC (IGBP-IHDP) program. The investigation was directed at the further development of the CLUE model (Conversion of Land Use and its Effects), which aimed at revealing driving factors of land use change at different hierarchical levels.

In April 1997 he was given the opportunity to direct his own thesis and he became a AIO Research assistant (PhD) at the Laboratory of Soil Science and Geology, Department of Environmental Sciences, Wageningen University, on the subject "Multi-scale landscape process modelling to support sustainable land use planning: a case study for the lower Guadalhorce valley South Spain". Except for a short delay after a momentary lapse of reason when he broke his ankle during fieldwork 1998, he has been able to finish all the work, which has resulted in this thesis.

At the moment (2001-2002) he is employed as an Associate Teacher at the Laboratory of Soil Science and Geology, responsible for developing and renewing several future courses of the new study program and teaching two major courses ("Land evaluation: exploration and variability" and "Sustainable land use in Álora, Spain: landscape scale geology, geomorphology and soils"). Furthermore, in the near future he will start a two year Postdoc project (2002-2004) at BenG "Landscape farming" in the VEL&VANLA region in Friesland, funded by the PE&RC research school of Wageningen University.

Appendix

LAPSUS Source Code

```
/  **          ***     *****    *****  **   **   *****
   **         ** **    **  **   **      **   **  **
   **        *******   ****      ****   **   **   ****
   **       **     **  **           **  **   **      **
   *******  **     **  **      *****    *****   *****
*****************************************************************
***                        LAPSUS 1.1                         ***
***                  J.M. Schoorl & A. Veldkamp               ***
*** LandscApe ProcesS modelling at mUlti dimensions and Scales ***
*** (C) Copyright 1997-2002 by Wageningen University          ***
*** 27-11-2000 -infiltration moved from sed_tr to q_out loop   ***
***             -removed root2 from dh for digonal flow instead ***
***              the dx length is adapted (d_x)               ***
*** 08-12-2000 -anti-sink: new sedimentation and erosion loop, ***
***              sediment is forced down stream,              ***
***              erosion is limited on-site                   ***
*** 15-09-2001 - for SA and GN experiments infil op 0.2*soildep***
***             - t_cap and det_r muliplied with d_x length   ***
*** (C) Copyright 2002 Soil science and Geology               ***
*****************************************************************

#include <bios.h>
#include <stdio.h>
#include <stdlib.h>
#include <conio.h>
#include <dos.h>
#include <math.h>
#include <alloc.h>
#include <string.h>

#define ROOT2 1.4142135
#define PI    3.1415926

typedef double MATHLEMS;
typedef MATELEMS *vector;

typedef int INTELEMS;
typedef INTELEMS *intvector;

vector *dtm,      // dem height values, change after dt
       *dtmnew,   // dummy matrix
       *q_mat,    // discharges for time t
       *sed_tr,   // sediment transport rate for each cell
       *dz_ero,   // dz lowering or erosion for each cell
       *dz_sed,   // dz higher or sedimentation for each cell
       *K_fac,    // local erosion K-factor
       *P_fac,    // local sedimentation P-factor
       *soildep,  // local soil depth
       *infil;    // local infiltration losses

intvector  *neigh_b, // 0 or 1 to check neighbours
           *error_m, // To store error locations as integer
           *soilmap, // integer numbers for soil map
           *lumap;   // numbers to indicate landuse

int  num_out,  // number of outputs during run
     numfile,  // output file number
     dh_nul,   // number of zero slope neighbours
     flat,     // number of zero slope neighbours
     low,      // number of lower neighbours
     high,     // number of higher neighbour
     sink,     // only higher neighbours
     top,      // only lower neighbours
     ps_flat,  // pseudo flat, no lows, one or more highs
     spill,    // no highs only one low
     round,    // loop counter
     s_ch,     // loop switch
     nr,nc,    // number of rows, number of columns
     S1_error, // error switches
     S2_error, //
     row,col,  // row column counter
     i,j,      // neighbour counter
     er_ifile, // input file error switch
     result,
      scan_int, // input file integer scan
      numtel,   // counter
      rr,rrr,   // extra neighbour loop counters
      cc,ccc,   //
      ii,jj,    //
      nb_ok,    // neighbour processing check
      direct,   // unique value for steepest descent
      lock,
      tel1,tel2,tel3,tel4,
      gncnt,mocnt,macnt,ricnt,
      intmax,intmin,intcoun,intout;
long  scan_lon,    // integer file inputs
      scan_cnt;    // integer file inputs
double h,dh,dh1,   //
       dh_maxi,    //
       inpu1,inpu2, // inputs to file
       inpu3,       // inputs to file
       dhmax,       // maximum erosion
       dhmin,dhtemp,
       dmax,dmin,
       NRO,NCO, // number of rows and columns
       CSIZE,
       t_cap,   // transport capacity
       det_r,   // detachmnet rate
       set_r,   // settlement rate
       tra_di,  // travel distance
       set_di,  // settlement distance
       gmsdp,   // local soil depths
       masdp,mosdp,risdp;

double  dcount,     // difference max, min counter
        dx,dy,      // grid size in both x and y
        d_x,        // length of dx finite element
        dh_tol,     // tolerance factor
        ET0,        // Annual Evapotranspiration losses
        dt,         // time step
        actual_t,   // Time counter for loop
        end_time,   // Total end time of loop
        out_t,      // Time control in time/simulation loop
        eff_prep,   // effective precipitation
        K_act,      // Actual erosion K-factor
        P_act,      // Actual sedimentation P-factor
        m,n,        // capacity slope and discharge exponents
        Slope,      // Gradient
        conv_fac,   // convergence/divergence factor
        dS,dz,dztot,// Difference in sediment/deposition/erosion
        scan_do.    // Input double from file
        slope_sum,  // Summation over lower slopes
        sedtr_loc,  // Local sediment transport rate
        all_grids,  // Total number of grids to stop loop
        fraction,   // fraction slope by slopesum
        frac_dis,   // fraction of discharge into lower grid
        frac_tr,    // fraction of transport rate
        q_out,      // discharge. runoff
        ds_left,    // unfulfilled sedimentation
        ds_leftl,
        dz_fill,
        dz_min,mmin,// minimum lowest neighbour
```

```
        dz_max,maxx,// maximum lowest neighbour, steepest descent
        dz_bal,     // balances to check dz
        dz_bal2,    // erosion/sedimentation balances
        sedbal,
        sedbal2,
        erobal,erobal2,
        erobalto,sedbalto,
        erocnt,     // check number of eroding grids
        sedcnt,     // check number of sedimentation grids
        sed_out,    // sediment transport output of system
        nb_check;   // check if all neighbour cells are processed
char    ch[30], f_name[30],filename[30];

/*******************************************************
** make_mat() makes/ declares matrices in the memory  **
**            both double as integer matrices         **
*******************************************************/
int make_mat()
{ result=1;  // double matrices
  dtm = (vector *) calloc(nr+1,sizeof(vector));
  if (dtm==NULL) result=0;
  dtmnew = (vector *) calloc(nr+1,sizeof(vector));
  if (dtmnew==NULL) result=0;
  q_mat = (vector *) calloc(nr+1,sizeof(vector));
  if (q_mat==NULL) result=0;
  sed_tr = (vector *) calloc(nr+1,sizeof(vector));
  if (sed_tr==NULL) result=0;
  dz_ero = (vector *) calloc(nr+1,sizeof(vector));
  if (dz_ero==NULL) result=0;
  dz_sed = (vector *) calloc(nr+1,sizeof(vector));
  if (dz_sed==NULL) result=0;
  K_fac = (vector *) calloc(nr+1,sizeof(vector));
  if (K_fac==NULL) result=0;
  P_fac = (vector *) calloc(nr+1,sizeof(vector));
  if (P_fac==NULL) result=0;
  soildep = (vector *) calloc(nr+1,sizeof(vector));
  if (soildep==NULL) result=0;
  infil = (vector *) calloc(nr+1,sizeof(vector));
  if (infil==NULL) result=0;
// integer matrices
  neigh_b = (intvector *) calloc(nr+1,sizeof(intvector));
  if (neigh_b==NULL)  result=0;
  error_m = (intvector *) calloc(nr+1,sizeof(intvector));
  if (error_m==NULL)  result=0;
  soilmap = (intvector *) calloc(nr+1,sizeof(intvector));
  if (soilmap==NULL)  result=0;
  lumap = (intvector *) calloc(nr+1,sizeof(intvector));
  if (lumap==NULL)  result=0;
  for(i=0;i<(nr+1);i++) {
    dtm[i]=(vector) calloc(nc+1,sizeof(MATELEMS));
    if(dtm[i]==NULL) result=0;
    dtmnew[i]=(vector) calloc(nc+1,sizeof(MATELEMS));
    if(dtmnew[i]==NULL) result=0;
    q_mat[i]=(vector) calloc(nc+1,sizeof(MATELEMS));
    if(q_mat[i]==NULL) result=0;
    sed_tr[i]=(vector) calloc(nc+1,sizeof(MATELEMS));
    if(sed_tr[i]==NULL) result=0;
    dz_ero[i]=(vector) calloc(nc+1,sizeof(MATELEMS));
    if(dz_ero[i]==NULL) result=0;
    dz_sed[i]=(vector) calloc(nc+1,sizeof(MATELEMS));
    if(dz_sed[i]==NULL) result=0;
    K_fac[i]=(vector) calloc(nc+1,sizeof(MATELEMS));
    if(K_fac[i]==NULL) result=0;
    P_fac[i]=(vector) calloc(nc+1,sizeof(MATELEMS));
    if(P_fac[i]==NULL) result=0;
    soildep[i]=(vector) calloc(nc+1,sizeof(MATELEMS));
    if(soildep[i]==NULL) result=0;
    infil[i]=(vector) calloc(nc+1,sizeof(MATELEMS));
    if(infil[i]==NULL) result=0;
    neigh_b[i]=(intvector) calloc(nc+1,sizeof(INTELEMS));
    if(neigh_b[i]==NULL) result=0;
    error_m[i]=(intvector) calloc(nc+1,sizeof(INTELEMS));
    if(error_m[i]==NULL) result=0;
    soilmap[i]=(intvector) calloc(nc+1,sizeof(INTELEMS));
    if(soilmap[i]==NULL) result=0;
    lumap[i]=(intvector) calloc(nc+1,sizeof(INTELEMS));
    if(lumap[i]==NULL) result=0;
  }
  return(result);
} // end make_mat()

/*******************************************************
** ini_mat()    fill matrices on zero values          **
*******************************************************/
void ini_mat(void)
{
  for(row=0;row<=nr;row++) {
    for(col=0;col<=nc;col++) {
        dtm[row][col] = 0.0;
        dtmnew[row][col] = 0.0;
        q_mat[row][col] = 0.0;
        sed_tr[row][col] = 0.0;
        dz_ero[row][col] = 0.0;
        dz_sed[row][col] = 0.0;
        K_fac[row][col] = 0.0;
        P_fac[row][col] = 0.0;
        soildep[row][col] = 0.0;
        infil[row][col] = 0.0;
        neigh_b[row][col] = 0;
        error_m[row][col] = 0;
        soilmap[row][col] = 0;
        lumap[row][col] = 0;
    }
  }
} // end ini_mat()

/*******************************************************
** free_mat()  free the matrices from the memory      **
*******************************************************/
void free_mat()
{
  for(i=0;i<(nr+1);i++) {
    free(lumap[i]);
    free(soilmap[i]);
    free(error_m[i]);
    free(neigh_b[i]);
    free(infil[i]);
    free(soildep[i]);
    free(P_fac[i]);
    free(K_fac[i]);
    free(dz_sed[i]);
    free(dz_ero[i]);
    free(sed_tr[i]);
    free(q_mat[i]);
    free(dtmnew[i]);
    free(dtm[i]);
  }
  free(lumap);
  free(soilmap);
  free(error_m);
  free(neigh_b);
  free(infil);
  free(soildep);
  free(P_fac);
  free(K_fac);
  free(dz_sed);
  free(dz_ero);
  free(sed_tr);
  free(q_mat);
  free(dtmnew);
  free(dtm);
} // end free_mat()

/*******************************************************
** ini_mod()  input data from the  parameter.TXT file **
**            parameters settings                     **
*******************************************************/
void ini_mod(char *name0) // *name0 is given in main()
{
  FILE *para;             // parameter file.txt
  strcpy(f_name,name0);
  strcat(f_name,".txt");
  para=fopen(f_name,"r");
  er_ifile=1; scan_cnt=0;
  if (para==NULL){
    (void)printf("Error: unable to open %s\n", f_name);
    er_ifile = NULL;
  }
  if( (er_ifile != NULL) ) {
    for (numtel=1;numtel<11;numtel++) {
      if (er_ifile==NULL){
        scan_lon = 0;
      }
      else {
        scan_lon = 0; scan_cnt++;
        fscanf(para,"%lf",&scan_do);
        scan_lon = cell(scan_do);
        if (numtel==1) NRO = scan_do;      // number of rows
        if (numtel==2) NCO = scan_do;      // number of cols
        if (numtel==3) CSIZE = scan_do;    // Cell size
        if (numtel==4) actual_t = scan_do;// Start time
        if (numtel==5) dt =scan_do;        // Time steps
        if (numtel==6) end_time =scan_do; // end time
        if (numtel==7) eff_prep =scan_do; // precipitation in mm
        if (numtel==8) m =scan_do;         // discharge exponent
        if (numtel==9) n =scan_do;         // slope exponent
        if (numtel==10) conv_fac=scan_do; //convergence/divergence
        switch (scan_lon){
          case 0:

          (void)printf(" File %s empty after %ld numbers\n",
                                    f_name,(scan_cnt-1));

          (void)printf(" Input file format error \n");
          er_ifile = NULL;
          break;
          default:
          break;
        }
```

```
    }
  }
  nr=(int)NRO; nc=(int)NCO;
  dx=CSIZE; dy=CSIZE;
  (void)printf(" Scanned %s header %ld numbers\n", f_name,
                                                scan_cnt);
  sprintf(ch," Results\n nr:%d nc:%d act t:%4.1f
                                dt:%4.1f\n",nr,nc,actual_t,dt);
  gotoxy(1,4); printf(ch);
  sprintf(ch," end t:%4.1f prec:%4.3f m:%4.1f n:%4.1f conv:%4.1f
  dx/dy: %4.1f\n",end_time,eff_prep,m,n,conv_fac,dx);
  gotoxy(1,6); printf(ch);
  getch();
 } else {
  (void)printf("input file format error/n");
  (void)printf("Press any key");
  getch();
 }
 fclose(parm);
} // end ini_mod(name0)*/

/*******************************************************
** inir_fil()  initialise double or floating points   **
**             read from file                         **
**             input data from the  ascii .TXT file   **
**  data starting from left down corner row=0 col=0   **
**  read from left col=0 to right col=nc till right   **
**  upper corner row=nr col=nc                        **
*******************************************************/
void inir_fil(char *name1, vector *map1)
{
 FILE *pp;                          // dem_in.txt, sdp.txt
 strcpy(f_name,name1);
 strcat(f_name,".txt");
 pp=fopen(f_name,"r");
 er_ifile=1; scan_cnt=0;
 if (pp==NULL){
  (void)printf("Error: unable to open %s\n", f_name);
  er_ifile = NULL;
 }
 if( (er_ifile != NULL) ) {
  for(row=0;row<nr;row++) {
   for(col=0;col<nc;col++) {
    if (er_ifile==NULL){
     scan_do = 0.0;
    } else {
     scan_do = 0.0; scan_cnt++;
     fscanf(pp,"%lf",&scan_do);
     map1[row][col]=scan_do;
    }
   }
  }
  (void)printf(" Scanned  %s header %ld numbers\n", f_name,
  scan_cnt);
 } else  {
  (void)printf("\n input file format error\n\n");
  (void)printf(" Press any key\n");
  getch();
 }
 fclose(pp);
} // end inir_fil(name1, map1)

/*******************************************************
** ini_intf() initialise integer  for this simulation **
**            read from file                           **
*******************************************************/
void ini_intf(char *name2, intvector *map2)
{
 FILE *in_file;
 strcpy(f_name,name2);
 strcat(f_name,".txt");   // extension
 in_file = fopen(f_name, "r");
 if (in_file==NULL) SL_error=1;
 else {
  for(row=0;row<nr;row++) {
   for(col=0;col<nc;col++) {
    fscanf(in_file,"%d",&scan_int);
    map2[row][col] = scan_int;
   }
  }
  fclose(in_file);
 }
} // end ini_intf(name2, map2)

/*******************************************************
** int_file()  output integers into a surfer .grd file   **
*******************************************************/
void int_file(char *name3,intvector *map3)
{
 FILE *p;
 int idx;
 intmax=0; intout=0;
 intmin=9999;
 idx=(int)dx;
 for(row=0;row<nr;row++) {
  for(col=0;col<nc;col++) {
   intcoun=map3[row][col];
   if (intcoun>intmax) intmax=intcoun;
   if (intcoun<intmin) intmin=intcoun;
  }
 }
 strcpy(f_name,name3);
 strcat(f_name,".grd");
 p=fopen(f_name,"w");
 fprintf(p,"DSAA \n");
 fprintf(p,"%3d %6d\n",nc,nr);
 fprintf(p,"%3d %6d\n",(idx),(nc*idx));
 fprintf(p,"%3d %6d\n",(idx),(nr*idx));
 fprintf(p,"%3d %6d\n",intmin,intmax);
 for(row=0;row<nr;row++) {
  if (row>0) fprintf(p,"\n");
  for(col=0;col<nc;col++) {
   intout=map3[row][col];
   if ((col+1)%(nc/2)==0) fprintf(p,"%d \n",intout);
   else fprintf(p,"%d ",intout);
  }
 }
 fclose(p);
} // end int_file()

/*******************************************************
** surf_file()  output doubles into a surfer .grd file   **
*******************************************************/
void surf_file(char *name4,vector *map4)
{
 FILE *ppp;
  int idx;
 dmax=0.0;
 dmin=9999.0;
  idx=(int)dx;
 for(row=0;row<nr;row++) {
  for(col=0;col<nc;col++) {
   dcount=map4[row][col];
   if (dcount>dmax) dmax=dcount;
   if (dcount<dmin) dmin=dcount;
  }
 }
 strcpy(f_name,name4);
 strcat(f_name,".grd");
 ppp=fopen(f_name,"w");

 fprintf(ppp,"DSAA \n");
 fprintf(ppp,"%3d %6d\n",nc,nr);
 fprintf(ppp,"%4.5f %4.5f \n",(dx),(nc*dx));
 fprintf(ppp,"%4.5f %4.5f \n",(dx),(nr*dx));
 fprintf(ppp,"%4.5f  %4.5f \n",dmin,dmax);
 for(row=0;row<nr;row++) {
  if (row>0) fprintf(ppp,"\n");
  for(col=0;col<nc;col++) {
   h=map4[row][col];
   if ((col+1)%(nc/2)==0) fprintf(ppp,"%4.5f \n",h);
   else fprintf(ppp,"%4.5f ",h);
  }
 }
 fclose(ppp);
} // end surf_file()

/*******************************************************
** logfile()  log all run output data into   .txt file**
*******************************************************/
void log_file(char *name5)
{
 FILE *pppp;
 strcpy(f_name,name5);
 strcat(f_name,".txt");
 pppp=fopen(f_name,"a");
  if (numfile==1){
    fprintf(pppp,"%6.6f initP %6.6f Duration
%6.6f\n",K_act,P_act,end_time);
   }
   fprintf(pppp,"%d out %6.6f ero %6.6f sed %6.6f ec %6.6f se
%6.6f\n",numfile,ds_bal,erobal,sedbal,erobalto,sedbalto);
 fclose(pppp);
} // end log_file()


/*******************************************************
** logfile()  log all run output data into   .txt file**
*******************************************************/
void sadis(char *name6)
{
 FILE *pppppp;
 strcpy(f_name,name6);
 strcat(f_name,".txt");
 pppppp=fopen(f_name,"a");
 fprintf(pppppp," %7.8f\n",input);
 fclose(pppppp);
} // end sadis()
```

```
/*********************************************************
** logfile()  log all run output data into   .txt file**
*********************************************************/
void saero(char *name7)
{
  FILE *ppppppp;
  strcpy(f_name,name7);
  strcat(f_name,".txt");
  ppppppp=fopen(f_name,"a");
  fprintf(ppppppp," %7.8f\n",inpu2);
  fclose(ppppppp);
} // end saero()

/*********************************************************
** logfile()  log all run output data into   .txt file**
*********************************************************/
void sased(char *name8)
{
  FILE *ppppppppp;
  strcpy(f_name,name8);
  strcat(f_name,".txt");
  ppppppppp=fopen(f_name,"a");
  fprintf(ppppppppp," %7.8f\n",inpu3);
  fclose(ppppppppp);
} // end sedis()

/*********************************************************
** calc_process()  actualise erosion/sedimentation   **
*********************************************************/
void calc_pro(void)
{
  for(row=0;row<nr;row++) {
    for(col=0;col<nc;col++) {
      soildep[row][col]+=((dz_ero[row][col]+dz_sed[row][col]));
      if (soildep[row][col]<0.0) soildep[row][col]=0.0;
      dtm[row][col]+=(dz_ero[row][col]+dz_sed[row][col]);
    }
  }
} // end calc_pro()

/*********************************************************
** ini_sok  Initialise the landuse= soil or geology      **
**          related parameters as erodibility K. P and   **
**          infiltration                                 **
*********************************************************/
void ini_sok(void)
{
for(row=0;row<nr;row++) {
  for(col=0;col<nc;col++) {
    K_fac[row][col]=K_act; P_fac[row][col]=P_act;
    infil[row][col]=dx*0.1;
// infil given with AWC ratios
    if (soilmap[row][col]==1) { // Holocene-Pleistocene colluvium
      K_fac[row][col]=K_act; P_fac[row][col]=P_act;
      infil[row][col]=dx*0.161*soildep[row][col];
    }
    if (soilmap[row][col]==2) { // Flysch, marls and sandstones
      K_fac[row][col]=1.5*K_act; P_fac[row][col]=1.5*P_act;
      infil[row][col]=dx*0.105*soildep[row][col];
    }
    if (soilmap[row][col]==3) { // Pliocene, sands/gravels
      K_fac[row][col]=K_act; P_fac[row][col]=P_act;
      infil[row][col]=dx*0.151*soildep[row][col];
    }
    if (soilmap[row][col]==4) { // Schists
      K_fac[row][col]=0.9*K_act; P_fac[row][col]=0.9*P_act;
      infil[row][col]=dx*0.135*soildep[row][col];
    }
    if (soilmap[row][col]==5) { // Gneiss
      K_fac[row][col]=0.7*K_act; P_fac[row][col]=0.7*P_act;
      infil[row][col]=dx*0.066*soildep[row][col];
    }
    if (soilmap[row][col]==6) { // Molasse/conglomerates
      K_fac[row][col]=0.5*K_act; P_fac[row][col]=0.5*P_act;
      infil[row][col]=dx*0.055*soildep[row][col];
    }
    if (soilmap[row][col]==7) { // Peridotite/Serpentenites
      K_fac[row][col]=0.3*K_act; P_fac[row][col]=0.3*P_act;
      infil[row][col]=dx*0.044*soildep[row][col];
    }
    if (lumap[row][col]==1) { // Citrus
      K_fac[row][col]*=0.5; P_fac[row][col]*=2.5;
      infil[row][col]*=1.0;
    }
    if (lumap[row][col]==2) { // Annuals
      K_fac[row][col]*=1.3; P_fac[row][col]*=1.3;
      infil[row][col]*=1.2;
    }
    if (lumap[row][col]==3) { // Olive
      K_fac[row][col]*=0.75;//Scen A
      P_fac[row][col]*=0.75;//Scen A
      infil[row][col]*=1.5;//Scen A
      K_fac[row][col]*=1.5;//Scen B
      P_fac[row][col]*=1.5;//Scen B
      infil[row][col]*=0.75;//Scen B
      K_fac[row][col]*=(0.675+((0.075)*actual_t));//Scen C
      P_fac[row][col]*=(0.675+((0.075)*actual_t));//Scen C
      infil[row][col]*=(1.575-((0.075)*actual_t));//Scen C
// Alternative scenario of linear vegetation regeneration
      K_fac[row][col]*=(1.5-((0.075)*actual_t));//Scen C1
      P_fac[row][col]*=(1.5-((0.075)*actual_t));//Scen C1
      infil[row][col]*=(0.675+((0.075)*actual_t));//Scen C1
// Altitude dependent abandonement highest first abandoned
      if (actual_t==1) {olihei=340.568;}
      if (actual_t==2) {olihei=305.159;}
      if (actual_t==3) {olihei=277.712;}
      if (actual_t==4) {olihei=257.645;}
      if (actual_t==5) {olihei=237.289;}
      if (actual_t==6) {olihei=216.514;}
      if (actual_t==7) {olihei=197.124;}
      if (actual_t==8) {olihei=180.238;}
      if (actual_t==9) {olihei=158.537;}
      if (actual_t==10) {olihei=100.00;}
      if (dtm[row][col]>olihei){
        K_fac[row][col]*=1.5;//Scen C2
        P_fac[row][col]*=1.5;//Scen C2
        infil[row][col]*=0.75;//Scen C2
      } else {
        K_fac[row][col]*=0.75;//Scen C2
        P_fac[row][col]*=0.75;//Scen C2
        infil[row][col]*=1.5;//Scen C2
      }
// Altitude dependent abandonement highest first abandoned
      if (actual_t==1) {olihei=158.537;}
      if (actual_t==2) {olihei=180.238;}
      if (actual_t==3) {olihei=197.124;}
      if (actual_t==4) {olihei=216.514;}
      if (actual_t==5) {olihei=237.289;}
      if (actual_t==6) {olihei=257.645;}
      if (actual_t==7) {olihei=277.712;}
      if (actual_t==8) {olihei=305.159;}
      if (actual_t==9) {olihei=340.568;}
      if (actual_t==10) {olihei=1200.00;}
      if (dtm[row][col]<=olihei){
        K_fac[row][col]*=1.5;//Scen C3
        P_fac[row][col]*=1.5;//Scen C3
        infil[row][col]*=0.75;//Scen C3
      } else {
        K_fac[row][col]*=0.75;//Scen C3
        P_fac[row][col]*=0.75;//Scen C3
        infil[row][col]*=1.5;//Scen C3
      }
    }
    if (lumap[row][col]==4) { // Nature
      K_fac[row][col]*=1.2; P_fac[row][col]*=1.2;
      infil[row][col]*=0.75;
    }
    if (lumap[row][col]==5) { // Riverbed/buildings/bare
      K_fac[row][col]*=0.01; P_fac[row][col]*=2.5;
      infil[row][col]*=0.0;
    }
  } //for
 } //for
} // end ini_sok()

/*********************************************************
** control()  checking for sinks. pits + error map   **
*********************************************************/
void control(void)
{
  char textch[100];
  rounds=0; s_ch=0;
  for(row=0;row<nr;row++) {
    for(col=0;col<nc;col++) {
      error_m[row][col] = 0;
    }
  }
  while (s_ch>=0)
  { // begin while
    sink=0; top=0; flat=0; round=0;ps_flat=0;spill=0;
    round++; s_ch=0; dh_maxi=0.000000000000;
    for(row=0;row<nr;row++) {
      for(col=0;col<nc;col++) {
        dh_nul=0; low=0; high=0;
        for(i=(-1);i<=1;i++) {
          for(j=(-1);j<=1;j++) {
            dh=0.000;
            if( ((row+i)>=0) && ((row+i)<nr) &&   // boundaries
                ((col+j)>=0) && ((col+j)<nc) &&
                      !((i==0)&&(j==0)) ) {
              dh_nul++;
              if((row!=row+i)&&(col!=col+j)){d_x=dx*ROOT2;}
              else {d_x=dx;}
              dh=(dtm[row][col]-dtm[row+i][col+j]);
              if (dh>dh_maxi) {dh_maxi=dh;}
              if (dh<0.000000) { // i,j is higher neighnour
                high++; dh_nul--;
```

```
            }
            if (dh>0.000000) { // i,j is lower neighbour
              low++; dh_nul--;
            }
          }//end if
        }//end for
      }//end for
// Sinks and pitts and flats after this move to next row / col
      if (low==8) {top++; error_m[row][col]=0;}
      if (high==8) { sink++; error_m[row][col]=-99;S2_error=1;}
      if (dh_nul==8) {flat++; error_m[row][col]=5;}
      if (((dh_nul+low)==8) && (low==1))
                              {spill++; error_m[row][col]=3;}
      if (((dh_nul+high)==8) &&!((dh_nul==0)||(high==0)))
                              {ps_flat++; error_m[row][col]=5;}
    }
  }
  sprintf(textch," sinks:%d tops:%d flats:%d  \n ps_flats:%d
  spills:%d  \n round:%d dhmax:%3.8f",sink,top,flat, ps_flat,
  spill, round, dh_maxi);
  gotoxy(1,14);
  printf(textch);
  if (s_ch==0) s_ch=(-1);
 } // end while
} // control()

/*************************************************************
** calc_qtr()  main calculations follow the wtaer downslope  **
**           until all neighbours are processed              **
**                determine the discharge q for this timestep **
**           and the transport rates capacities etc.         **
*************************************************************/
void calc_qtr(void)
{
  char chtext[100];
//set all start q values effective precipitation at time t
  nb_ok=0; nb_check=0.0; all_grids=0.0; ds_bal=0.0; sed_out=0.0;
  q_out=0.0; erocnt=0.0; sedcnt=0.0; sedbal=0.0; erobal=0.0;
  dhmin=-9999.0; dh_tol=0.00025; ET0=0.4373; sedbal2=0.0;
  erobal2=0.0; tel1=0; tel2=0; tel3=0; tel4=0;
  for(row=0;row<nr;row++) {
    for(col=0;col<nc;col++) {
// rainfall from input file dtmnew[row][col]
//    q_mat[row][col] =
              ((dtmnew[row][col]/1000.0)*ET0*dx)infil[row][col];
// normal effective precipitation
      q_mat[row][col] = (eff_prep*ET0)-infil[row][col];
      if (q_mat[row][col]<0.001) q_mat[row][col]=0.001;
      neigh_b[row][col] = 0;     // neighbour check is 0 is false
      sed_tr[row][col] = 0.0;
      ds_ero[row][col] = 0.0;
      dz_sed[row][col] = 0.0;
    }
  }
// into while loop for all grids if not all neighbours processed
all_grids=double(nr)*double(nc);
while (nb_check<all_grids)
  {// begin while
  for(row=0;row<nr;row++) {
    for(col=0;col<nc;col++) {
// into loop for surounding grids of certain grid
// Start first the slope_sum loop for all lower neighbour grids
      slope_sum=0.0; dhmax=0.0; dz_min=-9999.99; d_x=dx;
      direct=20; dz_max=-1.0;dhtemp=-99999.99; dhmin=(-9999.99);
      if (neigh_b[row][col]==0) {
// Repeat the loop to determine if all neigbours are processed
        nb_ok=1;
        for(i=(-1);i<=1;i++) {
          for(j=(-1);j<=1;j++) {
            dh=0.000;
              if( ((row+i)>=0) && ((row+i)<nr) &&   // boundaries
                  ((col+j)>=0) && ((col+j)<nc) &&
                              !((i==0)&&(j==0)) ) {
                dh=(dtm[row][col]-dtm[row+i][col+j]);
                if (dh<0.000){// select higher neighbour
                if (neigh_b[row+i][col+j]==0) {nb_ok=0;}
              }//end if
            }//end if
          }//end for
        }//end for
      }//end if
// Repeat loop determine flow if all draining neighbours are known
// but do this only once
      if ((nb_ok==1) && (neigh_b[row][col]==0)) {
        neigh_b[row][col]=1; // grid to be processed so set to 1
        for(i=(-1);i<=1;i++) {
          for(j=(-1);j<=1;j++) {
            dh=0.000000; dh1=0.000; dhtemp=-99999.99; d_x=dx;
            if( ((row+i)>=0) && ((row+i)<nr) &&   // boundaries
                ((col+j)>=0) && ((col+j)<nc) &&
                              !((i==0)&&(j==0)) ) {
              dh=(dtm[row][col]-dtm[row+i][col+j]);
              dh1=((dtm[row][col]+dz_sed[row][col])-
                          (dtm[row+i][col+j]+dz_ero[row+i][col+j]
                                  +dz_sed[row+i][col+j]));
              if((row!=row+i)&&(col!=col+j)){d_x=dx*ROOT2;
              } else {d_x=dx;}
              if (dh<0.000000){// i j is a higher neigbbour
                if (dh>dz_min) {dz_min=dh;}
                if ((dh<0.000000)) {// i j is a higher neighbour
                  if (dh1>dhmin) {dhmin=(dh1);}
                }
              }
              if (dh>0.000000){// i j is a lower neighbour
                if ((dh>0.000000)) {
                  if (dh1>dhmax-dh_tol) {dhmax=(dh1-dh_tol);}
                }
                dh=dh/d_x;
                if (dh>dz_max){ dz_max=dh; direct=(i*3+5+j);}
                dh=pow(dh,conv_fac);
                slope_sum=slope_sum+dh;
              }//end if
            }//end if
          }//end for
        }//end for
        if (dhmin==-9999.99){dhmin=0.0;}
          else {dhmin=(dhmin*(-1.0));}
        if (dhmax==0.0) {dhmax=dh_tol*-1.0;}
          else {dhmax=(dhmax*(-1.0));}
        for(i=(-1);i<=1;i++) {
          for(j=(-1);j<=1;j++) {
            dh=0.000000; fraction=0.0; t_cap=0.0;
            frac_dis=0.0; frac_tr=0.0; det_r=0.0;
            set_r=0.0; tra_di=0.0; set_di=0.0; d_x=dx;
            if( ((row+i)>=0) && ((row+i)<nr) &&   // boundaries
                    ((col+j)>=0) && ((col+j)<nc) &&
                              !((i==0)&&(j==0)) ) {
              dh=(dtm[row][col]-dtm[row+i][col+j]);
//dh=((dtm[row][col]+dz_ero[row][col]+dz_sed[row][col])-
(dtm[row+i][col+j]+dz_ero[row+i][col+j]+dz_sed[row+i][col+j]));
// Multiple Flow: If there are lower neighbours start evaluating
              if (dh>0.000000){
// Steepest descent only one neighbour
//              if ((i*3+5+j) == direct){
// fraction of discharge into a neighbour grid
                if((row!=row+i)&&(col!=col+j)){d_x=dx*ROOT2;}
                  else {d_x=dx;}
                Slope=dh/d_x;
                dh=dh/d_x;
                dh=pow(dh,conv_fac);
                fraction=(dh/slope_sum);
//                fraction=1.0;
                          frac_dis=(q_mat[row][col]*fraction);
                q_mat[row+i][col+j]+=frac_dis;
// Calc Capacity, detachment, settlement, travel/ settle distance
                t_cap = (pow(frac_dis,m))*(pow(Slope,n));
                det_r = (K_fac[row][col]*(frac_dis*Slope));
                set_r = (-1.0)*(P_fac[row][col]*(frac_dis*Slope));
                          t_cap*=d_x; det_r*=d_x; set_r*=d_x;
                dtmnew[row][col]=t_cap;
                  tra_di = (t_cap/det_r);
                set_di = (t_cap/set_r);
// Evaluate Transport rates and sedimentation/ erosion
// Sediment Transport Rate for de fraction of the discharge
  frac_tr=(sed_tr[row][col]*fraction*d_x);
   // Start a new alinea
  if (frac_tr == t_cap) sed_tr[row+i][col+j]+=(frac_tr/d_x);
  if (frac_tr < t_cap)
// Sediment rate of transport is lower than its capcity over slope
// Erosion
  {
     erocnt+=1.0; lock=0; dz_fill=0.0;
    sedtr_loc=t_cap+((frac_tr-t_cap)*exp(((d_x*(-1.0))/tra_di)));
    dS=sedtr_loc-frac_tr;
    if (dS>0.00) { // all erosion is processed sinks possible
      dz=(((-1.0)*((dS/1.0)*dt))/d_x);
         dz_fill=dz;
         if (dz<(dhmax)){
            sprintf(chtext,"dhmax erosion error");
          gotoxy(1,5);
          printf(chtext);
               dz_fill=(dhmax);
      }
         if (dhmax>=(dh_tol*-1.0)) {dz_fill=0.0;}
         dz_ero[row][col]=dz_ero[row][col]+dz_fill;
      dz_left=dz-dz_fill;
         dhmax-=dz_fill;
         erobal+=dz_fill;
         erobalto+=dz_fill;
         sedtr_loc=sedtr_loc+(dz_left*d_x);
      } //*/
    if (dS<0){ S1_error=1;}
  }
  if (frac_tr > t_cap)
// Sediment rate of transport is exceeding the capacity
// Deposition
  {
    sedcnt+=1.0; lock=0; dz_fill=0.0;
```

```
    sedtr_loc=t_cap+((frac_tr-t_cap)*exp((d_x/sed_di)));
    dS=sedtr_loc-frac_tr;
    if (dS<0.00){
      dz=(((-1.0)*((dS/1.0)*dt ))/d_x);
      if ( (dz>(dhmin-ds_ero[row][col]-dh_tol))) {
           ds_fill=(dhmin-dh_tol-ds_ero[row][col]);
            if (ds_fill<=dh_tol) ds_fill=0.0;
            if (dhmin<=dh_tol) ds_fill=0.0;
        ds_sed[row][col]=ds_sed[row][col]+ds_fill;
        ds_left=ds-ds_fill;
        dhmin-=ds_fill; lock++;
            dhmax-=ds_fill;
            if (dhmin<=dh_tol) {dhmin=dh_tol;}
            rr=row; cc=col; tel1++;
        while (ds_left>0.0){
              maxx=0.0;mmin=-9999.9;lock++;
              for(ii=(-1);ii<=1;ii++) {
            for(jj=(-1);jj<=1;jj++) {
               dh=0.000000;
                if( ((rr+ii)>=0) && ((rr+ii)<nr) &&   //
boundaries
                    ((cc+jj)>=0) && ((cc+jj)<nc) &&
                     !((ii==0)&&(jj==0)) ) {
                   dh=((dtm[rr][cc]+dz_ero[rr][cc]+ds_sed[rr][cc])-
(dtm[rr+ii][cc+jj]+dz_ero[rr+ii][cc+jj]+ds_sed[rr+ii][cc+jj]));
                    if (dh>0.000000){// i j is a lower neighbour
                    if (dh>maxx){
                        maxx=dh; rrr=rr+ii; ccc=cc+jj;
                       }
                   }//end if
                   }//end if
                 }//end for
           }//end for
           for(ii=(-1);ii<=1;ii++) {
             for(jj=(-1);jj<=1;jj++) {
                dh=0.000000;
                if( ((rrr+ii)>=0) && ((rrr+ii)<nr) && //boundaries
                    ((ccc+jj)>=0) && ((ccc+jj)<nc) &&
                     !((ii==0)&&(jj==0)) ) {
                   dh=((dtm[rrr][ccc]+dz_sed[rrr][ccc])-
(dtm[rrr+ii][ccc+jj]+dz_ero[rrr+ii][ccc+jj]+ds_sed[rrr+ii][ccc+jj]
));
                    if (dh<0.000000){// i j is a higher neighbour
                    if (dh>mmin) {mmin=dh;}
                   }//end if
                 }//end if
           }//end for
           }//end for
           if ((ds_left>((mmin*(-1.0))-dh_tol))){
             ds_left1=((mmin*(-1.0))-dh_tol);
             if (ds_left1<=dh_tol) ds_left1=0.0;
             if (mmin==(-9999.9)) ds_left1=0.0;
             dz_left=ds_left-ds_left1;
           } else { ds_left1=ds_left; ds_left=(-1.0);}
           ds_sed[rrr][ccc]=ds_sed[rrr][ccc]+ds_left1;
           if (ds_left>0.0) {rr=rrr; cc=ccc;}
           if (maxx==0.0){
             ds=dz-ds_left;
             sedtr_loc=sedtr_loc+((ds_left)*d_x);
             ds_left=-1.0;
           }
           if ((rr<0)||(cc<0)||(rr>=nr)||(cc>=nc)){
             dz=dz-ds_left;
             sedtr_loc=sedtr_loc+((dz_left)*d_x);
             ds_left=-1.0;
             sprintf(chtext,"Outof Area sedimentation error");
             gotoxy(1,3);
             printf(chtext);
           }
        } //end while */
      } // end if */
      if (dhmin<=dh_tol) tel3++;
      if ((dz<=((dhmin-dz_ero[row][col])-dh_tol))&&(lock==0)) {
        ds_sed[row][col]=ds_sed[row][col]+dz;
        dhmin=(dhmin-dz); lock++; tel2++;
        dhmax-=dz;
      }
      if (((dhmin-ds_ero[row][col])<=dh_tol)&&(lock==0)) {
        sedtr_loc=sedtr_loc+((dz)*d_x); dz=0.0; tel4++;
      }
      sedbal+=dz;
      sedbalto+=dz;
    }
  if (dS>0.00){ S1_error=1; }
  }
// after calculation the local tansport rate is added to the total
  sed_tr[row+i][col+j]+=(sedtr_loc/d_x);
// End of inspring alines
            }//end if
          }//end if boarders
        }//end for j
      }//end for i
    }//end if start process once
   }//end for col
  }//end for row
// check if all the grids are processed to leave this function
  nb_check=0.0;
  for(row=0;row<nr;row++) {
    for(col=0;col<nc;col++) {
      nb_check+=double(neigh_b[row][col]);
    }
  }
  sprintf(chtext,"Process nb_check: %8.1f to go
:%8.1f",nb_check,all_grids);
  gotoxy(1,8);
  printf(chtext);
}    // end while
   // tab correction towards end
// Outlet for 100 alora dem

  for(row=0;row<nr;row++) {   // divide by dx to get m per m
    for(col=0;col<nc;col++) {
        if (dtm[row][col]==0.0) {q_mat[row][col]=0.0;}
//      q_mat[row][col]=(q_mat[row][col]/dx);
    }
  }
//   sed_out=(sed_tr[72][141]); q_out=(q_mat[72][141]); //gneiss
   sed_out=(sed_tr[17][30]); q_out=(q_mat[17][30]);    //Sar
/*  sed_out=0.0;
   sed_out+=(dz_ero[22][30]+dz_sed[22][30]);//transect 4
   sed_out+=(dz_ero[21][30]+dz_sed[21][30]);
   sed_out+=(dz_ero[20][30]+dz_sed[20][30]);
   sed_out+=(dz_ero[19][30]+dz_sed[19][30]);
   sed_out+=(dz_ero[18][30]+dz_sed[18][30]);
   sed_out+=(dz_ero[17][30]+dz_sed[17][30]);
   sed_out/=1.009721;//*/
/*   sed_out+=(dz_ero[23][30]+dz_sed[23][30]);// transect 5
   sed_out+=(dz_ero[23][29]+dz_sed[23][29]);
   sed_out+=(dz_ero[23][28]+dz_sed[23][28]);
   sed_out+=(dz_ero[23][27]+dz_sed[23][27]);
   sed_out+=(dz_ero[23][26]+dz_sed[23][26]);
   sed_out+=(dz_ero[24][25]+dz_sed[24][25]);
   sed_out+=(dz_ero[25][24]+dz_sed[25][24]);*/
  sed_out=0.0;
   sed_out+=(dz_ero[64][46]+dz_sed[64][46]);//transect 2
   sed_out+=(dz_ero[63][47]+dz_sed[63][47]);
   sed_out+=(dz_ero[62][48]+dz_sed[62][48]);
   sed_out+=(dz_ero[61][49]+dz_sed[61][49]);
   sed_out+=(dz_ero[60][50]+dz_sed[60][50]);
   sed_out+=(dz_ero[59][51]+dz_sed[59][51]);
   sed_out+=(dz_ero[58][52]+dz_sed[58][52]);
   sed_out+=(dz_ero[57][53]+dz_sed[57][53]);
   sed_out+=(dz_ero[56][54]+dz_sed[56][54]);
   sed_out+=(dz_ero[55][55]+dz_sed[55][55]);
   sed_out+=(dz_ero[54][56]+dz_sed[54][56]);
   sed_out/=1.390098;//*/
  for(row=0;row<nr;row++) {
    for(col=0;col<nc;col++) {
        erobal2+=dz_ero[row][col];
        sedbal2+=dz_sed[row][col];
            inp1=q_mat[row][col];
            inp2=dz_ero[row][col];
            inp3=dz_sed[row][col];
            sprintf(filename,"gndis2");
            sadis(filename);
            sprintf(filename,"gnero2");
            saero(filename);
            sprintf(filename,"gnsed2");
            ssed(filename);//*/
    }
  }
   ds_bal=(sedbal+erobal);
   ds_bal2=(sedbal2+erobal2);
  sprintf(chtext,"dsbal: %6.6f %6.6f sed_out: %6.6f q_out:
%6.6f",ds_bal,ds_bal2,(sed_out*10000),q_out);
  gotoxy(1,10);
  printf(chtext);
  sprintf(chtext,"Erosion grids: %8.1f  Sediment. grids: %8.1f
",erocnt,sedcnt);
  gotoxy(1,11);
  printf(chtext);
  sprintf(chtext,"Balance Erol:%5.5f 2:%6.6f Sed1:%6.6f 2:%6.6f
",erobal,erobal2,sedbal,sedbal2);
  gotoxy(1,12);
  printf(chtext);
  sprintf(chtext,"Erobaltotal: %6.6f  Sedbalancetotal: %6.6f   %d
%d %d %d   ",erobalto,sedbalto,tel1,tel2,tel3,tel4);
  gotoxy(1,13);
  printf(chtext);
}// end calc_qtr()

/*****************************************************
** main()  main program with time loop and outputs   **
*****************************************************/
void main()
{
// Set main parametres and variables before simulation
   strcpy(filename, "paragnei");
```

```
   ini_mod(filename);
  num_out=1;       // Number of output files during simulation
  numfile=2;
//   K_act=0.000289;     // Actual K-factor Serp trans 4
   K_act=0.15;     // Actual K-factor Gneiss trans 2
   P_act=0.6;
   erobalto=0.0;
   sedbalto=0.0;
   S1_error=0;   S2_error=0;
  if( (make_mat()==1) ) {
    clrscr();
      ini_mat();
       strcpy(filename, "gneiss");
       inir_fil(filename,dtm);
       strcpy(filename, "gnsdp");
       inir_fil(filename,soildep);
//       strcpy(filename, "rain_2km");
//       inir_fil(filename,dtmnew);
//       strcpy(filename, "vege_2km");
//       ini_intf(filename,soilmap);
      if( (er_ifile != NULL) ) {
      gotoxy(1,3);
      printf("Matrices and DTM completed");
      gotoxy(1,4);
      printf("Matrices initialised (infil, K_fac etc..)");
        gotoxy(1,6);
        printf("Please press any key to start");
        clrscr();
      sprintf(ch,"Initial dt=%6.4f  Endtime %6.4f",dt,end_time);
      gotoxy(1,2);
      printf(ch);
  // Start the time loop
      while (actual_t<=end_time)
         {//begin while time loop
        sprintf(ch,"Time    %10.0f",actual_t);
        gotoxy(1,4);
        printf(ch);
           if ((S1_error==0)&&(S2_error==0)) {
          ini_sok();
          calc_qtr();
          calc_pro();
               control();
        }
        if (S1_error!=0) {
          sprintf(ch,"dS Error on Time:%10.0f",actual_t);
          gotoxy(1,4);
          printf(ch);
              actual_t=end_time+1;
        }
        if (S2_error!=0) {
          sprintf(ch,"sink Error on Time:%10.0f",actual_t);
          gotoxy(1,4);
          printf(ch);
              actual_t=end_time+1;
        }
        if (fmod(actual_t,end_time/num_out)==0) {
//              sprintf(filename,"log_2km");
//          log_file(filename);
          sprintf(filename,"gnero%d",numfile);
          surf_file(filename,dz_ero);
          sprintf(filename,"gnsed%d",numfile);
          surf_file(filename,dz_sed);
          sprintf(filename,"gndis%d",numfile);
          surf_file(filename,q_mat);
          sprintf(filename,"gndem%d",numfile);
           surf_file(filename,dtm);
//          sprintf(filename,"sdp%d",numfile);
//           surf_file(filename,soildep);
//          sprintf(filename,"infilD%d",numfile);
//           surf_file(filename,infil);
//          sprintf(filename,"gntra%d",numfile);
//           surf_file(filename,dtmnew);
//          sprintf(filename,"lu_in%d",numfile);
//          int_file(filename,lumap);
//          sprintf(filename,"geog_in",numfile);
//           int_file(filename,soilmap);
//          sprintf(filename,"err%d",numfile);
//           int_file(filename,error_m);
          gotoxy(1,6);
          sprintf(ch,"last file written: %d",numfile);
          printf(ch);
          numfile++;
        }
            actual_t+=dt;
        }//end while time loop
      gotoxy(1,18);
        free_mat();
      printf("End of Program");
      getch();
      } else  {
         printf("input DEM file error\n\n End of Program");
         getch();
    }
   } else  {
    printf("not enough memory for matrices\n");
    getch();
  }
} // end main
```